Ferdowsi University of Mashhad

Iranian Food Science and Technology Research Journal

Iranian food science and technology Association

Vol.20 No.6

2025

ISSN:1735-4161

Contents

Iranian Food Science and Technology Research Journal

Vol. 20 No. 6 2025

Published by: Ferdowsi University of Mashhad, (College of Agriculture), Iran
Executive Manager: N. Shahnoushi, Department of Agricultural Economics, Ferdowsi University of Mashhad, Iran

Publisher Ferdowsi University of Mashhad
Address: College of Agriculture, Ferdowsi University of Mashhad, Iran
P.O.BOX: 91775- 1163
Fax: (98)051-38787430
E-Mail: ifstrj@um.ac.ir
Web Site: https://ifstrj.um.ac.ir

Contents

Iranian Food Science and Technology Research Journal
Homepage: https://ifstrj.um.ac.ir

Research Article
Vol. 20, No. 6, Feb.-Mar., 2025, p. 105-118

Impact of Sprouting Time of Chickpea on the Physicochemical, Textural, Sensory, and Total Phenolic Characteristics of Falafel Prepared from Sprouted Chickpea Flour

K. Goharpour[1], F. Salehi[2*], A. Daraei Garmakhany[3]

1 and 2- M.Sc Student and Associate Professor, Department of Food Science and Technology, Faculty of Food Industry, Bu-Ali Sina University, Hamedan, Iran, respectively.
(*- Corresponding Author Email: F.Salehi@Basu.ac.ir)
3- Associate Professor, Department of Food Science and Technology, Faculty of Engineering and Natural Resources, Bu-Ali Sina University, Hamedan, Iran

Received: 17.06.2024
Revised: 22.11.2024
Accepted: 23.11.2024
Available Online: 07.01.2025

How to cite this article:
Goharpour, K., Salehi, F., & Daraei Garmakhany, A. (2025). Impact of sprouting time of chickpea on the physicochemical, textural, sensory, and total phenolic characteristics of falafel prepared from sprouted chickpea flour. *Iranian Food Science and Technology Research Journal*, *20*(6), 105-118. https://doi.org/10.22067/ifstrj.2024.88550.1339

Abstract

Falafel is considered as an inexpensive and nutritious product that contains various plant substances, vitamins, dietary fibers, and phenolic compounds. The aim of this research was to investigate the impact of sprouting time on the physicochemical characteristics of sprouted chickpea flour. Also, the effects of sprouting time on the physicochemical characteristics and sensory properties of falafel prepared from sprouted chickpea flour were examined. The finding of this research indicated that the sprouting process significantly increased the total phenolic content (from 284.17 to 720.98 µg gallic acid/g dry), antioxidant capacity (from 77.55% to 93.35%), and redness (from 7.65 to 11.39) of chickpea flour ($p<0.05$). While, it significantly decreased the lightness (from 70.81 to 57.07) and yellowness (from 43.71 to 25.62) of chickpea flour ($p<0.05$). The total phenolic content and antioxidant capacity of falafel prepared from flour of sprouted chickpea for two-days (48 hours) were significantly higher than those prepared from unsprouted chickpeas flour ($p<0.05$). The volume of falafel samples produced from unsprouted, one-day sprouted, and two-day sprouted chickpea flours was 18.75, 16.60, and 15.40 cm^3, respectively. The minimum oil uptake was observed in the sample prepared from chickpeas sprouted for two-days ($p<0.05$). The sprouting process did not have a significant impact on the firmness, cohesiveness, and chewiness of the falafel ($p>0.05$). In general, utilizing of one-day (24 hours) sprouted chickpea flour for the production of falafel is recommended due to the best flavor, the highest overall acceptance score, high content of phenolic compounds, high antioxidant capacity, and low oil absorption.

Keywords: Antioxidant capacity, Cohesiveness, Firmness, Oil absorption, Total phenolic

https://doi.org/10.22067/ifstrj.2024.88550.1339

Introduction

Legumes rank as the second most important crop globally, after cereals. In developing countries, a significant portion of people's dietary protein comes from various sources of legumes such as peas, green peas, mung beans, soybeans, beans, faba beans, and lentils. The protein content of legumes (20-50%) is relatively high compared to cereals and other starchy crops and roots (Elobuike *et al.*, 2021; Ghoshal & Kaushal, 2020; Salehi, 2023; Salehi *et al.*, 2024). Chickpeas (*Cicer arietinum* L.) are an excellent source of protein, carbohydrates, fiber, minerals (P, Mg, Ca, Fe, and K), and vitamins such as niacin, thiamin, riboflavin, B vitamins, and β-carotene (Bidkhori & Mohammadpour Karizaki, 2022; Doddamani *et al.*, 2014; Ghoshal & Kaushal, 2020).

The process of germination enhances legumes by changing their nutritional value, chemicals, and taste. This process is used to increase digestibility and improve nutritional value of legumes. During this process, the total phenolic content (TPC) and antioxidant capacity (AC) of legumes also increased (El-Adawy *et al.*, 2003; Karimi & Saremnezhad, 2020; Oghbaei & Prakash, 2016). The study conducted by Sofi *et al.* (2023) showed that the sprouting process increases the nutritional value, phenolic content, and AC of chickpea flour, and considerably improves the protein and starch digestibility of sprouted chickpea flour. Kim *et al.* (2022) also confirmed that germination of desi chickpeas led to increase TPC, total flavonoid content, antioxidant activity, and percentage of soluble proteins. The effect of addition sprouted mung bean flour at different levels (0-30%) on noodles properties was examined by Liu *et al.* (2018). Their findings confirmed that when more sprouted mung bean flour was added, the protein content of noodles increased.

Chickpeas are used as the main ingredient in ethnic and traditional Iranian foods such as Abgoosht, Ash, Shole, and falafel (Bidkhori & Mohammadpour Karizaki, 2022; Goharpour *et al.*, 2024). Falafel is considered as an inexpensive and nutritious product that contains various plant substances, various vitamins, dietary fibers, and bioactive components (Fikry *et al.*, 2021;Hojjati *et al.*, 2020). In a study by Goharpour *et al.* (2024) investigated the impacts of various drying methods of ground sprouted chickpeas on the quality, textural characteristics, and sensory properties of fried falafel, they found that fried falafel made from infrared drying of sprouted chickpeas scored the highest in terms of odor, flavor, and total acceptability.

During drying products, it is important to use the most suitable drying method and conditions (Khodadadi *et al.*, 2023). The most common method for dehydration agricultural crops is hot air drying (Khodadadi *et al.*, 2024).

The goal of this study was to estimate the impacts of sprouting time on the moisture content (MC), ash content, TPC, AC, color, and rehydration of sprouted chickpea flour. The effects of sprouting time on the physicochemical characteristics of falafel prepared from sprouted chickpea flour were also examined.

Materials and Methods

Sprouting Process

To conduct this research, packaged chickpeas were purchased from Sahar Company (Hamedan, Iran). After washing, the chickpeas were soaked in water at 25°C for 24 h. At this stage, one-third of the soaked peas were separated (Unsprouted sample). Afterwards, excess water was removed and chickpeas were sprouted in containers covered with thin towels at 25°C for 24 h (Day 1 sample) or 48 h (Day 2 sample) (Amin-Ekhlas *et al.*, 2024). Unsprouted and sprouted (after 24 and 48 h) chickpeas were ground (MK-G20NR, National, Japan) (Fig. 1).

Hot-air Drying

To dry the ground of unsprouted and sprouted (after 24 and 48 h) chickpeas, the samples were placed in a fan oven (Shimaz, Iran) at 70°C, until reached a constant weight (Amin-Ekhlas *et al.*, 2024).

Preparation of Falafel

The raw and fried falafels were prepared according to the approach described in our previous work (Goharpour *et al.*, 2024). The falafel recipe prepared included chickpea flour (70 g), water (100 g), salt (3.5 g, Toloo company, Iran), falafel spice (1.1 g), and baking powder (1 g, Bartar company, Iran). The prepared mixture was distributed evenly using a mold and placed in a deep fryer (Seven star, Model df02, Germany) at 150°C for 8 min.

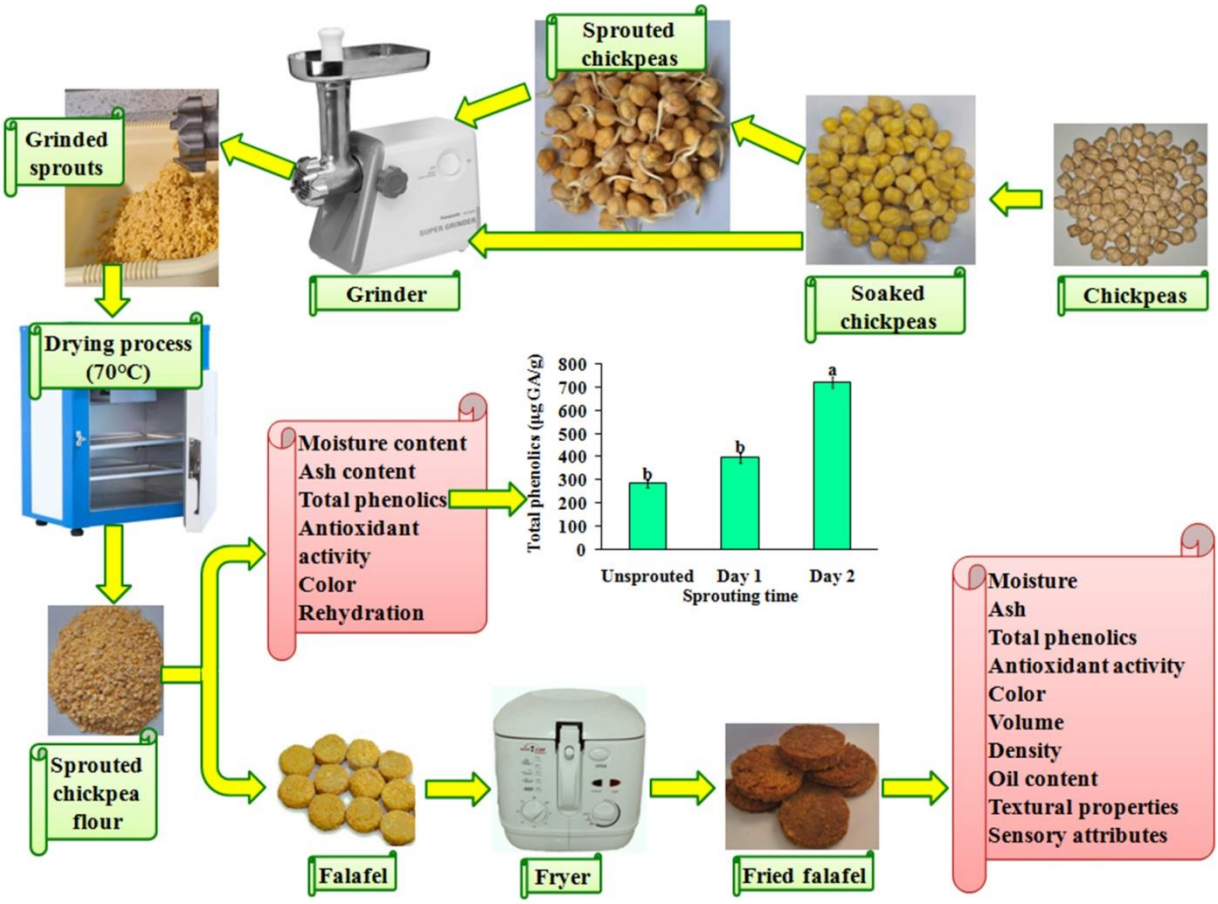

Fig. 1. Schematic of sprouted chickpea flour production and falafel making process

Moisture and Ash Contents

The MCs of chickpea flours (unsprouted and sprouted) and falafels were determined using an oven at 105°C for 5 h (Shimaz, Iran)(Amin-Ekhlas *et al.*, 2024). The ash contents of chickpea flours (unsprouted and sprouted) and falafels were determined using a laboratory electric furnace (Iran) at 550°C for 6 h (Goharpour *et al.*, 2024).

Total Phenolic Content

The TPCs of chickpea flours and falafels were determined according to the procedure described by Goharpour *et al.* (2024). The TPC of flours/falafels was calculated as Gallic acid equivalent (GA) using Folin-Ciocalteu's phenol reagent (Sigma-Aldrich, USA) and a UV-VIS spectrophotometer at 725 nm (XD-7500, Lovibond, Germany) (Salehi *et al.*, 2023a).

Antioxidant Activity

The AC of chickpea flours/falafels was determined as free radical scavenging activity using DPPH (2,2-Diphenyl-1-picrylhydrazyl, 0.1mM, Sigma-Aldrich, USA) and a UV-VIS spectrophotometer at 517 nm (XD-7500, Lovibond, Germany) (using Equation 1).

$$DPPH = \frac{\text{Absorbance of control - Absorbance of sample}}{\text{Absorbance of control}} \times 100 \quad (1)$$

Rehydration of Chickpea Flour

The rehydration test of chickpea flour was carried out in a water bath (R.J42, Pars Azma Co., Iran) at 50°C for 30 min (Salehi *et al.*, 2023b).

Color

Samples photos were taken with a scanner (HP Scanjet-300). The flour/falafel photos were converted from RGB color space to $L^*a^*b^*$ color space using a computer software (ImageJ, V.1.42e, USA) and its color space conversion plugin (Eftekhari *et al.*, 2023).

Volume and Density of Falafels

The volume and density of falafels were measured following the method described by Goharpour *et al.* (2024).

Oil Content (Soxhlet Extraction)

Conventional soxhlet extraction was performed in a laboratory soxhlet extractor using 3 g of falafel and approximately 75 mL of n-Hexane (extra pure, Arman Sina, Iran) at 80°C for 5 h (Behr E4, Germany).

Textural Properties

Puncture test: A texture analyzer (STM-5, Santam, Iran) was used for measuring the surface hardness of falafels. Puncture tests were performed using a cylindrical probe with a diameter of 5 mm, at a speed of 1 mm/s, and a penetration depth of 10 mm.

TPA test: Texture profile analysis (TPA) of falafel samples were carried out using the texture analyzer equipped with a 5 cm diameter cylindrical probe, 50% deformation, and a test speed of 1 mm/s.

Sensory Assessment

The sensory assessment was carried out after the falafels samples were fried. Food engineering students and professors participated in the evaluation of the sensory attributes of the fried falafels.

Statistical Analysis

A statistical analysis was performed to compare the average responses (using the Duncan's multiple range test), revealing significant differences with a 95% confidence level (employing the SPSS 21 software).

Results and Discussion

Sprouted Chickpea Flour Properties

The moisture and ash content of fresh chickpeas (unsoaked) were 6.89% and 3.40%. Table 1 shows the influence of sprouting time on the MC, ash content, AC, and rehydration of sprouted chickpea flour. The MC of unsprouted, sprouted after one-day, and sprouted after two-day samples was 9.13%, 7.77%, and 8.43%, respectively. The ash content of unsprouted, sprouted after one-day, and sprouted after two-day samples were 2.38%, 2.28%, and 2.22%, respectively. The results showed that there was no significant change in the ash content of sprouted chickpea flour during the sprouting process.

Table 1- Effect of sprouting time on the moisture, ash, antioxidant capacity, and rehydration of sprouted chickpea flour

Sprouting time	**Moisture content (%)**	**Ash content (%)**	Antioxidant capacity (%)	Rehydration ratio (%)
Unsprouted	9.13±0.05 [a]	2.38±0.12 [a]	77.55±3.72 [b]	366.47±16.45 [a]
Day 1	7.77±0.19 [c]	2.28±0.15 [a]	88.46±2.07 [a]	353.53±17.37 [a]
Day 2	8.43±0.12 [b]	2.22±0.10 [a]	93.35±1.32 [a]	341.73±1.67 [a]

Different letters within each column represent significance difference ($p<0.05$)

In this research, the TPC of fresh chickpea (unsoaked) was 254.37 µg GA/g dry. Sprouting of chickpeas increases the amount of phenolic compounds. Fig. 2 shows the effects of sprouting time on the total phenolics of sprouted chickpea flour. The total phenolics of

unsprouted, sprouted after one-day, and sprouted after two-day samples were 284.17, 395.38, and 720.98 µg GA/g dry, respectively. The results showed that there was a significant change in total phenolics of sprouted chickpea flour during the sprouting process. The increase in TPC after sprouting could be due to the enzymatic degradation of kernel structure of the samples, which helps in the more extraction of phenolic compounds (Kumar *et al.*, 2020). Goharpour *et al.* (2024) studied the impacts of different drying methods of ground sprouted chickpeas on the TPC of dried samples. Their findings showed that the TPC of hot air, infrared, and microwave dried samples were 463.42 µg GA/g dry, 766.20 µg GA/g dry, and 470.82 µg GA/g dry, respectively. In addition, Amin-Ekhlas *et al.* (2024) reported that the process of sprouting of wheat improves the TPC, and as a result, the flour made from the sprouts also had higher TPC.

Sprouting is a slow natural biochemical process that happens at low temperatures. It alters the metabolic activity and carbohydrate digestibility, and increases protein content, antioxidant activity, and nutrients bioavailability (Kumar *et al.*, 2020). During the sprouting process, the TPC of chickpea increased, which led to an increase in the AC of the product. In this study, the AC of unsprouted, one-day sprouted, and two-day sprouted chickpeas flours were 77.55%, 88.46%, and 93.35%, respectively. The sprouting process decreased the rehydration rate of the flours. As shown in the Table 1, as the sprouting time increased, the rehydration rate of sprouted chickpea flours was decreased from 366.47% to 341.73% ($p>0.05$).Gan *et al.* (2017) reported that hot-air dehydration not only enhanced the TPC and AC of sprouted mung beans, but also changed their color to brown. Kumar *et al.* (2020) studied the of sprouting on the TPC and AC of black chickpea. Their results showed that the effect of sprouting on TPC was positive but non-significant.

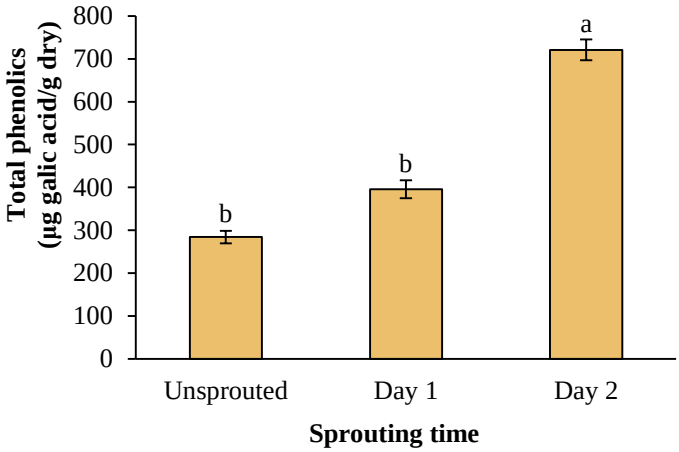

Fig. 2. Effect of sprouting time on the total phenolics of sprouted chickpea flour
Different letters above the columns indicate significant difference ($p<0.05$)

In this study, the lightness (L^*), redness (a^*), and yellowness (b^*) of fresh chickpea powder (unsoaked) were 60.79, 7.67, and 31.49 respectively. Table 2 shows the effects of sprouting time on the color parameters of sprouted chickpea flour. The sprouting process decreased the L^* and b^* indexes of the sprouted chickpea flours, while the a^* index of flours was increased. As shown in this table, as the sprouting time increased, the L^* and b^* indexes of sprouted chickpea flours significantly decreased from 70.81 to 57.07, and from 43.71 to 25.62, respectively ($p<0.05$). While, as the sprouting time increased, the a^* index of sprouted chickpea flours significantly increased from 7.65 to 11.39 ($p<0.05$). Reduction in color parameters in sprouted samples might be due to the change in carbohydrates and protein structure (Tian *et al.*, 2010). Ozturk *et al.* (2014) reported that sprouted wheat flour was

darker in color than unsprouted wheat flour. In addition, Javaheripour *et al.* (2022) reported that the addition of sprouted wheat flour to sponge cake formulations darkened the color of the samples and reduced the L^* parameter. This is likely due to the enhanced activity of the enzymes and the increased value sofreducing sugars in the sprouted grains. The study of Kumar *et al.* (2020) showed that sprouting process improved the physical and pasting properties of black chickpea (*Cicer arietinum*), whereas roasting improved the functional properties. The L^* index of sprouted grains considerably enhanced as compared with the dark color of roasted sample.

Table 2- Effect of sprouting time on the color parameters of sprouted chickpea flour

Sprouting time	Lightness	Redness	Yellowness
Unsprouted	70.81±1.42 [a]	7.65±0.14 [b]	43.71±0.66 [a]
Day 1	67.01±2.49 [b]	8.09±0.18 [b]	37.38±2.97 [b]
Day 2	57.07±2.52 [c]	11.39±0.45 [a]	25.62±2.52 [c]

Different letters within each column represent significance difference ($p<0.05$)

Moisture and Ash Contents of Falafel

Fig. 3 (a) displays the influence of sprouting time on the MC of falafel samples. The MC of falafel samples made from unsprouted, sprouted after one-day, and sprouted after two-days chickpea flours were 19.73%, 26.27%, and 24.80%, respectively. The MC of falafel made from sprouted chickpea flour was considerably higher than unsprouted chickpea flour ($p<0.05$). Serdaroglu (2006) used fat and oat flour in the production of beef patties. Their results confirmed that the addition of oat flour enhanced the baking properties of patties. Furthermore, adding oat flour reduced the water content of raw patties, whereas oat flour increased the water content of baked patties.

Fig. 3 (b) displays the influence of sprouting time on the ash content of samples. There was no considerable difference in ash content between falafel made from sprouted and unsprouted chickpea flour ($p>0.05$). The ash content of falafel samples prepared from unsprouted, sprouted after one-day, and sprouted after two-days chickpea flours were 5.19%, 5.40%, and 5.93%, respectively.

Total Phenolic Content and Antioxidant Capacity of Falafel

During the sprouting process, the amount of chickpea phenolic compounds increased, which led to an increase in the TPC and AC of the prepared falafel samples. Fig. 4 (a) and 4 (b) demonstrate the influence of sprouting time on the TPC and AC of falafel samples, respectively. The TPC of samples made from unsprouted, one-day sprouted, and two-days sprouted chickpea flours were 154.47, 245.73, and 264.23 µg GA/g dry, respectively. Also, the AC of samples made from unsprouted, sprouted after one-day, and sprouted after two-days chickpea flours were 71.88%, 78.89%, and 87.35%, respectively. The TPC and AC of falafel made from two-days sprouted chickpeas flours were considerably higher than falafel prepared from unsprouted chickpea flours ($p<0.05$).

Color of Falafel

The effect of sprouting time on the surface and core color parameters of falafel prepared from sprouted chickpea flours was reported in Table 3. The sprouting process did not have a considerable influence on the surface color of the falafel ($p>0.05$). The L^*, a^*, and b^* values of the falafel's surface were between 45.41 and 46.59, 14.95 and 15.57, and 29.62 and 32.12, respectively. The L^*, a^*, and b^* values of the falafel's core were between 55.18 and 60.65, 2.32 and 4.46, and 37.04 and 41.61, respectively. Goharpour *et al.* (2024) results showed that the L^*, a^*, and b^* values of the fried falafel's core were between 57.37 and 59.29, 3.66 and 6.88, and 40.50 and 43.31, respectively.

Volume

Fig. 5 displays the effect of sprouting time on the volume of falafel prepared from sprouted chickpea flours. The use of sprouted chickpeas to prepare falafel reduced the volume of falafel. The lowest volume was related to the sample made from the two-days sprouted chickpea. The volume of samples made from unsprouted, one-day sprouted, and two-day sprouted chickpea flours were 18.75, 16.60, and 15.40 cm^3, respectively. The results of this study showed that the use of sprouted chickpea flours did not have a considerable effect on the density of the falafel ($p>0.05$) and the density of falafel was between 886.86kg/$m^3$and 889.81 kg/m^3.

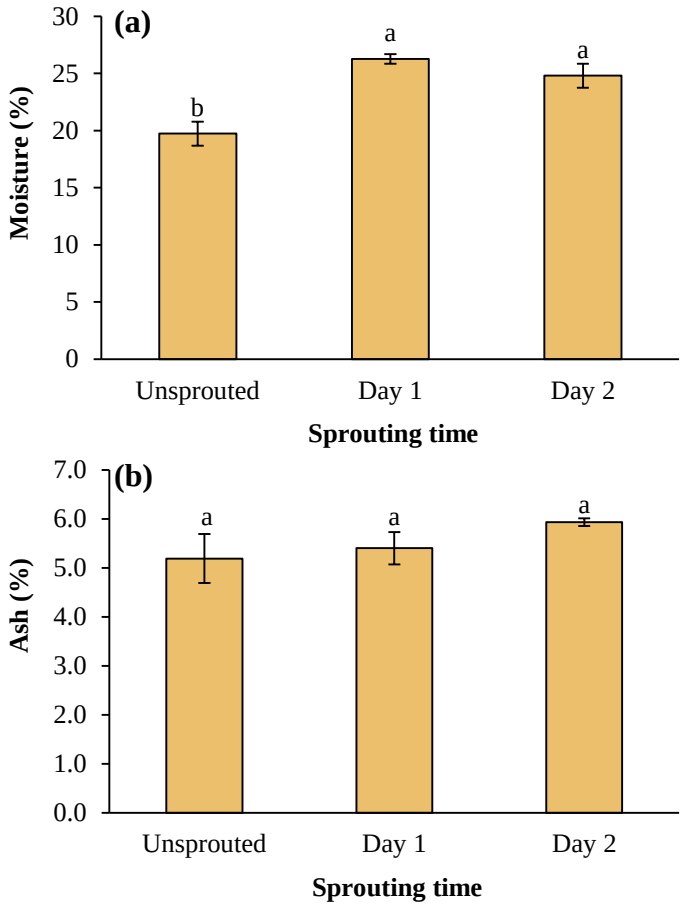

Fig. 3. Effect of chickpea sprouting time on the moisture (a) and ash (b) contents of falafels
Different letters above the columns indicate significant difference ($p<0.05$)

Table 3- Effect of chickpea sprouting time on the color parameters of falafels

Sprouting time	Surface color indexes			Core color indexes		
	Lightness	Redness	Yellowness	Lightness	Redness	Yellowness
Unsprouted	45.41±2.75 ^{a}	15.57±0.93 ^{a}	30.17±3.27 ^{a}	55.91±0.51 ^{b}	3.43±0.43 ^{b}	37.04±0.77 ^{a}
Day 1	45.98±1.40 ^{a}	15.44±0.47 ^{a}	29.62±4.32 ^{a}	60.65±0.91 ^{a}	2.32±0.42 ^{c}	41.61±1.94 ^{a}
Day 2	46.59±0.25 ^{a}	14.95±0.22 ^{a}	32.12±4.32 ^{a}	55.18±1.71 ^{b}	4.46±0.07 ^{a}	39.66±3.65 ^{a}

Different letters within each column represent significance difference ($p<0.05$)

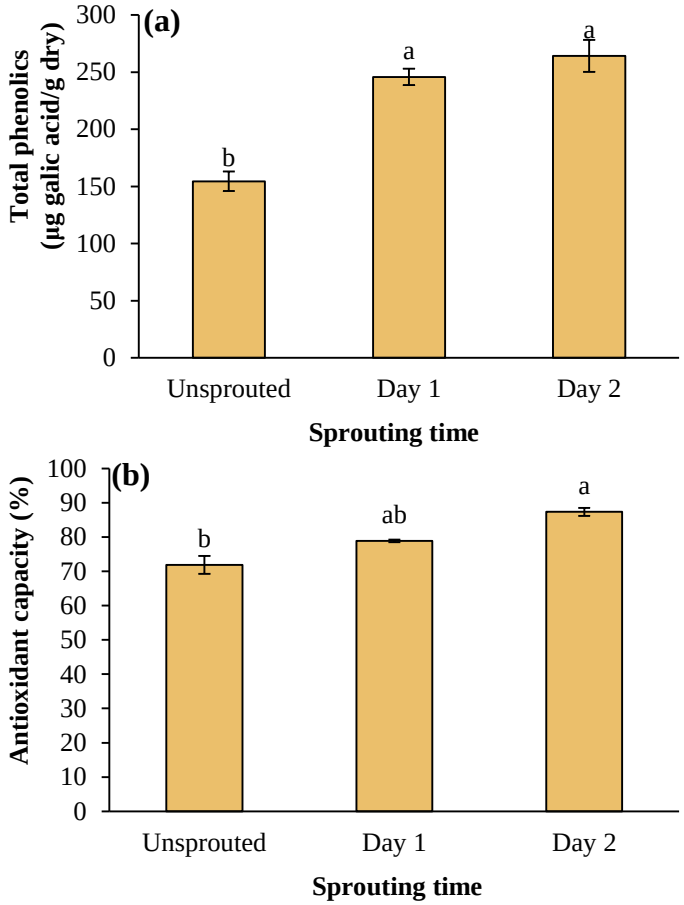

Fig. 4. Effect of chickpea sprouting time on the total phenolics content (a) and antioxidant capacity (b) of falafels
Different letters above the columns indicate significant difference ($p<0.05$)

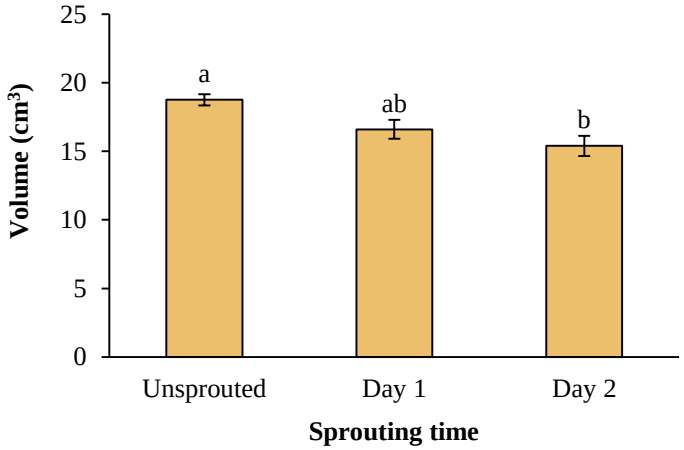

Fig. 5. Effect of chickpea sprouting time on the volume of falafels
Different letters above the columns indicate significant difference ($p<0.05$)

Oil Content of Falafel

Today, people are looking for low-fat content of food products (Daraei Garmakhany *et al.*, 2011). Fig. 6 displays the effect of sprouting time on the oil content of falafel prepared from sprouted chickpea flours. The use of sprouted chickpeas to prepare falafel reduced the oil absorption by falafel. The minimum oil uptake was related to falafel made from the two-day sprouted chickpea ($p<0.05$).

The oil content of samples made from unsprouted, one-day sprouted, and two-day sprouted chickpea flours were 22.56%, 21.67%, and 17.00%, respectively.

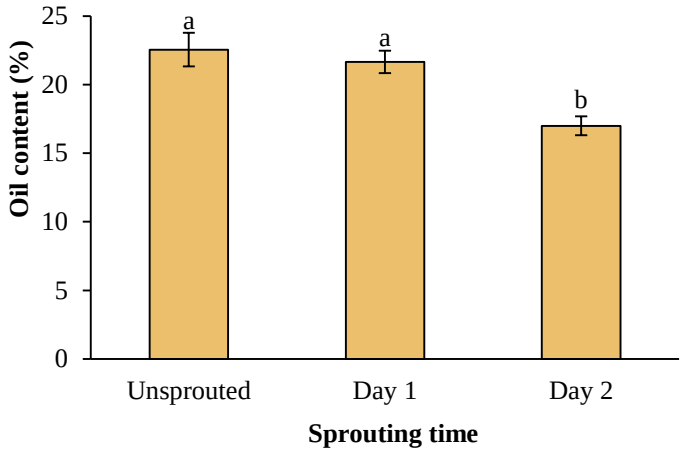

Fig. 6. Effect of chickpea sprouting time on the oil content of falafels
Different letters above the columns indicate significant difference ($p<0.05$)

Textural Properties of Falafels

Chickpea flour is commonly used as the main ingredient in falafel. Fig. 7 shows the effect of sprouting time on the texture hardness (puncture test) of falafel made from sprouted chickpea flours. The sprouting process did not have a considerable effect on the hardness of falafel ($p>0.05$). The hardness of falafel samples prepared from unsprouted, one-day sprouted, and two-days sprouted chickpea flours were 7.65 N, 8.94 N, and 7.47 N, respectively.

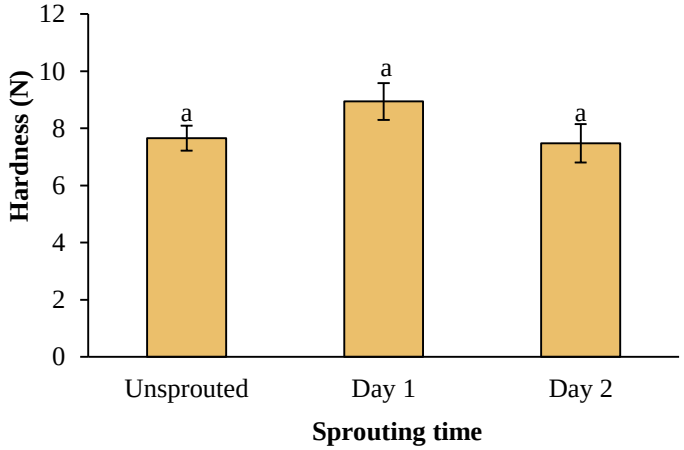

Fig. 7. Effect of chickpea sprouting time on the texture hardness (puncture test) of falafels
Same letters above the columns indicate no significant difference between means ($p>0.05$)

The texture is one of the main quality attributes of foods. Texture analysis tests are very useful in examining the texture of various foods and show a high correlation with sensory evaluation (Caine *et al.*, 2003). The firmness, cohesiveness, springiness, and chewiness values of falafel were between 45.90 N and 55.73 N, 0.60 and 0.72, 0.61 and 0.75, and 21.88 N and 25.14 N, respectively (Table 4). Goharpour *et al.* (2024) findings showed that the firmness, cohesiveness, springiness, and chewiness of the fried falafel were between 38.17 N and 91.56 N, 0.29 and 0.44, 0.48 and 0.58, and 5.38 N and 17.24 N, respectively.

Table 4- Effect of chickpea sprouting time on the textural properties (TPA test) of falafels

Sprouting time	Firmness (N)	Cohesiveness	Springiness	Chewiness (N)
Unsprouted	49.06±3.92 [a]	0.72±0.08 [a]	0.71±0.01 [a]	25.14±4.61 [a]
Day 1	55.73±2.19 [a]	0.70±0.21 [a]	0.61±0.05 [b]	24.44±8.74 [a]
Day 2	45.90±6.76 [a]	0.60±0.19 [a]	0.75±0.04 [a]	21.88±9.16 [a]

Different letters within each column represent significance difference ($p<0.05$)

Texture firmness is considered to be the maximum force observed in the for ceversustime graph (first cycle) during the TPA test. There is no considerable difference between falafel samples concerning firmness ($p>0.05$).

The TPA test is advice method that imitates the first two stages of chewing food and analyzes the texture of the product (Nishinari *et al.*, 2019). The cohesiveness parameter is a measure of the internal bond strength of the product. To estimate it, the ratio of the second cycle is at the first cycle in the TPA test graph was calculated. The use of sprouted chickpea flour to prepare falafel reduced the cohesiveness of falafel samples.

Springiness is the value or ratio at which a food samples returns to their original size/shape after being partially compressed among the tongue and palate (Meullenet *et al.*, 1998). Also, the springiness parameter or elastic describes the springiness state of a sample after the compressive force is removed. To calculate the springiness parameter, the ratio of the compression period of the second cycle to the first cycle in the TPA test graph is considered. The findings of this research demonstrated that the mean values of the springiness of falafel were between 0.61 and 0.75.

Chewiness describes the value of work required to chew the food products until it is swallowed (Meullenet *et al.*, 1998) and it is equal to firmness × cohesiveness × springiness. The findings of this research showed that the sprouting process did not have a significant effect on the chewiness of falafel ($p>0.05$). Off course, adding sprouted chickpeas flour to the falafel formulation decreases the cohesiveness of the texture, as well as, decreases the energy required for chewing falafel.

Sensory Evaluation of Falafel

The sprouting process greatly influences nutritional, biochemical, and sensory characteristics by improving chickpea quality and increasing its digestibility. Table 5 shows the effect of sprouting time on the sensory attributes of falafel made from sprouted chickpea flours. The sprouting process did not have a considerable influence on the surface brightness and core brightness of falafel ($p>0.05$). The appearance, odor, flavor, firmness, texture, and overall acceptance of falafel made from two-days sprouted chickpea flours were considerably lower than samples made from unsprouted flour ($p<0.05$). The highest texture acceptance score was related to falafel prepared from unsprouted chickpea flour. Falafel, made from one-day sprouted chickpeas, received the highest marks in terms of flavor and overall acceptance.

Conclusion

Various products such as falafel are made from ground and dried sprouted chickpea. In this work, the effect of sprouting time on the physicochemical characteristics of sprouted chickpea flour was examined. In addition, the effects of sprouting time on the physicochemical characteristics of falafel made from sprouted chickpea flour were studied. Sprouting of chickpea improves the TPC, so the flour made from the sprouts has a higher TPC and the highest AC. The sprouting process did not have a considerable effect on the ash content and rehydration rate of the sprouted chickpea flour ($p>0.05$). The TPC and AC of falafel made from two-day sprouted chickpea flours were considerably higher than falafel prepared from unsprouted chickpea flours ($p<0.05$). The sprouting process did not have a significant impact on the firmness,

cohesiveness, and chewiness of falafel ($p>0.05$). Using sprouted chickpea to prepare falafel reduced the cohesiveness and chewiness of falafel samples. It is recommended to use sprouted chickpea in the preparation of various food products. In addition, due to the highest sensory score, high TPC, high AC, high MC, and low oil absorption, it is recommended to use one-day sprouted chickpea flour for the production of falafel.

Table 5- Effect of chickpea sprouting time on the sensory attributes of fried falafels

Sprouting time	Surface brightness	Core brightness	Appearance acceptance	Odor acceptance	Flavor acceptance	Firmness	Texture acceptance	Overall acceptance
Unsprouted	7.40±0.80 ^{a}	7.90±1.30 ^{a}	8.00±0.45 ^{a}	8.20±0.75 ^{a}	7.20±1.25 ^{a}	7.30±0.78 ^{a}	8.10±0.54 ^{a}	7.70±0.46 ^{a}
Day 1	6.60±0.92 ^{a}	7.20±1.25 ^{a}	7.60±0.80 ^{a}	7.10±1.04 ^{b}	7.50±1.12 ^{a}	6.80±0.75 ^{a}	7.30±0.46 ^{b}	8.00±0.89 ^{a}
Day 2	6.80±1.83 ^{a}	6.90±1.22 ^{a}	6.90±0.70 ^{b}	4.70±1.27 ^{c}	4.60±1.02 ^{b}	5.10±0.70 ^{b}	4.90±1.22 ^{c}	5.40±1.11 ^{b}

Different letters within each column represent significance difference ($p<0.05$)

Author Contributions

Kimia Goharpour: Data curation, Formal analysis, Investigation, Software, Writing–original draft. **Fakhreddin Salehi**: Conceptualization, Data curation, Formal analysis, Investigation, Methodology, Project administration, Software, Supervision, Validation, Writing–original draft, Writing–review and editing. **Amir Daraei Garmakhany**: Conceptualization, Data curation, Investigation, Methodology, Supervision, Writing – original draft.

Founding Source

This work was supported by a grant from the Bu-Ali Sina University, Hamedan, Iran (Grant No. 402174 to Fakhreddin Salehi).

References

1. Amin-Ekhlas, S., Pajohi-Alamoti, M., & Salehi, F. (2024). Effect of ultrasonic and infrared treatments on microbial population, physicochemical properties, and total phenols of sprouted wheat powder. *Innovative Food Technologies*, *11*(3), 197-210. https://doi.org/10.22104/ift.2024.6712.2166
2. Bidkhori, P., & Mohammadpour Karizaki, V. (2022). Diffusion and kinetic modeling of water absorption process during soaking and cooking of chickpea. *Legume Science*, *4*(1), e116. https://doi.org/10.1002/leg3.116
3. Caine, W.R., Aalhus, J.L., Best, D.R., Dugan, M.E.R., & Jeremiah, L.E. (2003). Relationship of texture profile analysis and Warner-Bratzler shear force with sensory characteristics of beef rib steaks. *Meat Science*, *64*(4), 333-339. https://doi.org/10.1016/S0309-1740(02)00110-9
4. Daraei Garmakhany, A., Aghajani, N., & Kashiri, M. (2011). Use of hydrocolloids as edible covers to produce low fat French fries. *Latin American Applied Research*, *41*(3), 211-216.
5. Doddamani, D., Katta, M.A., Khan, A.W., Agarwal, G., Shah, T.M., & Varshney, R.K. (2014). CicArMiSatDB: the chickpea microsatellite database. *BMC Bioinformatics*, *15*(1), 212. https://doi.org/10.1186/1471-2105-15-212
6. Eftekhari, A., Salehi, F., Gohari Ardabili, A., & Aghajani, N. (2023). Effects of basil seed and guar gums coatings on sensory attributes and quality of dehydrated orange slices using osmotic-ultrasound method. *International Journal of Biological Macromolecules*, *253*, 127056. https://doi.org/10.1016/j.ijbiomac.2023.127056

7. El-Adawy, T.A., Rahma, E.H., El-Bedawey, A.A., & El-Beltagy, A.E. (2003). Nutritional potential and functional properties of germinated mung bean, pea and lentil seeds. *Plant Foods for Human Nutrition*, *58*(3), 1-13. https://doi.org/10.1023/B:QUAL.0000040339.48521.75
8. Elobuike, C.S., Idowu, M.A., Adeola, A.A., & Bakare, H.A. (2021). Nutritional and functional attributes of mungbean (*Vigna radiata* [L] Wilczek) flour as affected by sprouting time. *Legume Science*, *3*(4), e100. https://doi.org/10.1002/leg3.100
9. Fikry, M., Khalifa, I., Sami, R., Khojah, E., Ismail, K.A., & Dabbour, M. (2021). Optimization of the frying temperature and time for preparation of healthy falafel using air frying technology. *Foods*, *10*(11), 2567. https://doi.org/10.3390/foods10112567
10. Gan, R.-Y., Lui, W.-Y., Chan, C.-L., & Corke, H. (2017). Hot air drying induces browning and enhances phenolic content and antioxidant capacity in mung bean (*Vigna radiata* L.) sprouts. *Journal of Food Processing and Preservation*, *41*(1), e12846. https://doi.org/10.1111/jfpp.12846
11. Ghoshal, G., & Kaushal, K. (2020). Extraction, characterization, physicochemical and rheological properties of two different varieties of chickpea starch. *Legume Science*, *2*(1), e17. https://doi.org/10.1002/leg3.17
12. Goharpour, K., Salehi, F., & Daraei Garmakhany, A. (2024). Effects of different drying techniques of ground sprouted chickpeas on quality, textural properties, and sensory attributes of fried falafel. *Food Science & Nutrition*, *12*(9), 6328-6337. https://doi.org/10.1002/fsn3.4240
13. Hojjati, M., Mehrnia, M.A., Kakaaghazadeh, A., & Feghhi, S. (2020). Effects of edible hydrocolloids on quality characteristics of the fried falafels emphasize on decreases in oil uptakes. *Iranian Journal of Nutrition Sciences and Food Technology*, *14*(4), 77-88.
14. Javaheripour, N., Shahsoni Mojarad, L., Mahdikhani, S., & Inanloo, Y. (2022). The effect of adding quinoa flour and germinated wheat flour on the physicochemical ،microbial and sensory properties of sponge cake. *Journal of Food Science and Technology (Iran)*, *18*(119), 375-392. https://doi.org/10.52547/fsct.18.119.375
15. Karimi, A.S., & Saremnezhad, S. (2020). The effect of germination process on some functional properties of Iranian lentil cultivars. *Journal of Food Science and Technology (Iran)*, *17*(101), 167-176. https://doi.org/10.52547/fsct.17.101.167
16. Khodadadi, M., Masoumi, A., & Sadeghi, M. (2024). Drying, a practical technology for reduction of poultry litter (environmental) pollution: methods and their effects on important parameters. *Poultry Science*, *103*(12), 104277. https://doi.org/10.1016/j.psj.2024.104277
17. Khodadadi, M., Masoumi, A., Sadeghi, M., & Moheb, A. (2023). Optimization of drying specification and protein losses of poultry litter during drying process using response surface methodology. *Thermal Science and Engineering Progress*, *43*, 101958. https://doi.org/10.1016/j.tsep.2023.101958
18. Kim, S.M., Aung, T., & Kim, M.J. (2022). Optimization of germination conditions to enhance the antioxidant activity in chickpea (*Cicer arietimum* L.) using response surface methodology. *Korean Journal of Food Preservation*, *29*(4), 632-644.
19. Kumar, Y., Sharanagat, V.S., Singh, L., & Mani, S. (2020). Effect of germination and roasting on the proximate composition, total phenolics, and functional properties of black chickpea (*Cicer arietinum*). *Legume Science*, *2*(1), e20. https://doi.org/10.1002/leg3.20
20. Liu, Y., Xu, M., Wu, H., Jing, L., Gong, B., Gou, M., Zhao, K., & Li, W. (2018). The compositional, physicochemical and functional properties of germinated mung bean flour and its addition on quality of wheat flour noodle. *Journal of Food Science and Technology*, *55*(12), 5142-5152. https://doi.org/10.1007/s13197-018-3460-z
21. Meullenet, J.-F., Lyon, B.G., Carpenter, J.A., & Lyon, C.E. (1998). Relationship between sensory and instrumental texture profile attributes. *Journal of Sensory Studies*, *13*(1), 77-93. https://doi.org/10.1111/j.1745-459X.1998.tb00076.x

22. Nishinari, K., Fang, Y., & Rosenthal, A. (2019). Human oral processing and texture profile analysis parameters: Bridging the gap between the sensory evaluation and the instrumental measurements. *Journal of Texture Studies*, *50*(5), 369-380. https://doi.org/10.1111/jtxs.12404
23. Oghbaei, M., & Prakash, J. (2016). Effect of primary processing of cereals and legumes on its nutritional quality: A comprehensive review. *Cogent Food & Agriculture*, *2*(1), 1136015. https://doi.org/10.1080/23311932.2015.1136015
24. Ozturk, I., Sagdic, O., Tornuk, F., & Yetim, H. (2014). Effect of wheat sprout powder incorporation on lipid oxidation and physicochemical properties of beef patties. *International Journal of Food Science & Technology*, *49*(4), 1112-1121. https://doi.org/10.1111/ijfs.12407
25. Salehi, F. (2023). Effects of ultrasonic pretreatment and drying approaches on the drying kinetics and rehydration of sprouted mung beans. *Legume Science*, *5*(4), e211. https://doi.org/10.1002/leg3.211
26. Salehi, F., Amiri, M., & Ghazvineh, S. (2024). Effect of ultrasonic pretreatment on textural properties and sensory attributes of cooked faba beans. *Ultrasonics Sonochemistry*, *110*, 107040. https://doi.org/10.1016/j.ultsonch.2024.107040
27. Salehi, F., Ghazvineh, S., & Inanloodoghouz, M. (2023a). Effects of edible coatings and ultrasonic pretreatment on the phenolic content, antioxidant potential, drying rate, and rehydration ratio of sweet cherry. *Ultrasonics Sonochemistry*, *99*, 106565. https://doi.org/10.1016/j.ultsonch.2023.106565
28. Salehi, F., Razavi Kamran, H., & Goharpour, K. (2023b). Effects of ultrasound time, xanthan gum, and sucrose levels on the osmosis dehydration and appearance characteristics of grapefruit slices: process optimization using response surface methodology. *Ultrasonics Sonochemistry*, *98*, 106505. https://doi.org/10.1016/j.ultsonch.2023.106505
29. Serdaroglu, M. (2006). The characteristics of beef patties containing different levels of fat and oat flour. *International Journal of Food Science & Technology*, *41*(2), 147-153. https://doi.org/10.1111/j.1365-2621.2005.01041.x
30. Sofi, S.A., Rafiq, S., Singh, J., Mir, S.A., Sharma, S., Bakshi, P., McClements, D.J., Mousavi Khaneghah, A., & Dar, B.N. (2023). Impact of germination on structural, physicochemical, techno-functional, and digestion properties of desi chickpea (*Cicer arietinum* L.) flour. *Food Chemistry*, *405*, 135011. https://doi.org/10.1016/j.foodchem.2022.135011
31. Tian, B., Xie, B., Shi, J., Wu, J., Cai, Y., Xu, T., Xue, S., & Deng, Q. (2010). Physicochemical changes of oat seeds during germination. *Food Chemistry*, *119*(3), 1195-1200. https://doi.org/10.1016/j.foodchem.2009.08.035

نشریه پژوهشهای علوم و صنایع غذایی ایران
https://ifstrj.um.ac.ir

مقاله پژوهشی

جلد ۲۰، شماره ۶، بهمن-اسفند، ۱۴۰۳، ص. ۱۱۸-۱۰۵

تأثیر زمان جوانه‌زدن نخود بر ویژگی‌های فیزیکوشیمیایی، بافتی، حسی و فنل کل فلافل تهیه شده از آرد نخود جوانه‌زده

کیمیا گوهرپور[۱]- فخرالدین صالحی[۲*]- امیر دارایی گرمه‌خانی[۳]

تاریخ دریافت: ۱۴۰۳/۰۳/۲۸
تاریخ پذیرش: ۱۴۰۳/۰۹/۰۳

چکیده

فلافل یک محصول ارزان‌قیمت و مغذی است که حاوی مواد گیاهی مختلف، ویتامین، فیبرهای غذایی و ترکیبات فنلی است. هدف از این مطالعه بررسی تأثیر زمان جوانه زدن بر ویژگی‌های فیزیکوشیمیایی آرد نخود جوانه‌زده بود. همچنین اثرات زمان جوانه زدن بر ویژگی‌های فیزیکوشیمیایی و خصوصیات حسی فلافل تهیه شده از آرد نخود جوانه‌زده مورد بررسی قرار گرفت. یافته‌های این تحقیق نشان داد که فرآیند جوانه زدن به‌طور معنی‌داری مقدار فنل کل (از ۲۸۴/۱۷ به ۷۲۰/۹۸ میکروگرم اسید گالیک در گرم خشک)، ظرفیت آنتی‌اکسیدانی (از ۷۷/۵۵ در صد به ۹۳/۳۵ در صد) و قرمزی (از ۷/۶۵ به ۱۱/۳۹) آرد نخود را افزایش می‌دهد ($p<0.05$). در حالی‌که روشنایی (از ۷۰/۸۱ به ۵۷/۰۷) و زردی (از ۴۳/۷۱ به ۲۵/۶۲) آرد نخود به‌طور معنی‌داری کاهش یافت ($p<0.05$). محتوای فنل کل و ظرفیت آنتی‌اکسیدانی فلافل‌های تهیه شده از آرد نخود جوانه‌زده به مدت دو روز (۴۸ ساعت) به‌طور معنی‌داری بیشتر از فلافل تهیه شده از آرد نخود جوانه نزده بود ($p<0.05$). حجم نمونه‌های فلافل تهیه شده از آرد نخود جوانه نزده، جوانه‌زده به‌مدت یک روز و جوانه‌زده به‌مدت دو روز به‌ترتیب برابر ۱۸/۷۵، ۱۶/۶۰ و ۱۵/۴۰ سانتی‌متر مکعب بود. کمترین مقدار جذب روغن مربوط به نمونه تهیه شده از نخود جوانه‌زده به‌مدت دو روز بود ($p<0.05$). فرآیند جوانه زدن تأثیر معنی‌داری بر سفتی، انسجام و قابلیت جویدن فلافل‌ها نداشت ($p>0.05$). در مجموع، استفاده از آرد نخود جوانه‌زده به‌مدت یک روز (۲۴ ساعت) برای تولید فلافل به‌دلیل بهترین طعم، بیشترین امتیاز پذیرش کلی، محتوای بالای ترکیبات فنلی، ظرفیت آنتی‌اکسیدانی بالا و جذب کمتر روغن، توصیه می‌شود.

واژه‌های کلیدی: انسجام، جذب روغن، سفتی، ظرفیت آنتی‌اکسیدانی، فنل کل

۱ و ۲- به‌ترتیب دانشجوی کارشناسی ارشد و دانشیار، گروه علوم و صنایع غذایی، دانشکده صنایع غذایی، دانشگاه بوعلی سینا، همدان، ایران
(*- نویسنده مسئول: Email: F.Salehi@Basu.ac.ir)
۳- دانشیار، گروه مهندسی علوم و صنایع غذایی، دانشکده فنی و منابع طبیعی تویسرکان، دانشگاه بوعلی سینا، همدان، ایران
https://doi.org/10.22067/ifstrj.2024.88550.1339

Iranian Food Science and Technology Research Journal
Homepage: https://ifstrj.um.ac.ir

Research Article
Vol. 20, No. 6, Feb.-Mar., 2025, p. 119-136

Bioactive Components and Characterization of Extracted *Paeonia officinalis* using Ultrasonic and Microwave Assisted Maceration: Potential Evaluation as a Preservative in Panna Cotta

F. Fallahpour Sichani[1], H. Abbasi[2*]

1 and 2- M.Sc Graduate and Associate Professor, Department of Food Science and Technology, College Agriculture, Isfahan (Khorasgan) Branch, Islamic Azad University, Isfahan, Iran, respectively.
(*- Corresponding Author Email: H.Abbasi@khuisf.ac.ir)

Received: 22.07.2024
Revised: 02.10.2024
Accepted: 02.10.2024
Available Online: 07.01.2025

How to cite this article:
Fallahpour Sichani, F., & Abbasi, H. (2025). Bioactive components and characterization of extracted *Paeonia officinalis* using ultrasonic and microwave assisted maceration: Potential evaluation as a preservative in Panna cotta. *Iranian Food Science and Technology Research Journal*, *20*(6), 119-136. https://doi.org/10.22067/ifstrj.2024.89000.1350

Abstract

Preservatives are substances that can prevent or halt fermentation, acidification, and other processes that cause food to decompose. This study aims to extract the root of *Paeonia officinalis* with assistance of ultrasonic (40 kHz, 40 °C for 45 min) and microwave (400 watts, 40 °C, 5 min) maceration techniques, and evaluate the extraction yield, chemical compounds, antioxidant, and antimicrobial properties of the extracts. In the next phase, the best extract is incorporated at 2%, 4%, and 6% into the formulation of Panna cotta dessert to assess its effects on the physical, chemical, sensory, and microbial aspects of the product during storage. The findings reveal that the ultrasonic-assisted method improved the extraction efficiency of the extract. The extract had the highest levels of phenolic compounds (52.64±1.18 mg of gallic acid/g), antioxidant properties (76.33±0.47%), and antimicrobial activity against *Escherichia coli*, *Staphylococcus aureus*, and *Candida albicans*. The addition of the extract to Panna cotta reduces the rate of acid production and results in lower total populations of bacteria compared to the control sample at the end of storage period. The dessert containing 2% extract exhibited sensory characteristics (taste, color, odor, texture, and overall acceptance) similar to the control, while maintaining microbiological quality for a longer period. The ethanolic extract of *Paeonia officinalis* root obtained through the ultrasonic-assisted method can be introduced as an effective preservative for dairy desserts.

Keywords: Microwave, *Paeonia officinalis*, Preservatives, Rheological behavior, Ultrasonication

https://doi.org/10.22067/ifstrj.2024.89000.1350

Introduction

Preservatives play a crucial role in inhibiting or halting fermentation, acidification, and other processes that lead to food decomposition. The primary objective of using preservatives is to prevent the growth of microorganisms responsible for food spoilage and contamination, thereby extending the shelf life of products while maintaining their nutritional value, appearance, and organoleptic qualities (Silva & Lidon, 2016; Mirza *et al.*, 2017). However, concerns have emerged regarding the potential adverse effects of synthetic preservatives on human health, including allergies, cancer, attention-deficit/hyperactivity disorder (ADHD), brain damage, nausea, and heart disease (Gupta & Yadav, 2021). Consequently, both consumers and food producers have shown an increased interest in utilizing natural and organic additives as a safer alternative.

Paeonia officinalis is a flowering plant belonging to the Paeoniaceae family. The root of this plant contains proteins, alkaloids, tannins, saponins, glycosides, carbohydrates, flavonoids, and steroids. These compounds possess antioxidant and antimicrobial properties (Dulgheru & Burzo, 2010; Park *et al.*, 2021). The extract derived from the root of *Paeonia officinalis* inhibits the acetylcholinesterase enzyme and shows effectiveness in treating Alzheimer, migraine, and neuralgia (Adhami *et al.*, 2011). Based on studies of its sensory qualities, nutrients, and antioxidant activity, it could be used as a food additive (Dienaitė *et al.*, 2019).

The quality and quantity of herbal extracts are significantly influenced by the extraction process (Qamar *et al.*, 2021; Saboora *et al.*, 2014). Ultrasonic-assisted extraction, known for its simplicity and effectiveness, is particularly advantageous. By breaking down the cell wall, this method enhances the release of extracts. However, several factors such as moisture content, particle size, and type of solvent play an important role (Ghafoor *et al.*, 2009; Alupului *et al.*, 2009). In terms of antioxidant activity and enzyme inhibition of edible mushrooms, ultrasonic treatment has been shown to yield extracts rich in ergosterol when the appropriate extraction method is employed (Milovanovic *et al.*, 2021). Microwaves, as a heating method, have also gained widespread acceptance in the food industry, including for extraction processes, due to their cost-effectiveness and efficiency. Microwave treatment facilitates the extraction process by providing rapid, efficient heating that enhances solvent penetration, improves the yield of bioactive compounds, and reduces energy consumption. This makes it a highly advantageous method for industrial extraction processes (Lu *et al.*, 2017).

Due to their nutrient content, dairy products create favorable conditions for microorganisms to grow. To maintain their quality and enhance consumer satisfaction, researchers are exploring natural preservatives as an alternative to synthetic additives. Herbal preservatives such as pomegranate peel, *Melissa officinalis*, and *Valeriana officinalis* extracts have been tested as a natural preservatives in dairy products (Mahajan *et al.*, 2015; Sanjay *et al.*, 2020).

Panna Cotta, a dairy-based dessert, is particularly susceptible to spoilage due to its high moisture content, nutrient density, and neutral pH. These characteristics create a favorable environment for the growth of spoilage microorganisms. As a result, Panna Cotta is prone to rapid deterioration, leading to changes in texture, flavor, and safety. Additionally, the dessert can undergo acidification during storage, which may negatively impact its sensory qualities and shorten its shelf life. To mitigate these issues, traditional preservatives are often employed to inhibit microbial growth and prevent spoilage. However, there is increasing public concern over the use of synthetic preservatives, which have been associated with various health risks, including allergies, cancer, and ADHD. This has spurred interest in natural and organic alternatives that can effectively preserve food products while being perceived as safer and healthier options. The incorporation of natural

preservatives with antimicrobial and antioxidant properties into dairy desserts like Panna Cotta has gained significant attention. Plant-based extracts, such as those derived from *Paeonia officinalis*, offer a promising solution. These extracts contain bioactive compounds, including phenolics and flavonoids, that can inhibit the growth of spoilage microorganisms and delay oxidation processes, thereby extending the shelf life of the product without compromising its sensory attributes.

This study examined the compounds, including their antioxidant and antimicrobial properties, in *Paeonia officinalis* extract using ultrasonic- and microwave-assisted maceration techniques. In the second phase, based on the phenolic compound, antioxidant and antimicrobial activity results, the best extract was used as a preservative at various levels in the Panna cotta formulation, and the physical, chemical, sensory, and microbiological properties of the product were evaluated during storage.

Materials and Methods

Materials

The root of *Paeonia officinalis* was purchased from Isfahan medicinal plant market in Iran. Chemical compounds, such as ethanol, Folin-Ciocalteu's phenol reagent, 2,2-diphenyl-1-picrylhydrazyl (DPPH), sodium carbonate, gallic acid, methanol, phenolphthalein, and sodium hydroxide were purchased from Merck in Germany. *Staphylococcus aureus* (ATCC 25923), *Escherichia coli* (ATCC 25922), *Candida albicans* (J 905), and *Aspergillus niger* were obtained from Zistyakhte Company in Iran. The raw materials required to prepare Panna cotta, including milk, sugar, vanilla, gelatin, and cream, were purchased from local markets.

Extraction of Paeonia officinalis

The extraction process was carried out using the maceration method with 70% ethanol. For this purpose, 150 grams of dried *Paeonia officinalis* root were added to 600 mL of 70% ethanol and stirred at 25 °C for 2 h. The mixture was then filtered, and the extract was separated from the solvent using a rotary evaporator (40 °C, 80 rpm, 2 h) to Brix 50 (Ferioli *et al.*, 2020). The extracts were then stored in the dark at 4 °C. To evaluate the influence of ultrasonic and microwave treatments on the quantity and quality of the extracts, the solvent-sample mixture was subjected to 400 watts of microwave irradiation (LG, MH 8265), at 40 °C for 5 min with 30 s rest interval before separating the solvent. Ultrasonic waves were applied to the solvent-sample mixture in an ultrasound bath (WISD, 40kHz, South Korea) at 40 °C for 45 min with a power of 200 watts (Hoehn *et al.*, 2003). The extraction efficiency at Brix 50 was evaluated using the weight method (Hoehn *et al.*, 2003).

Characteristics of Extracts

pH of the extracts was evaluated using the pH meter (Ltd, Shanghai, Sanxin, China) and their density was determined using a digital densitometer.

Separation and identification of the extract's phytochemical compounds were performed using gas chromatography (Agilent 6890) connected to a mass spectrometer (HP 5973). The column of the device (Supelco SLB-5MS) had a length of 30 metres and an internal diameter of 0.25 mm. The sample was dissolved in methanol, and 0.6 microliters of the sample was injected into the column. The injection temperature was set to 280ºC in split mode. The column temperature started at 60 °C and then increased by 7 °C min^{-1}, maintaining it at 270 °C for 45 min. Helium was used as the carrier gas at a flow rate of 1 mL min^{-1}. (Mothana *et al.*, 2013)

To determine the antioxidant activity of the extract, 0.1 mL of the sample was mixed with 3.9 mL of DPPH and incubated in the dark for 30 min. The absorbance of the samples and the control (without extract) was measured using a spectrophotometer (Shimadzu, UV-1800/2600, Japan) at a wavelength of 517 nm. The percentage of DPPH inhibition was calculated using Eq. 1:

$$Percentage\ of\ inhibition\ (\%): \left(Contrc - \left(\frac{Sample\ OD}{Control\ OD} \right) \right) \times 100 \quad (1)$$

Where 'Sample OD' is the absorbance of the sample, and 'Control OD' is the absorbance of the control.

Total phenolic compounds in the extract were analyzed using the colorimetric method with Folin-Ciocalteu reagent. To perform this analysis, 0.1 mL of the extract was mixed with 2.5 mL of Folin-Ciocalteu reagent (diluted with water at a ratio of 10:1) and allowed to stand in the dark for 10 min. Next, 2 mL of sodium carbonate (7.5%) was added to the mixture, and after 45 min in the dark, the absorbance of the sample was measured using a spectrophotometer at a wavelength of 765 nm. The total phenolic content of the sample was then calculated in mg kg^{-1} using a standard solution of Gallic acid (Mothana *et al.*, 2013).

Antibacterial and Antifungal Activity of Extracts

The antibacterial and antifungal effects of the extracts were determined using the well plate method. For *Escherichia coli* (ATCC 25922) and *Staphylococcus aureus* (ATCC 25923), Mueller Hinton agar was utilized as the appropriate culture medium, while Potato Dextrose Agar (PDA) was used as the culture medium for *Aspergillus niger* (ATCC 9029) and *Candida albicans* (J 905). To prepare the microbial suspension, the strains were activated in nutrient broth, cultured on Tryptic soy agar, and incubated at 37 °C for 24 h. *Aspergillus niger* and *Candida albicans* were added to Potato dextrose broth, cultured linearly on PDA, and incubated at 30 °C for 24 h. A suspension of pure colonies of bacteria and fungi with a turbidity equivalent to 0.5 McFarland standard was prepared, and its absorbance was measured at a wavelength of 600 nm using a UV-Vis spectrophotometer. At an absorbance of 0.08-0.1, the concentration of bacteria and fungi was 1.5 x 10^8. To assess the antimicrobial activity of the extract, a standard microbial suspension was cultured on Mueller Hinton Agar for bacteria and PDA for fungi. The extract, sterilized using a 0.45 µm filter, and inoculated into designated holes in the cultures at concentrations of 10, 30, 50, 70, and 100%. Negative controls consisted of Mueller Hinton Broth (MHB) without the extract, while Tetracycline served as the positive control. The bacterial culture was incubated at 37 °C for 24 h and the fungus culture was kept at 30 °C for 3 to 5 days. The antibacterial activity was evaluated by measuring the diameter of the no-growth zone (mm) for microorganisms (Yeasmin *et al.*, 2016). The Minimum Inhibitory Concentration (MIC) and Minimum Bactericidal/Fungicidal Concentration (MBC/MFC) of the extracts were determined using the tube dilution method. Pure extract (1 mL) was added to the first tube containing 1 mL of MHB and mixed by tube vortex (Behdad, Iran). Dilutions were continued in subsequent tubes to create different concentrations of the extract. Then, 10 microliters of the microbial suspension were added to each tube. The positive control contained culture media with bacteria or fungi, but no extract, while the negative control consisted of culture media without bacteria, fungi, or extract. The culture tubes were incubated for 24 h at 37 °C to allow bacterial growth. To ensure accurate assessment of turbidity in the tubes, which may be affected by the colored solution, all inoculated tubes were also cultured on Mueller Hinton agar. Specifically, 10 µL of the suspension from each tube was transferred to Mueller Hinton agar plates and incubated (Sato *et al.*, 2018). To determine the MIC and MFC of fungi, PDB and PDA were used. The cultured tubes and plates were incubated for 48 h at 30 °C and then examined (Sato *et al.*, 2018).

Preparation of Panna Cotta

To prepare the dessert, a mixture of 500 grams of pasteurized milk, 55 grams of whipped cream, 25 grams of sugar, 1 gram of

vanilla, and 14 grams of gelatin was prepared. The mixture was then heated to 37 °C for 5 min. The mixure was cooled to the room temperature, and various concentrations of *Paeonia officinalis* extract (2%, 4%, and 6% w/w) were added to evaluate their impact on the sensory, microbiological, and chemical properties of the product. The samples were stored at 4 °C in polyethylene containers for 21 days.

Characteristics of the Product during the Storage Period

Acidity and pH of Samples

pH of the samples was measured at different time points (1, 7, 14, and 21 days) during the storage of the product at 4 °C using a digital pH meter (Elmentron pH-meter CP-501, Netherlands).

To determine the acid content in the sample, 9 grams of the dessert were titrated in distilled water with 0.1 N Sodium hydroxide. The acid content was reported as mg of citric acid per 100 g of the sample (AOAC 942.15).

Micribiological Properties

To assess the microbiological properties of the samples, a bacterial culture test was conducted using PCA. After 24 h of incubation at 35 °C, colony-forming units (CFUs) were counted. The proliferation and enumeration of yeasts and molds were carried out using Dichloran Rose-Bengal Chloramphenicol agar. Colony counting was performed after 72 h of incubation at 35 °C. Surface culture and incubation at 37 °C for 24 h was performed for *Staphylococcus aureus* on Mannitol Salt Agar, *Escherichia coli* on Eosin Methylene Blue Lactose Sucrose Agar, and Salmonella species on Salmonella Shigella Agar. (Chauhan *et al.*, 2020; Nottagh *et al.*, 2020).

Texture Analysis

Texture of the samples was evaluated using a back extrusion test. A texture analyzer (Santam/stm 20, Iran) equipped with a cylindrical probe of 29-mm diameter at a speed of 60 mm/s was utilized. The samples were placed in containers with a diameter of 36 mm, and their texture was assessed through a reciprocating pressure cycle at 4 °C (VanWees *et al.*, 2020).

The rheological evaluation of the samples was conducted using a Rheometer (Anton Paar Physica MCR 301, Austria). The apparent viscosity was measured across a range of 0.01-100 shear rates at 4 °C (Rezvani *et al.*, 2020). To assess the flow behavior of the samples, the values of shear stress versus shear rate were fitted using the power law equation (Eq. 2) in the Cure Expert 1.4 environment. The coefficient of determination (R^2) was determined to evaluate the fitness of models (Adeli & Samavati, 2015).

$$\delta = K(\gamma)^{n_p} \quad (2)$$

Where δ is the shear stress (Pa), γ is the shear rate (S-1), K is the consistency coefficient (Pa.sn) and n represents the flow behavior index (dimensionless).

The viscoelastic properties of the product were assessed using Cone & Plate geometry in an oscillation test. The strain sweep test was conducted at a constant frequency to evaluate the linear viscoelasticity. Furthermore, in the frequency sweep, the rheological parameters of the product were examined across a frequency range of 0.1 to 50 Hz (Rezvani *et al.*, 2020).

Sensory Analysis

A sensory evaluation was conducted 24 h after production, involving 20 panelists who participated in a 5-point hedonic scale testing. The samples were assessed and compared based on taste, color, texture, odor, and overall acceptance. The highest and lowest scores were assigned to the excellent and poor samples, respectively, for each attribute (Clark, 2009).

Statistical Analysis

Experiments were performen in triplicate and the results for the comparison of extracts from different methods were analyzed using a completely randomized design. In the second part of the research, the

qualitative characteristics of the samples were evaluated and compared using a completely randomized design-factorial test. Mean comparisons were performed using the minimum significant difference (LSD) at the 5% significance level.

Results and Discussion

The Extraction Efficiency and Compounds of the Extract

The extraction efficiency was assessed based on the weight of the extracts at Brix 50. The maceration method yielded an extraction efficiency of 14.7%, while maceration with assistance of microwave and ultrasonic achieved extraction efficiencies of 15.7% and 19%, respectively. A significantly higher extraction efficiency ($p<0.05$) was observed with ultrasonic-assisted extraction compared to the other methods. This can be attributed to the ability of ultrasonic waves with frequencies higher than 20 kHz to induce oscillations within the plant material and mechanically disrupt the cell walls, facilitating solvent access and the release of active components (Chemat *et al.*, 2017). Microwave-assisted extraction utilizes electric and magnetic fields generated by electromagnetic microwaves, which generate heat through bipolar rotation and ion conduction (Shirsath, 2012; Bagade & Patil, 2021). The heated solvent in the presence of microwave energy disrupts the matrix, leading to enhanced mass transfer. This explains the higher extraction efficiency observed in microwave-assisted extraction compared to the traditional maceration method (Shirsath, 2012; Bagade & Patil, 2021).

Table 1 presents the compounds identified in *Paeonia officinalis* extracts, including monoterpenes (trans-Linalool oxide, alpha-Terpinene), sesquiterpenes (Caryophyllene oxide, Humulene, alpha-Guaiene), and benzopyrans (Heneicosane, Encecalan, Benzaldehyde). The sesquiterpenes and benzopyrans were the predominant compounds in the *Paeonia officinalis* extract. Maceration yielded six identified compounds, with benzoic acid (19.04%), Heneicosane (15.81%), Humulene (6.93%), Benzaldehyde (3.99%), alpha-Terpinene (3.29%), and 1,3-dimethyl-benzene (1.29%) being the major components. In the microwave-assisted extract, five compounds were identified, with benzoic acid (14.44%), Benzaldehyde (5.74%), Humulene (4.49%), Heneicosane (3.30%), and Encecalan (2.64%) being the quantitatively significant ones. The ultrasonic-assisted extract contained seven identified compounds, with Caryophyllene oxide (35%), Benzoic acid (21.14%), Humulene (8.42%), Benzaldehyde (5.80%), alpha-Guaiene (4.22%), Encecalan (2.53%), and trans-Linalool oxide (1.95%) being the prominent. Notably, the ultrasonic-assisted extract showed higher concentrations of Benzoic acid, Benzaldehyde, and Humulene compared to other methods. Furthermore, the ultrasonic-assisted extract contained special compounds such as caryophyllene oxide, alpha-Guanine, and trans-linalool oxide, known for their antioxidant properties. The application of ultrasound in the solid-liquid phase creates a cycle of contraction and expansion, leading to the formation and collapse of bubbles (cavitation). This phenomenon induces oscillation of solid and liquid particles, enhancing the diffusion of soluble material from the solid phase to the solvent (Blanco-Llamero *et al.*, 2022). The increased extraction efficiency of the active compounds can be attributed to emulsification and tissue damage caused by ultrasound. Therefore, the ultrasonic-assisted extraction method exhibited significantly higher extraction efficiency for specific components of *Paeonia officinalis*, particularly Benzaldehyde, Benzoic acid, alpha-Guanine, Caryophyllene oxide, trans-linalool oxide, and Humulene, known for their antioxidant and antimicrobial activity.

Table 1- Components of aqueous-alcoholic *Paeonia officinalis* extracts

Compounds	Molecular Formula	*Retention Time* (min)	*Kovats Index*	Extraction method		
				Maceration	Microwave-assisted	Ultrasonic-assisted
2-hexenal	$C_6H_{10}O$	3.84	850	6.95%	-	2.50%
1,3-dimethyl-benzene	C_8H_{10}	4.576	897	1.29%	-	-
Benzaldehyde	C_6H_5CHO	5.741	960	3.99%	5.74%	5.80%
α-terpinene	$C_{10}H_{16}$	7.602	1021	3.29%	-	-
trans-Linalool oxide	$C_{10}H_{18}O_2$	7.181	1071	-	-	1.95%
Benzoicacid	$C_7H_6O_2$	9.023	1164	19.04%	14.44%	21.14%
α-guaiene	$C_{15}H_{24}$	10.984	1260	-	-	4.22%
2-butyl-2-octenal	$C_{12}H_{22}O$	12.043	1287	3.85%	-	-
Humulene	$C_{15}H_{24}$	13.802	1350	6.93%	4.49%	8.42%
caryophyllene oxide	$C_{15}H_{24}O$	14.55	1475	-	-	35%
Heptadecane	$C_{17}H_{36}$	15.99	1566	28.1%	33.16%	5.28%
Phytone	$C_{24}H_{48}O_7$	17.36	1609	-	4.05%	1.47%
Heneicosane	$C_{21}H_{44}$	19.56	1741	15.81%	3.30%	-
Encecalan	$C_{14}H_{16}O_3$	23.56	2056	-	2.64%	2.53%

Characteristics of the Aqueous-alcoholic Extract of *Paeonia officinalis*

Table 2 presents the quality characteristics of the aqueous-alcohol extracts of *Paeonia officinalis*. The extraction method had a significant impact on the pH of the extracts. The ultrasonic-assisted method produced extracts with significantly higher pH values compared to other methods ($p<0.05$). Additionally, the maceration method yielded extracts with significantly higher pH values than the microwave-assisted method ($p<0.05$). This variation in pH can be attributed to the differential solubility of *Paeonia officinalis* components, including phenols, flavonoids, anthocyanins, tannins, organic acids, carbohydrates, sugars, and other compounds, under different extraction conditions (Batinić *et al.*, 2022). The composition of compounds such as carbohydrates and proteins also contribute to changes in the pH of the extract (Ebringerová & Hromádková, 2010). The density of the extracts obtained through the ultrasonic-assisted method was significantly higher ($p<0.05$) compared to those produced through maceration. However, no significant difference in density was observed between the extracts obtained through ultrasonic and microwave-assisted extraction ($p<0.05$). As a result, the maceration extracts exhibited the lowest density, whereas the ultrasonic-assisted extracts had the highest density, as shown in Table 2. The variation in extract density can be attributed to the impact of extraction conditions on the extraction of different quantities and qualities of *Paeonia officinalis* compounds, such as phenols, flavonoids, anthocyanins, tannins, carbohydrates, sugars, and others (Batinić *et al.*, 2022).

The phenolic content and antioxidant activity in the extract obtained through ultrasound-assisted extraction was significantly higher ($p<0.05$) compared to the extract obtained through maceration. However, there was no significant difference between the ultrasound and microwave-assisted methods in this regard ($p<0.05$). Notably, the extract obtained through maceration exhibited the lowest total phenolic content as shown in Table2.

The superior extraction efficiency of phenolic components and antioxidant activity can be attributed to the shear forces and high energy produced by ultrasonic waves, which effectively disintegrate cell walls, enhance

mass transfer, and facilitate the release of their contents. Additionally, ultrasonic extraction reduces particle size, promoting better contact and diffusion of the solvent into the tissue (Kumar *et al.*, 2021). On the other hand, in microwave-assisted extraction, the energy from electromagnetic waves is converted to heat, leading to the evaporation of water and an increase in pressure within the cells. This process causes cell disintegration and facilitates the release of active compounds into the solvent, thereby enhancing the extraction yield of active compounds such as polyphenols (Kumar *et al.*, 2011). In a study carried out on comparing microwave-assisted extraction with traditional method for extraction of phenolic compounds from walnut leaves, it was found that microwave-assisted extraction demonstrated higher efficiency and required less time compared to the traditional method (Salimi & Majd, 2012).

Table 2- Physicochemical properties of *Paeonia officinalis* extract

Extraction method	Extraction efficiency (%)	pH	Density ($g.cm^{-3}$)	Phenolic compounds (mg of Gallic acid/g)	Antioxidant activity (%)
Maceration	14.73±0.33 ^{c}	4.28±0.01 ^{b}	1.07±0.07 ^{b}	46.60±0.87 ^{b}	42.06±1.34 ^{b}
Ultrasonic-assisted extraction	18.97±0.34 a	4.31±0.01 ^{a}	1.22±0.03 ^{a}	52.64±1.18 ^{a}	76.33±0.47 ^{a}
Microwave-assisted extraction	15.69±0.34 ^{b}	4.22±0.01 ^{c}	1.11±0.01 ^{ab}	49.73±1.03 ^{ab}	46.66±3.14 ^{b}
LSD	0.67	0.02	0.14	3.29	6.33

*In each column, means with different letters are significantly different at the 5 percent level of the LSD test.

Antimicrobial Properties of *Paeonia officinalis* Extract

Table 3 presents the impact of *Paeonia officinalis* extracts derived through different methods and their concentrations on microorganisms activity. The diameter of the zone of inhibition of *Escherichia coli* and *Staphylococcus aureus* by ultrasonic-assisted extract was significantly larger than the other extracts ($p<0.05$). The microwave-assisted extract exhibited greater antimicrobial properties compared to the maceration extract. However, in some concentrations, there was no significant difference in the antimicrobial activity between the maceration and microwave-assisted extracts ($p<0.05$). In the case of microwave-assisted extraction, the rapid rise in temperature and internal pressure accelerated the breakdown of cell walls and facilitated the release of antimicrobial compounds from tissue into the solvent (Swaathy *et al.*, 2014). At most concentrations, there were no significant variations among the *Paeonia officinalis* extracts produced using different methods in terms of their efficacy at inhibiting the growth of *Candida albicans* ($p<0.05$).

Table 4 displays the impact of different extraction methods on the minimum inhibitory concentration (MIC) and minimum lethal concentration (MLC) of *Paeonia officinalis* extract against microorganisms. The antibacterial activity of the maceration and ultrasonic-assisted extracts was greater than that of the microwave-assisted extract against *Escherichia coli*. The ultrasonic-assisted extract exhibited the lowest MIC and MLC values against *Candida albicans* and *Aspergillus niger* ($p<0.05$), while all extracts showed similar inhibitory and lethal effects on *Staphylococcus aureus* ($p<0.05$).

Table 3- Non-growth halo diameter of microorganisms near the different concentrations of *Paeonia officinalis* extracts

	Method	Concentration				
		10%	30%	50%	70%	100%
Escherichia coli	Maceration	13.50±2.12 a	19.00±1.41 a	15.50±0.71 b	19.00±2.83 a	24.00±1.41 b
	Ultrasonic-assisted	16.00±1.41 a	20.00±1.40 a	25.00±2.83 a	26.00±1.41 a	29.00±1.41 a
	Microwave-assisted	10.00±0.14 b	12.00±1.41 b	14.50±0.70 b	17.50±3.53 a	22.00±1.40 b
Staphylococcus aureus	Maceration	23.50±2.12 a	33.50±2.12 a	36.00±1.41 a	38.50±0.71 a	42.00±1.41 a
	Ultrasonic-assisted	25.00±1.41 a	30.00±2.83 a	37.50±3.54 a	32.50±3.54 a	42.00±2.83 a
	Microwave-assisted	20.00±1.41 a	16.50±2.11 b	20.00±1.41 b	20.00±1.41 b	24.00±1.41 b
Candida albicans	Maceration	10.00±0.71 a	14.00±1.41 a	21.50±2.12 a	21.50±0.71 a	28.50±2.12 a
	Ultrasonic-assisted	10.50±0.71 a	14.00±1.41 a	19.50±0.71 a	20.00±0.41 a	28.50±2.12 a
	Microwave-assisted	11.50±2.41 a	15.50±2.12 a	18.00±2.83 a	16.00±1.40 b	28.00±2.83 a

*In each column, means with different letters are significantly different at the five percent level of the LSD test.

Table 4- Effect of the *Paeonia officinalis* extract on the MIC and the MLC of microorganisms (µL/mL)

Extraction Method	*Escherichia coli*		*Staphylococcus aureus*		*Candida albicans*		*Aspergillus niger*	
	MLC	MIC	MLC	MIC	MLC	MIC	MLC	MIC
Maceration	12.50 b	10.00 b	25.00 a	12.50 a	25.00 a	12.50 a	50.00 a	30.00 a
Ultrasonic-assisted	12.50 b	10.00 b	25.00 a	12.50 a	12.50 b	6.25 b	25.00 b	20.00 b
Microwave-assisted	25.00 a	12.50 a	25.00 a	12.50 a	25.00 a	12.50 a	50.00 a	25.00 ab
LSD	2.91	1.84	2.95	1.60	3.95	1.67	5.95	6.36

*In each column, means with different letters are significantly different at the five percent level of the LSD test. Mean ± standard deviation

Consequently, we observed a higher level of antimicrobial activity in the ultrasonic-assisted extract compared to others. In this regard, it has been reported that the utilization of ultrasonic technology, through its ability to disrupt cell membranes and improve mass transfer, led to an increased extraction rate of compounds such as Benzoic acid and Benzaldehyde with antimicrobial and antioxidant properties from the roots of *Paeonia officinalis* (Lu *et al.*, 2017).

Characteristics of Panna Cotta during the Storage Period

pH is a critical factor that significantly impacts the quality of dairy desserts. As per the Iranian standard (IDS 1143), the acceptable pH range for dairy desserts is ranged between 3.6 and 6.8. In this study, the pH values of the control and other treatments fell within this standard range. The presence of different concentrations of aqueous-alcoholic extract from *Paeonia officinalis* root exerted a noticeable influence on the pH changes of Panna cotta during a 21-day storage period. The samples with extract exhibited lower pH values compared to the control. This increased acidity in the extract-containing samples during the initial storage period can be attributed to the presence of carboxyl groups in triterpenoids and organic acids, as well as the acidic nature of the compounds found in the root extract of *Paeonia officinalis*, including phenolic compounds (Stagos, 2019).

Over the course of 21-day storage period, the pH of the samples experienced a significant decrease ($p<0.05$) (Fig. 1-a). It can be attributed to microbial activity, which leads to the

production of acids (Barbieri *et al.*, 2019), as well as the breakdown of ester groups and their conversion into acids. The proliferation of acid-resistant non-pathogenic bacteria also contributes to pH fluctuations in the product (Stagos, 2019). However, the incorporation of the aqueous-alcoholic extract of *Paeonia officinalis* effectively mitigated the rate of pH reduction during storage, likely due to the extract's ability to inhibit microbial activity (Barbieri *et al.*, 2019). Consequently, the addition of the aqueous-alcoholic extract of *Paeonia officinalis* prevented excessive pH decline in Panna cotta during storage, resulting in higher pH values compared to the control after 7 days of storage. In a similar vein, the molded yogurt demonstrated an increase in acidity during storage, although the sample containing the highest concentration of spinach extract exhibited the lowest acid content (Ahmad *et al.*, 2022). In the other study, the acidity of ketchup was unaffected by different concentrations (0.2%, 0.5%, and 0.8%) of aqueous and ethanolic extract of black Hollyhocks during storage (Yourdkhani & Jafarpour, 2021).

There were no significant changes in the firmness of the samples produced with different concentrations of the extract and the control up to 7 days of storage ($p<0.05$), and there were no significant differences observed in samples at 14 days. However, on the 21st day of storage, a significant increase in sample stiffness was observed ($p<0.05$). The samples containing 2% and 4% of the extract exhibited a lower increase in stiffness compared to the others, resembling the control samples more closely at the beginning of production (Fig. 1-b). This increase in sample stiffness can be attributed to the phenomenon of water transfer from the gel structure of the product during the storage period, resulting in a denser texture (Djaoud *et al.*, 2020). Additionally, the interaction between the compounds in the extract, particularly the phenolic components, with proteins or polysaccharides is another factor contributing to the increased sample stiffness (Jridi *et al.*, 2015).

The total bacterial count in the samples with different concentrations of the extract and the control remained unchanged over 14 days ($p<0.05$). However, on the 21st day of storage, there was a significant decrease in the total bacterial of the samples with different extract concentrations compared to the control ($p<0.05$). This indicates that the extract is effective in reducing the overall bacterial count and maintaining the microbial quality of Panna cotta during extended storage periods ($p<0.05$). Higher concentrations of the extract (4% and 6%) were effective in reducing the bacterial population and preserving the microbial quality of the Panna cotta (Fig. 1-c). *Staphylococcus aureus*, *Escherichia coli*, and Salmonella were not observed in the samples. The presence of antimicrobial compounds in the alcoholic extract of *Paeonia officinalis*, such as Benzoic acid and Benzaldehyde, inhibits the growth of microorganisms, slows down their population growth, and ultimately prevents product spoilage. The interaction between polyphenols and proteins alters the biological activity of microorganisms and inhibits their growth and activity. Therefore, the polyphenol content in the extract limits the growth and activity of bacteria (Walter, 2021).

Rheological Properties of Panna Cotta

Fig. 2 illustrates the flow behavior of Panna cotta at the beginning (day 1) and end (day 21) of the storage period. The samples exhibited shear-thinning behavior, as indicated by a decrease in apparent viscosity with increasing shear rate. There were no significant differences in the flow behavior and consistency coefficients of the samples containing the extract and the control based on the Power-law model. However, the apparent viscosity of samples increased at the end of the storage period (day 21) compared to the initial viscosity, and the samples with higher extract concentrations had a significantly lower flow behavior index (Table 5). The increase in viscosity during storage is attributed to the reorganization of proteins and their hydration (Rezvani *et al.*, 2020).

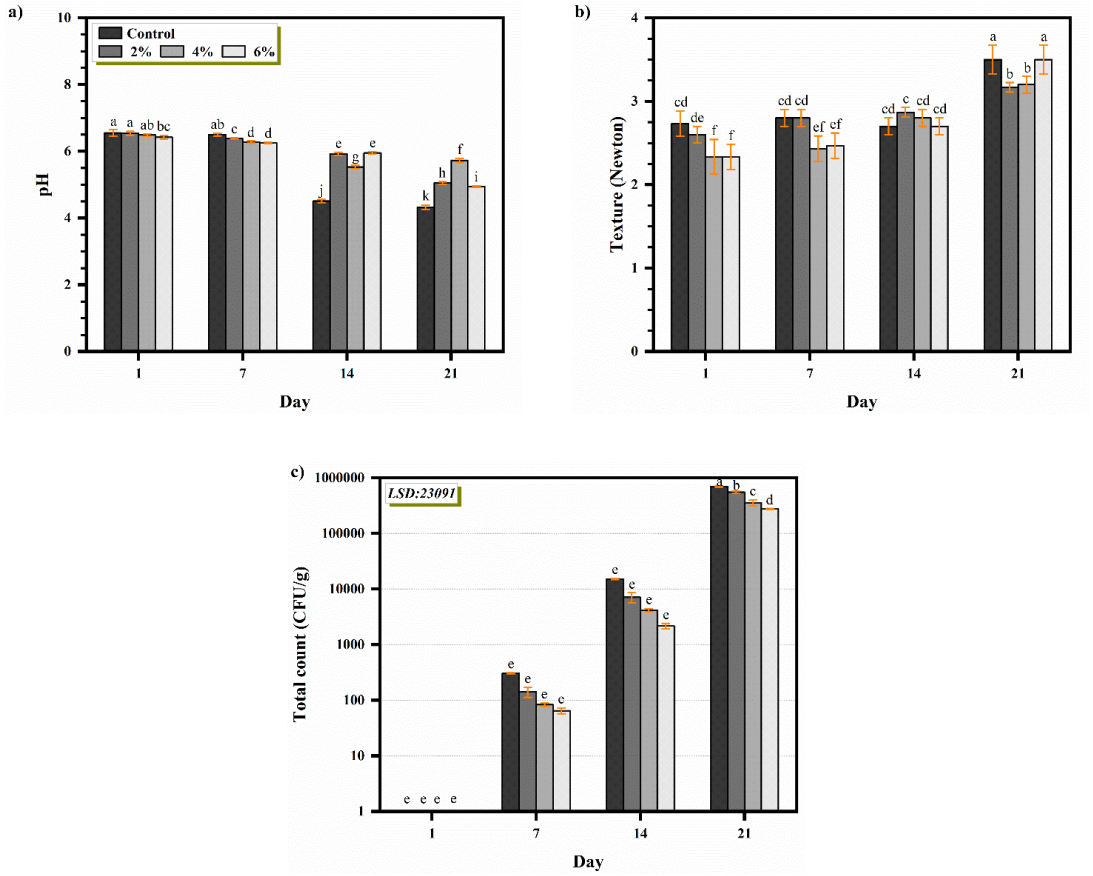

Fig. 1. Effect of different concentrations of aqueous-alcoholic extract of *Paeonia officinalis* and storage time on the quality of Panna cotta (each color is indicated in Fig. 1a).

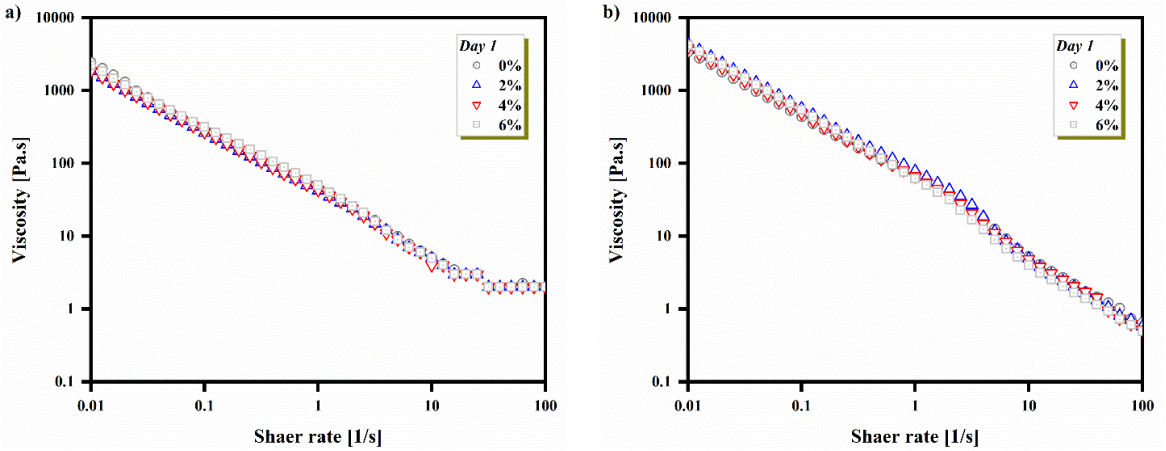

Fig. 2. Apparent viscosity of Panna cotta at (a) the beginning and (b) the end of the storage period

Table 5- Rheological parameters of the power law model in different samples

Storage period (Day)	Extract (%)	Rotation test	
		Consistency coefficient (K)	Flow behavior index (n)
1	0	40.205±3.344 ^{c}	0.265±0.021 ^{a}
	2	37.3±0.862 ^{c}	0.24±0.00 ^{ab}
	4	41.585±4.504 ^{c}	0.21±0.028 ^{bc}
	6	46.545±1.251 ^{c}	0.15±0.0141 ^{d}
21	0	64.225±6.795 ^{b}	0.165±0.021 ^{cd}
	2	81.31±4.751 ^{a}	0.13±0.00 ^{d}
	4	64.91±4.907 ^{b}	0.14±0.028 ^{d}
	6	62.745±1.661 ^{b}	0.081±0.024 ^{e}
LSD		9.27	0.047

*In each column, means with different letters are significantly different at the five percent level of the LSD test. Mean ± standard deviation

In the frequency sweep, the storage modulus (G') was higher than the viscous modulus (G"), indicating that the samples exhibited solid viscoelastic behavior. The slight changes in G' and G" with increasing frequency suggest the presence of a semi-gel-like structure in the samples. At the beginning of the storage period (day 1), the rheological properties of samples with different extract concentrations were similar. However, at the end of the storage period (day 21), the dessert containing 2% extract exhibited the highest elastic modulus (G'). On the other hand, the sample with 6% extract showed the highest damping factor (tan delta), indicating its weaker elastic behavior (Fig. 3).

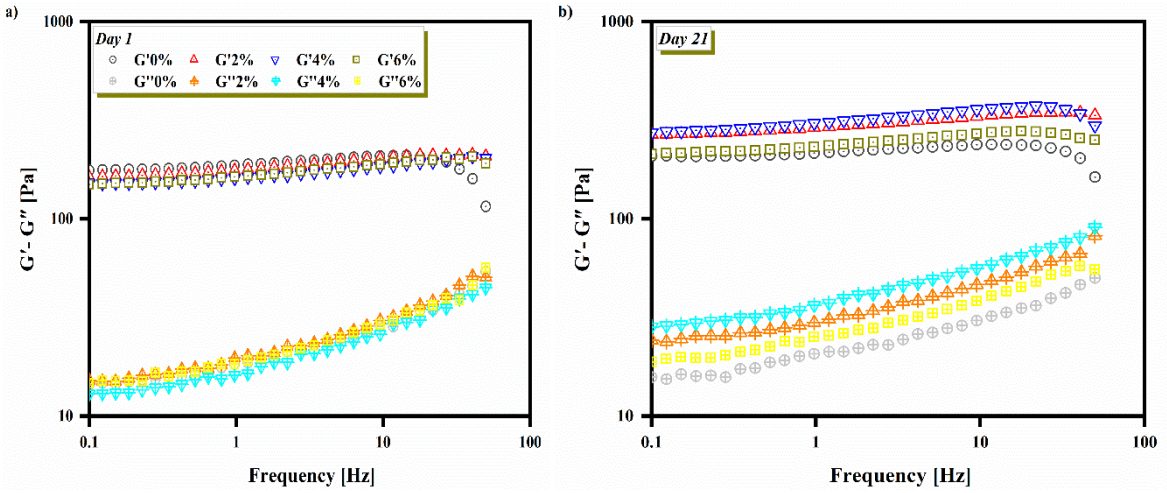

Fig. 3. Frequency sweep of different samples at (a) the beginning, and (b) the end of storage period

Sensory Analysis

The results of the sensory evaluation for Panna cotta prepared with different extract concentrations are presented in Fig. 4. The control and the sample with 2% extract received high scores and did not show significant differences in terms of taste, color, odor, texture, and overall acceptance ($p<0.05$). The sample with 4% extract had a similar color and odor to the control, and was preferred over the sample with 6% extract in terms of taste, color, odor, texture, and overall acceptance ($p<0.05$). Therefore, the sample with 2% extract closely resembled the control in sensory characteristics (taste, color, odor, texture, and overall acceptance). The presence of a bitter, astringent, or woody taste reduced the organoleptic perception of samples with high extract concentrations (Walter, 2021), leading to a decrease in overall acceptance. Similarly,

high concentrations of other extracts and essential oils used as preservatives in food have been reported to negatively affect the organoleptic quality of products. For example, the use of ginger extract in concentrations above 5% in yogurt has been found to significantly reduce overall acceptance (Ahmadi, 2020; Raikos, 2018).

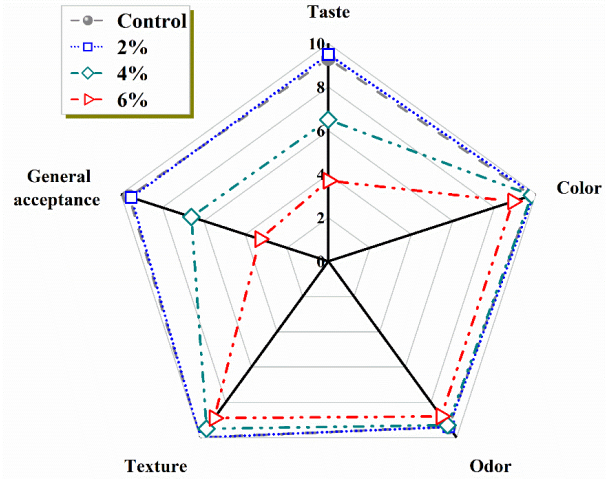

Fig. 4. Sensorial properties of Panna cotta samples

Conclusion

The findings of the current investigation demonstrated that the ultrasonic-assisted method exhibited superior extraction efficiency and yielded more potent compounds compared to the microwave-assisted method and traditional maceration. The ultrasonic-assisted extract showcased the highest content of phenolic compounds, exceptional antioxidant properties, and notable antimicrobial activity against *Escherichia coli*, *Staphylococcus aureus*, and *Candida albicans*. Furthermore, the pH, acidity, and firmness of the Panna cotta, formulated with varying concentrations of the extract, exhibited lower changes during storage compared to the control. The total bacterial population was also significantly lower in these samples compared to the control. Notably, the Panna cotta prepared using 2% *Paeonia officinalis* extract closely resembled the control in terms of texture, viscosity, and sensory characteristics, encompassing taste, odor, color, texture, and overall acceptance. It is concluded that ultrasonic-assisted extraction improves the yield and quality of bioactive compounds from *Paeonia officinalis* and can be used as a natural preservative in dairy desserts, such as Panna cotta. Future research on the long-term shelf life and effectiveness of *Paeonia officinalis* extract, along with other natural preservatives in various dairy products and storage conditions are recommended.

Declaration of Conflicting Interests

The authors declare that they have no known competing financial interests or personal relationships that could have appeared to influence the work reported in this paper.

Author Contributions

This article is extracted from Mrs. **Fallahpour Sichani**'s thesis presented at Islamic Azad University, Isfahan (Khorasgan) Branch under the supervision of Dr. Abbasi. Scientific and statistical analysis corrections were made by **Hajar Abbasi**.

Funding Sources

This research did not has receive any specific grant from funding agencies in the public, commercial, or not-for-profit sectors.

References

1. Adeli, M., & Samavati, V. (2015). Studies on the steady shear flow behavior and chemical properties of water-soluble polysaccharide from *Ziziphus lotus* fruit. *International Journal of Biological Macromolecules*, *72*, 580-587. https://doi.org/10.1016/j.ijbiomac.2014.08.047
2. Adhami, H.R., Farsam, H., & Krenn, L. (2011). Screening of medicinal plants from Iranian traditional medicine for acetylcholinesterase inhibition. *Phytotherapy Research*, *25*(8), 1148-1152. https://doi.org/10.1002/ptr.3409
3. Ahmad, I., Hao, M., Li, Y., Zhang, J., Ding, Y., & Lyu, F. (2022). Fortification of yogurt with bioactive functional foods and ingredients and associated challenges-A review. *Trends in food Science & Technology*, *129*, 558-580. https://doi.org/10.1016/j.tifs.2022.11.003
4. Ahmadi, S., Soleimanian-Zad, S., & Zaeim, D. (2020). Antibacterial and antifungal activity of the aqueous and methanolic extracts and essential oils of red beets *Beta vulgaris* leaves. *Zahedan Journal of Research in Medical Sciences*, *22*(3). https://doi.org/10.5812/zjrms.83725
5. Alupului, A., Calinescu, I., & Lavric, V. (2009, May). Ultrasonic vs. microwave extraction intensification of active principles from medicinal plants. *In AIDIC conference series* (Vol. 9, No. 2006, pp. 1-8). Milano, Italy: ERIS CTSrl. https://doi.org/10.3303/CET0917171
6. Bagade, S.B., & Patil, M. (2021). Recent advances in microwave assisted extraction of bioactive compounds from complex herbal samples: a review. *Critical Reviews in Analytical Chemistry*, *51*(2), 138-149. https://doi.org/10.1080/10408347.2019.1686966
7. Batinić, P., Milošević, M., Lukić, M., Prijić, Ž., Gordanić, S., Filipović, V., & Marković, T. (2022). In vitro evaluation of antioxidative activities of the extracts of petals of *Paeonia lactiflora* and *Calendula officinalis* incorporated in the new forms of biobased carriers. *Food and Feed Research*, *49*(1), 23-35. https://doi.org/10.5937/ffr0-36381
8. Blanco-Llamero, C., Fonseca, J., Durazzo, A., Lucarini, M., Santini, A., Señoráns, F.J., & Souto, E.B. (2022). Nutraceuticals and food-grade lipid nanoparticles: from natural sources to a circular bioeconomy approach. *Foods*, *11*(15), 2318. https://doi.org/10.3390/foods11152318
9. Chauhan, A., Jindal, T., Chauhan, A., & Jindal, T. (2020). Microbiological methods for food analysis. *Microbiological Methods for Environment, Food and Pharmaceutical Analysis*, 197-302. https://doi.org/10.1007/978-3-030-52024-3_8
10. Chemat, F., Rombaut, N., Sicaire, A.G., Meullemiestre, A., Fabiano-Tixier, A.S., & Abert-Vian, M. (2017). Ultrasound assisted extraction of food and natural products. Mechanisms, techniques, combinations, protocols and applications. A review. *Ultrasonics Sonochemistry*, *34*, 540-560. https://doi.org/10.1016/j.ultsonch.2016.06.035
11. Yin, C., Zhang, X., Li, K., Bai, Y., Yang, P., Li, C., & Song, X. (2022). Evaluation on the fresh eating quality of tree peony flowers. *Food Bioscience*, *47*, 101611. https://doi.org/10.1016/j.fbio.2022.101611
12. Clark, S., Costello, M., Drake, M., & Bodyfelt, F. (Eds.). (2009). *The sensory evaluation of dairy products* (Vol. 571). New York: Springer. https://doi.org/10.1007/978-3-031-30019-6
13. Dienaitė, L., Pukalskienė, M., Pukalskas, A., Pereira, C.V., Matias, A.A., & Venskutonis, P.R. (2019). Isolation of strong antioxidants from *Paeonia officinalis* roots and leaves and evaluation of their bioactivities. *Antioxidants*, *8*(8), 249. https://doi.org/10.3390/antiox8080249
14. Djaoud, K., Boulekbache-Makhlouf, L., Yahia, M., Mansouri, H., Mansouri, N., Madani, K., & Romero, A. (2020). Dairy dessert processing: Effect of sugar substitution by date syrup and powder on its quality characteristics. *Journal of Food Processing and Preservation*, *44*(5), e14414. https://doi.org/10.1111/jfpp.14414
15. Dulgheru, C., & Burzo, I. (2010). Contribution to knowledge the volatile oil from *Paeonia officinalis* L. *Flowers*, 639-641.

16. Ebringerová, A., & Hromádková, Z. (2010). An overview on the application of ultrasound in extraction, separation and purification of plant polysaccharides. *Central European Journal of Chemistry*, *8*, 243-257. https://doi.org/10.2478/s11532-010-0006-2
17. Ferioli, F., Giambanelli, E., D'Alessandro, V., & D'Antuono, L.F. (2020). Comparison of two extraction methods (high pressure extraction vs. maceration) for the total and relative amount of hydrophilic and lipophilic organosulfur compounds in garlic cloves and stems. An application to the Italian ecotype "Aglio Rosso di Sulmona"(Sulmona Red Garlic). *Food Chemistry*, *312*, 126086. https://doi.org/10.1016/j.foodchem.2019.126086
18. Ghafoor, K., Choi, Y.H., Jeon, J.Y., & Jo, I.H. (2009). Optimization of ultrasound-assisted extraction of phenolic compounds, antioxidants, and anthocyanins from grape (*Vitis vinifera*) seeds. *Journal of Agricultural and Food Chemistry*, *57*(11), 4988-4994. https://doi.org/10.1021/jf9001439
19. Gupta, R., & Yadav, R.K. (2021). Impact of chemical food preservatives on human health. *Palarch's Journal Of Archaeology Of Egypt/Egyptology*, *18*(15), 811-818.
20. Hoehn, E., Gasser, F., Guggenbühl, B., & Künsch, U. (2003). Efficacy of instrumental measurements for determination of minimum requirements of firmness, soluble solids, and acidity of several apple varieties in comparison to consumer expectations. *Postharvest Biology and Technology*, *27*(1), 27-37. https://doi.org/10.1016/S0925-5214(02)00190-4
21. Jridi, M., Souissi, N., Salem, M.B., Ayadi, M.A., Nasri, M., & Azabou, S. (2015). Tunisian date (*Phoenix dactylifera* L.) by-products: Characterization and potential effects on sensory, textural and antioxidant properties of dairy desserts. *Food Chemistry*, *188*, 8-15. https://doi.org/10.1016/j.foodchem.2015.04.107
22. Kaderides, K., Papaoikonomou, L., Serafim, M., & Goula, A.M. (2019). Microwave-assisted extraction of phenolics from pomegranate peels: Optimization, kinetics, and comparison with ultrasounds extraction. *Chemical Engineering and Processing-Process Intensification*, *137*, 1-11. https://doi.org/10.1016/j.cep.2019.01.006
23. Karo, F.Y.E.B., Sinaga, H., & Karo, T. (2021). The use of konjac flour as gelatine substitution in making panna cotta. *In IOP Conference Series: Earth and Environmental Science* (Vol. 782, No. 3, p. 032106). IOP Publishing. https://doi.org/10.1088/1755-1315/782/3/032106
24. Kumar, K., Srivastav, S., & Sharanagat, V.S. (2021). Ultrasound assisted extraction (UAE) of bioactive compounds from fruit and vegetable processing by-products: A review. *Ultrasonics Sonochemistry*, *70*, 105325. https://doi.org/10.1016/j.ultsonch.2020.105325
25. Lu, X., Zheng, Z., Li, H., Cao, R., Zheng, Y., Yu, H., & Zheng, B. (2017). Optimization of ultrasonic-microwave assisted extraction of oligosaccharides from lotus (*Nelumbo nucifera* Gaertn.) seeds. *Industrial Crops and Products*, *107*, 546-557. https://doi.org/10.1016/j.indcrop.2017.05.060
26. Mahajan, D., Bhat, Z.F., & Kumar, S. (2015). Pomegranate (*Punica granatum*) rind extract as a novel preservative in cheese. *Food Bioscience*, *12*, 47-53. https://doi.org/10.1016/j.fbio.2015.07.005
27. Milovanovic, I., Zengin, G., Maksimovic, S., & Tadic, V. (2021). Supercritical and ultrasound-assisted extracts from *Pleurotus pulmonarius* mushroom: chemical profiles, antioxidative, and enzyme-inhibitory properties. *Journal of the Science of Food and Agriculture*, *101*(6), 2284-2293. https://doi.org/10.1002/jsfa.10849
28. Mason, T., Chemat, F., & Vinatoru, M. (2011). The extraction of natural products using ultrasound or microwaves. *Current Organic Chemistry*, *15*(2), 237-247. https://doi.org/10.2174/138527211793979871
29. Mirza, S.K., Asema, U.K., & Kasim, S.S. (2017). To study the harmful effects of food preservatives on human health. *Journal of Medicinal Chemistry*, *2*, 610-616.

30. Mothana, R.A., Al-Said, M.S., Al-Yahya, M.A., Al-Rehaily, A.J., & Khaled, J.M. (2013). GC and GC/MS analysis of essential oil composition of the endemic Soqotraen *Leucas virgata* Balf. f. and its antimicrobial and antioxidant activities. *International Journal of Molecular Sciences*, *14*(11), 23129-23139. https://doi.org/10.3390/ijms141123129
31. Niko, Z.N., Ghajarbeygi, P., Mahmoudi, R., Mousavi, S., & Mardani, K. (2016). Inhibitory effects of aloe vera gel aqueous extract and *L. casei* against *E. coli* in yoghurt. *Journal of Biology and Today's World*, *5*(9), 157-162.
32. Nottagh, S., Hesari, J., Peighambardoust, S.H., Rezaei-Mokarram, R., & Jafarizadeh-Malmiri, H. (2020). Effectiveness of edible coating based on chitosan and Natamycin on biological, physico-chemical and organoleptic attributes of Iranian ultra-filtrated cheese. *Biologia*, *75*, 605-611. https://doi.org/10.2478/s11756-019-00378-w
33. Park, K.R., Lee, J.Y., Cho, M., Hong, J.T., & Yun, H.M. (2021). Biological mechanisms of paeonoside in the differentiation of pre-osteoblasts and the formation of mineralized nodules. *International Journal of Molecular Sciences*, *22*(13), 6899. https://doi.org/10.3390/ijms22136899
34. Peker, H., & Arslan, S. (2017). Effect of olive leaf extract on the quality of low fat apricot yogurt. *Journal of Food Processing and Preservation*, *41*(5), e13107. https://doi.org/10.1111/jfpp.13107
35. Pinzon, M.I., Sanchez, L.T., Garcia, O.R., Gutierrez, R., Luna, J.C., & Villa, C.C. (2020). Increasing shelf life of strawberries (*Fragaria* ssp.) by using a banana starch-chitosan-Aloe vera gel composite edible coating. *International Journal of Food Science & Technology*, *55*(1), 92-98. https://doi.org/10.1111/ijfs.14254
36. Qamar, S., Torres, Y.J., Parekh, H.S., & Falconer, J.R. (2021). Extraction of medicinal cannabinoids through supercritical carbon dioxide technologies: A review. *Journal of Chromatography B*, *1167*, 122581. https://doi.org/10.1016/j.jchromb.2021.122581
37. Raikos, V., Grant, S.B., Hayes, H., & Ranawana, V. (2018). Use of β-glucan from spent brewer's yeast as a thickener in skimmed yogurt: Physicochemical, textural, and structural properties related to sensory perception. *Journal of Dairy Science*, *101*(7), 5821-5831. https://doi.org/10.3168/jds.2017-14261
38. Rezvani, F., Abbasi, H., & Nourani, M. (2020). Effects of protein–polysaccharide interactions on the physical and textural characteristics of low-fat whipped cream. *Journal of Food Processing and Preservation*, *44*(10), e14743. https://doi.org/10.1111/jfpp.14743
39. Sato, Y., Unno, Y., Ubagai, T., & Ono, Y. (2018). Sub-minimum inhibitory concentrations of colistin and polymyxin B promote *Acinetobacter baumannii* biofilm formation. *PLoS One*, *13*(3), e0194556. https://doi.org/10.1371/journal.pone.0194556
40. Saboora, A., Pourbarat, F., & Fallah, H.H. (2014). Comparison of different extraction methods for optimizing antioxidant compounds in *Origanum majorana* L. *Journal of Food Quality*, 693-704.
41. Salimi, M., Majd, A., Sepahdar, Z., Azadmanesh, K., Irian, S., Ardestaniyan, M.H., & Rastkari, N. (2012). Cytotoxicity effects of various *Juglans regia* (walnut) leaf extracts in human cancer cell lines. *Pharmaceutical Biology*, *50*(11), 1416-1422. https://doi.org/10.3109/13880209.2012.682118
42. Sanjay, S.P., Asgar, S., Mishra, D., Kalyankar, S.D., & Patil, M.R. (2020). Effect of cinnamon powder addition on microbial quality of fresh Buttermilk. *International Journal of Current Microbiology and Applied Sciences*, *9*(10), 2005-2009.
43. Shirsath, S.R., Sonawane, S.H., & Gogate, P.R. (2012). Intensification of extraction of natural products using ultrasonic irradiations-A review of current status. *Chemical Engineering and Processing: Process Intensification*, *53*, 10-23. https://doi.org/10.1016/j.cep.2012.01.003
44. Silva, M.M., & Lidon, F.C. (2016). Food preservatives-An overview on applications and side effects. *Emirates Journal of Food and Agriculture*, *28*(6), 366.

45. Stagos, D. (2019). Antioxidant activity of polyphenolic plant extracts. *Antioxidants*, *9*(1), 19. https://doi.org/10.3390/antiox9010019
46. Barbieri, F., Montanari, C., Gardini, F., & Tabanelli, G. (2019). Biogenic amine production by lactic acid bacteria: A review. *Foods*, *8*(1), 17. https://doi.org/10.3390/foods8010017
47. Sun, X., Guo, X., Ji, M., Wu, J., Zhu, W., Wang, J., & Zhang, Q. (2019). Preservative effects of fish gelatin coating enriched with CUR/βCD emulsion on grass carp (*Ctenopharyngodon idellus*) fillets during storage at 4 C. *Food Chemistry*, *272*, 643-652. https://doi.org/10.1016/j.foodchem.2018.08.040
48. Swaathy, S., Kavitha, V., Pravin, A.S., Mandal, A.B., & Gnanamani, A. (2014). Microbial surfactant mediated degradation of anthracene in aqueous phase by marine *Bacillus licheniformis* MTCC 5514. *Biotechnology Reports*, *4*, 161-170. https://doi.org/10.1016/j.btre.2014.10.004
49. Toma, M., Vinatoru, M., Paniwnyk, L., & Mason, T.J. (2001). Investigation of the effects of ultrasound on vegetal tissues during solvent extraction. *Ultrasonics Sonochemistry*, *8*(2), 137-142. https://doi.org/10.1016/S1350-4177(00)00033-X
50. VanWees, S.R., Rankin, S.A., & Hartel, R.W. (2020). The microstructural, melting, rheological, and sensorial properties of high-overrun frozen desserts. *Journal of Texture Studies*, *51*(1), 92-100. https://doi.org/10.1111/jtxs.12461
51. Walter, M., Brzozowski, B., & Adamczak, M. (2021). Effect of supercritical extract from black poplar and basket willow on the quality of natural and probiotic drinkable yogurt. *Animals*, *11*(10), 2997. https://doi.org/10.3390/ani11102997
52. Yeasmin, D., Swarna, R.J., Nasrin, M., Parvez, S., & Alam, M.F. (2016). Phytochemical analysis and antioxidant activity of three flowers colours *Chrysanthemum moriflolium* Ramat. *International Journal of Biosciences*, *9*, 69-77.
53. Yourdkhani, E., & Jafarpour, A. (2021). The effect of aqueous and ethanolic extract of Hollyhock black (*Alcea rosea*) on physicochemical and antioxidant properties of ketchup sauce. *Food & Health*, *4*(3), 19-23.
54. Zuo, H.L., Zhang, Q.R., Chen, C., Yang, F.Q., Yu, H., & Hu, Y.J. (2021). Molecular evidence of herbal formula: a network-based analysis of Si-Wu decoction. *Phytochemical Analysis*, *32*(2), 198-205. https://doi.org/10.1002/pca.2965

نشریه پژوهشهای علوم و صنایع غذایی ایران
https://ifstrj.um.ac.ir

مقاله پژوهشی

جلد ۲۰، شماره ۶، بهمن-اسفند، ۱۴۰۳، ص. ۱۳۶-۱۱۹

بررسی ترکیبات و خواص کیفی عصاره *Paeonia officinalis* استخراج شده به روش غوطه‌وری با اعمال امواج ماوراءصوت و مایکروویو: ارزیابی بالقوه عصاره به‌عنوان یک نگهدارنده در دسر پاناکوتا

فرناز فلاحپور سیچانی[۱]- هاجر عباسی[۲*]

تاریخ دریافت: ۱۴۰۳/۰۴/۳۱
تاریخ پذیرش: ۱۴۰۳/۰۷/۱۱

چکیده

نگهدارنده‌ها موادی هستند که می‌توانند از تخمیر، اسیدی شدن و سایر فرآیندهایی که موجب فساد غذا می‌شوند، جلوگیری یا آن‌ها را متوقف کنند. این پژوهش با هدف استخراج عصاره ریشه گیاه *Paeonia officinalis* با کمک اعمال روش امواج فراصوت (۴۰ کیلوهرتز، ۴۰ درجه سانتی‌گراد به‌مدت ۴۵ دقیقه) و مایکروویو (۴۰۰ وات، ۴۰ درجه سانتی‌گراد، ۵ دقیقه) در روش غوطه‌وری و ارزیابی بازده استخراج، ترکیبات شیمیایی، خواص آنتی‌اکسیدانی و ضدمیکروبی عصاره‌ها انجام گرفت. در مرحله بعد، بهترین عصاره به میزان ۲، ۴ و ۶ درصد به فرمولاسیون دسر پاناکوتا اضافه شد تا اثرات آن بر ویژگی‌های فیزیکی، شیمیایی، حسی و میکروبی محصول در طول مدت نگهداری بررسی شود. یافته‌ها نشان می‌دهند که اعمال روش امواج فراصوت راندمان استخراج عصاره را بهبود می‌بخشد. این عصاره دارای بالاترین سطوح ترکیبات فنلی (۱/۱۸±۵۲/۶۴ میلی‌گرم اسید گالیک در هر گرم)، خواص آنتی‌اکسیدانی (۰/۴۷±۷۶/۳۳ درصد) و فعالیت ضد میکروبی در برابر *Escherichia coli*، *Staphylococcus aureus* و *Candida albicans* بوده است. افزودن عصاره به پاناکوتا نرخ تولید اسید را در محصول کاهش می‌دهد و منجر به کاهش جمعیت کل باکتری در مقایسه با نمونه شاهد در پایان دوره نگهداری می‌شود. دسر حاوی ۲ درصد عصاره ویژگی‌های حسی (طعم، رنگ، بو، بافت و پذیرش کلی) مشابه نمونه شاهد داشته در حالی‌که کیفیت میکروبیولوژیکی آن برای مدت طولانی‌تری حفظ گردید. عصاره اتانولی ریشه *Paeonia officinalis* که با اعمال روش امواج فراصوت در روش غوطه‌وری استخراج شده است، می‌تواند به‌عنوان یک نگهدارنده مؤثر برای دسرهای لبنی معرفی شود.

واژه‌های کلیدی: پائونیا، رفتار رئولوژیکی، فراصوت مایکروویو، نگهدارنده‌ها

۱ و ۲- به‌ترتیب دانش‌آموخته کارشناسی ارشد و دانشیار گروه علوم و صنایع غذایی، دانشکده کشاورزی، واحد اصفهان (خوراسگان)، دانشگاه آزاد اسلامی، اصفهان، ایران
(*- نویسنده مسئول: Email: H.abbasi@Khuisf.ac.ir)

https://doi.org/10.22067/ifstrj.2024.89000.1350

Iranian Food Science and Technology Research Journal

Homepage: https://ifstrj.um.ac.ir

Research Article
Vol. 20, No. 6, Feb.-Mar., 2025, p. 137-153

Fatty Acid Profile and Chemical Composition of Three Populations of Southern Cattail (*Typha domingensis*) from South of Iran

M. Shojaee Barjouee[1], M. Farasat[2,3], M. Tadayoni[4*]

1 and 4- Graduated Master's Student and Associate Professor, Department of Food Science and Technology, Ahvaz Branch, Islamic Azad University, Ahvaz, Iran, respectively.
2- Marine Pharmaceutical Science Research Center, Ahvaz Jundishapur University of Medical Sciences, Ahvaz, Iran
3- Assistant Professor, Departments of Agronomy and Biology, Ahvaz Branch, Islamic Azad University, Ahvaz, Iran
(*- Corresponding Author Email: me.tadayoni@iau.ac.ir)

Received: 09.09.2024
Revised: 25.11.2024
Accepted: 21.12.2024
Available Online: 07.01.2025

How to cite this article:
Shojaee Barjouee, M., Farasat, M., & Tadayoni, M. (2025). Fatty acid profile and chemical composition of three populations of southern cattail (*Typha domingensis*) from south of Iran. *Iranian Food Science and Technology Research Journal*, *20*(6), 137-153. https://doi.org/10.22067/ifstrj.2024. 89632.1365

Abstract

Lipids are comprised of heterogenous group of chemical compounds, the majority of which have fatty acids as part of their structure. Fatty acids (FAs) are essential for the normal functioning of all organisms. Polyunsaturated fatty acids with multiple double bonds (PUFAs), including omega-3 (n-3) and omega-6 (n-6) are known as beneficial chemicals for human health. Recent attempts to find and identify oils with special advantageous qualities have been prompted by the widespread use of vegetable oils in the food and other industries. Southern cattail (*Typha domingensis*) is a plant whose practically all parts are edible, particularly its starchy rhizomes, which have a protein composition comparable to corn or rice. In this study, to investigate the nutritional value of this plant, plant samples were collected from three locations in the south of Iran, including Shadegan Wetland, Hoveyzeh (Hoorolazim Wetland), and Hamidabad (Dez River). The oil content and fatty acid profile as well as some chemical compositions such as ash, moisture, fiber, protein, and carbohydrates were evaluated and compared. The oil was extracted using the Soxhlet technique, and the fatty acid composition was determined by GC/MS. The average oil content in aerial (stems and leaves) and underground (rhizomes and roots) organs was 2.62 and 1.52%, respectively. The samples contained 12 fatty acids, three of which were unsaturated and nine were saturated. In roots and rhizomes, the maximum proportion of unsaturated fatty acids including oleic acid (ω-9), linoleic acid (ω-6), alpha- linolenic acid (ω-3) was 65.85±1.51%, whereas in stems and leaves, it was 41.10±0.09%. The amounts of fiber, moisture, ash, protein, and carbohydrates in the samples ranged from 43.34 to 45.93%, 12.57 to 17.84%, 3.64 to 4.25%, 6.20 to 6.40%, and 23.19 to 32.18%, respectively. This plant's high fiber content with the capacity to grow quickly and widely in fresh and saline water make it a viable candidate for inclusion in human diet and animal feed through agricultural breeding initiatives.

Keywords: Fatty acid, Fiber, PUFAs, *Typha domingensis*

https://doi.org/10.22067/ifstrj.2024.89632.1365

Introduction

Compounds that are fatty, waxy, or oily and soluble in organic solvents but insoluble in polar solvents like water are known as lipids. Lipids play a crucial role in the human body's homeostatic processes. Some of the most essential bodily functions are facilitated by lipids. Major types of lipids are oils and fats, phospholipids, waxes, and steroids. Oils and fats are esters composed of three fatty acids and glycerol (Ahmed *et al*., 2024). Fatty acids (FAs) are essential for the normal functioning of all organisms. They are components of plasma membranes, serve as energy storage materials, and act as signaling molecules regulating cell growth and differentiation as well as gene expression (de Carvalho& Caramujo, 2018). Fatty acids (FAs) are primarily categorized as saturated (SFAs—without double bonds), monounsaturated (MUFAs—with one double bond), and polyunsaturated fatty acids (PUFAs—with two or up to six double bonds) (Orsavova *et al*., 2015). Polyunsaturated fatty acids are one of the most important components of cells, influencing the normal growth and function of both eukaryotic and prokaryotic organisms (Czumaj & Śledziński, 2020). The health benefits of polyunsaturated fatty acids, such as omega-3 (n-3) and omega-6 (n-6) are well established. According to Daley *et al*. (2010), two significant polyunsaturated fatty acids that are referred to as essential fatty acids are linoleic acid (C18:2) and alpha-linolenic acid (18:3). These long-chain polyunsaturated fatty acids significantly alter the body's physiology and biochemistry, which lowers the chance of cardiovascular illnesses. The n-6 to n-3 PUFA ratio is important for human health because the n-6 and n-3 metabolic pathways compete with one other for the same activities of elongation and desaturation enzymes. It has been found that a 5:1 consumption ratio of n-6/n-3 is sufficient for the human body to ensure good health. The consumption of omega-6 has altered significantly in the western diet throughout time, leading to a 20:1 n-6/n-3 ratio (Bishehkolaei & Pathak, 2024).

Type 2 diabetes is caused by a condition where the body becomes resistant to insulin. Consuming more saturated fats raises the risk of type 2 diabetes and insulin resistance (Pipoyan *et al*., 2021). Based on previous research, not all saturated fatty acids affect serum cholesterol in the same way. For instance, lauric acid (C12:0) and myristic acid (C14:0) have a greater total cholesterol-raising effect than palmitic acid (C16), while stearic acid (C18:0) has a neutral effect on serum cholesterol concentration (Daley *et al*., 2010). Saturated fatty acids (SFAs) of different chain lengths have unique metabolic and biological effects, and a few recent studies suggest that higher circulating concentrations of very long-chain fatty acids (VLSFAs) with 20 carbons or more, such as arachidic acid (C20:0), behenic acid (C22:0), and lignoceric acid (C24:0) are associated with a lower risk of diabetes, heart failure, atrial fibrillation, coronary heart disease, mortality, and sudden cardiac arrest (Fretts *et al*., 2019; Lemaitre & King, 2022). The findings of some researchers also indicate that saturated fat in some cases has an inverse relationship with type 2 diabetes related to obesity (Gershuni, 2018).

Fats and oils are valuable food compounds that, in addition to providing energy, play an important role in human health and survival and are in the group of essential foods (Leray, 2020). Vegetable oils are widely used in food and various industries. There is a lot of work done to enhance oilseeds, streamline procedures, and discover new sources. Parallel efforts have been undertaken in recent years to find and acquire oils with unique application qualities (Brahma *et al*., 2022).

Many plants situated in aquatic habitats, particularly wetlands, have gotten less attention in food research than plants found on land because of their restricted access. Because they are rich in food, wetlands have long been favored habitats for indigenous people all over the world. For example, apart from rice, cattail (*Typha* spp.) is a valuable food source found in rice-growing areas of China (Zhang *et al*., 2020). According to Hamdi & Assadi (2003),

there are 12 species of this genus that are found growing in aquatic environments in Iran, such as lakes, wetlands, and stagnant waters. One of these species that can shield lakes, estuaries, groundwater, other aquatic plants, and animals from erosion is *Typha domingensis*. Its roots can serve as a biological cleanser. This plant is found around the world, and a pH of 4 to 10 is ideal for it. Warm temperate climates are home to this species, and 30°C is the ideal temperature for seed germination (Bansal *et al*., 2019). It can be found in temperate, tropical, and subtropical parts of Africa, Asia, America, Australia, and the Mediterranean and sub-Mediterranean regions of Europe. It has also adapted in Hawaii. According to Uotila *et al*. (2010), this species successfully invades and dominates salty and tidal habitats. Research on the potential use of cattail pollen as a food source and its effects on human activity and the environment has revealed that cattail pollen can be a perfect supplemental source to alleviate the shortage of fruits and vegetables (Zhang *et al*., 2020). Nearly every portion of the plant can be eaten, but the rhizomes in particular are starchy and have a protein level akin to that of rice or corn (Pandey & Verma, 2018).

Apart from its nutritional worth, this plant is an excellent source of dietary fiber and has been traditionally utilized by the local community to treat various ailments. Numerous investigations have additionally demonstrated the plant's medicinal properties. For instance, the impact of fiber in *Typha angustifolia* L. rhizome flour was studied in rats with inflammatory bowel disease (IBD), and the findings indicated that 10% *T. angustifolia* rhizome flour was just as effective as prednisolone without exhibiting any synergistic effects. Rhizome flour was shown to contain coumarins, flavonoids, and saponins (Fruet *et al*., 2012). The cytotoxic effects of *T. domingensis* on human breast adenocarcinoma (MCF7), human ovarian adenocarcinoma (A2780), and human colon adenocarcinoma (HT29), as well as fibroblasts in the normal human fetal lung (MRC5), have been documented in another study, which also examined the antimicrobial, antioxidant, anticancer, thyroid inhibitory, and anti-inflammatory properties of *T. domingensis* (Khalid *et al*., 2022). Additionally, numerous studies have demonstrated that the plant's extract lowers blood pressure, cholesterol, triglycerides, and has an anti-atherosclerotic effect (Akram & Jabeen, 2022; Khalid *et al*., 2022).

Studies have demonstrated the impact of environmental variables on the fatty acid composition and quality of oil in plants (Labdelli *et al*., 2022). Numerous fresh and brackish waters in Iran are home to the southern cattail plant. In Khuzestan, this species is also found in the waters of many areas, including the three locations under study, where it has established large colonies. Water characteristics, particularly salinity, varied among the three study regions. The water at Shadegan Wetland was brackish in some areas and saline in others, with the lowest and maximum salinities occurring in the spring and summer, respectively. Hoveyzeh Wetland falls within the category of brackish water (Nasirian & Salehzadeh, 2019), but the Dez River has drinking freshwater (Azish *et al*., 2023). The purpose of this study was to examine the fatty acid profile of *Typha domingensis* under various geographic situations because this species is found in all three regions. Thus, the oil content and fatty acid composition of *T. domingensis* from three different geographic sites were analyzed and compared in this study. Along with the fatty acid profile, the chemical properties of the samples were evaluated and compared.

Materials and Methods

Sample Collecting

In April 2017, samples of *Typha domingensis'*s populatios were collected from three locations of Khuzestan province in the south of Iran including Shadegan Wetland (30° 44′582″ N, 48° 45′270 ″E), Hoveyzeh Protected Area (Hoorolazim Wetland) (31° 27′987 ″N, 47° 79′155 ″E) and Hamidabad (32° 24′267 ″N, 48° 34′200 ″E).

Oil Extraction

The aerial (stems and leaves) and underground (rhizome and roots) parts of the samples were separated after they were collected and cleaned with water. The cut portions were inspected under a stereomicroscope to make sure the subsurface and aerial portions were fully separated in order to guarantee the separation accuracy. It took 14 days for the samples to fully dry after being exposed to air in shade. 50 grams of each powder sample were placed in a Soxhlet apparatus, and 200 mL of 95% n-hexane solvent (Merck, Germany) was added to it. Then, it was placed under the reflux system for 8 hours. The gravimetric method was used to calculate the amount of oil (AOAC, 1995). To remove the hexane solvent from the oil, a rotary evaporator (Heidolph, 4000 Laborota) was used at a speed of 60 rpm and 50 °C for 45 minutes. Gas-liquid chromatography was used to determine the content of fatty acids as fatty acid methyl esters (FAME). Fatty acid methyl esters can be prepared using a variety of techniques (Ichihara *et al*., 2020). In order to prepare FAME, the extracted oil from the plant was methylated in the presence of hexane and 1 M methanolic KOH at 50 °C and finally stored at -18 °C for further analysis (ISO 5509, 2000).

GC/MS (Gas Liquid Chromatography/Mass Spectrometry)

To identify fatty acids, the samples (FAME) were injected in a gas chromatograph (Alginet 7890A GC System) with a mass selective detector (MSD5977A), equipped with an HP-5MS capillary column. Helium was used as carrier gas with a constant pressure of 33 psi. A constant flow of helium was maintained at a flow rate of 1.50 mL min^{-1}. The oven temperature started at 50°C, then increased to 230°C (25°C/min), and held at this temperature for 5 min. The fatty acids were identified by comparing their retention times with those of standards. The content of fatty acids was expressed as a percentage (Dieffenbacher & Pocklington, 1992).

Chemical Composition

Ash, moisture, and protein of the samples were determined using analysis methods of the Association of Official Analytical Chemists (AOAC, 2000). Total ash content was determined by burning the samples at 550°C according to the AOAC method 942.05. The moisture content was determined by drying the samples at 100°C for 3 hours according to the AOAC 925.10 method. Protein measurement was done by the Kjeldahl method in three stages of digestion, distillation, and titration (AOAC method 950.36). Total Nitrogen was determined, and the factor Nx6.25 was applied to convert the total nitrogen to protein content. Crude fiber content was determined using the Weende method according to the AOAC method 978.10 (AOAC, 2005).

The amount of carbohydrate content was measured by the Anthrone method. 100 µL of each extract and the standards were taken, and 3 ml of anthrone reagent was added to it. It was then placed in a boiling water bath for 20 minutes, and after cooling the samples, their absorbance was read at 620 nm with a spectrophotometer model 340 (HIITACHI). Anthrone reagent was used as a blank. Pure glucose concentrations of 0, 20, 40, 60, 80, 100, and 120 were used to draw the standard curve. The amount of carbohydrates was calculated using the standard curve (McCready *et al*., 1950). All values were calculated based on the percentage of plant dry weight.

Statistical Analysis

Data analysis was done using the SPSS 22.0 software. Means were compared with analysis of variance and post hoc tests. In order to estimate the correlation between variables, Pearson's correlation test was applied. The values of $p < 0.05$ were considered statistically significant. All measurements were repeated in 3 times.

Results and Discussion

The *Typha domingensis* samples were collected from 3 areas south of Iran, including: Shadegan Wetland, Hoveyzeh Wetland, and

Hamidabad (downstream of the Dez River). The oil was extracted by Soxhlet apparatus. The average percentage of oil in dry matter in the samples of underground and aerial organs was 1.52% and 2.62%, respectively. Table 1 shows the amount of oil in the aerial and underground parts of the samples from three collection locations. The findings demonstrated that there is a significant difference in the oil content between the aerial and underground parts, as well as between the samples of the three evaluated areas. Compared to rhizomes and roots, stems and leaves contained more oil. The highest amount of oil was found in Hamidabad (H2) samples and the lowest in Hoveyzeh (H1) samples (Table 1). After oil extraction, the composition of fatty acids in the oil was identified by gas chromatography. In general, 12 fatty acids, including 3 unsaturated and 9 saturated fatty acids, were identified. The fatty acids, their scientific names, and their structures are given in Table 2. Also, Fig. 1 shows the percentage of fatty acids in the underground part (including rhizome and root) and aerial parts (including stem and leaves) of the samples.

Saturated and Unsaturated Fatty Acids

Table 3 shows the percentage of saturated and unsaturated fatty acids in the oil of the studied samples. As can be seen in the table, the samples collected from Shadegan (S1) were free of myristic acid (C14). Arachidic acid (C20) was also not found in the root and rhizome of Hoveyzeh (H1) samples. Fatty acids C22, C14, C10, C8, and C4 showed the highest amount in both aerial (from 6.15 to 8.67%) and underground parts (from 8.58 to 9.26%) of H1 samples. Fatty acids C12 (lauric acid) and C16 (palmitic acid) showed the highest amount in the shoots of H2 samples (10.67 ± 0.03 %) and S1 samples (13.95 ± 0.06 %) respectively.

Table 1- Oil content of the root (underground parts), shoot (aerial parts) and the whole plant of the Cattail

Location	Sample code	Oil content (% DW)		
		*Root	Shoot	Whole plant
Shadegan	S1	1.58±0.07 b	2.81±0.01 a	2.19±0.07 a
Hoveyzeh	H1	1.19±0.02 b	2.13±0.07 b	1.66±0.05 b
Hamidabad	H2	1.79±0.59 a	2.91±0.69 a	2.35±0.07 a

Each value is expressed as the mean ±SD(n=3). Means with the same small letters in each column are not significantly different at $p< 0.05$ according to Duncan's Multiple Range test.
*Here root includes rhizome and root and, shoot includes stem and leaves.

Table 2- Fatty acids composition of cattail oil

Lipid Numbers	ω-n	Common Name	Structural Formula
C4	-	Butyric acid	$CH_3(CH_2)_2COOH$
C8	-	Caprylic acid	$CH_3(CH_2)_6COOH$
C10	-	Capric acid	$CH_3(CH_2)_8COOH$
C12	-	Lauric acid	$CH_3(CH_2)_{10}COOH$
C14	-	Myristic acid	$CH_3(CH_2)_{12}COOH$
C16	-	Palmitic acid	$CH_3(CH_2)_{14}COOH$
C18	-	Stearic acid	$CH_3(CH_2)_{16}COOH$
C20	-	Arachidic acid	$CH_3(CH_2)_{18}COOH$
C22	-	Behenic acid	$CH_3(CH_2)_{20}COOH$
C18:1	ω-9	Oleic acid	CH_3-$(CH_2)_7$-CH=CH-CH_2-(CH_2)-COOH
C18:2	ω-6	Linoleic acid	CH_3-$(CH_2)_4$-(CH=CH-$CH_2)_2$-$(CH_2)_6$-COOH
C18:3	ω-3	Alpha- Linolenic acid	CH_3-(CH2-CH=CH)$_3$-$(CH)_7$-COOH

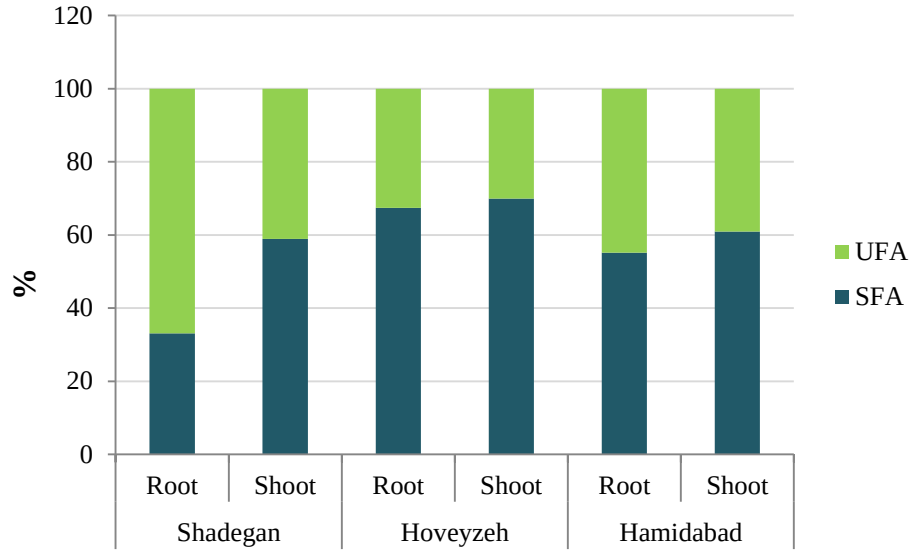

Fig. 1. Saturated and unsaturated fatty acids in the root (rhizome+root) and shoot (stems+leaves) of cattail (*Typha domingensis*) collected from the three study areas. SFA= Saturated Fatty Acids, UFA= Unsaturated Fatty Acids

C18 fatty acid (stearic acid) was generally more in the roots than in the shoots, and the highest value was found in the roots of S1 samples (17.28 ± 0.23%). Fatty acid C18:1 ω-9 (oleic acid) showed the highest amount in root (21.22 ± 0.21%) and shoot (13.66 ± 0.04%) of S1 samples. Fatty acid C18:2 ω-6 (linoleic acid) also showed the highest amount in the roots of S1 samples (25.43 ± 0.44%), followed by the shoots of H2 samples (16.74 ± 0.11). Fatty acid C18:3-3 ω-3(alpha- linolenic acid), similar to fatty acid C18:1, showed the highest amount in roots (19.19 ± 0.29%) and shoots (13.02 ± 0.09%) of S1 samples. Arachidic acid (C20) and behenic acid (C22) showed the highest amount in both aerial and underground parts in H2 and H1samples, respectively. The lowest amounts of unsaturated fatty acids were found in both roots and shoots of H1 samples (Table 3). With the exception of the underground organs of (Shadegan) S1 samples, in other samples, the amount of saturated fatty acids in the extracted oil was more than unsaturated fatty acids. Fig. 1 shows the percentage of saturated and unsaturated fatty acids in the oil obtained from the aerial and underground parts of the samples. As illustrated in the figure, the highest percentage of unsaturated fatty acids was found in S1 samples. This value was 65.85 ± 1.51% in roots and 41.10 ± 0.09% in shoots.

Lipids are considered one of the essential nutrients for humans. Lipid metabolism produces many bioactive lipid molecules that are essential mediators of numerous signaling pathways and also essential constituents of cell membranes. Any change in lipid metabolism can lead to a variation in the composition of the membrane and subsequently to a difference in its permeability (Orsavova *et al*., 2015). Plants are immobile organisms and cannot migrate from a stressful environment, and for this reason, they have complex alternatives to prevent the adverse effects of biotic stress factors such as viruses, bacteria, and fungi and non-biotic stress factors such as salinity, temperature, UV, and heavy metals (Guo *et al*., 2019; He & Ding, 2020). One of the most common defense mechanisms in plants against a variety of biotic and abiotic stressors is the high concentration of unsaturated fatty acids found in the membrane lipids of plant cells. In higher plants, the most common PUFAs are three 18-carbon (C18) species: oleic (OA, 18:1Δ9), linoleic (LA, 18:2Δ9,12), and α-linolenic (ALA, 18:3Δ9,12, 15) acids. These simple compounds play multiple vital roles and

are deeply related to abiotic and biotic stresses. They participate in stress responses and are precursors of plant hormones (He & Ding, 2020). Accumulation of unsaturated fatty acids such as ALA in plant membranes is a common abiotic stress response that leads to increased membrane fluidity and resistance to cold-induced membrane hardening. In addition to modulating membrane fluidity, C18 PUFAs act as intrinsic antioxidants. The double bonds in unsaturated fatty acids make them susceptible to reactive oxygen species (ROS), which are commonly produced as a result of stress. Overexpression of omega-3 fatty acid desaturases (FADs) is a general defense mechanism to induce stress responses in plants (Czumaj & Śledziński, 2020; Coniglio *et al*., 2023).

Table 3- The percentage of fatty acids in the roots and shoots of cattail samples

	Shadegan		**Hoveyzeh**		**Hamidabad**	
	Root	Shoot	Root	Shoot	Root	Shoot
C4	1.91 ± 0.01	6.92 ± 0.16	9.26 ± 0.32	8.57 ± 0.15	8.81 ± 0.74	7.33 ± 0.88
C8	1.34 ± 0.08	7.40 ± 0.10	8.58 ± 0.83	8.32 ± 0.10	2.10 ± 0.38	2.57 ± 0.23
C10	2.72 ± 0.15	5.89 ± 0.11	9.00 ± 0.18	8.67 ± 0.16	3.35 ± 0.07	5.13 ± 0.47
C12	4.30 ± 0.03	3.39 ± 0.07	4.46 ± 011	8.30 ± 0.02	7.80 ± 0.23	10.67 ± 0.03
C14	0.00	0.00	9.66 ± 0.1	6.78 ± 0.28	0.98 ± 0.17	5.49 ± 0.05
C16	2.37 ± 0.07	13.95 ± 0.06	9.54 ± 0.33	7.98 ± 0.55	4.35 ± 0.39	3.38 ± 0.14
C18	17.28 ± 0.23	9.60 ± 0.05	8.19 ± 0.05	8.20 ± 0.14	15.32 ± 0.05	11.57 ± 0.18
C20	1.47 ± 0.24	7.64 ± 0.25	0.00	6.96 ± 0.03	8.97 ± 0.27	9.63 ± 0.15
C22	1.74 ± 0.09	4.13 ± 0.05	8.69 ± 0.07	6.15 ± 0.15	3.43 ± 0.13	5.13 ± 0.24
C18:1 ω-9	21.43 ± 0.35	13.67 ± 0.06	10.17 ± 0.65	10.66 ± 0.02	15.35 ± 0.22	11.50 ± 0.16
C18:2 ω-6	26.17 ± 0.04	14.40 ± 0.09	12.18 ± 0.38	8.86 ± 0.18	19.23 ± 0.15	16.75 ± 0.20
C18:3 ω-3	19.28 ± 0.03	13.02 ± 0.17	10.28 ± 0.05	10.56 ± 0.10	10.30 ± 0.22	10.85 ± 0.03

The results of a 2017 study on avocados by Guzmán-Maldonado *et al*. (2017) showed that ripe fruits have more oil content than green and unripe fruits. The proportion of saturated fatty acids decreased to 28% as the plant aged, whereas the levels of linoleic acid (C18:2) and oleic acid (C18:1) increased by 20%. Their results revealed that the amount of oleic acid varied significantly depending on the location of the plants, with a 14% decrease at lower elevations.

In a study conducted in artificial micro-wetlands of Mexico on three aquatic macrophytes, including *T. domingenesis*, the results showed that in *T. domingenesis* leaves, in addition to unsaturated fatty acids C18:1 (35.35%), C18:2 (19.28%) and, C18:3(18.57%), fatty acids C16:2 ω 6, C16:1 ω 9, C16:1 ω 7, in small amounts below 1% have also been observed (Ruiz-Carrera *et al*., 2016). In the present work, the highest amount of C18:1, C18:2, and C18:3 was obtained with an average of 13.67, 16.75, and 13.02%, respectively, which shows lower values than those found in the mentioned study. The present study's sampling locations are located between 5 and 150 meters above sea level, whereas the altitude in Mexico is above 1000 meters. This difference in altitude may account for the significant variation in oleic acid levels between the study conducted by Ruiz-Carrera *et al*. (2016) and the current study.

According to earlier research, submerged and emergent aquatic macrophytes had higher total lipid contents than free floating and rooted floating macrophytes. It has been reported that in early autumn and at the peak of growth, there was a tendency for depositing total lipids in the tissue of submerged macrophytes, which shows that this period provides better conditions for development. The tendency to accumulate fat during this period of the year may be due to the conversion of proteins and carbohydrates into lipids (Ahmad Dar *et al*., 2013).

T. domingenesis is an emergent plant whose rhizome and roots are immersed in water, and part of its stem and leaves are above the water surface. In the current investigation, the

rhizome and roots had greater concentrations of unsaturated fatty acids than saturated fatty acids. A similar pattern was somewhat seen in the case of stems and leaves (Table 3). As previously noted, unsaturated fatty acid accumulation in plant organs can be brought on by adverse environmental conditions. The dumping of herbicides and pesticides into Shadegan wetland has caused the phenomenon of eutrophication, increased pollution, increased water salinity, and increased water alkalinity (pH > 9) according to a study on the effects of changes in the land use of Shadegan Wetland over a 15-year period (Raygani *et al*., 2020). The construction of a dam upstream of Hoveyzeh wetland has also caused drought and changes in the ecosystem of the wetland (Foladvand *et al*., 2014). Also, as a result of the entry of polluting sources into the Dez River, the increase of BOD and EC has been reported to a critical level for the Dez River (Ghorbani *et al*., 2022). Even though Azish *et al.* (2023) examined the water quality of the Dez River over a 10-year period and concluded that the Dez River has been experiencing an increase in salinity downstream, but the river water is still classified as freshwater.

According to the study on the fatty acid profiles and lipid alterations of algae *Diacronema vlkianum*, grown in different salinity, it was found that fatty acids react differently to intense salinity stress. The concentrations of C14, C16:1, C20:4, C20:5, and C22:6 was decreased, whereas the concentration of C16:1, C17:1, C18:2, and C18:3 increased as salinity increased (Cañavate & Fernández-Díaz, 2022). In the current investigation, it was found that myristic acid (C14) was absent in samples from Shadegan, which had a higher salinity than the other two regions. Interesting patterns were seen in the fatty acids in another investigation on lipid buildup in the mangrove-dwelling *Chlorella vulgaris* grown on culture medium. The concentration of C16 was increased at 30 ppt salinity after being largely unchanged in the range of 5 to 20 ppt salinity. A declining trend was observed in both C18 and C20 as salinity increased from 5 to 30 ppt. Up to 20 ppt, C18:2 displayed a fluctuating tendency; after that, it declined at 30 ppt, while C18:3 showed an increasing trend as salinity increased. These researchers found that high levels of C18:3n3 PUFA were present in the early growth phase, along with a variety of short, medium, and long chain fatty acids, particularly C20. They also found that C18:1 and C18:2 accumulated in the stationary growth phase at all salinities, serving as substrates for the cellular accumulation of C18:3. Mangrove organisms may have adapted to the salinity by adopting nonlinear growth patterns (Teh *et al*., 2021). The salinity of the habitat is considered as the main factors affecting the differences in the fatty acid profiles of *T. domingensis* plants in our study. According to the findings, samples from Hamidabad, which had the lowest water salinity, had higher levels of C20 than those from the other two areas. Furthermore, this fatty acid was absent from the roots of samples taken from the brackish-watered Hoveyzeh Wetland. The plant appears to be adapting to its environment through these changes in fatty acid levels.

Chemical Composition (Moisture, Ash, Protein, Fiber, and Carbohydrates)

In this study, the stems and leaves were evaluated for moisture, ash, protein, fiber, and carbohydrate content. Duncan's test and one-way analysis of variance revealed that there was a significant difference at the 1% level in the mean of all variables, including moisture, carbohydrate, protein, fiber, and ash, among the samples from the three locations under study. This indicates the impact of environmental conditions on the physico-chemical characteristics of the studied samples.

H2 and H1 samples had the highest and lowest moisture contents, respectively (17.84±0.07 and 12.57±0.08 %). In contrast, the H1 samples had the highest concentration of carbohydrates (32.18±0.18 %), while the H2 samples had the lowest (23.19±0.38 %). H2 samples had the highest protein content (6.40±0.01 %), whereas S1 samples had the

lowest (6.20±0.04 %). Fiber content was also highest in H2 samples (45.93±0.08 %) and lowest in H1 samples (43.14±0.0.16 %). Lastly, S1 samples had the highest ash content (4.25±0.04 %), whereas H1 samples had the lowest (3.64±0.03 %) (Table 4).

Table 4-Comparison of chemical composition of cattail shoots collected from different locations.

Location	Moisture (%)	Total Carbohydrate (%)	Crude Protein (%)	Crude Fiber (%)	Ash (%)
Shadegan	12.71±0.02 b	29.16±0.23 b	6.20±0.04 c	44.87±0.11 b	4.25±0.04 a
Hoveyzeh	12.57±0.08 b	32.18±0.18 a	6.34±0.01 b	43.14±0.16 c	3.64±0.03 c
Hamidabad	17.84±0.07 a	23.19±0.38 c	6.40±0.01 a	45.93±0.08 a	3.73±0.05 b

The means in each column with different letters are significantly different ($P < 0.05$). Each value is expressed as the mean ±SD(n=3).

In a study conducted in Nigeria, the nutritional and mineral composition of the whole plant of *T. domingensis* were investigated. The results revealed that this plant contains 57.81% moisture, 9.08% ash, 1.90% crude fat, 8.86% crude protein, 17.46% fiber, and 4.89% carbohydrates (Hassan *et al*., 2018). According to data from another study, the contents of aerial parts in terms of moisture, ash, crude fat, crude protein, fiber, and carbohydrates were 12.43, 9.98, 2.8, 12.25, 35.90, and 49.05%, respectively (El-Amier, 2013). In the underground parts, these compounds are reported as 21.56, 8.42, 1.5, 8.13, 27.47, and 62.9%, respectively. According to the aforementioned study, there was more fat in the aerial than in the underground portions, but there was a contrary trend in the percentage of carbohydrates, with greater values in the underground sections (El-Amier, 2013). In the present study, the fat content of the aerial parts was higher than the underground parts, which is consistent with the reports of El-Amier (2013). The stem and leaves of *T. domingensis* contain an ash level of 10.5%, according to Khider *et al*. (2012). The average amount of ash in the current study was 3.87%. However, the average carbohydrates calculated in the current study was 28.18%, while the average fiber was 44.65%. These findings are considerably different from Hassan *et al*.'s (2018) findings. In contrast to El-Amier's findings in Egypt, higher levels of fiber and lower levels of ash, protein, and carbohydrates were obtained in our study. Moreover, our study's ash content differs significantly from Khider *et al*.'s (2012) findings.

In order to find any physiological deficiencies in the growth cycle of *T. domingensis* in Lake Burullus, Egypt, the seasonal allocation of carbohydrates by this plant was assessed. According to the study, rhizomes were strong reservoirs for carbohydrate storage during the life cycle of *T. domingensis*. The largest part of non-structural carbohydrates was starch, whose concentration reached about 4.3 times that of water-soluble carbohydrates. In this study, it was reported that carbohydrates reach their lowest level in the plant in March (Eid & Shaltout, 2017). In the current investigation, sampling was completed in April. The fact that the sampling month in the experiments is nearly identical to the sampling period in the Eid and Shaltout study (which is likely the point at which the plant has achieved its lowest carbohydrate reserve) could be the cause of the lower amount of carbohydrates obtained in our study.

In our investigation, samples from all three regions showed high levels of fiber. Generally, controversial reports on fiber efficiency were found in literature. For instance, Shadhin *et al*. (2021) from Canada, indicated that the examined cattail samples had a fiber efficiency ranging from 18 to 30%. Additionally, 63% cellulose, 8.7% hemicellulose, 40% fiber, 8.9% moisture, 9.6% lignin and pectin, and other water-soluble materials were found in another investigation on *T. latifolia* (Chakma *et al*., 2017). The freshwater-dwelling samples from Hamidabad in our study, had a higher fiber content than the samples from the other two

studied regions, which contain more salinized water. Studies have indicated that the production of fiber may be impacted by salt. For instance, it has been noted that cotton is comparatively more resilient to abiotic stressors. But salinity stress can affect boll formation, resulting in detrimental impacts on biomass output and a 60% drop in fiber production. An increase in electrical conductivity (EC) influences the process of photosynthesis, cellulose deposition, and sugar transport, all of which have an indirect effect on fiber maturity. Because there is less cellulose deposition, the creation of mature fiber also declines (Maryum *et al.*, 2022). Variations in the fiber yield of *T. domingensis* species around the world could be caused by environmental factors like the EC of the habitat water, as well as the age and timing of sample collection.

In this species, Elhaak *et al*. (2015) found that while lignin behaved differently and was present in greater amounts in winter than summer, carbohydrates, cellulose, and hemicellulose were shown to be present in greater amounts in summer. In light of this, variations in the chemical composition from earlier studies may also be caused by the sampling season.

The essential place of carbohydrates in cell metabolism and their abundance compared to other organic osmolytes indicate their importance in plant defense. Carbohydrates, especially mono- and disaccharides, in addition to helping to regulate osmosis, affect plant survival (Farrokhzad *et al*., 2022). Saccharides are the main substrates used in respiratory processes, which provide energy for cellular defense responses and protection against pathogenic agents. Carbohydrates provide the carbon skeleton for the synthesis of defense compounds, including secondary metabolites such as flavonoids, stilbenes, and lignins (Jeandet *et al*., 2022). Dietary fiber consists of different parts such as cellulose, non-cellulosic polysaccharides such as hemicelluloses, and non-carbohydrate parts such as lignin. These are also the main structural components of the cell wall in plants (George *et al*., 2020). In the present study, the Pearson correlation coefficient between the variables showed a significant negative correlation between the amount of fiber and carbohydrates, which can indicate the conversion of carbohydrates into cellulose, hemicellulose, and defensive compounds such as lignin. The amount of fiber and ash showed a significant positive correlation with unsaturated fatty acids and a significant negative correlation with saturated fatty acids (Table 5). Ash usually represents the inorganic part of the plant. The amount of plant ash varies depending on the species, organ, and age of the plant and environmental conditions (Lacey *et al.*, 2018). According to a study conducted by Sarker *et al*. (2018), salt stress increased the amount of protein, ash, and dietary fiber in edible amaranth plants (*Amaranthus tricolor*) by 18%, 6%, and 16%, respectively. As previously mentioned, stress can lead to plants accumulating unsaturated fatty acids as a stress response (Coniglio *et al*., 2023). The increase in fiber and the accumulation of unsaturated fatty acids in these plants appear to be caused by environmental stresses, particularly the rise in salinity and water EC in the three sampling locations in recent years. This is demonstrated by the positive correlation that has been observed between these two parameters.

The cattail plant has many uses, and the practical potentials of this plant have been reported in various studies. *T. domingensis* is one of the most edible aquatic plants in the world. Its pollen is a wonderful food, and its unopened flowers and rhizome are edible. In some countries, such as Congo, Nigeria, and Argentina, indigenous communities use it as raw or cooked (Hellmuth, 2021). In a research in Nigeria, it has been suggested that *T. domingensis* fodder is a higher nutritional value and more economical alternative to sorghum straw for feeding cattle. The authors have indicated that the concentration of red blood cells in cows fed with such fodder has increased, and the total cost of feeding has decreased between 49.60 and 61.62 dollars

compared to the use of sorghum straw (John *et al*., 2022).

Table 5- Pearson's correlation coefficients between the variables

Variable	Carbohydrate	Protein	Fiber	Ash	SFA	UFA
Moisture	-0.012	0.116	-0.023	-0.072	0.039	-0.038
Carbohydrate	-	-0.233	-0.958**	-0.034	0.642	-0.637
Protein		-	0.089	-0.424	0.160	-0.160
Fiber			-	0.315	-0.832**	0.828**
Ash				-	-0.878*	0.791*
SFA					-	-1.000

Significant at the level 0.05*Significant at the level 0.01, **

It has been suggested that cattail fibers are a promising natural source for the production of oil absorbents (Cao *et al*., 2016). Physical and chemical properties, micro/nanostructure, and mechanical properties of cattail fiber have been investigated. The chemical component and infrared spectroscopic analysis show that the fiber of cattail plant has lignin content (20.6%) and wax content (11.5%), which lead to improved corrosion resistance, thermal stability, and lipophilic-hydrophobic properties of this fiber (Wu *et al*., 2021). Another advantage of this plant is its phytoremediation ability. It has been reported that *Typha* species exposed to urban sewage and metal pollutants are able to absorb metal elements in their roots and transfer them to the rhizome and leaves, so they are one of the best species for phytoremediation (Bonanno & Cirelli, 2017).

In addition to Khuzestan, *T. domingensis* is found in the waters of northern, northwestern, western, central, northeastern, and southeastern regions of Iran (Hamdi & Assadi, 2003). It is therefore a valuable economic species that can be utilized in a variety of industries, including the food industry, depending on the water conditions of its habitat. More thorough studies on the nutritional content and fiber characteristics of this aquatic plant, however, should be conducted in the future to investigate its application in a variety of industries. This plant has a potential to be included in the diet of humans and livestock, but despite the nutritional value of this plant, the safety of the plant's habitat and the absence of contamination by heavy metals should be ensured first, and then its cultivation and development should be considered for food consumption.

Conclusion

The oil content and fatty acid profile of the cattail (*Typha domingensis*) samples, as well as certain chemical compositions like ash, moisture, fiber, protein, and carbohydrates, were assessed in this study. The samples were collected from three different locations: Shadegan Wetland, Hoveyzeh, and Hamidabad (Dez River). The results showed that the oil content of the samples from the three assessed sites, from both the aerial and underground parts, differs significantly. Stems and leaves have higher oil content than rhizomes and roots. Overall, 12 fatty acids were found, comprising 3 unsaturated and 9 saturated fatty acids. In Shadegan samples, the highest concentration of polyunsaturated fatty acids (oleic acid, linoleic acid, and alpha-linolenic acid) was found. The amounts of fiber, moisture, ash, protein, and carbohydrates in the samples ranged from 43.34 (H1) to 45.93% (H2), 12.57 (H1) to 17.84% (H2), 3.64 (H1) to 4.25%(S1), 6.20 (S1) to 6.40% (H2), and 23.19 (H2) to 32.18% (H1), respectively. All the assessed components of the examined samples were significantly different. Due to the fact that this plant is widely distributed throughout Iran, researchers are encouraged to study its nutritional value and fiber qualities for application in a variety of industries, depending on its habitat.

Acknowledgment

The authors express their sincere gratitude to Mr. Behnam Amirshekari for his help in collecting samples and some experiments.

Author Contributions

M. Farasat: Conceptualization, Data curation, Formal analysis, Methodology, Writing–original draft, Writing–review and editing. **M. Tadayoni:** Conceptualization, Data curation, Formal analysis, Methodology, Writing–review and editing. **M. Shojaee Barjouee**: Data curation, Investigation, Formal analysis, Resources.

Funding Sources

This research did not receive any specific grant from funding agencies in the public, commercial, or not-for-profit sectors.

Conflict of Interest

The authors declare that there is no conflict of interest.

References

1. Ahmed, S., Shah, P., & Ahmed, O. (2024). Biochemistry, Lipids. In StatPearls [Internet]; StatPearls: Treasure Island, FL, USA.
2. Ahmad Dar, N., Hamid, A., Pandit, A.K., Ganai, B.A., Ullah Bhat, S., & Hussain, A. (2013). Total lipid content in macrophytes of Wular lake, A Ramsar site in Kashmir Himalaya. *International Journal of Plant Physiology and Biochemistry*, *5*(1), 11-15. https://doi.org/10.5897/IJPPB12.020
3. Akram, A., & Jabeen, Q. (2022). Pharmacological evaluation of *Typha domingensis* for its potentials against diet-induced hyperlipidemia and associated complications. *Tropical Journal of Pharmaceutical Research*, *21*(3), 563-569, https://doi.org/10.4314/tjpr.v21i3.16
4. AOAC. (1995). *Official methods of analysis 16th Ed*. Association of official analytical chemists. Washington DC, USA.
5. AOAC. (2000). *Official Methods of Analysis. 17th Edition*, The Association of Official Analytical Chemists, Gaithersburg, MD, USA.
6. AOAC. (2005). *Association of Official Analytical Chemist, Official Methods of Analysis. 18th Edition*, AOAC International, Gaithersburg, MD, USA.
7. Azish, S., Asareh, A., & Khodadadi Dehkordi, D. (2023). Quality assessment of Dez River water in terms of efficiency in pressurized irrigation systems. *Water Resources Engineering Journal*, *15*(55). https://doi.org/10.30495/wej.2023.17899.2031
8. Bansal, S., Lishawa, S.C., Newman, S., Tangen, B.A., Wilcox, D., Albert, D., Anteau, M.J., Chimney, M.J., Cressey, R.L., DeKeyser, E., Elgersma, K.J., Finkelstein, S.A., Freeland, J., Grosshans, R., Klug, P.E., Larkin, D.J., Lawrence, B.A., Linz, G., Marburger, J., Noe, G., Otto, C., Reo, N., Richards, J., Richardson, C., Schrank, A.J., Svedarsky, D., Travis, S., Tuchman, N., & Windham-Myers, L. (2019). *Typha* (cattail) invasion in North American wetlands: biology, regional problems, impacts, ecosystem services, and management. *Wetlands*, *39*(4), 645-684. https://doi.org/10.1007/s13157-019-01174-7
9. Bishehkolaei, M., & Pathak, Y. (2024). Influence of omega n-6/n-3 ratio on cardiovascular disease and nutritional interventions, *Human Nutrition & Metabolism*, *37*, 200275. https://doi.org/10.1016/j.hnm.2024.200275
10. Brahma, S., Nath, B., Basumatary, B., Das, B., Saikia, P., Patir, K., & Basumatary, S. (2022). Biodiesel production from mixed oils: A sustainable approach towards industrial biofuel production. *Chemical Engineering Journal Advances*, *10*, 100284. https://doi.org/10.1016/j.ceja.2022.100284
11. Bonanno, G., & Cirelli, G.L. (2017). Comparative analysis of element concentrations and translocation in three wetland congener plants: *Typha domingensis*, *Typha latifolia* and *Typha*

angustifolia. *Ecotoxicology and Environmental Safety*, *143*, 92-101. https://doi.org/10.1016/j.ecoenv.2017.05.021

12. Cañavate, J-P., & Fernández-Díaz, C. (2022). Salinity induces unique changes in lipid classes and fatty acids of the estuarine haptophyte *Diacronema vlkianum*. *European Journal of Phycology*, *57*(3), 297-317. https://doi.org/10.1080/09670262.2021.1970234
13. Cao, S., Dong, T., Xu, G., & Wang, F. (2016). Study on structure and wetting characteristic of cattail fibers as natural materials for oil sorption. *Environmental Technology*, *37*(24), 3193-9. https://doi.org/10.1080/09593330.2016.1181111.
14. Chakma, K., Cicek, N., & Rahman, M. (2017). Fiber extraction efficiency, quality and characterization of cattail fibres for textile applications. CSBE/SCGAB 2017 Annual Conference, Canad Inns Polo Park, Winnipeg, Manitoba, 6-10 August 2017.
15. Coniglio, S., Shumskaya, M., & Vassiliou, E. (2023). Unsaturated fatty acids and their immunomodulatory properties. *Biology*, *12*(2), 279. https://doi.org/10.3390/biology12020279
16. Czumaj, A., & Śledziński, T. (2020). Biological role of unsaturated fatty acid desaturases in health and disease. *Nutrients*, *12*(2), 356. https://doi.org/10.3390/nu12020356
17. Daley, C.A., Abbott, A., & Doyle, P.S. (2010). A review of fatty acid profiles and antioxidant content in grass-fed and grain-fed beef. *Nutrition Journal, 9*, 10. https://doi.org/10.1186/1475-2891-9-10
18. de Carvalho, C.C.C.R., & Caramujo, MJ. (2018). The various roles of fatty acids. *Molecules*. *9*, *23*(10), 2583. https://doi.org/ 10.3390/molecules23102583.
19. Dieffenbacher, A.,& Pocklington, W.D. (1992).*Standard Methods for the Analysis of Oils, Fats and Derivatives, 1st Supplement to the 7th Edition* (*IUPAC Chemical Data*), Wiley, 184 pages.
20. Eid, E.M., & Shaltout, K.H. (2017). Seasonal allocation of carbohydrates between aboveand below-ground organs of *Typha domingensis*. *Feddes Repertorium*, *128*, 1–10, https://doi.org/10.1002/fedr.201600004
21. El-Amier, Y.A. (2013). Spatial distribution and nutritive value of two *Typha* species in Egypt. *Egyptian Journal of Botany*, *53*(1), 91-113.
22. Elhaak, M.A., Mohsen, A.A., Hamada, E.A.M., & El-Gebaly, F.E. (2015). Biofuel production from phragmites australis (cav.) and *Typha domingensis* (Pers.) plants of Burullus Lake. *Egyptian Journal of Experimental Biology*, *11*(2), 237–243.
23. Farrokhzad, Y., Babaei, A., Yadollahi, A., Beyraghdar Kashkooli, A., & Mokhtassi-Bidgoli, A. (2022). *In vitro* rooting, plant growth, monosaccharide profile and anatomical analysis of *Phalaenopsis* regenerants under different regions of visible light. *South African Journal of Botany*, *149*, 622-631. https://doi.org/10.1016/j.sajb.2022.06.039
24. Foladvand, S., Sayad, G., Hemadi, K., & Moazed, H. (2014). Assessing changes in quality and quantity of entering stream to Hor-Al-Azim Wetland regarding Karkhe Dam construction. *Journal of Irrigation Sciences and Engineering*, (JISE), *36*(4), 1-8. https://doi.org/20.1001.1.25885952.1392.36.4.1.8
25. Fretts, A.M., Imamura, F., Marklund, M., Micha, R., Wu, J.H.Y., Murphy, R.A., Chien, K.L., McKnight, B., Tintle, N., Forouhi, N.G., Qureshi, W.T., Virtanen, J.K., Wong, K., Wood, A.C., Lankinen, M., Rajaobelina, K., Harris, T.B., Djoussé, L., Harris, B., Wareham, N.J., Steffen, L.M., Laakso,M., Veenstra, J., Samieri, C., Brouwer, I.A., Yu, C.I., Koulman, A., Steffen, B.T., Helmer, C., Sotoodehnia, N., Siscovick, D., Gudnason, V., InterAct Consortium; Wagenknecht, L., Voutilainen, S., Tsai, M.Y., Uusitupa, M., Kalsbeek, A., Berr, C., Mozaffarian, D., & Lemaitre, R.N. (2019). Associations of circulating very-long-chain saturated fatty acids and incident type 2 diabetes: a pooled analysis of prospective cohort studies. *The American Journal* of *Clinical Nutrition*, 1, 109(4), 1216-1223. https://doi.org/10.1093/ajcn/nqz005

26. Fruet, A.C., Seito, L.N., Rall, V.L., & Di Stasi, LC. (2012). Dietary intervention with narrow-leaved cattail rhizome flour (*Typha angustifolia* L.) prevents intestinal inflammation in the trinitrobenzenesulphonic acid model of rat colitis. *BMC Complementary and Alternative Medicine*. https://doi.org/10.1186/1472-6882-12-62
27. George, N., Andersson, A.A.M., Andersson, R., & Kamal-Eldin, A. (2020). Lignin is the main determinant of total dietary fiber differences between date fruit (*Phoenix dactylifera* L.) varieties.
28. *NFS Journal*, 21, 16-21. https://doi.org/10.1016/j.nfs.2020.08.002.
29. Gershuni, V.M. (2018). Saturated fat: Part of a healthy diet. *Current Nutrition Reports*, *7*(3), 85-96. https://doi.org/10.1007/s13668-018-0238-x
30. Ghorbani, Z., Amanipoor, H., & Battaleb-Looie, S. (2022). Water quality simulation of Dez River in Iran using QUAL2KW model. *Geocarto International*, *37*(4), 1126-1138. https://doi.org/10.1080/10106049.2020.1762763
31. Guo, Q., Liu, L., & Barkla, B.J. (2019). Membrane lipid remodeling in response to salinity. *International Journal of Molecular Sciences*, *20*, 4264. https://doi.org/10.3390/ijms20174264
32. Guzmán-Maldonado, S.H., Osuna-García, J.A., & Herrera-González, J.A. (2017). Effect of locality and maturity on the fatty acid profile of avocado 'Hass' fruit. *Revista mexicana de ciencias agrícolas*, *8*(19), 3885-3896. https://doi.org/10.29312/remexca.v0i19.657
33. Hamdi, S.M.M., & Assadi, M. (2003). *Flora of Iran No.42*: Typhaceae, Research Institute of Forests and Rungelands, Tehran, Iran.
34. Hassan, U.F., Hassan, H.F., Baba, H., & Suleiman, A.S. (2018). The feed quality status of whole *Typha domingensis* plant. *International Journal of Scientific & Engineering Research*, *9*(5), 1609-1617.
35. He, M., & Ding, N.Z. (2020). Plant unsaturated fatty acids: Multiple roles in stress response. *Frontiers in Plant Science*, *11*, Article 562785, https://doi.org/10.3389/fpls.2020.562785
36. Hellmuth, N. (2021). *Edible plants of wetlands Cattail, Tule Typha domingensis*. Flaar Mesoamerica, Guatemala.
37. Ichihara, K., Kohsaka, C., Tomari, N., Yamamoto, Y., & Masumura, T. (2020). Determination of free fatty acids in plasma by gas chromatography. *Analytical Biochemistry*, 15, 603, 113810. https://doi.org/10.1016/j.ab.2020.113810
38. ISO. (2000). Animal and vegetable fats and Oils–preparation of methyl esters of fatty acid / 5509 /ISO https://standards.iteh.ai/catalog/standards/sist/37abc0ea-3e75-4531-bb43-c6912f85a0c5/iso-5590-2000
39. Jeandet, P., Formela-Luboińska, M., Labudda, M., & Morkunas, I. (2022). The role of sugars in plant responses to stress and their regulatory function during development. *International Journal of Molecular Sciences*, *5*, 23(9), 5161. https://doi.org/10.3390/ijms23095161
40. John, M.O., Rufai, M.A., Sunday, A.J., Fernando, E., Richard, K., Eva, I., Maidala, A., Amos, M., Chana, M., Hannatu, C., & A, O.S. (2022). Cattail (*Typha domingensis*) silage improves feed intake, blood profile, economics of production, and growth performance of beef cattle. *Tropical Animal Health and Production*, *12*, *54*(1), 48. https://doi.org/10.1007/s11250-022-03066-1
41. Khalid, A., Algarni, A.S., Homeida, H.E., Sultana, S., Javed, S.A., Rehman, Z.U., Abdalla, H., Alhazmi, H.A., Albratty, M., & Abdalla, A.N. (2022). Phytochemical, Cytotoxic, and Antimicrobial Evaluation of *Tribulus terrestris* L., *Typha domingensis* Pers., and *Ricinus communis* L.: Scientific Evidences for Folkloric Uses. *Evidence-Based Complementary and Alternative Medicine*, *27*, 6519712. https://doi.org/10.1155/2022/6519712
42. Khider, T.O., Omer, S., & Taha, O. (2012). Alkaline pulping of *Typha domingensis* stems from Sudan. *World Applied Sciences Journal*, *16*(3), 331-336.

43. Labdelli, A., Tahirine, M., Foughalia, A., Zemour, K., Cerny, M., Adda, A., Simon, V., & Merah, O. (2022). Effect of ecotype and environment on oil content, fatty acid, and sterol composition of seed, kernel, and epicarp of the Atlas pistachio. *Agronomy*, *12*(12), 3200. https://doi.org/10.3390/agronomy12123200
44. Lacey, J.A., Aston, J.E., & Thompson, V.S. (2018). Wear properties of ash minerals in biomass. *Perspective* 6, article 119, https://doi.org/10.3389/fenrg.2018.00119
45. Lemaitre, R.N., & King, I.B. (2022). Very long-chain saturated fatty acids and diabetes and cardiovascular disease. *Current Opinion in Lipidology*, *1,33*(1), 76-82. https://doi.org/10.1097/MOL
46. Leray, C. (2020). Lipids and Health. *Oilseeds and fats, Crops and Lipids*, 27, 25. https://doi.org/10.1051/ocl/2020018
47. Maryum, Z., Luqman, T., Nadeem, S, Khan, S.M.U.D., Wang, B., Ditta, A., & Khan, M.K.R. (2022). An overview of salinity stress, mechanism of salinity tolerance and strategies for its management in cotton. *Frontiers in Plant Science*, *13*, 907937 https://doi.org/10.3389/fpls.2022.907937
48. McCready, M.R., Guggols, J., Silviera, V., & Owens, S.H. (1950). Determination of starch and amylose in vegetables. *Analytical Chemistry*, *22*, 1156-1158. https://doi.org/10.1021/ac60045a016
49. Nasirian, H., & Salehzadeh, A. (2019). Effect of seasonality on the population density of wetland aquatic insects: A case study of the Hawr Al Azim and Shadegan wetlands, Iran. *Vet World*, *12*(4), 584-592. https://doi.org/10.14202/vetworld.2019.584-592
50. Orsavova, J., Misurcova, L., Ambrozova, J.V., Vicha, R., & Mlcek, J. (2015). Fatty acids composition of vegetable oils and its contribution to dietary energy intake and dependence of cardiovascular mortality on dietary intake of fatty acids. *International Journal of Molecular Sciences*, *16*, 12871-12890. https://doi.org/10.3390/ijms160612871
51. Pandey, A., & Verma, R.K. (2018). Taxonomical and pharmacological status of *Typha*: A Review, *Annals of Plant Sciences*, *7*(3), 2101-2106. https://doi.org/10.21746/aps.2018.7.3.2
52. Pipoyan, D., Stepanyan, S., Stepanyan, S., Beglaryan, M., Costantini, L., Molinari, R., & Merendino, N. (2021). The effect of trans fatty acids on human health: Regulation and consumption patterns. *Foods*, *10*(10), 2452. https://doi.org/10.3390/foods10102452
53. Raygani, B., Goodarzi, F., Talebi, A., Talaeian Araghi, M., & Hashemi, H. (2020). Assessment of the probable impacts of land use changes on water quality in shadeghan wetland using remotely sensed data. *Journal of Spatial Analysis Environmental Hazards*, *7*(2), 33-48. https://doi.org/10.29252/jsaeh.7.2.33
54. Ruiz-Carreraa, V., Hernández-Piedraa, G., Arredondo-Vegab, B.O., & Sánchez, A.J. (2016). Fatty acids in leaf and seed of three emergent aquatic macrophytes. *Revista Latinoamericana de Química*, *44*(1-3), 7-15.
55. Sarker, U., Islam, M.T., & Oba, S. (2018). Salinity stress accelerates nutrients, dietary fiber, minerals, phytochemicals and antioxidant activity in Amaranthus tricolor leaves. *PLoS One*. *1;13*(11), e0206388. https://doi.org/10.1371/journal.pone.0206388
56. Shadhin, M., Rahman, M., Jayaraman, R., & Mann, D. (2021). Novel cattail fiber composites: converting waste biomass into reinforcement for composites. *Bioresources and Bioprocessing*, *8*(1), 101. https://doi.org/10.1186/s40643-021-00453-8
57. Teh, K.Y., Loh, S.H., Aziz, A., Takahashi, K., Mohd Effendy, A.V., & Cha, T.S. (2021). Lipid accumulation patterns and role of different fatty acid types towards mitigating salinity fluctuations in *Chlorella vulgaris*. *Scientific Reports*, *11*, 438. https://doi.org/10.1038/s41598-020-79950-3

58. Uotila, P., Raus, T., Tomović, G., & Niketić, M. (2010). *Typha domingensis* (Typhaceae) new to Serbia. *Botanica Serbica, 34*(2), 111-114.
59. Wu, S., Zhang, J., Li, C., Wang, F., Shi, L., Tao, M., Weng, B., Yan, B., Guo, Y., & Chen, Y. (2021). Characterization of potential cellulose fiber from cattail fiber: A study on micro/nano structure and other properties. *International Journal of Biological Macromolecules*, *193*(A), 27-37. https://doi.org/10.1016/j.ijbiomac.2021.10.088
60. Zhang, Y., van Geel, B., & Gosling, W.D. (2020). *Typha* as a wetland food resource: evidence from the Tianluoshan site, Lower Yangtze Region, China. *Vegetation History and Archaeobotany, 29*, 51–60. https://doi.org/10.1007/s00334-019-00735-4

نشریه پژوهشهای علوم و صنایع غذایی ایران
https://ifstrj.um.ac.ir

مقاله پژوهشی

جلد ۲۰، شماره ۶، بهمن-اسفند، ۱۴۰۳، ص. ۱۵۳-۱۳۷

پروفایل اسید چرب و ترکیب شیمیایی سه جمعیت لویی (*Typha domingensis*) از جنوب ایران

مونا شجاعی برجوئی[۱]- معصومه فراست[۲و۳]- مهرنوش تدینی[۴*]

چکیده

لیپیدها گروه بزرگی از ترکیبات شیمیایی با ا سیدهای چرب در ساختار خود ه ستند که برای عملکرد طبیعی همه موجودات ضروری‌اند. ا سیدهای چرب غیرا شباع چندگانه با پیوندهای م ضاعف متعدد از جمله امگا-۳ و امگا-۶ به‌عنوان ترکیبات شیمیایی مفید برای سلامت ان سان شناخته می شوند. اخیرا تلاش زیادی برای یافتن روغن‌هایی با ویژگی‌های سودمند ویژه، به‌دلیل استفاده گسترده از روغن‌های گیاهی در صنایع غذایی و دیگر صنایع انجام شده است. لویی جنوبی گیاهی است که تقریباً تمام قسمت‌های آن خوراکی است بویژه ریزوم‌های نشاسته‌ای آن که دارای ترکیب پروتئینی قابل مقایسه با ذرت یا برنج است. در این تحقیق، نمونه‌های گیاهی از سه نقطه جنوب ایران شامل تالاب شادگان، هویزه (تالاب هورالعظیم) و حمیدآباد (رودخانه دز) جمع آوری و محتوای روغن و نوع اسیدهای چرب و همچنین برخی ترکیبات شیمیایی از جمله خاکستر، رطوبت، فیبر، پروتئین و کربوهیدرات آنها ارزیابی و مقایسه شد. روغن با استفاده از تکنیک سوکسله استخراج شد و ترکیب اسیدهای چرب توسط GC/MS تعیین شد. میانگین میزان روغن در اندام‌های هوایی (ساقه و برگ) و زیرزمینی (ریزوم و ریشه) به‌ترتیب ۲/۶۲ و ۱/۵۲ در صد بود. نمونه‌ها حاوی ۱۲ اسید چرب بودند که ۳ ا سید چرب غیرا شباع و ۹ اسید چرب اشباع بودند. در ریشه و ریزوم بیشترین نسبت اسیدهای چرب غیراشباع شامل اولئیک اسید، اسید لینولئیک، اسید آلفا-لینولنیک ۱/۵۱±۶۵/۸۵ درصد و در ساقه و برگ ۰/۰۹±۴۱/۱۰ درصد بود. مقادیر فیبر، رطوبت، خاکستر، پروتئین و کربوهیدرات‌ها در نمونه‌ها به‌ترتیب از ۴۳,۳۴ تا ۴۵,۹۳- ۱۲,۵۷ تا ۱۷,۸۴- ۳,۶۴ تا ۴,۲۵- ۶,۲۰ تا ۶,۴۰ درصد و ۲۳,۱۹ تا ۳۲,۱۸ درصد متغیر بود. محتوای فیبر بالا و ظرفیت این گیاه برای رشد سریع و گسترده در آب شیرین و شور، آن را به یک کاندید مناسب برای گنجاندن در رژیم غذایی انسان و حیوان از طریق طرح‌های ا صلاحی کشاورزی تبدیل می‌کند.

واژه‌های کلیدی: اسید چرب، PUFAs، فیبر، *Typha domingensis*

۱ و ۴- به‌ترتیب کارشناس ارشد فارغ‌التحصیل و دانشیار، گروه علوم و صنایع غذایی، واحد اهواز، دانشگاه آزاد اسلامی، اهواز، ایران
۲- مرکز تحقیقات علوم دارویی دریایی، دانشگاه علوم پزشکی جندی شاپور اهواز، اهواز، ایران
۳- استادیار، گروه‌های زراعت و زیست‌شناسی، واحد اهواز، دانشگاه آزاد اسلامی، اهواز، ایران
(*- نویسنده مسئول: Email: me.tadayoni@iau.ac.ir)

https://doi.org/10.22067/ifstrj.2024.89632.1365

Iranian Food Science and Technology Research Journal
Homepage: https://ifstrj.um.ac.ir

Research Article
Vol. 20, No. 6, Feb.-Mar., 2025, p. 155-169

Development of Fermentation-induced Soymilk Gel: Effects of Different Lactic Acid Bacteria on the Physicochemical Characteristics

F. Rahmani[1], A. Moayedi[2*], M. Khomeiri[3], M. Kashiri[2]

1, 2 and 3- Ph.D. Student, Associate Professor and Professor, Department of Food Science and Technology, Faculty of Food Science, Gorgan University of Agricultural Sciences and Natural Resources, Gorgan, Iran, respectively.
(*- Corresponding Author Email: amoayedi@gau.ac.ir)

Received: 11.09.2024
Revised: 08.12.2024
Accepted: 10.12.2024
Available Online: 07.01.2025

How to cite this article:
Rahmani, F., Moayedi, A., Khomeiri, M., & Kashiri, M. (2025). Development of fermentation-induced soymilk gel: effects of different lactic acid bacteria on the physicochemical characteristics. *Iranian Food Science and Technology Research Journal*, *20*(6), 155-169. https://doi.org/10.22067/ifstrj.2024.89764.1366

Abstract

Nowadays, plant-based dairy alternatives have gained considerable attention. However, the textural and sensorial characteristics of plant-based products limit their acceptance. The exploitation of lactic acid bacteria has been proposed as a promising approach to developing plant-based dairy analogs. In this study, the performance of three proteolytic lactic acid bacteria in the induction of soymilk gelation was compared and their effects on the physicochemical properties of resulting gels were investigated. *Lactiplantibacillus plantarum MCM4*, *Streptococcus thermophilus*, and *Weissella confusa MDM8*) were inoculated to the soy milk matrix, and incubated at 37 °C until reaching pH 4.7. To understand the effects of acidifying and proteolytic activity of starter culture, syneresis, cell counts, free amino acid content (O-phthalaldehyde method), evaluation of proteolysis using sodium dodecyl sulfate-polyacrylamide gel electrophoresis (SDS-PAGE) and textural parameters of soymilk gels during fermentation were investigated. There was a significant difference among the strains in terms of viable cell counts and proteolytic activity during fermentation ($p < 0.05$). The amount of syneresis was also different among the resulted gels as it was in the range from 61% (sample fermented with *S. thermophilus*) to 69.5% (fermented with *L. plantarum* MCM4). The main soy proteins were degraded to different extents as a function of fermentation time. Texture analysis showed that fermentation of soymilk with *W. confusa MDM8* resulted in soy gel with higher firmness and consistency, while the sample fermented with *L. plantarum MCM4* had higher adhesiveness and viscosity index. Overall, it can be concluded that *L. plantarum* MCM4, *W. confusa MDM8*, and *S. thermophilus* can be introduced as starter cultures for the production of novel soymilk gels with reasonable properties.

Keywords*:* Dairy alternatives, Lactic acid bacteria, Plant-based Proteins, Sustainable food production

https://doi.org/10.22067/ifstrj.2024.89764.1366

Introduction

Animal welfare, medical reasons such as cow's milk allergy and lactose intolerance, ethical concerns, and sustainable food production have all increased the demand for plant-based alternatives to dairy products (McCarthy *et al.*, 2017; Rastogi *et al.*, 2022). Because of their high protein content, and health-promoting effects, soy products have received much attention for the development of plant-based dairy alternatives. However, the sensory characteristics of soy-based products such as soy milk, soy gel, and soy protein isolate are not yet satisfactory and further research should be conducted to find suifie processes to mimic dairy products with better texture, aroma, taste, and shelf life (Genet *et al.*, 2023). Soymilk is a good source of protein for plant-based products and the concept of soymilk gel is significant in the food industry due to its various applications and benefits (Yang *et al.*, 2020). Soymilk gel can be used as a substitute for milk fat in cheese production, which can enhance the saturated/unsaturated fat balance in cheese without compromising nutritional value, making it beneficial for individuals with health issues related to saturated fatty acid and cholesterol content in dairy products (Rojas-Nery *et al.*, 2015). During the formation of soymilk gel, the coagulant may influence the extent of denaturation, while the electrostatic effect can disrupt the electric double layer on the protein colloid's surface, leading to increased aggregation and the development of a gel. The formation of the soymilk gel network is affected by various factors, including protein sources, the presence of stabilizers, pH, and temperature. Bacterial fermentation can be regarded as an alternative method for preparing soy gel instead of chemical coagulants (Wang *et al.*, 2022). Among the bacteria, lactic acid bacteria (LAB) have a unique place in the fermentation of plant-based products as they are recognized as safe, and have the potential to produce bioactive metabolites (such as bacteriocins and bioactive peptides) and aromatic compounds as well as reduce anti-nutritional components. Additionally, LAB increase the product shelf life because of the production of organic acids and hydrogen peroxide (Kong *et al.*, 2022; Mishra & Mishra, 2018; Somjid *et al.*, 2022). In this regard, certain LAB displayed favorable technological and functional attributes, such as protein hydrolysis, acidification, exopolysaccharide production (EPS), and aroma generation, which can improve the sensory characteristics of plant-based dairy products (Böni et *al.*, 2016; García-Cano *et al.*, 2019; Kamarinou *et al.*, 2022; Kong *et al.*, 2022).

This study analyzes the relationship between the textural and physicochemical characteristics of fermented soymilk gel and the proteolytic and acidifying activity of three LAB strains. In this regard, syneresis, cell counts, proteolysis (O-phthalaldehyde method), evaluation of proteolysis using SDS-PAGE, and textural parameters of soymilk gels during fermentation were compared. This work aims to provide a better understanding of texture modulation and physicochemical properties in plant protein substitutes by investigating the proteolytic ability of LAB in soy milk. Understanding this ability can help us introduce a starter for plant-based alternatives with desirable texture, flavor, and less allergenicity.

Materials and Methods

Chemicals and Bacterial Strains

L. plantarum MCM4, W. confusa MDM8, and *S. thermophilus* used in this study had been previously isolated from cabbage pickle (Karimian *et al.*, 2020), sourdough (Khanlari *et al.*, 2021) and yogurt (Moslemi *et al.*, 2023), respectively and stored in the microbial collection at the Department of Food Science and Technology (Gorgan University of Agricultural Sciences and Natural Resources, Gorgan, Iran). The frozen cultures were activated by subculturing in De Man–Rogosa–Sharpe (MRS) broth and incubating at 37 °C for 24 h. Dithiotritol (DTT) and L-Serine were purchased from Biobasic Co. (Canada). The chemicals and reagents for SDS-PAGE analysis were purchased from Sigma Aldrich (St.Louis,

Missouri, United States). Microbial culture media and other chemicals (OPA, sodium dodecyl sulfate, and di-sodium tetraborate) were purchased from Merck Co. (Darmstadt, Hesse, Germany).

Soymilk and Doy Gel Preparation

The preparation steps of soy milk gel are shown in Fig. 1 (Saraniya & Jeevaratnam, 2015). Yellow soybeans (Katul variety from the local farms, Golestan province) were soaked in water (1:3, w/v) for 10 h and ground with the blender (Philips, Netherlands,1400 W) (1:5 w/v, soy: distilled water). The mixture was then filtered and mixed with 1% glucose and soy protein isolate (SPI) until reaching 10% dry matter and heated at 95 ◦C for 15 min. After cooling to room temperature, bacterial suspensions (*L. plantarum MCM4, W. confusa MDM8, or S. thermophilus*) with optical density (OD) of 1 at 600 nm were inoculated (2% v/v). The inoculated soymilk was incubated at 37˚C until reaching pH 4.7. The fermentation was terminated by cooling the soymilk gels to 4°C.

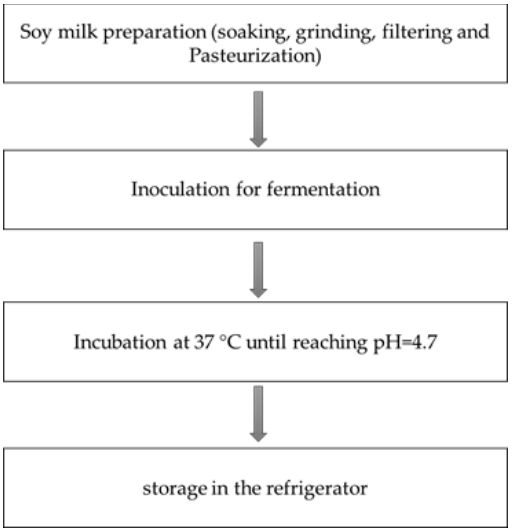

Fig. 1. Production process of soymilk gel

Determination of pH and Titratable Acidity

The pH levels of the samples were assessed with a digital pH meter throughout the fermentation process of soy milk. For titratable acidity (TA) determination, 10 grams of sample was diluted with 90 ml of distilled water and titrated with 0.1 mol/L NaOH. TA was reported as % lactic acid (Rahmani *et al.*, 2021).

Measurement of the Syneresis Value

The extent of syneresis was measured according to the method described by Rahmani et al. Tubes containing 20 grams of samples were centrifuged (10°C) at 4000 × g for 15 min. The weight percentage of released water after centrifugation was calculated and reported as syneresis extent (Rahmani *et al.*, 2021).

$$\text{Syneresis}=\frac{W1}{W2}\times 100 \quad (1)$$

where W1 is the weight of the supernatant and W2 is the weight of the sample.

Determination of Zeta-Potential

The zeta potential of soymilk gel was measured using a laser diffraction and dynamic light scattering analyzer (CORDOUAN Technologies, France). For zeta-potential measurements, the mixtures were diluted 100-fold with deionized water and placed into a specialized capillary cuvette containing two electrodes (Masiá *et al.*, 2022).

Viable Cell Counts

The changes in viable LAB cell counts (as Log CFU/mL) during fermentation were

evaluated using the pour plate technique. After preparing the serial dilutions, one mL of appropriate dilution from each sample was transferred into the plate and 15 ml of MRS agar was added. The plates were then incubated at 37 °C for 48 h, and the colonies were counted (only plates with 30-300 colonies). Two sequential dilutions for each sample (three replications) were analyzed. The following formula was used for cell count determination (Taheri *et al.*, 2019) :

$$N = \frac{\Sigma Ci}{V(n1 + 0.1n2)d} \quad (2)$$

where C represents the total number of colonies counted on all plates; V is the volume applied to each plate (in mL); n1 is the number of plates counted in the first dilution; n2 is the number of plates counted in the second dilution, and d is the dilution factor for the initial count.

Evaluation of Proteolysis Using OPA

The proteolysis in the soymilk was evaluated by measuring free amino groups (L-serine equivalent) using the OPA reagent (Shakerian *et al.*, 2015). Aliquot of 2.5 ml of fermented soymilk or soy gel was mixed with 5 ml of 5 % TCA in a test tube. The mixture was centrifuged at ۲000 × g for 1۰ min and filtered through a Wathman (0.45 µ) filter paper. Then, 200 µL of filtrate was added to 3 ml of OPA reagent and the absorbance of the mixture was read at 340 nm (UV-visible spectrophotometer, model Photonix Ar2015, IRAN) after 2 min incubation at room temperature. L-serine was used as standard amino acid for the quantification. The OPA reagent was prepared using the method outlined by Shakerian et al. (2015). In summary, 2.5 ml of 20% w/v SDS was added to a glass flask containing 25 ml of 100 mM sodium tetraborate. Then, 40 mg OPA reagent (previously dissolved in 1 ml methanol) was added to the flask. Finally, 150 µl of 20 mM dithiothreitol (DTT) was added to the flask and distilled water was then added to reach the final volume of 50 ml.

Sodium Dodecyl Sulfate-polyacrylamide Gel Electrophoresis (SDS-PAGE) Analysis

SDS-PAGE analysis was performed as described by Shirotani *et al*. using a 15% separating gel and 4% stacking gel. Samples were mixed with Tris buffer containing (10 mM Tris–HCl buffer, pH 8-9, 10% glycerol, 2.5% SDS, 5% β-mercaptoethanol, and 0.002% bromophenol blue), then heated at 95ºC for 5 min. Finally, 25 µL of the prepared sample was injected into the electrophoresis gel. The period of electrophoresis was 4 h at 130 volts, then, protein bands were stained with Coomassie Brilliant Blue followed by a destaining solution containing 10% acetic acid and 10% methanol. Standard protein markers with a molecular weight range of 11 to 180 kDa were used to determine the molecular weight range of the proteins and hydrolysates (Shirotani *et al.*, 2021).

Texture Profile Analysis (TPA)

The back-extrusion test was conducted by a Texture Analyzer instrument (Brookfield CT3-10Kg, USA). The test was conducted using a cylindrical probe (40 mm diameter) at a 1 mm/s rate to 3 cm penetration. The soymilk gels kept at 4 °C for 24 h were taken out 60 min before testing to achieve room temperature. The textural parameters including firmness, consistency, adhesiveness, and viscosity were calculated via mean values obtained from a force-time curve (Shams-Abadi & Razavi, 2021).

Statistical Analysis

Data analysis was conducted using SPSS software (version 20). The mean values were compared to each other using the Duncan multiple range test ($p \leq 0.05$).

Results and Discussion

Titratable Acidity and pH

Changes in titratable acidity and pH during fermentation are shown in Fig. 2 (a) and (b), respectively. As shown in Fig. 2, in the control group, acidity remained stable during 9 h incubation. In soymilk fermented with *L. plantarum* MCM4 and *S. thermophilus*, acidity increased from 0.18 to 0.38% and 0.49%

respectively after 8 h of incubation. Also, the titratable acidity of soymilk fermented with *W. confusa MDM8* increased over time and reached 0.43% within 9 h. This shows the potential of tested LAB in consuming the sugars in soymilk (oligosaccharides, raffinose, stachyose, sucrose, and glucose) (Wang *et al.*, 2003). The isoelectric pH of soy proteins has been reported to be 4.5-5.0, and therefore reaching this pH is the beginning of gelation (Ningtyas *et al.*, 2021) (Fig. 3). Tang et al. reported that after pH approached the PI during fermentation, the electrostatic force between the proteins decreased and resulted in formation of SPI gel (Tang *et al.*, 2006).

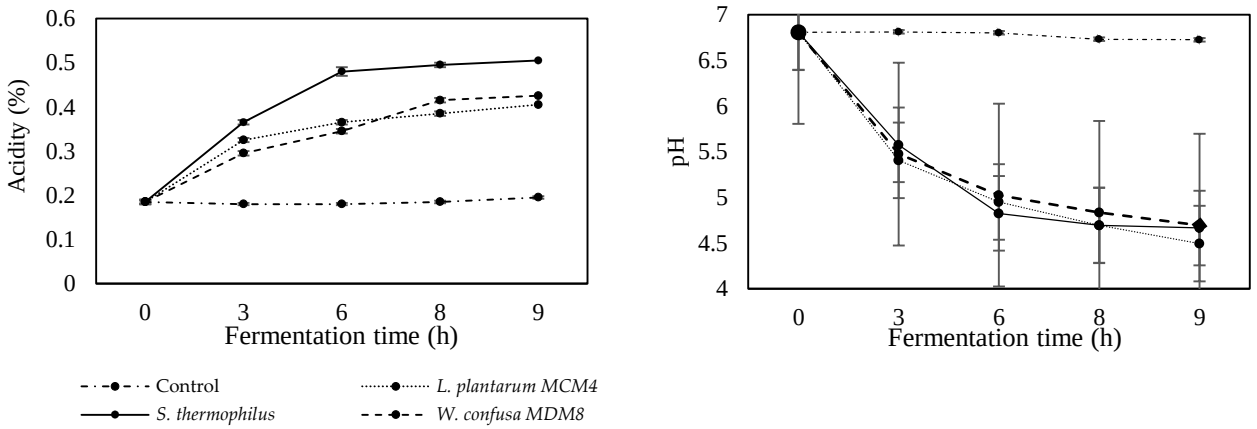

(a) **(b)**

Fig. 2. Change in titratable acidity (a) and pH values (b) of soymilk inoculated with different LAB strains during fermentation

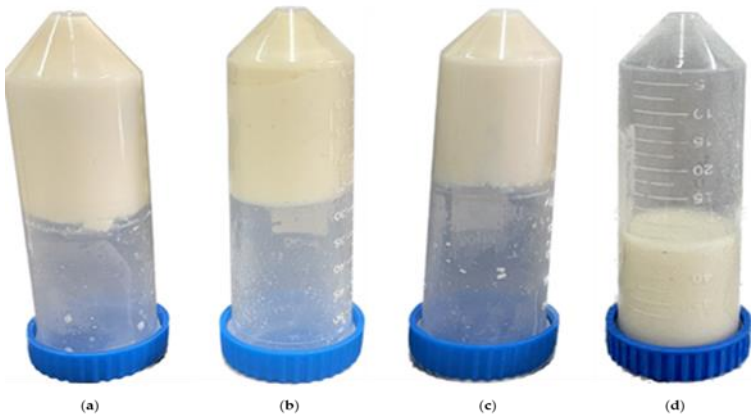

Fig. 3. Soymilk samples fermented with (a) *L. plantarum MCM4* after 8 h of fermentation; (b) *W. confusa MDM8* after 9 h of fermentation; (c) *S. thermophilus* after 8 h of fermentation; (d) unfermented (Control) after 9 h incubation

Zeta Potential

The results of measuring the zeta potential of soymilk before and after fermentation are shown in Table 1. The zeta potential, which is influenced by the pH of the dispersed phase, reflects the electrostatic interactions between protein molecules and is considered the main factor in protein aggregation (Klost *et al.*, 2020). Our results in this study show that the value of zeta potential significantly decreased from '-13.15' to ≈0. These results were similar to the results of Wang *et al.*, who showed that protein surface charges changed during fermentation and consequently the electrostatic

repulsion between them decreased. This can be mainly attributed to the neutralization of the negative charge on the original protein surface due to an increase in H^+ concentration. On the estimation of zeta-potential, it was seen that minimum surface charge was obtained at the isoelectric pH and the electrostatic repulsion is the main influence factor on aggregation behavior (Wang & Guo, 2016; Xing *et al.*, 2019).

Table 1- Zeta-potential of soymilk gel at t = 0 h and after reaching the pH= 4.7 during fermentation

Samples	Time(h)	pH	Zeta Potential/mV
*Control**	0	6.8±0.0	-13.15
Lactiplantibacillus plantarum MCM4	0	6.8±0.0	-13.15
Weissella confusa MDM8	0	6.8±0.0	-13.15
Streptococcus thermophilus	0	6.8±0.0	-13.15
Control	8	6.8±0.1	-13.15
Control	9	6.8±0.1	-13.15
Lactiplantibacillus plantarum MCM4	8	4.7±0.0	≈0
Streptococcus thermophilus	8	۴.۷±0.1	≈0
Weissella confusa MDM8	9	4.7±0.1	≈0

*Control: Unfermented soy milk

Cell Count

The cell counts of *L. plantarum MCM4*, *W. confusa MDM8*, and *S. thermophilus* in soymilk during fermentation are shown in Fig. 4. The viable cell count in samples fermented with *L. plantarum* MCM4, *S. thermophilus*, and *W. confusa MDM*8 was 6.42, 5.96, and 6.04 log CFU/ml respectively at the time of inoculation, which was increased to 7.43, 7.32, and 7.49 log CFU/ml at the end of fermentation (reaching pH=4.7). The metabolic processes occurring during the growth of lactic acid bacteria (LAB) resulted in acid production. The observed rise in titratable acidity, coupled with a reduction in pH value, signified the generation of acid during the fermentation of soy milk. All strains demonstrated a consistent increase in titratable acidity throughout the fermentation period, which was following the results of Leksono et al. (Leksono *et al.*, 2022) Considering the higher cell counts of *W. confusa MDM8* after 9h, and longer time for reaching pH 4.7, it can be concluded that it has a lower acidification activity than *L. plantarum MCM4* and *S. thermophilus* in soy milk and therefore weaker coagulation ability.

Proteolysis (FAA Content)

Free amino acid (FAA) content (mg/mL, L-Serine equivalent) in the fermented and unfermented samples is shown in Fig. 5. *L. plantarum MCM4* exhibited highest proteolytic activity (1.12 mg/mL), followed by *S. thermophilus* (1.07 mg/mL) and *W. confusa MDM8* (0.98 mg/mL) ($p< .05$). In the research conducted by Atashgahi et al., *L. plantarum MCM4* exhibited the most significant proteolytic activity in soy whey based on OPA method (Atashgahi *et al.*, 2024). The complex biosystem fermentation comprises enzymes derived from both the raw materials and microorganisms, which are responsible for hydrolysis reactions, including proteolysis (Joshi *et al.*, 2018). Microbial proteolysis can improve plant protein digestibility and bioactivity and reduce protein allergenicity (Worsztynowicz *et al.*, 2019). In this study, FAA content in all three inoculated samples increased during fermentation showing the affinity of tested LAB for soy proteins. In a study that used *Lactobacillus helveticus* for fermentation, the immunoreactivity of the soluble soy protein (β-conglycinin) decreased significantly (Meinlschmidt *et al.*, 2016). Meinlschmidt *et al*. reported that a combination of strain-specific proteolytic activity and acidic protein denaturation may cause the reduced immunoreactivity of β-conglycinin. Acidification is an aspect of LAB fermentation that may serve as a method to create a peptide

pool within a plant-based context (Gänzle *et al.*, 2008). Proteolytic system of LAB have the potential to increase protein solubility, an interesting property that could be used as a technological tool for stabilizing and producing complex plant-based products (Gänzle, 2015) leading to fermented plant-based milk a potential added value with multifunctional properties compared to nonproteolytic strains (Worsztynowicz *et al.*, 2019).

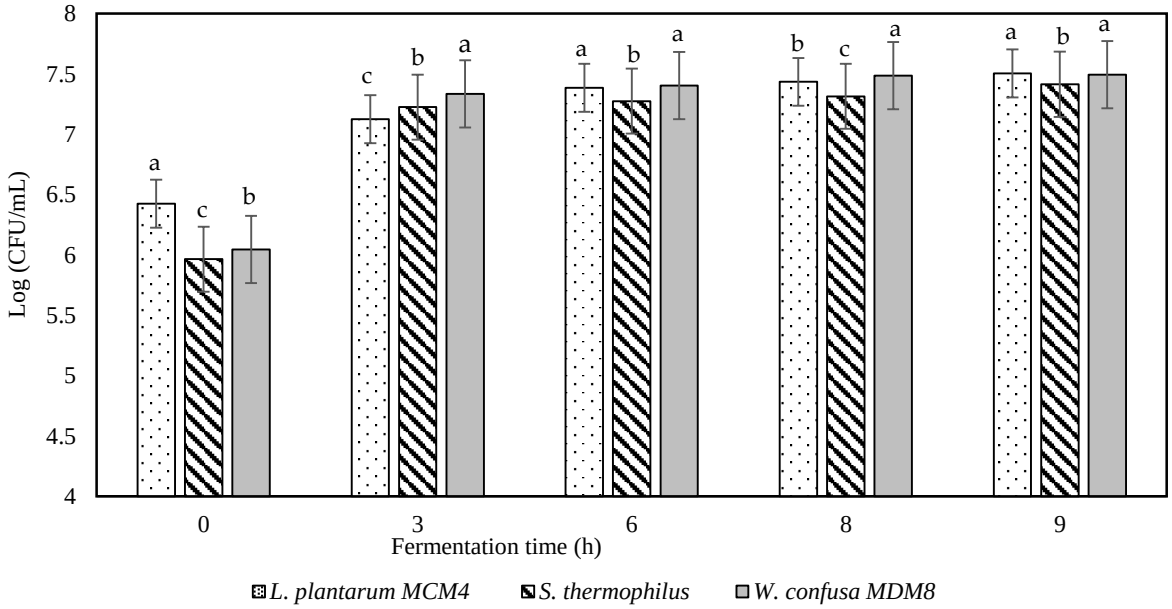

Fig. 4. Cell count (log cfu/ml) of Lactiplantibacillus plantarum MCM4, Streptococcus thermophilus, and Weissella confusa MDM8 in soymilk during fermentation

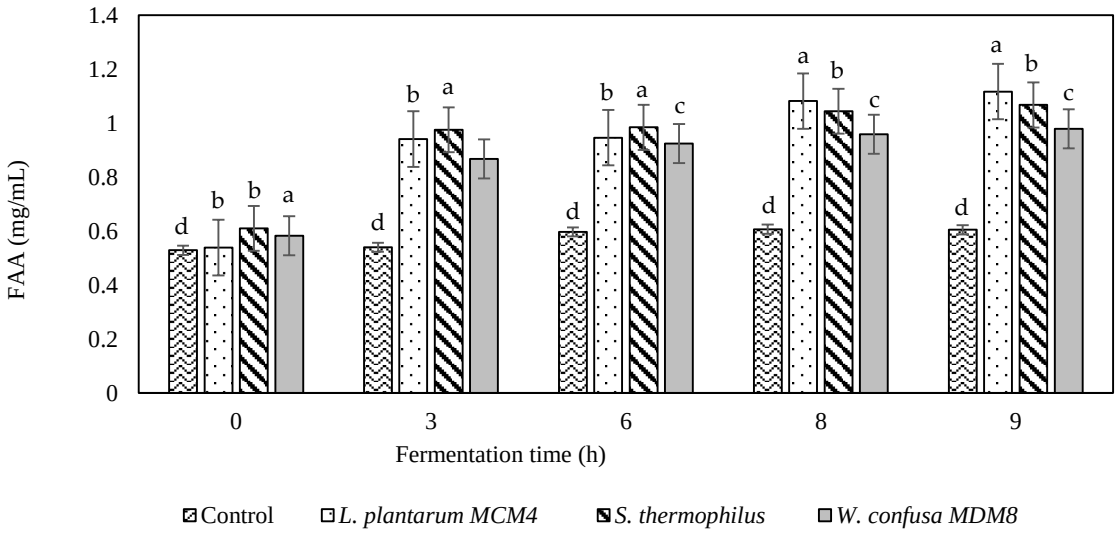

Fig. 5. Free amino acid (FAA) content (mg/ml, L-Serine equivalent) of soymilk fermented with *Lactiplantibacillus plantarum MCM4, Streptococcus thermophilus,* and *Weissella confusa MDM8* and Control sample for 0, 3, 6, 8 and 9h of fermentation

SDS-PAGE Analysis

Changes in soymilk protein profile during the fermentation process are shown in SDS-PAGE pattern (Fig. 6). In all fermented samples the band density of most of the proteins reduced after 3 h of fermentation and disappeared after the end of fermentation. Also, the SDS-PAGE pattern shows that new bands were derived from the acidic subunit of glycinin and the glycinin A5 subunit. The ability of proteolysis may vary due to differences in microbial species, the secreted protease as well as its ability to degrade protein (Yang *et al.*, 2020). *W. confusa MDM8* showed the highest degradation of β-subunits and acidic subunits of glycinin at the end of fermentation. It is essential to note that β-conglycinin was broken down more easily than glycinin in all strains. The phenomenon was probably due to the difference in structural characteristics between β-conglycinin and glycinin. Glycinin has a compact structure stabilized by disulfide bonds which makes it more difficult for the microorganism to access the cleavage sites. Glycinin and β-conglycinin are the two major proteins of soybean which make up approximately 40% and 30% of the total soybean proteins, respectively. Among the legume proteins, soy proteins have particular interest as they are connected to allergenicity (Meinlschmidt *et al.*, 2016). Many studies proved that the hydrolysis of allergenic proteins by enzymes secreted from LAB is an effective method to reduce soy allergenicity and easy digestion of the final product (Aguirre *et al.*, 2014; Holzhauser *et al.*, 2009; Tavano, 2013). In addition, soy protein is a protein of large molecular size, which is why products made from soybeans usually have a grainy texture (Shewry *et al.*, 1995). The results of electrophoresis showed that microbial proteolysis can break down large soy protein molecules into smaller peptide fragments and may solve the problem of granular texture (Li *et al.*, 2013).

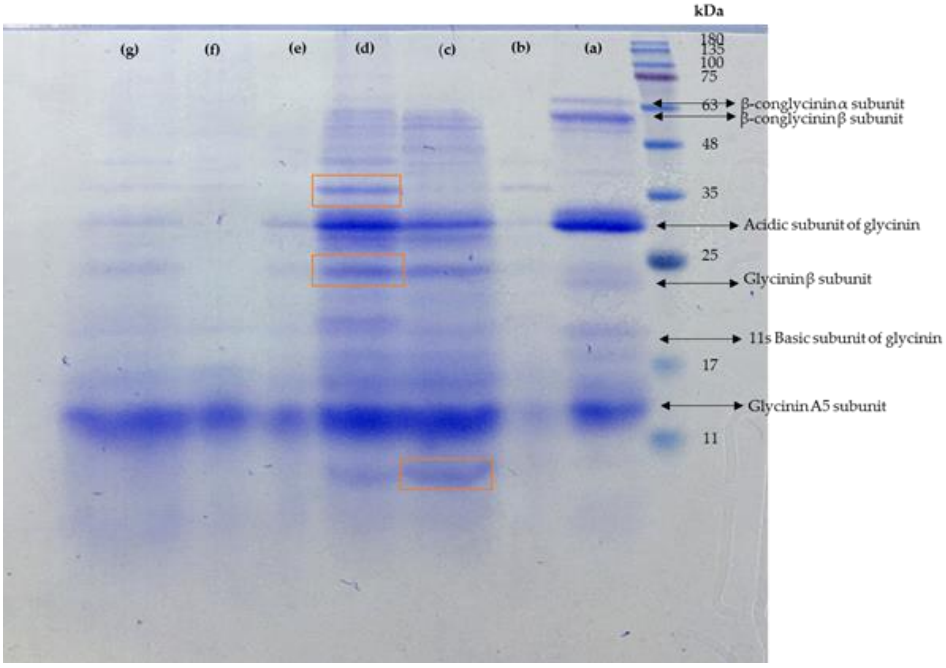

Fig. 6. SDS-PAGE profiles of soymilk fermented by three LAB strains and control sample during fermentation. (Lane a) control, unfermented soymilk - incubated for 9h; (Lane b) fermented soymilk for 9h with *Weissella confusa MDM8* ;(Lane c) fermented soymilk for 3h with *Weissella confusa MDM8* ;(Lane d) fermented soymilk for 3h with *Lactiplantibacillus plantarum MCM4*;(Lane e) fermented soymilk for 8h with *Lactiplantibacillus plantarum MCM4;*(Lane f) fermented soymilk for 3h with *Streptococcus thermophilus*;(Lane g) fermented soymilk for 8h with *Streptococcus thermophiles*

Syneresis in Soymilk Gels

The syneresis value of different soymilk gels was quantified at the end of fermentation and the results are presented in Fig. 7. There was a significant difference in the syneresis value among the samples. In soymilk gels fermented with *L. plantarum MCM4*, *S. thermophilus*, and *W. confusa MDM8*, the syneresis values were 69.5, 61 and 66%, respectively. Kuipers et al. reported that soy protein gels with elevated degree of hydrolysis showed higher syneresis (Kuipers *et al.*, 2005) which is in line with our results indicating higher syneresis in the gels fermented with *L. plantarum MCM4* with higher proteolysis, which could be due to greater contraction of the protein matrix. It is essential to note that β-conglycinin was broken down more easily than glycinin in all strains (Beal *et al.*, 1999). Such results were not in agreement with the results of our study, as soymilk fermented with *L. plantarum MCM4* had more syneresis than soymilk fermented with *W. confusa MDM8*, while its fermentation time was less. The length of fermentation is another factor that could affect the degree of syneresis and the texture of the gel (Purohit *et al.*, 2009). Furthermore, the effect of EPS on gel texture and syneresis is very important. EPS can bind water and enhance the viscosity and firmness of the gels (Folkenberg *et al.*, 2006). The functionality of EPS depends on their structural characteristics such as molar mass, degree of branching, and charge (De Vuyst & Degeest, 1999) and also the concentration of EPS (Mende *et al.*, 2013). Considering that the effect of EPS on the properties of fermented soymilk gel was not investigated in the present study, this can be a suggestion for future studies.

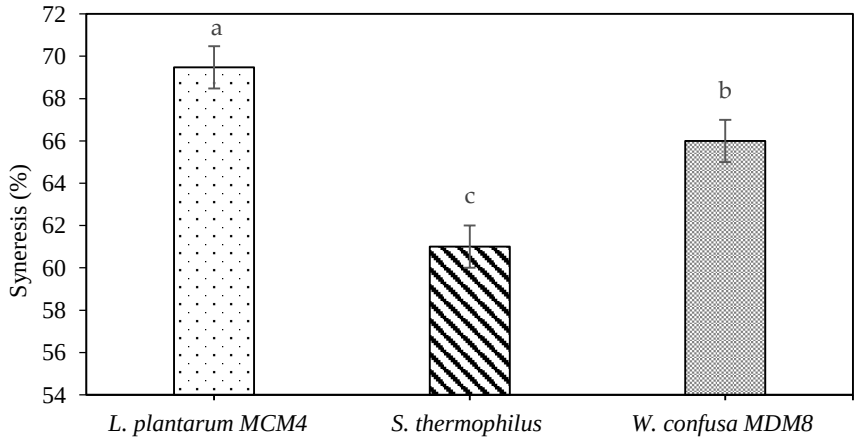

Fig. 7. Comparison of Syneresis of soymilk gel by inoculation of three LAB (*Lactiplantibacillus plantarum MCM4, Streptococcus thermophilus,* and *Weissella confusa MDM8*) at the end of fermentation

Texture

Texture parameters of the soymilk gels were assessed using back extrusion testing after 24h storage at 4 ˚C (Table 2). The adhesiveness of soy milk gels can be understood in terms of the adhesive force required to surpass the surface adsorption forces acting between the particles. Consequently, it can be inferred that a more robust gel structure and a denser protein network will result in a greater adhesive force (Shahbandari *et al.*, 2016), and the maximum force applied during compression is called firmness, while consistency refers to the thickness of the sample (Ciron *et al.*, 2010). The viscosity index is also the extrusion energy of adhesion when it increases, more resistance is required when pulling out the sample (Nasaruddin *et al.*, 2012). Generally, sample fermented with *S. thermophilus* showed the lowest values of textural characteristics and sample fermented with *L. plantarum MCM4* had higher consistency, adhesiveness, and

viscosity index. Moreover, sample fermented with *W. confusa MDM8* had the highest hardness. The final pH values of the gels were similar, but the difference in acidification rate could affect subtle differences in the microstructure (Liu *et al.*, 2023). In Cavallieri *et al.*'s study on the acidic cold set gelation of whey proteins, it was reported that at lower acidification rates the structure was stronger, probably due to a more organized formation during the slower acidification process. During slow acidification conditions, the molecular rearrangements occur in parallel with pH reduction and have enough time to interact and consequently organize the structure (Cavallieri & Da Cunha, 2008). In general, our results show that the use of LAB isolated from plant sources may be a useful strategy for improving the textural characteristics of plant-based suspensions because they can be better adapted to plant proteins. Korcz and Varga stated that EPS-producing LAB can induce textural properties in plant-based products because added hydrocolloids led to improve the clean products (Korcz & Varga, 2021). In another study, it was reported that fermentation with an EPS-producing strain of *Weissella confusa* increased the viscosity and water-holding capacity of the product compared to fermentation with non-EPS-producing LAB strains (Lorusso *et al.*, 2018). Also, in the study of Zannini *et al*., fermentation by *Weissella cibaria* resulted in the production of a quinoa-based yogurt product as viscous as dairy yogurt. They attributed the textural properties to extensive proteolysis of the protein matrix and increased viscosity to the production of high molecular-weight EPS (Zannini *et al.*, 2018).

Table 2- Texture characteristics of fermented soy milk gels**

Samples	Firmness (N)	Consistency (N*s)	Adhesiveness (N)	Viscosity index (N*s)
Fermented soy milk with *Lactiplantibacillus plantarum MCM4*	0.7755 ± 0.02^{b}	24.4665 ± 0.14^{a}	-0.503 ± 0.02^{b}	-1.21 ± 0.14^{b}
Fermented soy milk with *S. thermophilus*	0.5425 ± 0.04^{c}	11.4345 ± 0.20^{b}	-0.2785 ± 0.03^{a}	-0.79 ± 0.08^{a}
Fermented soy milk with *Weissella confusa MDM8*	1.132 ± 0.04^{a}	24.408 ± 0.04^{a}	-0.479 ± 0.02^{b}	-1.05 ± 0.04^{ab}

**Mean values ± SD. Samples with different superscripted letters in the same column are significantly different ($P < 0.05$).

Conclusion

The shift towards healthier and sustainable food consumption requires more studies on plant-based proteins. Plant-based gel has gained growing attention from the food industry, because many food systems, such as processed meats and cheeses, are plant-based gels. This work aims to evaluate the possibility of using LAB as a starter culture in the production of soy protein-based gels as a novel approach for healthier foods. The results of the present study clearly showed that the choice of applied microorganisms has a decisive role in the textural and physical characteristics of soymilk gels. In comparison to other samples, soymilk gel induced by fermentation with *Weissella confusa MDM8* was found to be more favorable in terms of physical and proteolytic properties. Although it took longer to reach the desired pH, SDS-PAGE analysis showed higher proteolysis and the resulting gel had better textural characteristics. Analysis of sensory properties, flavor, and shelf life of soy milk gel produced by such LAB strains can be the subject of future research.

Author Contributions

F. Rahmani: Funding acquisition, investigation, writing-original draft; **A. Moayedi:** Project administration, supervision, conceptualization, writing–review and editing; **M. Khomeiri:** Data curation, methodology; **M. Kashiri:** Formal analysis, software.

Funding Sources

This research was funded by Gorgan University of Agricultural Sciences and Natural Resources, Iran. This research is also partially funded by Iran Industrial States Company (regional office in Golestan province, Iran).

Acknowledgments

Mrs. Zahra Zareie is acknowledged for her technical support.

Conflict of Interest

The authors declare no conflicts of interest.

Data Availability Statement: The data presented in this study are available in article.

References

1. Aguirre, L., Hebert, E.M., Garro, M.S., & de Giori, G.S. (2014). Proteolytic activity of Lactobacillus strains on soybean proteins. *LWT-Food Science and Technology*, *59*(2), 780-785. https://doi.org/10.1016/j.lwt.2014.06.061
2. Atashgahi, S., Moayedi, A., Sadeghi Mahoonak, A., Shahiri Tabarestani, H., & Sadeghi, A. (2024). Enhancement of antioxidant activity and bioactive compounds in soy whey fermented with *Lactiplantibacillus plantarum* and *Weissella confusa*. *Iranian Food Science and Technology Research Journal*, *20*(3), 65-79. https://doi.org/10.22067/ifstrj.2024.87477.1325
3. Beal, C., Skokanova, J., Latrille, E., Martin, N., & Corrieu, G. (1999). Combined effects of culture conditions and storage time on acidification and viscosity of stirred yogurt. *Journal of Dairy Science*, *82*(4), 673-681. https://doi.org/10.3168/jds.S0022-0302(99)75283-5
4. Böni, L., Rühs, P.A., Windhab, E.J., Fischer, P., & Kuster, S. (2016). Gelation of soy milk with hagfish exudate creates a flocculated and fibrous emulsion-and particle gel. *PLoS One*, *11*(1), e0147022. https://doi.org/10.1371/journal.pone.0147022
5. Cavallieri, A.L.F., & Da Cunha, R.L. (2008). The effects of acidification rate, pH and ageing time on the acidic cold set gelation of whey proteins. *Food Hydrocolloids*, *22*(3), 439-448.
6. Ciron, C., Gee, V., Kelly, A., & Auty, M. (2010). Comparison of the effects of high-pressure microfluidization and conventional homogenization of milk on particle size, water retention and texture of non-fat and low-fat yoghurts. *International Dairy Journal*, *20*(5), 314-320. https://doi.org/10.1016/j.idairyj.2009.11.018
7. De Vuyst, L., & Degeest, B. (1999). Heteropolysaccharides from lactic acid bacteria. *FEMS Microbiology Reviews*, *23*(2), 153-177. https://doi.org/10.1111/j.1574-6976.1999.tb00395.x
8. Folkenberg, D.M., Dejmek, P., Skriver, A., Guldager, H.S., & Ipsen, R. (2006). Sensory and rheological screening of exopolysaccharide producing strains of bacterial yoghurt cultures. *International Dairy Journal*, *16*(2), 111-118. https://doi.org/10.1016/j.idairyj.2004.10.013
9. Gänzle, M.G. (2015). Lactic metabolism revisited: metabolism of lactic acid bacteria in food fermentations and food spoilage. *Current Opinion in Food Science*, *2*, 106-117. https://doi.org/10.1016/j.cofs.2015.03.001
10. Gänzle, M.G., Loponen, J., & Gobbetti, M. (2008). Proteolysis in sourdough fermentations: mechanisms and potential for improved bread quality. *Trends in Food Science & Technology*, *19*(10), 513-521. https://doi.org/10.1016/j.tifs.2008.04.002
11. García-Cano, I., Rocha-Mendoza, D., Ortega-Anaya, J., Wang, K., Kosmerl, E., & Jiménez-Flores, R. (2019). Lactic acid bacteria isolated from dairy products as potential producers of lipolytic, proteolytic and antibacterial proteins. *Applied Microbiology and Biotechnology*, *103*, 5243-5257. https://doi.org/10.1007/s00253-019-09844-6
12. Genet, B.M., Xiao, H., Christensen, L.F., Laforce, I.N., Mohammadifar, M.A., Bang-Berthelsen, C.H., & Hansen, E.B. (2023). Selection of proteolytic LAB starter cultures for acidification of soy based dairy alternatives. *LWT*, *184*, 115082.

13. Holzhauser, T., Wackermann, O., Ballmer-Weber, B.K., Bindslev-Jensen, C., Scibilia, J., Perono-Garoffo, L., Utsumi, S., Poulsen, L.K., & Vieths, S. (2009). Soybean (*Glycine max*) allergy in Europe: Gly m 5 (β-conglycinin) and Gly m 6 (glycinin) are potential diagnostic markers for severe allergic reactions to soy. *Journal of Allergy and Clinical Immunology*, *123*(2), 452-458. e454. https://doi.org/10.1016/j.jaci.2008.09.034
14. Joshi, R., Sharma, V., & Kuila, A. (2018). Fermentation technology: current status and future prospects. *Principles and Applications of Fermentation Technology*, 1-13. https://doi.org/10.1002/9781119460381
15. Kamarinou, C.S., Papadopoulou, O.S., Doulgeraki, A.I., Tassou, C.C., Galanis, A., Chorianopoulos, N.G., & Argyri, A.A. (2022). Mapping the key technological and functional characteristics of indigenous lactic acid bacteria isolated from Greek traditional dairy products. *Microorganisms*, *10*(2), 246. https://doi.org/10.3390/microorganisms10020246
16. Karimian, E., Moayedi, A., Khomeiri, M., Aalami, M., & Mahoonak, A.S. (2020). Application of high-GABA producing *Lactobacillus plantarum* isolated from traditional cabbage pickle in the production of functional fermented whey-based formulate. *Journal of Food Measurement and Characterization*, *14*, 3408-3416. https://doi.org/10.1007/s11694-020-00587-x
17. Khanlari, Z., Moayedi, A., Ebrahimi, P., Khomeiri, M., & Sadeghi, A. (2021). Enhancement of γ-aminobutyric acid (GABA) content in fermented milk by using *Enterococcus faecium* and *Weissella confusa* isolated from sourdough. *Journal of Food Processing and Preservation*, *45*(10), e15869. https://doi.org/10.1111/jfpp.15869
18. Klost, M., Brzeski, C., & Drusch, S. (2020). Effect of protein aggregation on rheological properties of pea protein gels. *Food Hydrocolloids*, *108*, 106036. https://doi.org/10.1016/j.foodhyd.2020.106036
19. Kong, X., Xiao, Z., Du, M., Wang, K., Yu, W., Chen, Y., Liu, Z., Cheng, Y., & Gan, J. (2022). Physicochemical, textural, and sensorial properties of soy yogurt as affected by addition of low acyl gellan gum. *Gels*, *8*(7), 453.
20. Korcz, E., & Varga, L. (2021). Exopolysaccharides from lactic acid bacteria: Techno-functional application in the food industry. *Trends in Food Science & Technology*, *110*, 375-384. https://doi.org/10.1016/j.tifs.2021.02.014
21. Kuipers, B.J., van Koningsveld, G.A., Alting, A.C., Driehuis, F., Gruppen, H., & Voragen, A.G. (2005). Enzymatic hydrolysis as a means of expanding the cold gelation conditions of soy proteins. *Journal of Agricultural and Food Chemistry*, *53*(4), 1031-1038. https://doi.org/10.1021/jf048622h
22. Leksono, B.Y., Cahyanto, M.N., Rahayu, E.S., Yanti, R., & Utami, T. (2022). Enhancement of antioxidant activities in black soy milk through isoflavone aglycone production during indigenous lactic acid bacteria fermentation. *Fermentation*, *8*(7), 326.
23. Li, Q., Xia, Y., Zhou, L., & Xie, J. (2013). Evaluation of the rheological, textural, microstructural and sensory properties of soy cheese spreads. *Food and Bioproducts Processing*, *91*(4), 429-439. https://doi.org/10.1016/j.fbp.2013.03.001
24. Liu, L., Huang, Y., Zhang, X., Zeng, J., Zou, J., Zhang, L., & Gong, P. (2023). Texture analysis and physicochemical characteristics of fermented soymilk gel by different lactic acid bacteria. *Food Hydrocolloids*, *136*, 108252. https://doi.org/10.1016/j.foodhyd.2022.108252
25. Lorusso, A., Coda, R., Montemurro, M., & Rizzello, C.G. (2018). Use of selected lactic acid bacteria and quinoa flour for manufacturing novel yogurt-like beverages. *Foods*, *7*(4), 51. https://doi.org/10.3390/foods7040051
26. Masiá, C., Jensen, P.E., Petersen, I.L., & Buldo, P. (2022). Design of a functional pea protein matrix for fermented plant-based cheese. *Foods*, *11*(2), 178. https://doi.org/10.3390/foods11020178

27. McCarthy, K., Parker, M., Ameerally, A., Drake, S., & Drake, M. (2017). Drivers of choice for fluid milk versus plant-based alternatives: What are consumer perceptions of fluid milk? *Journal of Dairy Science*, *100*(8), 6125-6138.
28. Meinlschmidt, P., Ueberham, E., Lehmann, J., Schweiggert-Weisz, U., & Eisner, P. (2016). Immunoreactivity, sensory and physicochemical properties of fermented soy protein isolate. *Food Chemistry*, *205*, 229-238.
29. Mende, S., Peter, M., Bartels, K., Dong, T., Rohm, H., & Jaros, D. (2013). Concentration dependent effects of dextran on the physical properties of acid milk gels. *Carbohydrate Polymers*, *98*(2), 1389-1396. https://doi.org/10.1016/j.carbpol.2013.07.072
30. Mishra, S., & Mishra, H.N. (2018). Comparative study of the synbiotic effect of inulin and fructooligosaccharide with probiotics with regard to the various properties of fermented soy milk. *Food Science and Technology International*, *24*(7), 564-575. https://doi.org/10.1177/1082013218776529
31. Moslemi, M., Moayedi, A., Khomeiri, M., & Maghsoudlou, Y. (2023). Development of a whey-based beverage with enhanced levels of conjugated linoleic acid (CLA) as facilitated by endogenous walnut lipase. *Food Chemistry: X*, *17*, 100547. https://doi.org/10.1016/j.fochx.2022.100547
32. Nasaruddin, F., Chin, N., & Yusof, Y. (2012). Effect of processing on instrumental textural properties of traditional dodol using back extrusion. *International Journal of Food Properties*, *15*(3), 495-506. https://doi.org/10.1080/10942912.2010.491932
33. Ningtyas, D.W., Tam, B., Bhandari, B., & Prakash, S. (2021). Effect of different types and concentrations of fat on the physico-chemical properties of soy protein isolate gel. *Food Hydrocolloids*, *111*, 106226. https://doi.org/10.1016/j.foodhyd.2020.106226
34. Purohit, D., Hassan, A., Bhatia, E., Zhang, X., & Dwivedi, C. (2009). Rheological, sensorial, and chemopreventive properties of milk fermented with exopolysaccharide-producing lactic cultures. *Journal of Dairy Science*, *92*(3), 847-856. https://doi.org/10.3168/jds.2008-1256
35. Rahmani, F., Gandomi, H., Noori, N., Faraki, A., & Farzaneh, M. (2021). Microbial, physiochemical and functional properties of probiotic yogurt containing *Lactobacillus acidophilus* and *Bifidobacterium bifidum* enriched by green tea aqueous extract. *Food Science & Nutrition*, *9*(10), 5536-5545. https://doi.org/10.1002/fsn3.2512
36. Rastogi, Y.R., Thakur, R., Thakur, P., Mittal, A., Chakrabarti, S., Siwal, S.S., Thakur, V.K., Saini, R.V., & Saini, A.K. (2022). Food fermentation–significance to public health and sustainability challenges of modern diet and food systems. *International Journal of Food Microbiology*, *371*, 109666.
37. Rojas-Nery, E., Garcia-Martinez, I., & Totosaus, A. (2015). Effect of emulsified soy oil with different carrageenans in rennet-coagulated milk gels. *International Food Research Journal*, *22*(2), 606.
38. Saraniya, A., & Jeevaratnam, K. (2015). In vitro probiotic evaluation of phytase producing *Lactobacillus* species isolated from Uttapam batter and their application in soy milk fermentation. *Journal of Food Science and Technology*, *52*, 5631-5640.
39. Shahbandari, J., Golkar, A., Taghavi, S.M., & Amiri, A. (2016). Effect of storage period on physicochemical, textural, microbial and sensory characteristics of stirred soy yogurt. *International Journal of Farming and Allied Sciences*, *5*(6), 476-484.
40. Shakerian, M., Razavi, S.H., Ziai, S.A., Khodaiyan, F., Yarmand, M.S., & Moayedi, A. (2015). Proteolytic and ACE-inhibitory activities of probiotic yogurt containing non-viable bacteria as affected by different levels of fat, inulin and starter culture. *Journal of Food Science and Technology*, *52*, 2428-2433. https://doi.org/10.1007/s13197-013-1202-9

41. Shams-Abadi, S.T., & Razavi, S.M.A. (2021). Cress seed gum improves rheological, textural and physicochemical properties of native wheat starch-sucrose mixture. *International Journal of Biological Macromolecules*, *181*, 945-955. https://doi.org/10.1016/j.ijbiomac.2021.04.093
42. Shewry, P.R., Napier, J.A., & Tatham, A.S. (1995). Seed storage proteins: structures and biosynthesis. *The Plant Cell*, *7*(7), 945. https://doi.org/10.1105/tpc.7.7.945
43. Shirotani, N., Hougaard, A.B., Lametsch, R., Petersen, M.A., Rattray, F.P., & Ipsen, R. (2021). Proteolytic activity of selected commercial *Lactobacillus helveticus* strains on soy protein isolates. *Food Chemistry*, *340*, 128152. https://doi.org/10.1016/j.foodchem.2020.128152
44. Somjid, P., Panpipat, W., Cheong, L.-Z., & Chaijan, M. (2022). Comparative effect of cricket protein powder and soy protein isolate on gel properties of Indian mackerel surimi. *Foods*, *11*(21), 3445. https://doi.org/10.3390/foods11213445
45. Taheri, S., Khomeiri, M., Aalami, M., & Moayedi, A. (2019). Non-fermented synbiotic drink based on lactic cheese whey which incorporates *Lactobacillus rhamnosus* GG and *Lactobacillus paracasei*. *International Journal of Food Studies*, *8*(2). https://doi.org/10.7455/ijfs/8.2.2019.a9
46. Tang, J., Luan, F., & Chen, X. (2006). Binding analysis of glycyrrhetinic acid to human serum albumin: fluorescence spectroscopy, FTIR, and molecular modeling. *Bioorganic & Medicinal Chemistry*, *14*(9), 3210-3217. https://doi.org/10.1016/j.bmc.2005.12.034
47. Tavano, O.L. (2013). Protein hydrolysis using proteases: An important tool for food biotechnology. *Journal of Molecular Catalysis B: Enzymatic*, *90*, 1-11. https://doi.org/10.1016/j.molcatb.2013.01.011
48. Wang, R., & Guo, S. (2016). Effects of endogenous small molecular compounds on the rheological properties, texture and microstructure of soymilk coagulum: Removal of phytate using ultrafiltration. *Food Chemistry*, *211*, 521-529. https://doi.org/10.1016/j.foodchem.2016.05.086
49. Wang, T., Chen, X., Wang, N., Wu, N., Jiang, L., Wu, F., Yu, D., Cheng, J., & Wang, L. (2022). Effect of electrochemical treatment on the formation and characteristics of induced soybean milk gel. *Journal of Food Engineering*, *323*, 111007. https://doi.org/10.1016/j.jfoodeng.2022.111007
50. Wang, Y.-C., Yu, R.-C., Yang, H.-Y., & Chou, C.-C. (2003). Sugar and acid contents in soymilk fermented with lactic acid bacteria alone or simultaneously with bifidobacteria. *Food Microbiology*, *20*(3), 333-338. https://doi.org/10.1016/S0740-0020(02)00125-9
51. Worsztynowicz, P., Schmidt, A.O., Białas, W., & Grajek, W. (2019). Identification and partial characterization of proteolytic activity of *Enterococcus faecalis* relevant to their application in dairy industry. *Acta Biochimica Polonica*, *66*(1), 61-69. https://doi.org/10.18388/abp.2018_2714
52. Xing, G., Giosafatto, C.V.L., Rui, X., Dong, M., & Mariniello, L. (2019). Microbial transglutaminase-mediated polymerization in the presence of lactic acid bacteria affects antigenicity of soy protein component present in bio-tofu. *Journal of Functional Foods*, *53*, 292-298. https://doi.org/10.1016/j.jff.2018.12.035
53. Yang, H., Qu, Y., Li, J., Liu, X., Wu, R., & Wu, J. (2020). Improvement of the protein quality and degradation of allergens in soybean meal by combination fermentation and enzymatic hydrolysis. *LWT*, *128*, 109442. https://doi.org/10.1016/j.lwt.2020.109442
54. Yang, X., Su, Y., & Li, L. (2020). Study of soybean gel induced by *Lactobacillus plantarum*: Protein structure and intermolecular interaction. *LWT*, *119*, 108794. https://doi.org/10.1016/j.lwt.2019.108794
55. Zannini, E., Jeske, S., Lynch, K.M., & Arendt, E.K. (2018). Development of novel quinoa-based yoghurt fermented with dextran producer Weissella cibaria MG1. *International Journal of Food Microbiology*, *268*, 19-26. https://doi.org/10.1016/j.ijfoodmicro.2018.01.001

نشریه پژوهشهای علوم و صنایع غذایی ایران
https://ifstrj.um.ac.ir

مقاله پژوهشی
جلد ۲۰، شماره ۶، بهمن-اسفند، ۱۴۰۳، ص. ۱۶۹-۱۵۵

تولید ژل شیرسویا تخمیری: تأثیر لاکتیک اسید باکتری‌های مختلف بر ویژگی‌های فیزیکوشیمیایی

فاطمه رحمانی[۱]- علی مویدی[۲*]- مرتضی خمیری[۳]- محبوبه کشیری[۲]

تاریخ دریافت: ۱۴۰۳/۰۶/۲۱
تاریخ پذیرش: ۱۴۰۳/۰۹/۲۰

چکیده

امروزه فرآورده‌های گیاهی جایگزین لبنی توجه زیادی را به خود جلب نموده است. با این حال، ویژگی‌های بافتی و حسی نامطلوب این محصولات پذیرش آن‌ها را محدود کرده است. بطور کلی استفاده از باکتری‌های لاکتیک اسید، به‌عنوان رویکردی نویدبخش برای توسعه آنالوگ‌های لبنی بر پایه گیاه پیشنهاد شده است. در این مطالعه، پتانسیل سه باکتری اسید لاکتیک پروتئولیتیک در ایجاد ژل شیرسویا مورد مقایسه قرار گرفت و تأثیر آن‌ها بر ویژگی‌های فیزیکو-شیمیایی ژل حاصله بررسی شد. *Lactiplantibacillus plantarum MCM4*، *Streptococcus thermophilus* و *Weissella confusa MDM8* به ماتریس شیر سویا تلقیح و تا رسیدن به pH حدود ۴/۷ گرمخانه‌گذاری شد. به‌منظور درک تأثیر سرعت اسیدیفیکاسیون و فعالیت پروتئولیتیک کشت‌های آغازگر مورد استفاده، سینرزیس، شمارش سلولی، محتوای آمینواسید آزاد (به روش اورتوفتال آلدهید)، الگوی SDS-PAGE و پارامترهای بافتی ژل حاصله ارزیابی شد. هر سه سویه باکتریایی، توانستند شیر سویا را منعقد کنند، با این حال *L. plantarum MCM4* فعالیت تولید اسید سریع‌تری در دمای ۳۷ درجه سانتی‌گراد نشان داد. بین سه سویه مورد مطالعه، از نظر شمارش سلولی و فعالیت پروتئولیتیک در طی تخمیر تفاوت معنی‌داری وجود داشت ($p<۰,۰۵$). همچنین مقدار سینرزیس نیز در بین ژل‌های به‌دست آمده متفاوت بود و در محدوده ۶۱٪ (نمونه تخمیر شده با *S. thermophilus*) تا ۶۹,۵٪ (نمونه تخمیر شده با *L. plantarum MCM4*) قرار داشت. علاوه بر این، سه سویه مورد مطالعه توانستند پروتئین‌های اصلی سویا را در طول تخمیر، هیدرولیز کنند. تجزیه و تحلیل بافت نشان داد که تخمیر شیر سویا با *W. confusa MDM8* منجر به ژل سویا با سفتی و قوام بالاتر شده است، در حالی‌که نمونه تخمیر شده با *L. plantarum MCM4* دارای چسبندگی و شاخص ویسکوزیته بالاتری بود. به‌طور کلی می‌توان نتیجه گرفت که *L. plantarum MCM4*، *W. confusa MDM8* و *S. thermophilus* را می‌توان به‌عنوان کشت‌های آغازگر برای تولید ژل‌های جدید شیر سویا با ویژگی‌های مناسب معرفی کرد.

واژه‌های کلیدی: باکتری‌های لاکتیک اسید، پروتئین‌های گیاهی، تولید غذا پایدار، جایگزین‌های لبنی

۱، ۲ و ۳- به‌ترتیب دانشجوی دکتری، دانشیار و استاد گروه علوم و صنایع غذایی، دانشکده صنایع غذایی، دانشگاه علوم کشاورزی و منابع طبیعی گرگان، گرگان، ایران
(*- نویسنده مسئول: Email: amoayedi@gau.ac.ir)

https://doi.org/10.22067/ifstrj.2024.89764.1366

Iranian Food Science and Technology Research Journal
Homepage: https://ifstrj.um.ac.ir

Review Article
Vol. 20, No. 6, Feb.-Mar., 2025, p. 171-200

Biodegradable Packaging Made from Proteins

S. Sahraee[1], J. Milani[2*]

1 and 2- Ph.D. Graduate of Food Science and Technology and Professor, Department of Food Science and Technology, Sari Agricultural Sciences and Natural Resources University, Sari, Iran, respectively.
(*- Corresponding Author Email: jmilany@yahoo.com)

Received: 22.05.2024
Revised: 04.08.2024
Accepted: 07.09.2024
Available Online: 07.01.2025

How to cite this article:
Sahraee, S., & Milani, J. (2025). Biodegradable packaging made from proteins. *Iranian Food Science and Technology Research Journal*, *20*(6), 171-200. https://doi.org/10.22067/ifstrj.2024.88166.1334

Abstract

Protein films have gained significant attention in the development of sustainable packaging materials due to their exceptional properties and versatility. These films offer superior gas barrier properties, specific mechanical characteristics, and enhanced intermolecular connection capabilities compared to other biopolymers. Researchers are exploring innovative methods to enhance the film-forming properties of proteins, improve their mechanical strength, and optimize their gas barrier performance. Various protein sources, such as gelatin, whey protein, soy protein, corn zein, wheat gluten, and casein, are being investigated for film fabrication. Techniques to modify protein films, including the incorporation of additives, crosslinking agents, and nanomaterials, are being explored to enhance their properties. The development of protein-based composite films, by blending proteins with other biopolymers or synthetic materials, is also being explored to achieve improved performance and functionality. Advancements in processing technologies, such as film casting, extrusion, and electrospinning, enable precise control over the thickness, morphology, and structural properties of protein films. These films not only offer enhanced barrier properties but also possess biodegradability and renewable characteristics, aligning with the increasing demand for eco-friendly packaging solutions. The preparation and improvement of protein films hold significant potential for revolutionizing the packaging industry and contributing to a greener and more environmentally friendly future. This review provides an overview of current research and advancements in the field, addressing various protein sources, film modification techniques, processing methods, challenges, and future prospects.

Keywords: Degradable, Food packaging, Nanotechnology, Physicochemical properties, Protein

Introduction

Film-fabricating biopolymers play a crucial role in the development of sustainable packaging materials. Among these biopolymers, proteins have gained significant attention due to their exceptional properties and versatility. Protein films offer superior gas barrier properties, specific mechanical characteristics, and enhanced intermolecular connection capabilities compared to polysaccharide-based and lipid-based films (Balaguer *et al*., 2013).

The unique ability of proteins to form intricate networks and induce plasticity and elasticity makes them an ideal choice for packaging applications. These films can be used as a component in biopolymer-based packaging materials, providing enhanced protection and preservation for various products (Du *et al*., 2018).

The increasing demand for sustainable packaging solutions has led to a growing interest in the preparation and improvement of protein films. Researchers and scientists are

https://doi.org/10.22067/ifstrj.2024.88166.1334

exploring innovative methods to enhance the film-forming properties of proteins, improve their mechanical strength, and optimize their gas barrier performance (Garavand *et al*., 2020).

Efforts are being made to identify suitable protein sources that can be used for film fabrication, such as gelatin, whey protein, soy protein, corn zein, wheat gluten and casein. These proteins offer a wide range of functional properties, making them suitable for different applications in the packaging industry (Yu *et al*., 2021).

Additionally, researchers are investigating various techniques to modify protein films, including the incorporation of additives, crosslinking agents, and nanomaterials. These modifications aim to enhance the film's mechanical properties, increase its resistance to moisture and oxygen permeability, and prolong the shelf life of packaged products (Farhan *et al*., 2017).

Furthermore, the development of protein-based composite films, by blending proteins with other biopolymers or synthetic materials, is being explored. This approach allows for the combination of desirable properties from different materials, resulting in films with improved performance and functionality (Winotapun *et al*., 2019).

In recent years, advancements in processing technologies, such as film casting, extrusion, and electrospinning, have enabled the production of protein films with precise control over their thickness, morphology, and structural properties. These techniques offer opportunities to tailor the film properties according to specific packaging requirements (*Jariyasakoolroj et al*., 2020).

The preparation and improvement of protein films hold significant potential for the development of sustainable packaging materials. These films not only offer enhanced barrier properties but also possess biodegradability and renewable characteristics, aligning with the growing demand for eco-friendly packaging solutions (Wang *et al*., 2017).

This paper aims to provide an overview of the current research and advancements in the preparation and improvement of protein films for packaging applications. The various protein sources, film modification techniques, and processing methods employed to enhance the performance of protein films were discussed. The challenges and future prospects in this field were also addressed.

Overall, the preparation and improvement of protein films have the potential to revolutionize the packaging industry, offering sustainable alternatives to conventional materials and contributing to a greener and more environmentally friendly future.

Different Methods of Packaging Film Preparation

There are several different preparation methods for packaging films, each with its own advantages and suitability for specific applications.

The Solution Casting Method

The solution casting method involves dissolving the film-forming material in a solvent to create a solution, which is then poured onto a flat surface or a mold and allowed to dry or solidify, resulting in a thin film.

In order to use this method some crucial factors should be taken into consideration. The solvent must effectively dissolve the material without degrading it and should have a high volatility to facilitate easy removal. The solid material (polymer, composite, etc.) is added to the solvent and stirred at a controlled temperature until a clear solution is obtained. The concentration of the material in the solution is adjusted according to the desired final thickness and properties of the cast film. The prepared solution is poured into molds or on casting surfaces (e.g., glass plates) to achieve the desired geometry. Sometimes, methods like spin coating or knife-over-edge can be used to spread the solution uniformly over the substrate. The solvent is allowed to evaporate gradually at room temperature or under controlled heating conditions. The rate of

evaporation influences the uniformity and properties of the final product. Care must be taken to avoid defects such as bubbles or uneven thickness during this stage. After solvent evaporation, the cast film may require curing (chemical crosslinking, thermal treatment) to enhance its properties. Further treatments such as annealing or surface treatment can be performed to improve film performance.

These kinds of films can be applied for packaging, electronic devices, and medical applications, coating technologies for enhancing surface properties, electrical conductivity, or barrier properties, composite materials**,** and nanocomposites.

The Extrusion

The extruder is a machine that consists of a screw inside a heated barrel. The screw rotates and conveys the raw material forward while also applying heat and pressure to melting the materials. The temperature in the barrel is carefully controlled to reach the melting point of the chosen material. As the raw material melts, it becomes a viscous mass suitable for further processing. There are several ways to form the film after extrusion. Blown Film Extrusion: The melted material is extruded through a circular die, creating a tube. Air is then blown into this tube, causing it to expand and form a thin-walled film. The film is cooled and pulled upward through an adjustable frame. Cast Film Extrusion: The melted raw material is extruded through a flat die, producing a continuous sheet. This sheet is immediately cooled on a flat surface (cast roll) and then wound up into rolls. In both blown and cast film processes, the film is cooled rapidly after exiting the extruder to stabilize its structure and hold the desired thickness. Once cooled, the film is typically wound into large rolls. This roll format is convenient for storage and shipping, and allows for further process such as printing or laminating.

Compression Molding

Compression molding involves shaping and solidifying the film-forming material in a mold cavity using heat and pressure, commonly employed for thermoplastic materials.

Lamination

Lamination is a process where multiple layers of films are bonded together to create a composite film, achieved through adhesive lamination, heat lamination, or extrusion lamination. Lastly, co-extrusion allows for the simultaneous extrusion of multiple layers of different materials, resulting in a multi-layered film with combined properties and functionalities (Yu *et al.*, 2021).

These are just a few examples of the various preparation methods for packaging films. The choice of method depends on factors such as the desired properties of the film, the film-forming material, and the intended application of the packaging film.

Physical Properties of Protein Films

Film Solubility

To assess solubility, conditioned protein films are weighed and immersed in distilled water. After stirring, undissolved material is centrifuged, dried, and weighed. Solubility is calculated by subtracting the weight of the remaining dry substance from the initial film weight (Pengbo *et al*., 2023).

Protein films exhibit solubility ranging from 16-72%. Comparatively, gelatin films display higher solubility than whey protein films. Moreover, fish gelatin films demonstrate superior solubility when compared to mammalian gelatin films. This disparity may be attributed to reduced intra-chain and inter-chain connections, as well as the presence of lysine, hydroxyl-lysine residues, and their aldehyde derivatives. Conversely, whey protein films exhibit lower solubility due to protein denaturation and the loss of their native three-dimensional structure. Consequently, sulfhydryl groups surface on the protein molecules, leading to covalent connections between them, thus decreasing solubility

(Hadidi *et al*., 2022). Water solubility is a significant characteristic for packaging films as it prevents water penetration or leakage in the packaged product. However, in certain applications like encapsulating nutrients or utilizing films as food additives, water permeability and solubility are evaluated as desirable features.

The solubility of whey protein films in water is reduced when subjected to UV treatment. This outcome is attributed to the impact of radiation on whey protein denaturation, resulting in the exposure of sulfide groups and subsequent intermolecular reactions. Notably, high-dose ultraviolet radiation, approximately 12 J/cm2, significantly decreases film solubility. Furthermore, denaturation induced by UV rays leads to the formation of hydrophobic surfaces in protein molecules, primarily through covalent bonding between aromatic amino acids and disulfide bonds. During the denaturation process, hydrophobic regions of the proteins migrate to the surface, thereby increasing the hydrophobicity of the protein film (Galus *et al*., 2016).

Film WVP

Various techniques exist to measure water vapor permeability (WVP) of protein films. Here are some commonly employed methods in recent studies.

Gravimetric method entails monitoring the weight gain of a film sample over a specific duration when subjected to a controlled humidity environment (Chaudhary *et al*., 2020).

Electrochemical sensors, such as quartz crystal microbalances (QCM) or surface acoustic wave (SAW) sensors, offer a means to evaluate alterations in film mass resulting from water vapor absorption (Velaga *et al*., 2018).

Permeation cells comprise of two chambers that are divided by the film sample. The film allows water vapor to permeate through it, and on the opposite side, techniques such as gas chromatography or infrared spectroscopy are employed to measure the concentration of the permeated vapor (Kao *et al*., 2014).

Dynamic vapor sorption (DVS) is a technique that assesses the sorption and desorption characteristics of a film in response to controlled humidity levels (Velaga *et al*., 2018).

Coulometric Karl Fischer titration is a technique that entails subjecting a film to a controlled water vapor gradient and quantifying the rate of water vapor transmission through the film using Karl Fischer titration (Kim *et al*., 2020).

Mathematical modeling employs Fick's laws of diffusion to estimate water vapor permeability. By taking into account factors such as film thickness, diffusion coefficient, and environmental conditions, these models can calculate WVP. However, for accurate modeling, it is necessary to possess knowledge of film properties and validate the models against experimental data (Pengbo *et al*., 2023).

The selection of a method relies on factors including desired accuracy, sensitivity, equipment availability, and the specific properties of the protein film under examination. It is crucial to evaluate the limitations and benefits of each method when choosing a suitable technique for measuring WVP in protein films.

In the majority of food packaging studies, the assessment of water vapor permeability in the film is conducted using the method outlined in ATSM 1993 (Alak *et al*., 2019). This method involves affixing films of precise dimensions and weight onto vials filled with dry silica gel. Subsequently, these vials are weighed and positioned within a conditioned desiccator containing distilled water at a temperature of 20 degrees Celsius. The rate at which water vapor passes through the films can be determined using the subsequent formula.

$$WVP = \frac{\Delta w \times L}{\Delta t \times A \times \Delta P} \quad (1)$$

Where $\Delta w/\Delta t$ is the mass change of vials per time unit, L is the thickness of the films, A is the exposed surface of the film and ΔP is the water vapor pressure difference between outside and inside of the film.

The soy protein isolate film exhibited a lower WVP compared to gelatin films due to its higher surface hydrophobicity (dos Santos Paglione *et al*., 2019).

Additionally, an increased protein content in the surimi film could potentially result in a higher concentration of polar groups. These polar groups have the ability to absorb more moisture from the surrounding environment, thereby influencing the WVP of the films. It was also suggested that film thickness played a role in this phenomenon.

Nevertheless, certain protein films, particularly the WPC film, demonstrated a low WVP. This could potentially be attributed to the denaturation of whey protein, which is facilitated by the intra-molecular and inter-molecular crosslinking of amino acid residues. Additionally, the formation of disulfide crosslinks and hydrophobic bonds may contribute to the reduction in WVP values. Typically, the moisture migration through films is regulated by the film's network. Films possessing a denser structure have the ability to more efficiently impede the moisture migration compared to those with a less compact structure (Galus *et al*., 2016).

Light Transmission

Various methods can be employed to measure the light transmission of biodegradable packaging films. Some commonly utilized techniques include spectrophotometry and haze measurement. Spectrophotometry entails passing a light beam through the film and assessing the intensity of transmitted light at different wavelengths. This method offers insights into the film's transparency and enables quantitative analysis of light transmission (Hadidi *et al*., 2022). Haze measurement, on the other hand, quantifies the extent of light scattering as it traverses the film, thereby indicating the film's clarity. Instruments like haze meters or haze-gloss meters are employed to measure haze values (Garavand *et al*., 2020).

Transparency can be visually evaluated by comparing the film to a standard transparent material. Although this method is subjective and may not yield precise quantitative data, it is commonly employed for quick evaluations (Yu *et al*., 2021).

Ultraviolet-visible (UV-Vis) spectroscopy measures light absorption and transmission in the UV and visible range. This technique offers insights into the film's capability to block or transmit specific light wavelengths (Velaga *et al*., 2018).

Fourier Transform Infrared (FTIR) spectroscopy gauges the absorption of infrared light by the film. It aids in analyzing the film's chemical composition and identifying specific functional groups that could impact light transmission (Nisar *et al*., 2018).

Colorimetry involves measuring the film's color using colorimeters or spectrophotometers. This method provides information about the film's color properties, which can indirectly influence light transmission (Nor Adilah *et al*., 2021).

It is worth noting that different methods may be more suitable for specific types of packaging films or research objectives. The choice of measurement technique depends on factors such as the desired level of precision, sensitivity, cost, and availability of equipment.

Light transmission of protein films can vary depending on several factors, including the specific protein used, film thickness, processing methods, and any additives or modifications applied. Whey protein films typically exhibit good transparency and light transmission properties. They can allow a significant amount of light to pass through, resulting in relatively high transmittance values. However, the exact level of light transmission can be influenced by factors such as film thickness and the presence of any plasticizers or crosslinking agents (Galus *et al*., 2016). Soy protein films can have varying degrees of light transmission depending on the specific type of soy protein used and the film formulation. In general, soy protein films tend to be less transparent compared to whey protein films. The presence of soy protein aggregates or other impurities can contribute to reduced light transmission. Gelatin films are known for their excellent light transparency. They can allow a

significant amount of light to pass through, resulting in high transmittance values. Gelatin films are often used as edible coatings or packaging due to their clarity and visual appeal (Nor Adilah *et al*., 2021). Casein films generally tend to have lower light transmission compared to whey or gelatin films (Matías *et al*., 2018).

Protein-based films have been found to exhibit superior UV light blocking properties compared to PVC wrap films. This is attributed to the high content of aromatic amino acids in the protein-based structure, which enables them to effectively absorb UV light. As a result, protein-based films are considered more transparent than PVC films and are suitable for use in food packaging (Jariyasakoolroj *et al*., 2020).

The protein-based films exhibit a visual appearance similar to that of PVC films, characterized by uniform transparency. These films are flexible, homogeneous, and possess smooth surfaces devoid of any observable pores or cracks. Placing them over a white background allows the background color to remain clearly visible, highlighting the transparency of the protein-based films (Nor Adilah *et al*., 2021).

Tensile Strength

Various methods are employed to measure the mechanical properties of protein films.

Tensile testing involves subjecting a film sample to controlled tension until it breaks. The applied force and resulting deformation are measured, allowing for the determination of properties such as tensile strength, elongation at break, Young's modulus, and toughness. Tensile testing provides valuable information on the film's ability to withstand stretching or pulling forces (Jariyasakoolroj *et al*., 2020).

Compression testing involves applying a compressive force to a film sample and measuring the resulting deformation. It is particularly useful for assessing the ability of protein films to withstand pressure or impacts (Winotapun *et al*., 2019).

Flexural testing, also known as three-point or four-point bending, measures the film's resistance to bending. This method provides information on the film's flexural strength, modulus of elasticity, and flexibility (Yu *et al*., 2021).

Puncture testing assesses the film's resistance to penetration by measuring the force required to puncture the film with a sharp probe (Xiao *et al*., 2021).

Nanoindentation is a technique used to measure the mechanical properties of thin films at a micro- or nanoscale level. A small probe is indented into the film, and the resulting force-displacement curve is analyzed to determine properties such as hardness, elastic modulus, and viscoelastic behavior. Nanoindentation provides detailed information about the film's mechanical response at small scales (Winotapun *et al*., 2019).

Dynamic mechanical analysis (DMA) involves subjecting a film sample to oscillatory forces or deformations over a range of frequencies and temperatures. It measures the film's viscoelastic properties, including storage modulus, loss modulus, and damping behavior. DMA is particularly useful for studying the film's response to dynamic or cyclic loading conditions (Velaga *et al*., 2018).

The mechanical properties of protein films can vary depending on factors such as the protein source, film formulation, processing conditions, and any additives or modifications applied.

Tensile strength measures the maximum stress a film can withstand before breaking. Whey protein films have been reported to exhibit relatively high tensile strength, indicating good resistance to stretching or pulling forces. The high tensile strength (TS) of WPC film at 6.14 MPa indicated a brittle nature that makes it unsuitable for industrial applications. This brittleness can be attributed to intermolecular chain interactions, including disulfide bonding, hydrogen bonding, hydrophobic interactions, and electrostatic forces between protein chains (Galus *et al*., 2016). Soy protein films generally have lower

tensile strength compared to whey protein films (Xu *et al.*, 2017). Gelatin films also have moderate tensile strength but can be improved with crosslinking agents or plasticizers (Nor Adilah *et al.*, 2021). Casein films typically have lower tensile strength compared to other protein films (Matías *et al.*, 2018).

Elongation at break measures the ability of a film to stretch before breaking. The low elongation at break (EAB) value of whey protein films indicated good flexibility. This could be attributed to the unfolded structure and covalent disulfide bonding present in the film, which contribute to its higher strength and ability to withstand greater deformations. Soy protein films usually have lower elongation at break compared to whey protein films. Gelatin films can have moderate elongation at break, which can be enhanced with plasticizers. Casein films generally have lower elongation at break compared to other protein films (Pengbo *et al.*, 2023).

Young's modulus is a measure of the stiffness or rigidity of a film. Whey protein films typically have lower Young's modulus values, indicating good flexibility. Soy protein films can have moderate to high Young's modulus, indicating higher stiffness. Gelatin films generally have lower Young's modulus compared to soy protein films. Casein films can have moderate to high Young's modulus depending on the specific casein type and film formulation (Kaewprachu *et al.*, 2016).

Toughness measures the ability of a film to absorb energy before breaking. Whey protein films have been reported to have good toughness, indicating resistance to fracture. Soy protein films generally have lower toughness compared to whey protein films. Gelatin films can have moderate toughness, which can be improved with plasticizers or crosslinking agents. Casein films typically have lower toughness compared to other protein films (Hadidi *et al.*, 2022).

Thermal Properties

Several methods are used to measure thermal properties of protein films. Differential Scanning Calorimetry (DSC) is a widely used method that measures the heat flow into or out of a sample as it undergoes temperature changes. This technique can provide information about the thermal transitions of protein films, such as denaturation or melting temperatures, enthalpy changes, and heat capacity. DSC is particularly useful for studying the thermal stability and transitions of protein films (Wang *et al.*, 2017).

Thermogravimetric Analysis (TGA) measures the weight changes of a sample as it is subjected to controlled temperature conditions. This method can determine the thermal stability and degradation behavior of protein films. TGA provides information about the onset, rate, and extent of thermal decomposition or mass loss, which can be used to assess the thermal stability and decomposition kinetics of protein films (Winotapun *et al.*, 2019).

DMA used to measure the viscoelastic properties of protein films as a function of temperature. This technique applies a controlled oscillatory force or deformation to a sample while subjecting it to a temperature ramp. DMA can provide information about the glass transition temperature (Tg) of protein films, as well as changes in storage modulus, loss modulus, and damping behavior with temperature (Wang *et al.*, 2017).

Infrared Spectroscopy (IR) can be used to analyze the molecular vibrations and structural changes in protein films as a result of temperature variations. This technique can provide information about changes in protein secondary structure, hydrogen bonding, and conformational changes induced by temperature (Xiao *et al.*, 2021).

Thermal Conductivity Measurement can be used to determine the ability of protein films to conduct heat. These methods involve measuring the heat transfer through a film sample under controlled temperature conditions, providing information about the thermal insulation or conductivity properties of protein films (Jensen *et al.*, 2015).

Comparing the DSC results of different protein films can provide insights into their thermal behavior and stability.

Denaturation temperature (Td): Td is the temperature at which protein molecules undergo structural changes, leading to unfolding or denaturation. Comparing the Td values of different protein films can indicate their thermal stability. Films with higher Td values are generally more stable and resistant to heat-induced structural changes.

Denaturation enthalpy (ΔH): ΔH represents the amount of heat absorbed or released during protein denaturation. Comparing the ΔH values of protein films can provide information about the energy required for denaturation. Higher ΔH values indicate a higher degree of protein unfolding or denaturation.

Glass transition temperature (Tg): Tg is the temperature at which an amorphous material, such as a protein film, transitions from a glassy to a rubbery state. Comparing the Tg values of different protein films can indicate their molecular mobility and flexibility at different temperatures. Films with higher Tg values tend to be more rigid and have lower molecular mobility.

Melting temperature (Tm): Tm is the temperature at which a protein film transforms from a solid to a liquid state. Comparing the Tm values of different protein films can provide insights into their thermal stability and the presence of ordered secondary structures, such as alpha-helices or beta-sheets. Higher Tm values indicate a higher degree of thermal stability (Lee *et al*., 2010).

The Tm values of protein films can vary depending on the source of the protein. Different proteins have different amino acid compositions, secondary structures, and molecular interactions, which can influence their melting behavior. For example, proteins with predominantly alpha-helical structures may have higher Tm values compared to those with predominantly beta-sheet structures. Also, the Tm values of protein films can be influenced by factors such as film formulation and processing conditions. Parameters like film thickness, protein concentration, plasticizers, crosslinking agents, and drying methods can affect the Tm values. It is important to ensure consistent film formulation and processing conditions when comparing Tm values. Protein modifications, such as chemical crosslinking or enzymatic modifications, can alter the Tm values of protein films. These modifications can affect the protein's structural stability and interactions, leading to changes in the Tm values. Comparisons should be made between films with similar modification methods or with appropriate controls. The way by which protein films are prepared and handled can impact their Tm values. Factors such as sample purity, hydration level, and sample handling can affect the protein's structural stability and, consequently, the Tm values. It is crucial to ensure consistent and appropriate sample preparation methods for accurate Tm comparisons (Winotapun *et al*., 2019).

Additionally, it is important to interpret the Tm values in conjunction with other thermal and structural characterization techniques to gain a comprehensive understanding of the protein films' properties.

Comparing the melting temperature (Tm) values of whey protein, soy protein, gelatin, and casein films can provide insights into their thermal stability and structural characteristics. Whey protein films typically exhibit Tm values in the range of 60-75°C. Whey proteins, derived from milk, are known to have a relatively lower Tm compared to proteins with predominantly alpha-helical structures (Galus *et al*., 2016). Soy protein films generally have Tm values in the range of 80-100°C. Soy proteins, derived from soybeans, often contain proteins with a higher proportion of beta-sheet structures, which can contribute to higher Tm values (Xiao *et al*., 2021). Gelatin films typically have Tm values in the range of 25-40°C. Gelatin, derived from collagen, is composed mainly of random coil structures. As a result, gelatin films have relatively lower Tm values compared to proteins with more ordered secondary structures like alpha-helices or beta-sheets (Li *et al*., 2021). Casein films generally exhibit Tm

values in the range of 40-60°C. Casein, derived from milk, consists of a mixture of proteins with varying secondary structures (Matías *et al*., 2018).

Oxygen Permeability

The oxygen permeability of protein films can be measured using various techniques.

Oxygen Transmission Rate (OTR) Measurement: involves measuring the rate at which oxygen passes through a protein film. It typically utilizes a permeation cell, where the film is placed between two chambers. One chamber is filled with oxygen, while the other is maintained at a lower oxygen concentration or a vacuum. The flow of oxygen through the film is measured over time using sensors or detectors, providing the OTR value (Bagheri *et al*., 2019).

Gas Permeation Testing: involves exposing the protein film to a known concentration of oxygen and measuring the oxygen permeating through the film. This can be done using techniques such as gas chromatography or mass spectrometry, which analyze the oxygen concentration before and after passing through the film (Acquah *et al.*, 2020).

Dynamic Headspace Analysis: involves placing the protein film as a barrier between a sample containing oxygen and a detector. The oxygen permeates through the film into the detector, and the change in oxygen concentration over time is measured. This technique is often used for films with specific applications, such as food packaging (Velaga *et al*., 2018).

Electrochemical sensors, such as oxygen sensors or oxygen electrodes, can be used to measure the oxygen permeability of protein films. These sensors measure changes in electrical signals or current caused by the oxygen permeating through the film (Wang *et al*., 2017).

Optical techniques, such as fluorescence quenching or phosphorescence quenching, can be used to measure the oxygen permeability of protein films. These methods rely on the change in fluorescence or phosphorescence intensity of a dye or probe embedded in the film, which is affected by the presence of oxygen (Velaga *et al*., 2018).

Whey protein films generally have relatively high oxygen permeability. This is due to the presence of hydrophilic regions in whey proteins that can facilitate the diffusion of oxygen molecules. Soy protein films typically exhibit moderate to low oxygen permeability. Soy proteins have a more compact structure compared to whey proteins, which can restrict the movement of oxygen molecules through the film. Additionally, the presence of hydrophobic regions in soy proteins can further limit oxygen permeability. Gelatin films generally have high oxygen permeability. Gelatin, derived from collagen, consists of random coil structures that create pathways for oxygen molecules to pass through the film easily. The high oxygen permeability of gelatin films can be advantageous for certain applications, such as wound dressings, where oxygen diffusion is desirable. Casein films typically have moderate to low oxygen permeability. Casein proteins have a complex structure, consisting of different subunits and a combination of alpha-helices and beta-sheets. This structure can hinder the movement of oxygen molecules through the film, resulting in lower oxygen permeability compared to whey protein films (Kaewprachu *et al*., 2016).

Microstructure of Protein Films

The scanning electron microscope (SEM) is commonly used to study the microstructure of protein films. The protein film sample needs to be properly prepared for SEM analysis. This typically involves fixing the film onto a suitable substrate, such as a glass slide or a metal stub. The sample may also need to be dehydrated or freeze-dried, depending on the nature of the protein film and the desired analysis. To enhance the conductivity of the sample and prevent charging effects during SEM imaging, a thin conductive coating is often applied to the protein film. Common coating materials include gold, gold-palladium, or carbon. The

coating can be applied using techniques like sputter coating or carbon evaporation. The prepared sample is then loaded into the SEM chamber, and the instrument is set up accordingly. This involves adjusting the vacuum level, optimizing the electron beam parameters (e.g., accelerating voltage, beam current), and selecting the appropriate imaging mode (e.g., secondary electron imaging, backscattered electron imaging). Once the instrument is properly set up, the protein film sample can be imaged using the SEM. The electron beam scans the sample surface, and interactions between the beam and the sample generate signals that are detected and translated into an image. Secondary electron imaging provides high-resolution surface morphology information, while backscattered electron imaging can provide compositional contrast (Pengbo *et al*., 2023).

The acquired SEM images can be analyzed to study the microstructure of the protein film. This may involve measuring film thickness, observing surface topography, evaluating pore size and distribution, or assessing the presence of cracks, defects, or other structural features. Quantitative analysis can be performed using specialized software to obtain statistical data on various parameters. It allows researchers to visualize and understand the microstructural features of the films, aiding in the development and optimization of protein film-based materials for various applications.

Chemical Properties

The Fourier Transform Infrared (FTIR) Spectroscopy

FTIR spectroscopy method is commonly used to study the chemical structure of protein films.

The protein film sample needs to be properly prepared for FTIR analysis. This typically involves depositing the film onto a suitable substrate, such as a potassium bromide (KBr) pellet or a specialized FTIR sample holder. The sample should be sufficiently thin and uniform to allow for accurate spectral analysis. The FTIR instrument is set up for analysis. This involves calibrating the instrument, purging the system to remove any interfering gases, and ensuring that all components are properly aligned. The instrument is typically equipped with an infrared light source, an interferometer, and a detector. The prepared protein film sample is placed in the FTIR instrument, and the measurement is conducted. The instrument emits infrared light that passes through the sample, and the resulting transmitted or reflected light is detected. The instrument records the intensity of the light at different wavelengths across the infrared spectrum. The recorded infrared spectrum is analyzed to obtain information about the chemical structure of the protein film. Protein films exhibit characteristic absorption bands in the infrared region, which correspond to specific functional groups and molecular vibrations. These absorption bands provide information about the types of chemical bonds present in the film, such as amide bonds (peptide bonds) and functional groups like -OH, -NH, and -C=O. The FTIR spectrum is interpreted by comparing it to reference spectra or using spectral libraries to identify specific functional groups and molecular vibrations. The positions and intensities of absorption peaks in the spectrum can provide information about the protein secondary structure, presence of specific amino acid residues, and any chemical modifications or interactions within the film. This information is valuable in understanding the structure-function relationship of protein films and can aid in optimizing their performance for various applications, such as food packaging, biomedical materials, or sensors (Yu *et al*., 2021).

The FTIR results of whey protein film, soy protein film, and gelatin film can provide insights into their chemical structure and composition. Here is a comparison of the FTIR characteristics of these protein films (Galus *et al*., 2016).

The whey protein film typically exhibits a strong and broad amide I band in the range of 1600-1700 cm^{-1}. This band is associated with the stretching vibrations of the C=O bonds in

the protein backbone, providing information about the secondary structure of the protein film. The amide II band, located around 1500-1600 cm^{-1}, represents the bending vibrations of the N-H bond and the stretching vibrations of the C-N bond. It provides information about the presence of various secondary structures, such as alpha-helices and beta-sheets, within the whey protein film (Galus *et al*., 2016).

Additional characteristic bands may appear in the whey protein film FTIR spectrum, such as the amide III band (1200-1300 cm^{-1}) and the amide A band (3000-3500 cm^{-1}), which provide information about the presence of specific amino acid residues and hydrogen bonding interactions. On the other hand, the soy protein film typically shows a narrower and less intense amide I band compared to whey protein. The position and shape of this band can provide information about the secondary structure of the soy protein film, such as the presence of beta-sheets or random coil structures. The amide II band in the soy protein film FTIR spectrum typically exhibits multiple peaks or shoulders, indicating the presence of different secondary structures and molecular vibrations. Similar to whey protein, the soy protein film FTIR spectrum may also show characteristic bands related to specific amino acid residues and hydrogen bonding interactions. The gelatin film typically exhibits a broad and intense amide I band, similar to whey protein (Han *et al*., 2016). The position and shape of this band can provide information about the secondary structure of the gelatin film, which is influenced by the presence of collagen in the gelatin. The amide II band in the gelatin film FTIR spectrum typically shows multiple peaks or shoulders, similar to soy protein. This indicates the presence of various secondary structures and molecular vibrations within the gelatin film (Alak *et al*., 2019). The FTIR spectrum of the gelatin film may also show characteristic bands related to specific amino acid residues and hydrogen bonding interactions, similar to whey protein and soy protein. It's important to note that the FTIR results may vary for different studies and experimental setups.

The X-ray Diffraction (XRD)

XRD method is commonly used to study the crystalline structure and orientation of materials, including certain types of protein films that exhibit crystallinity.

The protein film sample needs to be properly prepared for XRD analysis. This typically involves depositing the film onto a suitable substrate, such as a glass slide or a specialized XRD sample holder. The sample should be sufficiently thin and uniform to allow for accurate X-ray diffraction measurements. The XRD instrument is set up for analysis. This involves calibrating the instrument, aligning the X-ray source, and positioning the detector. The instrument typically uses a high-energy X-ray source, such as a rotating anode generator or a synchrotron radiation source, to produce X-rays. The prepared protein film sample is placed in the XRD instrument, and the measurement is conducted. The X-rays are directed onto the sample, and the resulting diffracted X-rays are detected. The instrument records the intensity of diffracted X-rays at different angles. The recorded XRD pattern is analyzed to obtain information about the crystalline structure of the protein film. XRD patterns consist of a series of sharp peaks that correspond to the scattering of X-rays by crystal planes within the material. The positions and intensities of these peaks provide information about the arrangement of atoms within the crystal lattice. The XRD pattern is interpreted by analyzing the positions and intensities of the diffraction peaks. This analysis can provide information about parameters such as the lattice spacing, crystal symmetry, crystal orientation, and crystallite size of the protein film. By comparing the XRD pattern to known crystal structures or using crystallographic software, researchers can identify the specific crystalline phases present in the film (Balaguer *et al*., 2013).

It's important to note that not all protein films exhibit crystallinity, and XRD analysis may not be suitable for samples that are amorphous or have low crystallinity. In such

cases, other techniques like FTIR or solid-state NMR spectroscopy may be more appropriate for studying the chemical structure of protein films.

Whey protein films are typically amorphous or semi-crystalline, meaning they may not exhibit distinct crystalline peaks in the XRD pattern. Soy protein films and gelatin films can also be amorphous or semi-crystalline, but they may exhibit some level of crystallinity depending on their preparation methods and processing conditions (Galus *et al*., 2016).

If any crystalline peaks are observed in the XRD patterns, the crystal structure can be analyzed. Whey protein films are primarily composed of globular proteins like β-lactoglobulin, which do not typically exhibit well-defined crystal structures. Soy protein films, on the other hand, may contain proteins like glycinin and β-conglycinin, which can form crystalline structures. Gelatin films, derived from collagen, may also exhibit some degree of crystallinity in the form of collagen fibrils (Alak *et al*., 2019).

Antimicrobial Properties

Gelatin films have been extensively studied for their antimicrobial properties, making them valuable for applications in food packaging and biomedical materials. These films exhibit antimicrobial activity against a wide range of microorganisms, including bacteria, fungi, and some viruses. The presence of natural antimicrobial peptides and proteins, such as collagen-derived peptides, in gelatin contributes to this effect. These peptides disrupt microbial cell membranes and interfere with essential cellular processes, inhibiting the growth and proliferation of microorganisms (Li *et al*., 2020).

Gelatin films have demonstrated effectiveness against both Gram-positive and Gram-negative bacteria, including *Escherichia coli*, *Staphylococcus aureus*, *Salmonella enterica*, and *Listeria monocytogenes*. They have also exhibited inhibitory effects on various fungi, such as *Candida albicans* and *Aspergillus niger*. The mechanisms underlying the antimicrobial properties of gelatin films can vary. Some studies suggest that the release of antimicrobial peptides from the gelatin matrix disrupts microbial membranes, while other mechanisms involve chelation of essential metal ions required for microbial growth or the alteration of pH levels, creating unfavorable conditions for microbial survival (Alak *et al*., 2019).

Incorporating antimicrobial agents such as essential oils, plant extracts, or nanoparticles into the gelatin matrix enhances their antimicrobial properties (Table 1). Modifying the film structure, such as through cross-linking or blending with other polymers, can also affect the release rate and efficacy of antimicrobial compounds (Karimi *et al*., 2022).

Gelatin films with antimicrobial properties find potential applications in food packaging to extend the shelf life of perishable products by inhibiting microbial growth. They can also be utilized in wound dressings or biomedical devices to prevent infection. However, it is important to note that the effectiveness of gelatin films may vary depending on the specific application and the targeted microorganisms. Further research and optimization of gelatin film formulations and processing techniques hold promise for enhancing their antimicrobial efficacy and expanding their applications in diverse fields (Alak *et al*., 2019)

Whey protein films have demonstrated antimicrobial activity against various microorganisms, including bacteria and fungi. The presence of bioactive peptides derived from whey proteins, such as lactoferrin, lactoperoxidase, and immunoglobulins, is responsible for this antimicrobial effect. These peptides possess antimicrobial properties and can inhibit the growth and proliferation of microorganisms through various mechanisms. They can disrupt microbial cell membranes, leading to cell leakage and death. Additionally, they may interfere with microbial enzyme systems or nutrient uptake, inhibiting their growth. Some peptides exhibit antimicrobial activity by inducing oxidative stress or

modulating the immune response of the host (Galus *et al*., 2016).

Notable bacteria that have been shown to be affected by whey protein films include *Escherichia coli, Staphylococcus aureus, Salmonella enterica,* and *Listeria monocytogenes*. Whey protein films have also exhibited inhibitory effects on various fungi, such as *Candida albicans* and *Aspergillus niger* (Kaewprachu *et al*., 2016).

Casein protein films have also demonstrated antimicrobial properties. Casein-derived peptides, such as lactoferricin and casocidin, exhibit antimicrobial activity against various bacteria and fungi. These peptides can disrupt microbial membranes or interfere with microbial enzyme systems, leading to cell death or growth inhibition (Matías *et al*., 2018).

Soy peptides, such as soybean trypsin inhibitors and lunasin, have shown antimicrobial activity against bacteria and fungi. Corn zein films have shown potential antimicrobial properties. Zein is a prolamin protein found in corn, and studies have reported its inhibitory effects against bacteria and fungi. The antimicrobial activity of corn zein films is attributed to the hydrophobic nature of zein, which can disrupt microbial cell membranes (dos Santos Paglione *et al.*, 2019).

Table 1- Incorporation of different essential oils in protein film as antimicrobial food packaging

Protein film	Added essential oil	The type of food applied for	reference
Gelatin	Clove	Fish	(Karimi *et al*., 2022)
Whey protein isolate	Garlic, rosemary, and oregano	Fresh beef	(Hadidi *et al*., 2022)
Casein	Origanum Volgare L.	Cherry tomato	(Matías et al., 2018)
Soy protein	Oregano and thyme	Fresh ground beef	(Martelli-Tosi *et al*., 2018)
Gluten	Star anise	Snacks	(Bagheri *et al*., 2019)
Zein	Cinamon and mustard	Tomatoes	(Sayadi *et al*., 2021)

Antioxidant Properties

Gelatin protein films have been investigated for their antioxidant properties. Gelatin protein films have demonstrated radical scavenging activity, meaning they can neutralize free radicals and prevent oxidative damage. Free radicals are highly reactive molecules that can cause cellular damage and contribute to various diseases. Gelatin films containing natural antioxidants, such as phenolic compounds or flavonoids, have shown effective radical scavenging activity, reducing the levels of harmful free radicals (Table 2). Gelatin protein films have been found to possess metal-chelating properties. Certain metal ions, such as iron and copper, can catalyze free radical formation through Fenton and Haber-Weiss reactions, leading to oxidative stress. Gelatin films containing chelating agents can bind to these metal ions and inhibit their ability to generate free radicals, thereby reducing oxidative damage. These films have shown the ability to inhibit lipid oxidation, which is a major cause of food spoilage and deterioration. Lipid oxidation can lead to the formation of harmful compounds and rancidity in food products. Gelatin films with antioxidant properties can prevent or delay lipid oxidation by scavenging free radicals or inhibiting the initiation and propagation of lipid oxidation reactions. These films can also serve as protective barriers, preserving the antioxidant activity of incorporated compounds. By encapsulating antioxidants within the gelatin matrix, the films can shield them from degradation caused by environmental factors, such as oxygen or light (Table 2). This helps to maintain the stability and efficacy of antioxidants, ensuring their long-term antioxidant activity (Hadidi *et al*., 2022).

Whey protein films have demonstrated antioxidant properties due to the presence of bioactive peptides, such as lactoferrin and lactoperoxidase. These peptides exhibit radical scavenging activity and can effectively neutralize free radicals, providing protection against oxidative stress. Whey protein films have also shown hydrogen peroxide scavenging

and metal-chelating properties, further contributing to their antioxidant activity (Yu *et al*., 2021).

Soy protein and corn zein films have been investigated for their antioxidant properties. Antioxidant compounds present in soy, such as isoflavones and phenolic compounds, contribute to the antioxidant activity of soy protein films. These compounds exhibit radical scavenging activity and can inhibit lipid oxidation. Soy protein films also possess metal-chelating properties, further enhancing their antioxidant potential (Jensen *et al*., 2015).

Table 2- Different antioxidant types used in protein packaging film for food products

	Type of antioxidants	Classifications	Examples of antioxidants	Examples of films applied in	Food product	Reference
Antioxidants	Primery	Synthetic	BHA, BTA	Corn Zein	Turkey	(Sahraee *et al*., 2019)
		Natural	Plant extracts and essential oils	Gelatin	Fish oil	(Sahraee *et al*., 2019)
	Secondary	Chelators	EDTA	Whey protein	Turkey frankfurter	(Galus *et al*., 2016)
			Polylactic acid	Zein	Fish fillet	(Sayadi *et al*., 2021)
		UV absorbers	Nanoparticles	Gelatin	Bakery products	(Milani *et al*., 2015)
		Single oxygen quenchers	Carotenoids	Gelatin	Porks	(Alak *et al*., 2019)
			Polyphenols	Casein	Cheese	(Salajegheh *et al*., 2020)
		Oxygen scavengers	Metal oxide	Gelatin	Cake	(Karimi *et al*., 2022)
			Ascorbic acid	Whey protein	Roasted peanuts	(Garavand *et al*., 2020)

Protein Sources for Food Packaging

Gelatin

Gelatin possesses a range of properties which makes it highly suitable for packaging film applications. Firstly, gelatin exhibits excellent film-forming properties, allowing it to be easily processed into films. These films are thin, flexible, and transparent, while also possessing good mechanical strength. This combination of properties makes gelatin an ideal material for packaging films, as it can provide a protective barrier while maintaining the integrity of the packaged product.

In addition to its film-forming capabilities, gelatin is a natural protein derived from collagen, making it biodegradable. This means that gelatin can be broken down by microorganisms, enzymes, and natural processes over time, resulting in eco-friendly disposal. The biodegradability of gelatin is a highly desirable property for packaging films, as it helps to reduce environmental impact and waste accumulation.

Furthermore, gelatin films exhibit good water vapor barrier properties, enabling them to effectively control the moisture content of packaged products. This is crucial in maintaining the freshness and quality of perishable goods, as it helps prevent moisture loss or gain, thereby extending the shelf life of the products.

While not as effective as synthetic materials, gelatin films also provide a certain level of oxygen barrier properties. This property is important for packaging applications, as it helps slow down the oxidation process and preserve the quality and shelf life of oxygen-sensitive products.

Moreover, gelatin is compatible with various active ingredients, allowing for the incorporation of functional additives into gelatin films. This enhances their performance and offers additional benefits such as antioxidant or antimicrobial properties. Gelatin can also be modified or blended with other materials to enhance its properties and tailor it to specific packaging needs.

Lastly, gelatin is widely used in the food industry and is considered safe for consumption. This makes gelatin films suitable for direct food contact applications, such as food packaging or edible films and coatings or encapsulation (Alak *et al*., 2019).

While gelatin offers numerous desirable properties for packaging film, it is important to consider its disadvantages as well. Gelatin films can be sensitive to moisture, which can result in changes to their mechanical properties, such as increased brittleness or reduced strength. This sensitivity limits their use in high-humidity environments or for products with high moisture content. Additionally, gelatin has a relatively low melting point, making it unsuitable for heat-resistant packaging applications like microwaveable or hot-fill packaging.

Furthermore, gelatin films have limited resistance to water and fat, which can cause them to soften, lose structural integrity, or interact unfavorably with the packaged product. This limitation poses challenges for packaging products with high water or fat content. While gelatin films provide some barrier properties, they may not match the performance of synthetic materials in terms of oxygen or moisture barriers. Thus, their use may be restricted in certain packaging applications requiring higher barrier properties.

Another consideration is the limited shelf life of gelatin films, particularly those derived from animal sources, due to their biodegradability and susceptibility to microbial growth. This can be problematic for long-term storage or products requiring extended shelf life. Additionally, gelatin, derived from animal sources like collagen, can potentially trigger allergic reactions in individuals with specific allergies to animal proteins. This restricts the use of gelatin films in certain applications, particularly in allergen-sensitive industries or for products targeting specific consumer groups (Karimi *et al*., 2022).

Ongoing research and development efforts aim to address these limitations and enhance the overall performance of gelatin films. Moreover, alternative sources of gelatin, such as plant-based or modified gelatins, are being explored to overcome some of these disadvantages.

Gelatin for film packaging is primarily derived from animal sources, particularly from the collagen found in the skin, bones, and connective tissues of animals. Gelatin derived from bovine sources, such as cows or cattle; gelatin derived from porcine sources, such as pigs; and gelatin from poultry sources, including chicken and turkey, are widely used in the food and packaging industries.

It's important to note that gelatin derived from animal sources may pose challenges related to religious or dietary restrictions, allergenic potential, or ethical considerations for certain individuals or industries.

In recent years, there has been increasing interest in exploring alternative sources of gelatin to address these concerns. Some alternative sources being explored include fish gelatin derived from fish skins and scales, as well as plant-based gelatin substitutes, such as modified starches or proteins from sources like seaweed or legumes. These alternative sources offer potential solutions for individuals or industries seeking non-animal-derived options for gelatin-based packaging films.

To improve the properties of gelatin as packaging film, various additives can be incorporated. These additives can enhance specific characteristics or address limitations of gelatin films. Here are some commonly used additives (Winotapun *et al*., 2019).

Common plasticizers used in gelatin film include glycerol, sorbitol, polyethylene glycol, and propylene glycol. These additives help reduce brittleness and increase the film's ability

to conform to different shapes or packaging requirements.

Crosslinking agents like glutaraldehyde, genipin, and transglutaminase can be added to promote crosslinking between gelatin molecules, resulting in improved film properties.

Natural antioxidants, such as vitamin E, ascorbic acid, or plant-derived extracts, can be added to enhance the film's stability and prolong the shelf life of the packaged product (Table 2).

Colorants, such as natural or synthetic pigments or dyes, can be added to gelatin films to provide visual appeal, branding, or product differentiation. These additives help create attractive packaging designs or enhance the appearance of the film.

Antimicrobial agents can be incorporated into gelatin films to inhibit the growth of microorganisms and extend the shelf life of the packaged product. Examples of antimicrobial additives include essential oils, chitosan, or silver nanoparticles (Table 1).

Various additives can be used to enhance the barrier properties of gelatin films. For example, montmorillonite clay can be added to improve oxygen barrier properties, while lipids or waxes can enhance moisture barrier properties.

Fillers, such as cellulose fibers or nanoparticles, can be added to improve the mechanical strength, thermal resistance, or barrier properties of gelatin films. These additives help enhance the overall performance and durability of the film.

Montmorillonite clay nanoparticles, such as organically modified montmorillonite (OMMT), have been studied to enhance the barrier properties of gelatin films. These nanoparticles can improve the oxygen and water vapor barrier properties, mechanical strength, and thermal stability of gelatin films (Wang *et al*., 2017).

Metal oxide nanoparticles, such as titanium dioxide (TiO2) or zinc oxide (ZnO), have been explored for their UV-blocking properties in gelatin films. These nanoparticles can enhance the film's resistance to UV radiation, thereby protecting the packaged product from photochemical degradation (Garavand *et al*., 2020).

Silver nanoparticles (AgNPs) have gained attention for their antimicrobial properties. When incorporated into gelatin films, they can inhibit the growth of microorganisms, extending the shelf life of the packaged product and providing an additional protective barrier against contamination (Kim *et al*., 2020).

Cellulose nanocrystals (CNCs) derived from cellulose fibers have been investigated as reinforcing agents in gelatin films. These nanoparticles can enhance the mechanical properties, such as tensile strength and elasticity, of gelatin films, making them more suitable for packaging applications (Kao *et al*., 2014).

Chitosan nanoparticles have been studied for their potential as antimicrobial agents in gelatin films (Garavand *et al*., 2020).

Hybrid nanoparticles combining the antimicrobial properties of silver nanoparticles with the barrier-enhancing properties of nanoclays have been investigated. These hybrid nanoparticles can provide both antimicrobial and barrier functionalities to gelatin films, making them suitable for food packaging applications (Jariyasakoolroj *et al*., 2020).

Several essential oils have been studied and used in gelatin films to improve their packaging properties. Rosemary essential oil is known for its antioxidant and antimicrobial properties. When incorporated into gelatin films, it can help extend the shelf life of packaged products by inhibiting the growth of microorganisms and reducing oxidative degradation (Velaga *et al*., 2018).

Thyme, oregano, cinnamon, lemongrass, tea tree essential oils have strong antimicrobial properties, making them a valuable additives for gelatin films. It can help inhibit the growth of bacteria and fungi, thereby enhancing the safety and shelf life of the packaged product (Farhan *et al*., 2017).

Gelatin film is used as packaging for a variety of foods. Gelatin films are commonly used to package confectionery items such as

gummy candies, jelly beans, marshmallows, and fruit snacks. The film provides a protective barrier, enhances the product's appearance, and helps maintain freshness. Gelatin films can also be used for packaging dairy products like yogurts, puddings, and custards. The film helps prevent moisture loss, maintains product texture, and extends shelf life. Gelatin films are sometimes used for packaging meat and poultry products such as deli meats, sausages, and pâtés. The film can help improve product presentation, prevent moisture loss, and provide a protective barrier against contaminants. Gelatin films can be utilized for packaging bakery items like cakes, pastries, and cookies. The film helps retain moisture, preserve freshness, and protect the product during transportation. Gelatin films are also used for packaging pet foods, including treats and wet pet food products. The film helps maintain product quality, prevent spoilage, and provide an attractive presentation (Alak *et al*., 2019).

Whey Protein

Whey protein, derived from milk during the cheese-making process, possesses a range of favorable properties that render it suitable for packaging film applications. With excellent film-forming properties, whey protein can be processed into thin films or coatings, serving as a base material for packaging films. Moreover, whey protein films are biodegradable, ensuring they naturally break down over time without causing harm to the environment. This makes them a sustainable alternative to conventional plastic packaging materials (Galus *et al*., 2011).

Additionally, whey protein films display robust mechanical strength, enabling them to withstand handling and transportation without tearing or breaking easily. This characteristic makes them suitable for packaging a diverse range of products.

Considering whey protein's safety for human consumption and its common usage in food products, whey protein films are generally deemed safe for direct food contact, making them an ideal choice for food packaging.

Notably, whey protein is a byproduct of the dairy industry, rendering it a renewable and sustainable resource. By utilizing whey protein for packaging films, waste can be reduced, and a circular economy can be promoted (Pengbo *et al*., 2023).

While whey protein offers several favorable properties for packaging film, it is essential to consider its drawbacks. Whey protein films can be sensitive to moisture, resulting in reduced mechanical strength and barrier properties. This limits their use in applications requiring high moisture resistance. Additionally, whey protein films have lower heat resistance compared to synthetic films, restricting their suitability for high-temperature processes like sterilization or hot filling.

Moreover, whey protein films exhibit solubility in water, which can be considered disadvantageous in certain packaging applications. The processing of whey protein into films can be challenging due to its high viscosity and tendency to form gels.

Furthermore, whey protein as a valuable food ingredient may increase the production costs of packaging films compared to conventional plastics. This cost factor can limit the widespread adoption of whey protein-based films in certain applications. The availability of whey protein as a raw material for film production may also be constrained by the supply and demand dynamics of the dairy industry, impacting the scalability and commercial viability of whey protein-based packaging films.

Additionally, whey protein films may be sensitive to ultraviolet (UV) light, leading to discoloration and degradation over time. With advancing technology, these limitations may be mitigated, making whey protein films more viable for a broader range of packaging applications (Matías *et al*., 2018).

Whey protein concentrate (WPC) and whey protein isolate (WPI) are both forms of protein derived from whey, a byproduct of the cheese-making process. The main difference between whey protein concentrate (WPC) and whey protein isolate (WPI) lies in their protein

content and processing methods. WPC typically contains around 70-80% protein, while WPI has a higher protein content, usually around 90% or higher. This is because WPI undergoes additional processing steps to remove more non-protein components, such as lactose and fats.

Whey protein concentrate is produced by filtering and drying whey, resulting in a powder that retains a portion of the non-protein components naturally present in milk. On the other hand, whey protein isolate goes through further processing, including additional filtration or ion exchange, to remove more of the non-protein components, resulting in a more pure protein powder. WPI is generally more expensive than WPC due to the additional processing required to achieve higher protein content and remove more non-protein components (Chaudhary *et al.*, 2020).

Various additives have been utilized to enhance the properties of whey protein as a packaging film. Plasticizers, Cross-linking agents, Antioxidants and fillers or reinforcements like cellulose nanofibers, chitosan fibers, and starches can be incorporated to enhance mechanical properties, barrier properties, and stability. Coating agents such as lipids (e.g., fatty acids, waxes) and polysaccharides (e.g., chitosan, alginate) are employed to improve water vapor resistance and barrier properties. Additionally, colorants and flavorings can be added for visual appeal or to provide specific taste or aroma to the packaged product.

Blending with polymers like starch, alginate, or chitosan, can improve the mechanical strength, barrier properties, and stability of whey protein films (Galus *et al.*, 2016).

Various essential oils have been studied for their potential to improve the properties of whey protein films. Oregano oil has been investigated for its antimicrobial properties when incorporated into whey protein films. It has shown potential in inhibiting the growth of bacteria and fungi, thereby extending the shelf life of packaged products. Thyme oil, cinnamon, clove, rosemary, and tea tree oil have been explored for their antimicrobial and antioxidant activities. It has been used as an additive in whey protein films to improve their barrier properties, mechanical strength, and resistance to oxidation.

Whey protein films have shown promise as edible coatings for fruits and vegetables, offering potential to extend their shelf life, maintain quality, and reduce post-harvest losses. Additionally, these films have been investigated as coatings for meat and poultry products, aiming to improve quality, prevent moisture loss, and enhance shelf life. By acting as barriers against oxygen and microbial growth, whey protein films contribute to maintaining the freshness and safety of packaged meat.

Moreover, whey protein films have been studied for packaging dairy products such as cheese, yogurt, and milk. These films offer potential benefits in terms of preserving freshness, preventing moisture migration, and enhancing the overall quality and shelf life of these products. Furthermore, whey protein films have been explored for coating bakery and confectionery products like bread, cookies, chocolates, and candies. By utilizing these films, the freshness and quality of these products can be preserved while preventing moisture-related issues.

Leguminaceae Proteins (Soy Beans, Pea, etc.)

Proteins derived from legumes, specifically those belonging to the Leguminaceae family such as soybeans, lentils, and peas, possess several advantageous properties that make them well-suited for packaging films. These proteins exhibit excellent film-forming abilities, enabling the creation of thin and flexible films suitable for packaging applications. Moreover, they have the capability to form cohesive and continuous films, providing a protective barrier for packaged products.

Leguminaceae protein films demonstrate commendable barrier properties, including resistance to moisture, oxygen, and UV light.

Additionally, these proteins enhance the mechanical strength of packaging films, improving tensile strength, elasticity, and puncture resistance (Rani *et al*., 2020).

One notable advantage of Leguminaceae proteins is their plant-based origin, rendering them biodegradable and renewable. In addition, Leguminaceae proteins can be modified or blended with other ingredients to enhance their functional properties. For instance, blending these proteins with plasticizers or other polymers can improve film flexibility, elongation, and moisture resistance. This versatility allows for customization and adaptation to specific packaging needs (Sani *et al*., 2021).

Several members of the Leguminaceae family have been studied for their potential use in packaging film making.

Extensive research has been conducted on the use of soy protein films derived from Glycine max for various packaging applications. Soy protein isolates or concentrates have been utilized to create films with commendable mechanical strength, barrier properties, and biodegradability.

Studies have examined the impact of soy protein films on food quality, sensory attributes, and shelf life extension. Applications include coating fruits, vegetables, and meat products, as well as packaging bakery goods, snacks, and dairy products (Han *et al*., 2018).

Researchers have explored surface modification techniques to improve the properties of soy protein films. Surface treatments, such as plasma treatment, chemical modification, or coating with other materials, have been investigated to enhance film functionality, such as water resistance, antimicrobial properties, and controlled release of active compounds.

Antioxidants such as tocopherols (vitamin E), ascorbic acid (vitamin C), and polyphenols have been incorporated into soy protein films to enhance their oxidative stability. Natural antimicrobial compounds like essential oils, plant extracts, and bacteriocins have been used to improve the antimicrobial properties of soy protein films.

Glycerol and sorbitol are commonly used plasticizers in soy protein films. They help reduce film brittleness and enhance film elongation and tensile strength.

Nanomaterials such as silver nanoparticles, zinc oxide nanoparticles, and cellulose nanofibers have been studied for their potential to improve soy protein film quality.

Emulsifiers like lecithin or other food-grade surfactants can improve the emulsion stability and film-forming properties of soy protein films. They can help create more uniform films with improved mechanical strength and barrier properties (Martelli-Tosi *et al*., 2018).

Pea protein films, derived from Pisum sativum, have emerged as a promising alternative to soy protein films. By utilizing pea protein isolates or concentrates, films with excellent film-forming ability, barrier properties, and mechanical strength have been developed.

To further enhance film properties, pea protein can be blended with other polymers. Blending pea protein with chitosan, alginate, or starch, for instance, can significantly improve film flexibility, water resistance, and barrier properties (Du *et al*., 2018).

Pea protein films exhibit moderate barrier properties, characterized by low water vapor permeability (WVP) and oxygen permeability (OP) values. Moreover, the thermal stability of these films has been found to be satisfactory for packaging applications.

Lentil protein films possess a range of properties that make them well-suited for packaging applications. Notably, they exhibit impressive mechanical strength and flexibility. With desirable tensile strength and elongation at break, these films can withstand handling and packaging processes without easily breaking or tearing.

In terms of barrier properties, lentil protein films fall within the moderate to excellent range. Over time, these films naturally degrade, offering a more sustainable alternative to

conventional plastic films (Acquah *et al.*, 2020).

However, it is important to note that lentil protein films can be sensitive to moisture. Without proper protection or modification, they have the potential to absorb water and compromise their mechanical properties. To address this issue, strategies such as cross-linking or incorporating hydrophobic additives like fatty acids, waxes, lipids, and silanes can be employed to enhance the water resistance of lentil protein films.

Another advantageous characteristic of lentil protein films is their good transparency. This allows for visual inspection of the packaged products, ensuring quality control. They are compatible with a diverse range of food products, including fruits, vegetables, bakery goods, snacks, and meat products (Ortiz *et al.*, 2018).

Chickpea (Cicer arietinum) protein films have been investigated as a potential packaging material. Researchers extracted protein from chickpea flour and prepared film-forming solutions by dissolving the protein in a suitable solvent. Further optimization of the formulation and processing conditions could enhance the performance of chickpea protein films for broader applications in food packaging (Du *et al.*, 2018).

Graminacea Protein Films

Several members of the Graminaceae family, also known as the grass family, have been studied for their filmmaking capability (Balaguer *et al.*, 2013).

Rice protein, wheat gluten, corn zein, and barley protein have been extensively studied for their film-forming properties, making them a promising material for the development of edible films (Hager *et al.*, 2019).

Wheat proteins possess valuable elastic and cohesive properties that make them suitable for non-food applications, including the production of garbage bags. Additionally, wheat proteins can be utilized as edible coatings in various food applications. For example, when used as coatings on shell eggs, degradable polymers and oils derived from wheat proteins can effectively inhibit microbial invasion and enhance shell strength. The development of degradable films and coatings using wheat gluten opens up new marketing opportunities for this versatile ingredient (Bagheri *et al.*, 2019).

Zein, a type of alcohol-soluble prolamine storage protein found in corn, was divided into four classes (α-zein, β-zein, γ-zein, and δ-zein) based on solubility and sequence homology. Among these classes, α-zein constitutes the majority, accounting for 70-85% of the total zein mass, while γ-zein is the second most abundant, making up 10-20% of the fraction. All zein classes are rich in hydrophobic and neutral amino acids like leucine, proline, and alanine, with some polar amino acid residues such as glutamine also present. α-Zein is composed of highly similar repeat units and has a high α-helix content (Fazeli *et al.*, 2022). Notably, zein differs from other proteins in that it is almost devoid of lysine and tryptophan, and contains only a small amount of arginine and histidine residues. These unique amino acid compositions contribute to its distinct solubility, which is primarily limited to acetone, acetic acid, aqueous alcohols, and aqueous alkaline solutions. Due to Zein protein unique features, such as filmmaking, significant thermal stability and gas barrier, it seems suitable for food packaging. Zein edible films and coatings create a transparent yellowish, brilliant, and elastic appearance and show exceptional preservative features in food packaging (Sayadi *et al.*, 2021).

Barley, a key grain in brewing, is used in both raw and malted forms, often combined with other grains. The endosperm is vital for plant growth due to its nutrient content. Brewers' spent grain, a major by-product of brewing, has sparked interest in sustainable utilization of its protein content. This aligns with the industry's goal to reduce waste, which includes significant liquid and solid by-products per beer production. Harnessing barley proteins, valued for their nutritional

quality, presents promising opportunities in the food sector (Yang *et al*., 2015).

By combining other film base materials with barley protein, such as gelatin, it is possible to achieve improved characteristics like tensile strength and percent elongation (Karimi *et al*., 2022).

Advances in Protein-based Film Technology

Film Preparation through Thermoplastic Method

Edible films offer a means to effectively regulate the movement of substances within food or between the food and its surroundings. The wide variety of proteins, with their countless arrangements of amino acids, enables a range of interactions and chemical reactions to occur as proteins denature and link together during heat processing. Two primary processes can be employed to create edible films (Fig. 1). The "wet process" involves dispersing or dissolving biopolymers in a film-forming solution (known as solution-casting), followed by the evaporation of the solvent. On the other hand, the "dry process" relies on the thermoplastic properties exhibited by certain proteins and polysaccharides at low moisture levels, using compression molding and extrusion.

The thermoplastic method for film making involves the use of heat and pressure to transform a polymer or biopolymer into a pliable and moldable state, allowing it to be shaped into a film.

A suitable thermoplastic polymer or biopolymer is chosen based on its desired properties, such as film strength, flexibility, and barrier properties. The polymer is typically combined with other ingredients, such as plasticizers, to improve its processability and final film properties. These additives help to reduce the glass transition temperature of the polymer, making it easier to shape and mold. The mixture is heated to a temperature above the glass transition or melting point of the polymer. This causes the polymer chains to become mobile and allows for the formation of a viscous, molten state. The molten polymer is then subjected to pressure and shaped into a thin film using various techniques, such as compression molding or extrusion. Compression molding involves placing the molten polymer between two plates and applying pressure to form a film, while extrusion involves forcing the molten polymer through a die to create a continuous film. Once the desired film shape is achieved, the film is rapidly cooled to solidify the polymer chains and lock them into place. This solidification process can be achieved by cooling the film using chilled rollers or immersing it in a cooling bath. After solidification, the film may undergo additional treatments, such as annealing or stretching, to further enhance its mechanical properties and performance (Velaga *et al*., 2018).

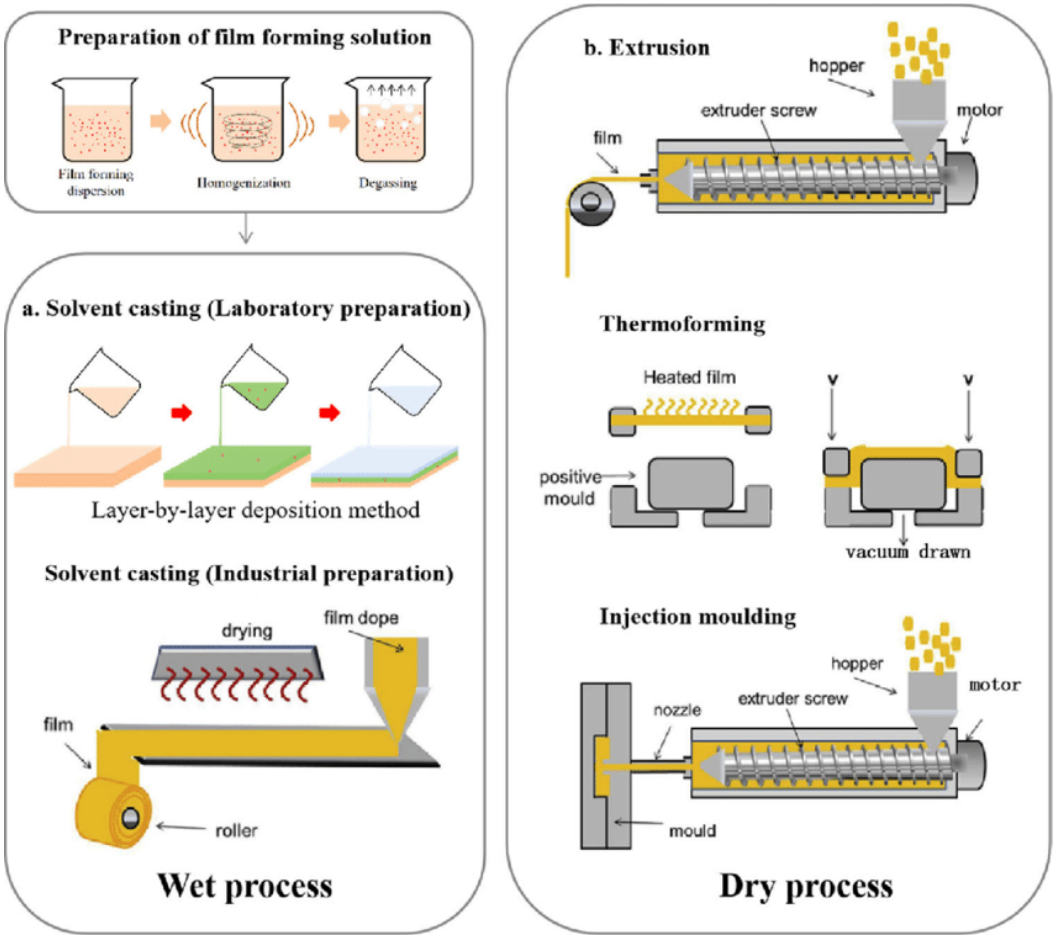

Fig. 1. Schematic of Film preparation through casting and thermoplastic method (Chen et al., 2021)

Wheat gluten, corn zein, soy protein, myofibrillar proteins, and whey proteins have all been successfully transformed into films using methods like compression molding and extrusion. These thermoplastic processes present a highly efficient way to manufacture edible films on a large scale, thanks to the use of low moisture levels, high temperatures, and short processing times. The addition of water, glycerol, sorbitol, sucrose, and other plasticizers allows the proteins to undergo transition into a glassy state, making them easier to shape and process without losing their integrity (Cheng *et al*., 2021).

The specific ways in which proteins interact during thermoplastic processing are not fully understood. The reactivity of proteins is influenced by their physicochemical environment and the thermomechanical treatment they undergo. The type and quantity of plasticizer used can also impact protein reactivity and the properties of the extruded material. For instance, a study examining the effect of different plasticizers on gluten protein reactivity found that octanoic and lactic acids hindered protein aggregation, despite the high mixing temperatures employed, which typically promote aggregation. The aggregation of gluten proteins is believed to involve reactions between sulfhydryl and disulfide groups. However, under acidic conditions, these reactions are less favorable as sulfhydryl acts as a catalyst. Whey protein films that were compression-molded with water as a plasticizer resulted in brittle and insoluble films, whereas those plasticized with glycerol were flexible, and their solubility depended on the temperatures used during film formation (Yang *et al.*, 2015).

In the case of corn zein, it was extruded into sheets along with fatty acids. Stable extrusion runs were achieved due to the binding of the fatty acids to the zein surface, as indicated by differential scanning calorimetry (DSC). This binding phenomenon prevented the separation of lipid phases and the sticking of zein onto the extruder barrel (Salajegheh *et al*., 2020).

Nanocomposite Protein Films

The use of biodegradable packaging materials has certain limitations as they cannot completely replicate the characteristics of petroleum-based materials. However, the incorporation of nano-sized materials allows for the modification of these materials, providing similar properties to traditional packaging materials. A nanocomposite film is created by blending a biopolymer with nanofillers to form a solid material system with multiple phases. When producing nanocomposites through the casting method, it is essential to first disperse the nanoparticles (NPs) in water, as they are typically sold in agglomerated microscopic forms. By incorporating various nanomaterials (ranging from 1 to 100 nm) into plant protein-based films, their barrier, optical, mechanical, and antimicrobial properties can be enhanced. This modification alters the physicochemical and functional characteristics of the films, opening up possibilities for their use as multifunctional ingredients in food products. Nanomaterials possess unique chemical, biological, electrical, thermal, mechanical, optical, and magnetic properties that differ from those of bulk materials (Garavand *et al*., 2020).

There are various examples of nanocomposite protein films that have been developed by incorporating nanomaterials into protein-based matrices.

Gelatin can be combined with nanoclays to create composite films. The addition of nanoclays improves the mechanical properties and barrier performance of the gelatin film. The addition of nanoclays can significantly increase the tensile strength, stiffness, and toughness of gelatin films. The clay particles create a reinforcing network within the gelatin matrix, improving its mechanical performance. Nanoclays can enhance the barrier properties of gelatin films, particularly against gases, such as oxygen and carbon dioxide, and water vapor. The presence of the nanoclays creates tortuous paths for gas and moisture molecules, slowing down their permeation through the film. Nano clay particles can improve the thermal stability of gelatin films. They act as heat barriers, reducing the rate of heat transfer through the film and enhancing its resistance to high temperatures. Depending on the type and concentration of nanoclays used, they can also influence the transparency of gelatin films. In some cases, the addition of nanoclays can lead to a slight reduction in film transparency, which may be desirable for certain applications. The improved barrier properties of nanoclay-reinforced gelatin films can help extend the shelf life of food products by reducing oxygen and moisture permeation. This can help in preserving the quality and freshness of the packaged goods (Winotapun *et al*., 2019).

Gelatin can be combined with silver nanoparticles to create antimicrobial composite films. The silver nanoparticles provide antimicrobial properties to the film, making it suitable for food packaging applications. Soy protein isolate can be combined with graphene oxide, a two-dimensional nanomaterial, to create composite films. The addition of graphene oxide improves the mechanical strength and barrier properties of soy protein film. Whey protein isolate can be blended with zinc oxide nanoparticles to create nanocomposite films. The incorporation of zinc oxide nanoparticles enhances the antimicrobial and barrier properties of whey protein film. Corn zein can be combined with nanoclays to create composite films. The addition of nanoclays improves the mechanical properties and barrier performance of corn zein film (Yu *et al*., 2021).

Non-thermal Techniques for Improving Film Properties

Protein films, due to their limited mechanical strength, tendency to rupture, and poor water resistance, are not suitable for use in the food industry. However, there are various non-thermal and thermal techniques available to address these limitations and modify the properties of protein films. Techniques such as microwave, ultrasound, cold-plasma, irradiation, and high-pressure processing can be employed to enhance the mechanical strength, water resistance, and overall performance of protein films (Jariyasakoolroj *et al*., 2020).

These techniques work by reducing particle size, promoting intermolecular electrostatic repulsion between protein molecules, and facilitating cross-linking. By modifying the protein films using these methods, their properties can be significantly improved. This is particularly important in the food industry, as modified protein films with excellent barrier properties can help reduce food waste and environmental pollution. Additionally, they contribute to enhancing the quality, safety, and security of food products. Non-thermal and thermal techniques offer effective ways to overcome the limitations of protein films, making them more suitable for use in the food industry. These modifications not only enhance the mechanical strength and water resistance of the films but also improve their barrier properties, leading to a range of benefits for food preservation and sustainability.

Non-thermal techniques encompass a range of methods from physics, chemistry, and biology that do not require heating to induce changes in a system. These techniques, such as microwave, ultrasound, high-pressure processing, irradiation, and cold plasma, have been widely utilized to improve the properties of protein-based edible films (Kao *et al*., 2014).

The drying process for whey protein isolate (WPI) edible films involved the use of microwave drying. It took approximately 5 minutes to dry the films in a microwave oven. Interestingly, both microwave drying and drying at room conditions yielded comparable results in terms of water vapor permeability (WVP) for the WPI films. Additionally, the application of microwave drying led to increased values in elongation and tensile strength for the films (Galus *et al*., 2016).

Ultrasound was used to unfold the pea protein isolate and expose hydrophobic groups on the protein surface. This resulted in both dissociation of PPI and formation of larger aggregates. Additionally, FE-SEM analysis showed that ultrasound reduced cracks and protein aggregates on the surface of the PPI film. The film structure was examined using FTIR, which revealed shifts in peak positions in the amide I and II regions, indicating changes in the protein's secondary structure due to ultrasound. These structural modifications led to improvements in the properties of the PPI films. Specifically, ultrasound greatly enhanced film transparency, significantly increased film tensile strength (while not affecting elongation at break), and reduced moisture content and water vapor permeability of the film (Moosavi *et al*., 2020).

A study was conducted to explore the effects of various cold plasma treatments on the modification of whey and gluten protein film properties. Atomic force microscopy (AFM) images showed that whey protein films became significantly rougher after plasma treatment, while the roughness of treated gluten films decreased dramatically. Additionally, the tensile strength of the films improved significantly after 10-minute treatment. Fourier-transform infrared spectroscopy (FTIR) revealed the introduction of functional groups such as C-O and O=C bonds, as well as the creation of cross-links, which could potentially lead to changes in various film properties. Furthermore, both edible polymers exhibited a significant decrease in gas permeability (Yang *et al*., 2015).

Conclusion

Biodegradable protein-based packaging offers a promising solution to address the environmental concerns associated with traditional plastic packaging materials. The physical properties of protein-based packaging films, such as flexibility, strength, and barrier

properties, make them suitable for various packaging applications. Additionally, their chemical properties, including biodegradability and compatibility with food products, further enhance their appeal. The antimicrobial and antioxidant properties exhibited by certain protein sources add an additional layer of functionality to these films, making them ideal for extending the shelf life of perishable goods. With a wide range of protein sources available, including plant-based and animal-based, there is ample opportunity for customization and optimization of protein-based packaging films. Furthermore, recent advancements in the field, such as the incorporation of bioactive compounds and the use of nanotechnology, have opened up new possibilities for improving the performance and functionality of protein-based packaging. However, challenges still exist, including the need for standardized production processes, scaling up manufacturing, and ensuring cost-effectiveness. Continued research and development efforts are essential to overcome these challenges and fully realize the potential of biodegradable protein-based packaging as a sustainable alternative in the packaging industry. Overall, protein-based packaging films represent an exciting and promising avenue for environmentally friendly packaging solutions with desirable physical and chemical properties, antimicrobial and antioxidant capabilities, and potential for further advancements and innovation.

Author Contributions

Samar Sahraee: Conceptualization, research and review, validation, writing-original draft, **Jafar M. Milani:** Project management, supervision, writing-reviewing and editing

Founding Sources

This research did not receive any specific funding from the public, commercial, or non-profit sectors.

References

1. Acquah, C., Zhang, Y., Dubé, M.A., & Udenigwe, C.C. (2020). Formation and characterization of protein-based films from yellow pea (*Pisum sativum*) protein isolate and concentrate for edible applications. *Current Research in Food Science, 2,* 61-69. https://doi.org/10.1016/j.crfs.2019.11.008
2. Alak, G., Guler, K., Ucar, A., Parlak, V., Kocaman, E.M., Yanık, T., & Atamanalp, M. (2019). Quinoa as polymer in edible films with essential oil: Effects on rainbow trout fillets shelf life. *Journal of Food Processing and Preservation, 43*(12), 1-11. https://doi.org/10.1111/jfpp.14268
3. Bagheri, V., Ghanbarzadeh, B., Ayaseh, A., Ostadrahimi, A., Ehsani, A., Alizadeh-Sani, M., & Adun, P.A. (2019). The optimization of physico-mechanical properties of bionanocomposite films based on gluten/carboxymethyl cellulose/cellulose nanofiber using response surface methodology. *Polymer Testing, 78,* https://doi.org/10.1016/j.polymertesting.2019.105989
4. Balaguer, M.P., Lopez-Carballo, G., Catala, R., Gavara, R., & Hernandez-Munoz, P. (2013). Antifungal properties of gliadin films incorporating cinnamaldehyde and application in active food packaging of bread and cheese spread foodstuffs. *International Journal of Food Microbiology, 166*(3), 369-377. https://doi.org/10.1016/j.ijfoodmicro.2013.08.012
5. Chen, W., & Ma, S., Wang, Q., McClements, D., Xuebo, L., Ngai, T., & Liu, F. (2021). Fortification of edible films with bioactive agents: a review of their formation, properties, and application in food preservation. *Critical Reviews in Food Science and Nutrition, 62,* 1-27. https://doi.org/10.1080/10408398.2021.1881435
6. Cheng, J., & Cui, L. (2021). Effects of high-intensity ultrasound on the structural, optical, mechanical and physicochemical properties of pea protein isolate-based edible film, *Ultrasonics Sonochemistry, 80.* https://doi.org/10.1016/j.ultsonch.2021.105809

7. Chaudhary, P., Fatima, F., & Kumar, A. (2020). Relevance of nanomaterials in food packaging and its advanced future prospects. *Journal of Inorganic and Organometallic Polymers and Materials, 30*(12), 5180-5192. https://doi.org/10.1007/S10904-020-01674-8
8. dos Santos Paglione, I., Galindo, M.V., de Medeiros, J.A.S., Yamashita, F., Alvim, I.D., Grosso, C.R.F., Sakanaka, L.S., & Shirai, M.A. (2019). Comparative study of the properties of soy protein concentrate films containing free and encapsulated oregano essential oil. *Food Packaging and Shelf Life, 22*. https://doi.org/10.1016/j.fpsl.2019.100419
9. Du, M., Xie, J., Gong, B., Xu, X., Tang, W., Li, X., Li, C., & Xie, M. (2018). Extraction, physicochemical characteristics and functional properties of Mung bean protein. *Food Hydrocolloids, 76,* 131-140. https://doi.org/10.1016/J.FOODHYD.2017.01.003
10. Farhan, A., & Hani, N.M. (2017). Characterization of edible packaging films based on semi-refined appa-carrageenan plasticized with glycerol and sorbitol. *Food Hydrocolloids, 64,* 48. https://doi.org/10.1016/j.foodhyd.2016.10.034
11. Fazeli, M., Alizadeh, M., & Pirsa, S. (2022). Nanocomposite film based on gluten modified with *Heracleum persicum* essence/ MgO/ Polypyrrole: Investigation of physicochemical and electrical properties. *Journal of Polymers and Environment, 30,* 954-970. https://doi.org/10.1007/s10924-021-02253-9
12. Galus, S., & Kadzińska, J. (2016). Moisture sensitivity, optical, mechanical and structural properties of whey protein-based edible films incorporated with rapeseed oil. *Food Technology and Biotechnology, 54*(1), 78-89. https://doi.org/10.17113/ftb.54.01.16.3889
13. Garavand, F., Cacciotti, I., Vahedikia, N., Rehman, A., Tarhan, Ö., Akbari-Alavijeh, S., Shaddel, R., Rashidinejad, A., Nejatian, M., & Jafarzadeh, S. (2020). A comprehensive review on the nanocomposites loaded with chitosan nanoparticles for food packaging. *Critical Reviews in Food Science and Nutrition,* 1-34. https://doi.org/10.1080/10408398.2020.1843133
14. Hadidi, M., Jafarzadeh, S., Forough, M., Garavand, F., Alizadeh, S., Salehabadi, A., Mousavi Khaneghah, A., & Jafari, M. (2022). Plant protein-based food packaging films; recent advances in fabrication, characterization, and applications. *Trends in Food Science and Technology, 120,* 154-173. https://doi.org/10.1016/j.tifs.2022.01.013
15. Hager, J.V., Rawles, S.D., Xiong, Y.L., Newman, M.C., Thompson, K.R., & Webster, C.D. (2019). Listeria monocytogenes is inhibited on fillets of cold-smoked sunshine bass, *Morone chrysops* × *Morone saxatilis*, with an edible corn zein-based coating incorporated with lemongrass essential oil or nisin. *Journal of the World Aquaculture Society, 50*(3), 575-592. https://doi.org/10.1111/jwas.12573
16. Han, Y., Yu, M., & Wang, L. (2018). Preparation and characterization of antioxidant soy protein isolate films incorporating licorice residue extract. *Food Hydrocolloids, 75,* 13-21. https://doi.org/10.1016/j.foodhyd.2017.09.020
17. Hashemi Moosavi, M., Khani, M., Shokri, B., Hosseini, M., & Shojaee Aliabadi, S., Mirmoghtadaie, L. (2020). Modifications of protein-based films using cold plasma. *International Journal of Biological Macromolecules, 142,* 769-777. https://doi.org/10.1016/j.ijbiomac.2019.10.017
18. Jariyasakoolroj, P., Leelaphiwat, P., & Harnkarnsujarit, N. (2020). Advances in research and development of bioplastic for food packaging. *Journal of the Science of Food and Agriculture, 100,* 5032-5045. https://doi.org/10.1002/jsfa.9497
19. Jensen, A., Lim, L.T., Barbut, S., & Marcone, M. (2015). Development and characterization of soy protein films incorporated with cellulose fibers using a hot surface casting technique. *LWT - Food Science and Technology, 60,* 162-170. https://doi.org/10.1016/j.lwt.2014.09.027

20. Kaewprachu, P., Osako, K., Benjakul, S., Tongdeesoontorn, W., & Rawdkuen, S. (2016). Biodegradable protein-based films and their properties: a comparative study. *Packaging Technology and Science, 29*, 77-90. https://doi.org/10.1002/pts.2183
21. Kao, M.J., Hsu, F.C., & Peng, D.X. (2014). Synthesis and characterization of Sio_2 nanoparticles and their efficacy in chemical mechanical polishing steel substrate. *Advances in Materials Science and Engineering*, 1-8. https://doi.org/10.1155/2014/691967
22. Kim, I., Viswanathan, K., Kasi, G., Thanakkasaranee, S., Sadeghi, K., & Seo, J. (2020). ZnO nanostructures in active antibacterial food packaging: Preparation methods, antimicrobial mechanisms, safety issues, future prospects, and challenges. *Food Reviews International*, 1-29. https://doi.org/10.1080/87559129.2020.1737709
23. Karimi, P., Zandi, M., & Ganjloo, A. (2022). Evaluation of physicochemical, mechanical, and antimicrobial properties of gelatin-sodium alginate-yarrow (*Achillea millefolium* L.) essential oil film. *Journal of Food Processing and Preservation, 46*(7), https://doi.org/10.1111/jfpp.16632
24. Lee, J., & Kim, K.M. (2010). Characteristics of soy protein isolate-montmorillonite composite films. *Journal of Applied Polymer Science, 118*, 2257-2263. https://doi.org/10.1002/app.31316
25. Li, J., Jiang, S., Wei, Y., Li, X., Shi, S.Q., Zhang, W., & Li, J. (2021). Facile fabrication of tough, strong, and biodegradable soy protein-based composite films with excellent UV-blocking performance. *Composites Part B: Engineering, 211*, 108645. https://doi.org/10.1016/j.compositesb.2021.108645
26. Li, X., Yang, X., Deng, H., Guo, Y., & Xue, J. (2020). Gelatin films incorporated with thymol nanoemulsions: Physical properties and antimicrobial activities. *International Journal of Bioligcal Micromolecules, 150*, 161-168. https://doi.org/10.1016/j.ijbiomac. 2020.02.066
27. Martelli-Tosi, M., Masson, M.M., Silva, N.C., Esposto, B.S., Barros, T.T., Assis, O.B.G., & Tapia-Blácido, D.R. (2018). Soybean straw nanocellulose produced by enzymatic or acid treatment as a reinforcing filler in soy protein isolate films. *Carbohydrate Polymers, 198*, 61-68. https://doi.org/10.1016/j.carbpol.2018.06.053
28. Matías, L., Picchio, M., Linck, Y.G., Monti, G.A., Gugliotta, L.M., Minari, R.J., & Alvarezigarzabal, C.I. (2018). Casein films crosslinked by tannic acid for food packaging applications. *Food Hydrocolloids, 84*, 424-434. https://doi.org/10.1016/j.foodhyd.2018.06.028
29. Milani, J., & Sahraee, S. (2015). Functional edible coatings and films for fresh cut food products. *Advances in Food Products, 37*(2), 78-80. https://doi.org/10.1021/acsomega.3c03459
30. Nisar, T., Wang, Z.-C., Yang, X., Tian, Y., Iqbal, M., & Guo, Y. (2018). Characterization of citrus pectin films integrated with clove bud essential oil: Physical, thermal, barrier, antioxidant and antibacterial properties. *International Journal of Biological Macromolecules, 106*, 670-680. https://doi.org/10.1016/j.ijbiomac.2017.08.068
31. Nor Adilah, A., Gun Hean, C., & Nur Hanani, Z.A. (2021). Incorporation of graphene oxide to enhance fish gelatin as bio-packaging material. *Food Packaging and Shelf Life, 28*, 100679. https://doi.org/10.1016/j.fpsl.2021.100679
32. Ortiz, C.M., Salgado, P.R., Dufresne, A., & Mauri, A.N. (2018). Microfibrillated cellulose addition improved the physicochemical and bioactive properties of biodegradable films based on soy protein and clove essential oil. *Food Hydrocolloids, 79*, 416-427. https://doi.org/10.1016/j.foodhyd.2018.01.011
33. Pengbo, C., Tianlun, S., Weilin, L., Mengyu, L., Mingxiao, Y., Weixue, Z., Yanzhuo, S., Yuting, D., & Jianhua, L. (2023). Advanced review on type II collagen and peptide: preparation, functional activities and food industry application, *Critical Reviews in Food Science and Nutrition*, 1-18. https://doi.org/10.1080/10408398.2023.2236699
34. Rani, S., Kumar, K.D., Mandal, S., & Kumar, R. (2020). Functionalized carbon dot nanoparticles reinforced soy protein isolate biopolymeric film. *Journal of Polymer Research, 27*, 1-10. https://doi.org/10.1007/s10965-020-02276-1

35. Sahraee, S., Milani, J., Regenstein, J., & Samadi Kafil, H. (2019). Protection of foods against oxidative deterioration using edible films and coatings: A review. *Food Bioscience, 32.* https://doi.org/10.1016/j.fbio.2019.100451
36. Salajegheh, F., Tajeddin, B., Panahi, B., & Karimi, H. (2020). Effect of edible coatings based on zein and chitosan and the use of Roman aniseed oil on the microbial activity of Mazafati dates. *Journal of Food and Bioprocess Engineering, 3,* 178-184. https://doi.org/10.22059/JFABE.2020.306636.1058
37. Sani, I.K., Rasul, N.H., Asdagh, A., Pirsa, S., & Ghazanfarirad, N. (2021). Development of antimicrobial/antioxidant nanocomposite film based on fish skin gelatin and chickpea protein isolated containing Microencapsulated *Nigella sativa* essential oil and copper sulfide nanoparticles for extending minced meat shelf life. *Materials Research Express*, *9*(2), https://doi.org/10.1088/2053-1591/ac50d6
38. Sayadi, M., Mojaddar Langroodi, A., & Jafarpour, D. (2021). Impact of zein coating impregnated with ginger extract and *Pimpinella anisum* essential oil on the shelf life of bovine meat packaged in modified atmosphere. *Journal of Food Measurement and Characterization*, 1-14. https://doi.org/10.1007/s11694-021-01096-1
39. Velaga, S.P., Nikjoo, D., & Vuddanda, P.R. (2018). Experimental studies and modeling of the drying kinetics of multicomponent polymer films. *AAPS American Association of Pharmaceutical Scientists, 19,* 425-435. https://doi.org/10.1208/s12249-017-0836-8
40. Wang, Y., Zhao, X., Feng, Z., Lu, G., Sun, T., & Xu, Y. (2017). Crystalline-phase-induced formation of fibre-in-tube TiO 2–SnO 2 fibres for a humidity sensor. *CrystEngComm, 19,* 5528-5531. https://doi.org/10.1039/C7CE01106G
41. Winotapun, C., Phattarateera, S., Aontee, A., Junsook, N., Daud, W., Kerddonfag, N., & Chinsirikul, W. (2019). Development of multilayer films with improved aroma barrier properties for durian packaging application. *Packaging Technology and Science, 32*, 405-418. https://doi.org/10.1002/pts.2452
42. Xiao, Y., Liu, Y., Kang, S., Cui, M., & Xu, H. (2021). Development of pH-responsive antioxidant soy protein isolate films incorporated with cellulose nanocrystals and curcumin nanocapsules to monitor shrimp freshness. *Food Hydrocolloids, 120,* 106893. https://doi.org/10.1016/j.foodhyd.2021.106893
43. Xu, L., Zhang, H., Lv, X., Chi, Y., Wu, Y., & Shao, H. (2017). Internal quality of coated eggs with soy protein isolate and montmorillonite: effects of storage conditions. *International Journal of Food Properties, 20,* 1921-1934. https://doi.org/10.1080/10942912.2016.1224896
44. Yang, W., Kenny, J. M., & Puglia, D. (2015). Structure and properties of biodegradable wheat gluten bionanocomposites containing lignin nanoparticles. *Industrial Crops and Products, 74,* 348-356. https://doi.org/10.1016/j.indcrop.2015.05.032
45. Yu, Y., Zheng, J., Li, J., Lu, L., Yan, J., Zhang, L., & Wang, L. (2021). Applications of two-dimensional materials in food packaging. *Trends in Food Science & Technology, 110,* 443-457. https://doi.org/10.1016/j.tifs.2021.02.021

نشریه پژوهشهای علوم و صنایع غذایی ایران
https://ifstrj.um.ac.ir

مقاله مروری

جلد ۲۰، شماره ۶، بهمن-اسفند، ۱۴۰۳، ص. ۲۰۰-۱۷۱

بسته‌بندی زیست‌تخریب‌پذیر ساخته‌شده از پروتئین

ثمر صحرائی[۱]- جعفر محمدزاده میلاتی[۱*]

تاریخ دریافت: ۱۴۰۳/۰۳/۰۲
تاریخ پذیرش: ۱۴۰۳/۰۶/۱۷

چکیده

فیلم‌های پروتئینی به‌دلیل ویژگی‌های منحصر به فرد و قابلیت‌های تطبیق‌پذیری خود، توجه زیادی در زمینه توسعه مواد بسته‌بندی پایدار جلب کرده‌اند. این فیلم‌ها به خاطر ممانعت از نفوذپذیری گازها، ویژگی‌های مکانیکی خاص و قابلیت‌های اتصال بین مولکولی، نسبت به سایر پلیمرهای زیستی بی شتر مورد توجه قرار گرفته‌اند. در سال‌های اخیر، محققان به برر سی روش‌های جدیدی برای بهبود خواص فیلم سازی، افزایش ا ستحکام مکانیکی و کاهش نفوذپذیری به گازها در فیلم‌های پروتئینی پرداخته‌اند. منابع پروتئینی مختلفی مانند ژلاتین، پروتئین آب پنیر، پروتئین سویا، زئین ذرت، گلوتن گندم و کازئین برای ساخت این فیلم‌ها مورد بررسی قرار گرفته‌اند. تکنیک‌هایی مانند ترکیب افزودنی‌ها، استفاده از عوامل اتصال‌دهنده عرضی و به‌کارگیری نانومواد، برای بهبود خواص این فیلم‌ها در حال اکتشاف هستند. همچنین، فیلم‌های کامپوزیتی بر پایه پروتئین با ترکیب پروتئین‌ها با دیگر پلیمرهای زیستی یا مواد مصنوعی به‌منظور دستیابی به عملکرد بهبود یافته تولید شده‌اند. پیشرفت‌ها در فناوری‌های تولید مانند قالب‌ریزی فیلم، اکستروژن و الکتروریسی، کنترل دقیق ضخامت، مورفولوژی و ویژگی‌های ساختاری فیلم‌های پروتئینی را امکان‌پذیر کرده است. این فیلم‌ها نه تنها ویژگی‌های نفوذپذیری بسیار خوبی دارند، بلکه زیست تخریب‌پذیری و تجدیدپذیری نیز از دیگر مزایای آن‌هاست که با افزایش تقاضا برای تولید بسته‌بندی‌های سازگار با محیط‌زیست هم‌راستا است. بهبود و تهیه فیلم‌های پروتئینی دارای پتانسیل قابل توجهی برای متحول کردن صنعت بسته‌بندی و کمک به ساخت دنیایی سبزتر و محیط زیست‌دوستانه تر می‌باشد. این مقاله به بررسی تحقیقات و پیشرفت‌های کنونی در این حوزه می‌پردازد و منابع مختلف پروتئین، تکنیک‌های اصلاح فیلم، روش‌های تولید، چالش‌ها و چشم‌اندازهای آینده را مورد بررسی قرار می‌دهد.

واژه‌های کلیدی: بسته‌بندی مواد غذایی، پروتئین، تجزیه‌پذیر، خواص فیزیکوشیمیایی، نانوتکنولوژی

۱ و ۲- به‌ترتیب دانش‌آموخته دکتری و استاد گروه علوم و مهندسی صنایع غذایی، دانشگاه علوم کشاورزی و منابع طبیعی ساری، ساری، ایران
(*- نویسنده مسئول: Email: jmilany@yahoo.com)

https://doi.org/10.22067/ifstrj.2024.88166.1334

Iranian Food Science and Technology Research Journal
Homepage: https://ifstrj.um.ac.ir

Review Article
Vol. 20, No. 6, Feb.-Mar., 2025, p. 201-224

Detection of Adulteration of Ground Meat by Spectral-based Techniques and Artificial Intelligence (2020-2024)

A. Kazemi[1*], A. Mahmoudi[2], M. Khojastehnazhand[3]

1 and 2- Ph.D. Student and Professor, Department of Biosystems Engineering, University of Tabriz, Tabriz, Iran, respectively.
(Corresponding Author Email: A.Kazemi@tabrizu.ac.ir)
3- Associate Professor, Department of Mechanical Engineering, University of Bonab, Bonab, Iran

Received: 22.05.2024
Revised: 09.09.2024
Accepted: 09.09.2024
Available Online: 09.09.2024

How to cite this article:
Kazemi, A., Mahmoudi, A., & Khojastehnazhand, M. (2025). Detection of adulteration of ground meat by spectral-based techniques and artificial intelligence (2020-2024). *Iranian Food Science and Technology Research Journal, 20*(6), 201-224. https://doi.org/10.22067/ifstrj.2024.88158.1335

Abstract

Meat is a significant source of important nutrients and has a vital role in the human diet. Lack of monitoring of the quality and safety of meat can result in posing health threats. Determining safety through chemical methods is costly and time-consuming, without the ability to monitor in real-time. Therefore, nowadays assessing the quality of meat by applying spectral techniques such as spectroscopic and spectral imaging, considered as promising tools and these strategies have recently undergone swift advancements and garnered heightened public attention. Therefore, the purpose of the present review paper is to give an overview of the latest advancements in spectral methods for assessing ground meat safety. The basic working principles, fundamental settings, analysis process, and applications of these techniques are described. By investigating the practical utilization possibilities of spectral detection technologies in the evaluation of meat safety, researchers discussed the present challenges and upcoming research prospects. Furthermore, the newest advances in the application of artificial intelligence accompanied by the mentioned techniques were also discussed.

Keywords: Adulteration, Machine learning, Minced meat, NIR spectroscopy, Spectral imaging

https://doi.org/10.22067/ifstrj.2024.88158.1335

Introduction

Meat is one of the necessary food products for human diet, which is regularly used by consumers due to its nutritional value and pleasantness. The authenticity of minced meat is among the most important criteria for customers to be considered in their meat purchasing. Some people are willing to pay more for safety certified meat products (Miller, Carr, Ramsey, Crockett, & Hoover, 2001). However, economic profits and easiness of substituting high commercial value meat with cheaper and low quality meat in minced meat increase the possibility of adulteration of meat (Kazemi, Mahmoudi, Veladi, Javanmard, & Khojastehnazhand, 2022). Processing activities on meat like grinding can expose the minced meat to the substitution adulteration. This is due to difficulty of minced meat identification, because of removal of morphological features (Kamruzzaman, Makino, & Oshita, 2016). This enables individuals to potentially commit fraud by replacing or substituting lower-grade meat. Therefore, meat industry has been challenged by some adulteration activities and it is significant to control the authenticity of this product intensively, because of high usage of meat among people and direct relation of its safety to the health of society. In addition to the economic aftermaths, the adulteration of meat species substitution can cause more issues like religious problems (presence of pork in halal meat products or beef in Hindu diets) (López-Maestresalas *et al*., 2019).

Thus, in order to prevent this issue, some traditional chemical methods, instrumental methods, sensory evaluations, and screening techniques have been utilized, over time. Some of the mentioned techniques include immunological detection and DNA-based approaches e.g. enzyme-linked immunosorbent assay (ELISA) and Polymerase Chain Reaction (PCR and real-time PCR) (Edwards *et al*., 2021). Despite their reliability, specificity, and sensitivity features, these authentication methods suffer from various limitations such as being destructive, laborious and costly. Moreover, they need intricate laboratory activities carried out by professional personnel (Edwards, Manley, Hoffman, & Williams, 2021).

The drawbacks of traditional approaches have led to the creation of rapid, non-destructive, precise, and repeatable analytical methods for verifying and detecting contaminants in minced meat items. Recently, there has been considerable attention to the development of a fast and non-destructive technique that can be effectively utilized in a food processing setting.

Currently, researchers have suggested spectral and imaging acquisition methods, along with Artificial Intelligence (AI), to non-destructively assess meat and its products. The application of authentication and/or adulterant detection has been explored through techniques like Near Infrared (NIR) spectroscopy, Raman spectroscopy, Fourier transform infrared spectroscopy, and spectral imaging (Shawky, El-Khair, & Selim, 2020). Nondestructive spectroscopic and spectral imaging methods provide a major advantage in that they allow for measuring the chemical and physical data of foodstuffs while preserving the substance intact. Its superiority over traditional methods is demonstrated by its ease of use, speed, cost-effectiveness, and ability to automate repetitive tasks. Moreover, their ability to conduct analyses quickly and efficiently makes them valuable tools for both online and in-situ detection, which is considered beneficial from industrial perspective.

Some of the reviews have discussed these methods applications for meat assessments. However, these papers have covered various aspects of applications like quality and safety of meat. There is no comprehensive review on the recent applications of spectroscopic and spectral imaging techniques for exclusively minced meat and safety of minced meat. Furthermore, the newest developments of AI including wavelength selection algorithms and deep learning is also discussed in the present review.

The review explores the theoretical foundation and contemporary uses of these

emerging methods, along with their distinguishing features and also prospects for future advancements. The present review covers researches performed from 2020 until now, as far as our knowledge a comprehensive review in this era has not been published yet.

Spectroscopic Methods

NIR Spectroscopy

The division of the infrared region in the electromagnetic spectrum includes near-, mid-, and far- infrared (Stark, Luchter, & Margoshes, 1986). Utilizing spectra information combined with statistical algorithms, the NIRs technique has been widely and extensively reported as one of the top optical methods for monitoring meat characteristics.

Near Infrared (NIR) spectroscopy is a fast, nondestructive and highly sensitive method, which eliminates the need for sample preparation and gives qualitative and quantitative information about chemical compositions of sample (Leng *et al*., 2020). The absorption of specific frequencies from the light source by each sample in NIR spectroscopy initiates the occurrence of overtones and vibrational changes within molecules bands, which are basically consisted of CH, OH, CO, and NH groups (Kazemi *et al*., 2022). Thus, the NIR spectrum is formed when molecular vibration transitions occur, crossing from a ground state to a state of higher energy.

In general, NIR spectroscopy has three modes of operation. Reflectance, transmission, and absorbance. Transmission mode can be utilized for detection of transparent liquid like water content and fecal or rumen contamination in minced meat samples (Dixit *et al*., 2017). Reflectance mode is the most common mode in meat analysis and can be used for detection of adulteration and chemical compositions of minced meat (Dixit *et al*., 2017). The NIR system encompasses several key components, including an illuminator, a spectrometer for selecting wavelengths, a sample holder, a photoelectric sensor for evaluating light intensity and converting it into electrical signals, and a computer. After being illuminated by the light source, the sample reflects, transmits, or diffuses its rays which are then detected by an interferometric system. Ultimately, for additional analysis, the collected data from the NIR spectrum will be sent to a computer by the detector.

This technique has its own advantages and disadvantages. The main advantages of this technique is that it is non-destructive and does not require sample preparation. Another merit of NIR spectroscopy is its capability to conduct reflectance measurements, thus making it a feasible choice for measuring inhomogeneous samples (Dixit *et al*., 2017). In addition, with its unique capability to utilize a light-fiber probe and separate the sampling position from the spectrometer, NIR emerges as the most flexible optical technology, perfectly suited for online process monitoring.

A drawback of NIR is that its spectrum is affected by interference from the background, including noise and overlapping bands. This leads to redundant variables and a high degree of collinearity. Furthermore, when recording the reflection spectrum, different light scattering phenomena occur as a result of numerous absorption bands overlapping. This leads to the complexity of the spectral information, and lacks of precise structural composition required for analysis of spectral data. (Guo, Ni, & Kokot, 2016). Therefore, the use of some multivariate analysis is essential for extracting chemically significant information from NIR spectra and create calibration models that connect spectral features with the quality and safety parameters of samples.

Studies have been done to explore meat authentication and the majority of such studies were done in 2020. For example, NIR spectroscopy in the range of 12.500-5400 cm^{-1} was applied to detect pork and duck meat in minced beef. In this study, Discriminant Analysis (DA) and Partial Least Square (PLS) models with various wavelength selection and preprocessing techniques were applied. DA model with selected wavelength and without preprocessing methods had the best

performance with 100% and 91.5% for binary and ternary dataset, respectively (Leng *et al.*, 2020). In another research, the capability of NIR spectroscopy technique for authentication of turkey meat was investigated by Barbin and coworkers in 2020. The spectral data within the 400 to 2500 nm was collected and analyzed for both raw materials and prepared turkey items, with the goal of using it for quality assurance and verification purposes. PCA and linear discriminant analysis (LDA) models were employed to explore the classification of samples and presented acceptable results (Barbin, Badaro, Honorato, Ida, & Shimokomaki, 2020). Similarly in another study, visible/near-infrared (VIS/NIR) reflectance spectroscopy accompanied with multivariate methods were applied to detect adulteration in minced beef. Deep Convolution Neural Network (DCNN) and PCA models identified the type of adulteration with accuracy of over 99%. In prediction of adulteration levels, Random Forest (RF) model with selected wavelengths had the best results for beef adulterated with pork, and Coefficient of Determination of Prediction (R^2_p) and Root Mean Square Error of Prediction RMSEP were 0.973 and 2.145, respectively (Weng *et al.*, 2020). In another research, the evaluation of capability of a portable near-infrared (NIR) spectrometer to detect adulterants in ground meat was explored. For binary mixtures, R^2_c and R^2_p values were between 0.78 and 0.99. Optimal results were obtained when predicting chicken content in beef mixtures (R^2_c = 0.98; R^2_p = 0.99; RMSEC= 4.5 wt%; RMSEP = 3.5 wt%; Limit of Detection (LOD)= 3.4 wt.%, Limit of quantification (LOQ)= 11.2 wt%). For ternary mixtures, analytical outcomes were acceptable only for predicting beef content with the following values: R^2_c= 0.98, R^2_p = 0.93, RMSEC = 3.6 wt.%, RMSEP = 4.7 wt. %, LOD = 4.7 wt.%. and LOQ 15.7% by weight (Silva *et al.*, 2020). In another study, a portable VIS-NIR spectrometer (400-1000 nm) and a portable NIR spectrometer (900-1700 nm) were used to distinguish between halal meat types and pork as non-halal meat, and also to distinguish between whole meat and pork. For the application of differentiating between halal and non-halal meat types, the utilized one-class classification (OCC) approach, particularly with the employment of VIS-NIR sensors achieved to the classification rate of 95-100% accuracy (Dashti *et al.*, 2021). In a recent study, the adulteration of chicken meat and fat in lamb was explored with VIS/NIR spectroscopy and multivariate methods. Various preprocessing techniques were applied to remove unwanted information from spectral data. PCA model as unsupervised and Support Vector Machine (SVM) and Soft Independent Modeling Class Analogies (SIMCA) as supervised models were employed to detect adulteration in nine and three class datasets. SVM had outcomes of 56.15% and 80.70% for classification of nine and three class datasets (Kazemi, Mahmoudi, Veladi, & Javanmard, 2022). Also, another study by the same research group, reported the classification of pure lamb from adulterated lamb with fat with 5%, 10%, 15%, and 20% (w/w) adulteration levels. Linear Discriminant Analysis (LDA) model with Savitzky-Golay smoothing preprocessing had results of 100% and 86.2% accuracy for two and five class datasets (Kazemi *et al.*, 2022). The 2D conventional neural network (CNN) and sized-adaptive online NIRS data were used in the study by Bai et al, to classify minced samples of pure mutton, pork, and duck, as well as adulterated mutton with pork and duck. According to the results, spectral information significantly affected the model's accuracy; for the same validation set, the maximum difference was 12.06%. For all datasets, the accuracy of the CNN model with per-direction average spectral information, Extreme Learning Machine (ELM) classifier, and 7 × 7 convolution kernel was above 99.56% (Bai *et al.*, 2022).

Another research focused on testing the possibility of utilizing the fat portion as an indicator of authenticity was performed by NIR spectroscopy. Models for the target class were created using the Data Driven version of Soft Independent Modelling of Class Analogy (DD-

SIMCA), following multivariate exploration. In both calibration and validation, the use of Standard Normal Variate SNV pre-treated data along with 4 PCs achieved outstanding results, yielding a sensitivity and specificity of 100% (Totaro *et al*., 2023).

In another study conducted by Hoffman et al, the evaluation of the performance of portable Near Infrared (NIR) spectroscopy to identify binary mixtures of lamb, emu, camel, and beef sources was explored. The NIR spectra of the meat mixtures were analyzed using principal component analysis (PCA) and partial least squares discriminant analysis (PLS-DA). The cross-validation coefficient of determination (R^2_{cv}) obtained for determining the proportion of species in binary mixtures was above 90%, and the standard error of cross-validation (SECV) ranged from 12.6 to 15% w/w (Hoffman *et al*., 2023).

Two approaches combining deep learning and two-dimensional correlation spectroscopy (2DCOS) methods and Partial Least Square-Discriminant Analysis PLS-DA model have been used to analyze mutton adulteration in beef (Wang *et al*., 2024). Analyzing the effects of different proportions of mixing chicken, duck, pork with beef or mutton through synchronized 2DCOS images reveals different patterns of chemical information changes in spectra under different adulteration scenarios. ResNet's deep learning method can achieve high accuracy (100%) models and has the advantage of effectively extracting 2DCOS feature information. Meanwhile, the accuracy range of the PLS-DA model test set was 32.97% to 50.64, depending on whether the raw or preprocessed spectral data matrix was used.

Fourier Transform Infrared (FTIR) Spectroscopy

Among spectroscopy techniques, FTIR spectroscopy is known as a fast, simple, and economical technique with least sample preparation. In comparison to traditional infrared techniques, this fingerprinting method offers more benefits including ability to detect components of small size samples, high precision and accuracy, data collection ability in controlled temperatures and pressures (Deniz *et al*., 2018). In FTIR spectroscopy, the interference between two IR beams is used to get signal (interferogram), which is based on difference in path length of two beams (Stuart, 2004). The beam splitter receives an incident beam of light that has been collimated from an external polychromatic infrared radiation source. A portion of it is reflected to mobile mirror while another part is transferred to the stationary mirror. The returning beams from mirrors retrace their path and return to the beam splitter and then interfere. Because of interfere, the intensity of each beam returning to the source is different and depends on difference in the path of the beam. This process is done by a Michelson interferometer. The Michelson interferometer is a device that splits an incident light beam in to two perpendicular paths using a beam splitter. Fig.1. displays the Michelson interferometer in its most basic configuration.

The interference is created when two resultant beams are recombined after a path difference. A photodetector can measure the emergent beam's intensity as a function of the path difference, and the path difference can be controlled and modified (Banerjee). The produced signal then is transformed to frequencies that form a signal by Fourier transform algorithms. FTIR spectroscopy technique can be applied to acquire spectral data from solid, liquid, or gas (Chai *et al*., 2020). In order to prepare solid materials to light beam of spectrophotometer, they can be mixed with potassium bromide (KBr) and subsequently pressed to form a small disc. One of the main problems of using this material is the low reproducibility of prepared samples due to some conditions like utilized ratio and homogeneousness required to be the same for all samples.

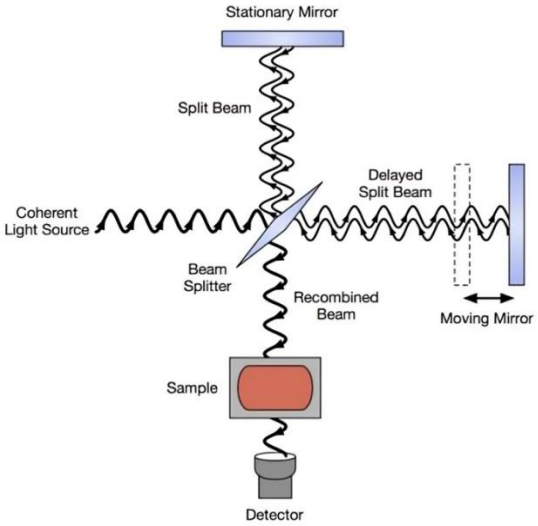

Fig. 1. Schematic diagram of the Michelson interferometer (Banerjee)

Nowadays, Attenuated Total Reflectance (ATR) FTIR has solved this problem which does not require addition of KBr and needs small volume of sample. It also allows for rapid analysis. In spite of some practical applications of FTIR spectroscopy particularly in food safety issues, there are some industrial challenges of this technique like the interpretation of FTIR spectra especially for complicated samples like polysaccharides can be difficult (Hong, Yin, Nie, & Xie, 2021) and sample preparation in this technique can be time-consuming and crucial step.

In a study by Mabood *et al*, FT-NIR spectrophotometer combined with PCA, PLS-DA, and PLSR models was applied to detect and quantify pork meat in other meats. In order to predict the amount of pork meat in other meats, PLSR model was used which had R^2_{cv} = 0.977 and RMSECV = 1.08% (Mabood *et al*., 2020). In another application of ATR-FTIR spectroscopy for meat industry, Keshavarzi et al, applied this technique to explore adulteration of chicken in beef. PCA model was applied for two kinds of data: data without any preprocessing techniques in the whole range of spectra and preprocessed spectral data with focusing on 1700-1070 cm^{-1} range of spectra. Clustering of meat kinds with PCA model on data in transmission mode was successfully done. Furthermore, the preprocessed ATR_FTIR spectrum was used to prepare PLSR and Artificial Neural Network (ANN) models for prediction of adulteration amounts. ANN model outperformed with R^2 of 0.999 for prediction dataset (Keshavarzi, Barzegari Banadkoki, Faizi, Zolghadri, & Shirazi, 2020). In the same year, the research group of Candogan investigated discrimination of pork, horse or donkey meat in beef. Hierarchical Cluster Analysis (HCA) in the region of 1480-1425 cm^{-1} separated all pure beef, pure donkey meat and adulterated samples with sensitivity and specificity of 100% (CANDOĞAN, DENİZ, ALTUNTAŞ, Naşit, & Demiralp, 2020).

In another study, the application of FTIR spectra combined with neural network classifier and different dimensionality reduction techniques was investigated for classification of lamb fat. The feature selection algorithms showed better performance of classification on the dataset collected from dairy lamb carcasses from 89.70% with the full feature set to 91.80% and 93.89% for SVM and PCA, respectively (Alaiz-Rodriguez & Parnell, 2020).

Furthermore, Siddiqui et al, explored application of FTIR spectroscopy for detection of adulteration of beef, chicken, and lamb in lard. PCA model could separate samples with using three principal components. Beef and lamb samples for both adulterated and pure

samples had the highest classification accuracy value of 85% with multiclass support vector machine (M-SVM), whereas chicken had the lowest value of 78% for each category (Siddiqui *et al*., 2021). In another investigation, detection of presence of beef liver in beef patties was explored by FTIR spectroscopy. this technique was able to detect adulterated samples at 5% concentration (Abidin, Rosli, Bujang, Nordin, & Nizar, 2021). The feasibility of utilizing portable Fourier transform infrared spectroscopy (FTIR) in combination with multivariate classification techniques was examined by Dashti et al, to classify ground meat, lamb, chicken, and pork samples for the assessment of carnivorous speciation. Examinations were conducted employing Partial Least Squares Discriminant Analysis (PLS-DA) and Support Vector Machines (SVM) with Radial Basis Functions (RBF) serving as the kernel function. SVM performs better than PLS-DA with an overall accuracy of 90% and 98% on ATR-FTIR and DR-FTIR datasets, respectively (Dashti *et al*., 2022).

Raman Spectroscopy

Raman spectroscopy is another nondestructive spectroscopic technique which has proved its capability and includes some advantages like simple operation, no requirements for sample preparation, less interference by water, and ability to provide structural information of chemical elements (Khaled, Parrish, & Adedeji, 2021). This technique is based on inelastic scattering of light on the molecule level. When a sample is illuminated by an external laser beam, molecules are excited by photons and their vibrational energy levels are changed from ground state to unstable state. Then, excited level returns to initial level of energy by photon emission (Pchelkina, Chernukha, Fedulova, & Ilyin, 2022). There are two types of photon scattering based on difference between photons and molecules: elastic scattering and inelastic scattering (Butler *et al*., 2016). Elastic scattering, also known as Rayleigh scattering, happens when there is no energy exchange and the frequency of incident and scattered photons is the same. In contrast, in elastic or Raman scattering, a little amount of energy exchange happens between scattered photons and target molecules (Butler *et al*., 2016). The result of this exchange between sample and light is formation of virtual level. Then, due to the instability of formed virtual level, photons are scattered to a fairly stable level. There is no energy transfer between incident light and scattered light when photons come back to the initial level. This process of elastic collisions is called Rayleigh scattering (Pchelkina *et al*., 2022). The majority of studies that have applied Raman spectroscopy for meat safety are before 2020, and due to the purpose of present review which is based on exploring researches after 2020, we mentioned only two studies after 2020. Table.1, summarizes the research on the safety of minced beef performed by spectroscopic methods between 2020 and 2024. Robert et al, assessed the ability of Raman spectroscopy combined with three chemometric methods (PCA, PLS-DA, and SVM) to differentiate red meat samples (beef, lamb, and vension). The outcomes of linear and non-linear kernels of SVM model were 87% and 90%, respectively (Robert *et al*., 2021). Similarly, Saleem et al, applied Raman spectroscopy technique to differentiate goat, cow, and buffalo fat samples with 532-785 nm. They found that saturated fatty acids at Raman bands of 1060, 1080, and 1440 cm^{-1} were relatively higher in buffalo fats (Saleem, Amin, & Irfan, 2021).

Table 1- Application of spectroscopic methods for meat safety

Technique	Investigated parameter	Chemometrics	Results	References
NIR	Adulteration: Pork and duck meat in minced beef	DA PLSR	R_p=95.80% RMSEP=7.27	(Leng *et al.*, 2020)
NIR	Discrimination: Turkey cuts	PCA LDA	Accuracy=80%	(Barbin *et al*., 2020)
VIS/NIR	Adulteration: Pork and beef heart in minced beef	SVM RF PLSR DCNN	R^2_p=0.96 RMSEP=2.75	(Weng *et al*., 2020)
NIR	Adulteration: Chicken/beef; beef/pork;pork/chicken	PLS SVR	R^2_c=0.78 R^2_p=0.99	(Silva *et al*., 2020)
VIS/NIR and NIR	Distinguish: Halal meat vs. pork	SVM PLS-DA	CCR=95-100%	(Dashti *et al.*, 2021)
VIS/NIR	Adulteration: Chicken and fat in lamb	PCA SVM SIMCA	Accuracy= 80.70%	(Kazemi, Mahmoudi, Veladi, & Javanmard, 2022)
VIS/NIR	Adulteration: Fat in lamb	PCA LDA	Accuracy= 100%	(Kazemi *et al*., 2022)
NIR	Classification: Mutton, pork, and duck	CNN	Accuracy= 99.56%	(Bai *et al.*, 2022)
NIR	Authenticity= Fat portion	DD-SIMCA	Sensitivity=100%	(Totaro *et al*., 2023)
NIR	adulteration: adulterants of exotic meat species	PCA PLS-DA	R^2_{cv}= 90% SECV=12.6-15%	(Hoffman *et al*., 2023)
2DCOS	Adulteration: Mutton in beef	Resnet deep learning PLS-DA	Accuracy=100%	(Wang *et al*., 2024)
FTIR	Adulteration: Pork meat in other meats	PCA PLS-DA	R^2=0.97 RMSECV=1.08%	(Mabood *et al*., 2020)
FTIR	Adulteration: Chicken in beef	PCA PLSR ANN	R^2=0.99	(Keshavarzi *et al*., 2020)
FTIR	Discrimination: Pork, horse, and donkey in beef	HCA	Sensitivity=100%	(CANDOĞAN *et al*., 2020)
FTIR	Classification of lamb fat	PCA SVM PLS	Accuracy=85.60%	(Alaiz-Rodriguez & Parnell, 2020)
FTIR	Adulteration: Beef, chicken, lamb in lard	M-SVM PCA	Accuracy=85%	(Siddiqui *et al.*, 2021)
FTIR	Adulteration: Beef liver in beef patties	-	-	(Abidin *et al.*, 2021)
FTIR	Classification: Lamb, chicken, and pork	PLS-DA SVM	Accuracy=98%	(Dashti *et al*., 2022)
Raman	Differentiation: Beef, lamb, vension	PCA PLS-DA SVM	Accuracy=90%	(Robert *et al*., 2021)
Raman	Differentiation: Goat, cow, and buffalo fat	PCA	-	(Saleem *et al*., 2021)

In a study by Robert *et al*, the researchers investigated the use of Raman spectroscopy in combination with three chemical analysis techniques to distinguish between beef, lamb, and game samples. They used PLS-DA and SVM classification methods to develop a model for identifying different types of meat, and PCA for exploratory purposes. The results showed that both linear and nonlinear kernel SVM models achieved high sensitivities and specificities, with sensitivities exceeding 87% and 90% respectively, and specificities exceeding 88% when tested against a separate set of samples. The PLS-DA model also demonstrated an accuracy of over 80% in correctly classifying each type of meat (Robert *et al*., 2021).

In order to apply Raman spectroscopy in industrial sector some limitations, like interference of fluorescent with Raman signals which make it difficult to get accurate measurements and requirement of some specialized instrumentation should be solved.

Spectral Imaging

Electromagnetic spectrum includes a wide range of electromagnetic radiation, each with its own unique wavelengths and frequencies. These various types of waves, such as ultraviolet, visible, infrared, microwave, and radio waves, have distinct electromagnetic features like energy levels, propagation traits, and interactions with matter. This makes them necessary for research in different scientific fields. Visible light is an electromagnetic radiation that is visible by human eye and is limited in the range of wavelength between 380 and 780 nanometers. Many well-established methods based on vision and image processing are based on this particular spectral region (Reinhard *et al*., 2010). Recent developments in sensor technology have made it possible to acquire images at a wide scope of electromagnetic wavelengths. These approaches encompass hyperspectral and multi-spectral images, which cover a wider range of spectral bands than the conventional three bands employed in visible spectrum imaging.

In order to get an increased level of spectral resolution, hyperspectral Imaging (HSI) and also Multispectral Imaging (MSI) methods take multitudinous images at compact and adjacent spectral bands encompassing a greater range of electromagnetic spectrum. These developed imaging techniques are known as imaging spectroscopy (Zahra *et al*., 2023).

Spectral sensors are employed to gather information through images, with each image capturing a district portion of the electromagnetic spectrum called a spectral band. There are various ways to collect spectral data, each with its own strengths and weaknesses. The whiskbroom method is a technique that entails installing a line of detectors on a mobile platform; as the platform progresses, the detectors gather information from a small section of the ground, referred to as a swatch. The data that is utilized to generate a visual representation of the scene, where every individual pixel holds specific spectral information (Zahra *et al*., 2023). The pushbroom technique is another approach that involves scanning a single axis and creating an image by either moving the camera or the objects being captured. To prevent spatial distortions in the collected data, the movement should be constant (Zahra *et al*., 2023). By switching out narrow bandpass filters in front of the camera lens or by utilizing electronically tunable filters, wavelength scanning techniques are possible to collect spectral image cubes. A typical NIR-HIS setup consists of a camera, a spectrometer, a detector, a light source, and a movable platform. A spectral image is typically represented as a cube, with the first two dimensions representing spatial information and the third dimension representing a collection of spectral images taken at various wavelengths. The challenge of performing hypercube analysis arises from the application of multivariate statistical methods (Cheng, Nicolai, & Sun, 2017). Moreover, the utilization of hypercube data in classification and prediction models frequently necessitates dimensionality reduction due to their large dimension and size. Preprocessing data from a hypercube often involves various techniques including interference correction, dimensionality reduction, and feature extraction (Oliveri *et al*., 2014). Then, models are used to establish correlations, classifications, prediction, and validations. Table 2 presents the summary of researches for the application of spectral imaging for minced meat safety.

Rady & Adedeji, explored the capability of hyperspectral imaging (400-1000nm) as a nondestructive approach to detect, differentiate, and quantify adulterants sourced from both plants and animals in minced beef and pork.

Table 2- The spectral imaging application for ground meat safety

Application	Technique	Spectral range	Model	Results	Reference
Adulteration: Plant and animal-based adulterants in minced beef and pork	HSI	400-1000nm	SVM LDA PLS-DA	Accuracy= 100%	(Rady & Adedeji, 2020)
Adulteration: Leaf lard in minced pork	HSI	400-1000nm	PCR PLSR	R2p = 0.98 RMSEP = 4.87%	(Jiang *et al*., 2020)
Adulteration: Minced chicken in minced beef	HSI	380-1000nm	GD-RC	R=0.98 RMSEP=0.03	(Zhao *et al*., 2020)
Adulteration: Minced pork jawl in minced pork	NIR-HSI	400-1000nm	PLSR	R2p=0.95 RPD=4.54	(Jiang *et al*., 2020)
Adulteration: Adulterants in minced beef	HSI	350-2500nm	RF	Accuracy=96.87%	(Guo *et al*., 2020)
Distinguish: Pork and duck rolls in mutton roll	HSI	400-1000nm	PLS-DA	Accuracy=100%	(Jiang *et al*., 2021)
Adulteration: SPP in ground beef	HSI	400-1000nm	PLSR	Rp = 0.99 LOD=0.74% RPD=8.45	(Jiang *et al*., 2022)
Adulteration; Duck meat in lamb	VIS-NIR-HSI SWIR-HSI	900-1700nm 400-1000nm	PLSR	R2p=0.98 RMSEP=0.98 RPD=5.62	(Jing-yuan *et al*., 2022)
Authentication of meat samples	VIS-NIR-HSI SWIR-HSI	400-1000nm 1116-1670nm	SVM ANN-BPN	Accuracy=96%	(Dashti *et al*., 2023)
Adulteration: Starch in minced chicken meat	HSI	400-1000nm	SVM CNN	Accuracy=98.6%	(Yang *et al*., 2023)
Adulteration: Minced chicken and turkey and pork in minced beef meat	HSI	400-1000nm	PLSR	R2p=0.96 RMSEP=2.9% RPD=5.4	(Achata *et al*., 2023)
Adulteration of alpacha meat with pork, chicken, and beef	NIR-HSI	-	DD-SIMCA PLSR PCA	Sensitivity=100%	(Cruz-Tirado *et al*., 2024)

The meat and non-meat samples used in our study included beef (chuck rust), pork (Boston butt), chicken thigh, textured vegetable protein (TVP) (Red Mill, Milwaukie, Oregon, USA) that contains 50% soy protein, and wheat gluten (WG) (TruTex RS 65, MGP Atchison, Kansas, USA) with 75% protein. Using the chosen wavelengths from the test set, the classification models produced optimal results with classification rates of 75-100% and 100% for pure and adulterated samples, respectively. Whereas, depending on the type of adulterants, the rates ranged from 83% to 100% (Rady & Adedeji, 2020). In another research, application of hyperspectral imaging (HSI) for detection of adulteration of leaf lard adulteration in minced pork was investigated. The average spectra extracted from regions of interest (ROIs) were subjected to distinct mathematical pre-processing. Then, quantitative calibration models (PCR, PLSR) with various wavelength selection algorithms (Principal Component (PC) loadings, two-dimensional correlation spectroscopy (2D-COS), competitive adaptive reweighted sampling (CARs), and Regression Coefficients (R_C)) were applied. The best outcomes of PLSR model with R_C wavelength selection algorithm were 0.98 and 4.87% for R^2 and RMSEP, respectively (Jiang *et al*., 2020). Zhao et al, employed the combination of hyperspectral imaging and Gaussian distribution of regression coefficient (GD-RC) model to visually detect adulteration of minced chicken in minced beef. The binary GD-RC model performed better than the uniform GD-RC model. The best technique had an average error (ARE) of 2.8%, a correlation coefficient (r) of 0.9831, and a root mean square prediction error (RMSEP) of 0.0319 (Zhao *et al*., 2020).

The combined usage of PLSR and NIR-HIS enabled the detection of minced pork contamination with minced pork jowl meat by collecting data between 400 and 1000 nm. The best performing model, with R^2_p = 0.9549 and residual predicted deviation (RPD)= 4.54, is spectra preprocessed with standard normal variables (SNV), and with partial least squares regression (PLSR) models. Additionally, to

precisely choose important wavelengths connected to adulteration identification, principal component (PC) loadings, two-dimensional correlation spectroscopy (2D-COS), and regression coefficients (RC) were applied and yielded acceptable results (Jiang, Cheng, & Shi, 2020).

Similarly, in another research, the capability of hyperspectral reflectance spectroscopy in detection of minced beef adulteration was assessed. Random Forest (RF) model yielded the best accuracy of 96.87% in prediction set with selected wavelengths (Guo *et al*., 2020). Similarly, the potential of use of hyperspectral imaging (HSI) technique to identify any adulteration of offal in ground beef was investigated. PLSR models based on full spectra showed the best performance with R^2_P of 0.98, RMSEP = 4.25%, and Ratio Performance Deviation (RPD) of 7.53 in prediction set (Jiang *et al*., 2020).

Examining the potential of multivariate data analysis alongside HSI, the research done by Jiang et al, investigated the ability to distinguish between raw and cooked mutton rolls with substitutions of pork and duck rolls. The highest rate of 100% classification was achieved in all sets with the application of different models and preprocessing techniques, specifically through the use of the PLS-DA model developed by raw spectra (Jiang, Yang, & Shi, 2021). In another study, the use of hyperspectral imaging technology in conjunction with characteristic variable screening for the quick and nondestructive identification of adulterated fox meat in minced mutton was investigate. When paired with the 2-dimensional correlation- SVR model, hyperspectral imaging can efficiently achieve quantitative detection of contaminated fox meat in minced mutton (Bai et al, 2021). In other study, HSI in spectral range of 400-1000 nm accompanied with multivariate analysis and wavelength selection algorithms was applied to detect soybean protein powder (SPP) in ground beef. The final outcomes displayed that simplified PLSR model based on six selected wavelengths from PC loadings acquired R_p = 0.993, RPD = 8.45, and LOD of 0.74 (Jiang *et al*., 2022).

The visible/near infrared (400-1000nm) and short-wave near-infrared (900-1700 nm) HSI method was employed in another research to detect adulteration of duck meat in lamb. Different models, preprocessing and wavelength selection algorithms were applied and the best outcome was with SNV-SPA-PLSS model in short-wave near infrared band with prediction set (R^2_p = 0.986, RMSEP = 0.058, RPD = 5.62) (Jing-yuan, Jun-qin, Mei, Xing-hai, & Ye-lin, 2022).

Similarly, the effectiveness of visible-near infrared hyperspectral imaging (VIS-NIR-HSI) and shortwave infrared hyperspectral imaging (SWIR-HSI) accompanied with different classification and regression methods were reported for meat authentication by (Dashti *et al*., 2023). the obtained results proved that VIS-NIR-HSI technique outperformed SWIR-HSI. Combination of HSI and transfer learning was employed to detect starch in minced chicken meat (Yang *et al*., 2023). Two classification models were compared. Models were built on acquired hyperspectral data from samples. Additionally, a classification model based on the GoogleNet network pretrained on the ImageNet collection was developed to detect starch in minced chicken meat. The model based on the GoogleNet network showed a better classification accuracy, up to 98.6%, according to the results.

A different study conducted by Achata and colleagues in 2023 examined the use of Hyperspectral imaging (HSI) within a specific spectral range, combined with multivariate analysis. The purpose of this study was to determine if it is possible to create a universal model for detecting the presence of other meats in ground meat samples. To predict the quantity of Minced Beef meat (MBM) in scanned samples, various approaches including different spectral pre-treatments, the partial least squares regression (PLSR) methodology, the ensemble Monte Carlo variable selection method (EMCVS), and combinations of any two of these methods were examined. The researchers

used data from MBM contaminated with chicken and turkey meats to create a beef prediction model. They tested the accuracy of the model by using data from MBM contaminated with pork meat at various levels of adulteration. They used a combination of the asymmetric least squares and standard normal variate techniques to analyze the reflectance spectra. The results showed good prediction accuracy with 23 specific wavelengths, achieving an R^2_p value of 0.96, an RMSEP of 2.9%, and an RPD of 5.4 (Achata *et al*., 2023).

The study conducted by Cruz-Tirado et al, utilized the Portable NIR Spectrometer and NIR-HIS methods, which do not involve the use of chemicals, to identify the presence of pork, chicken, and beef in alpaca meat at varying concentrations (0-50% w/w). The samples were classified into pure and non-pure alpaca meat using Principal Component Analysis (PCA), with both instruments providing spectral data. To authenticate pure alpaca meat, a single-class data-driven soft independent class analogy (DD-SIMCA) model was developed and validated. The DD-SIMCA model, using spectra obtained from both instruments, achieved perfect sensitivity and specificity (100%) when applied to an external sample set. Moreover, the NIR-HIS-based partial least squares regression (PLSR) outperformed the portable NIR spectrometer in accurately predicting contaminant concentrations in alpaca meat (Cruz-Tirado *et al*., 2024).

Artificial Intelligence

Data analysis is the keystone that connects the desired sample characteristics to the NIR absorption or transmittance measurements. The primary objective is to enhance both the reliability and accuracy of analytical results. For instance, the combination of spectral data and pattern recognition techniques can effectively address authentication issues in commodities like pharmaceutical, food, and cosmetics (Chophi, Sharma, Jossan, & Singh, 2021). With advancements in artificial intelligence, big data, and cloud computing, new ideas, approaches, and strategies are constantly revitalizing the field of statistical analysis techniques. Fig.2, illustrates how machine learning algorithms convert the NIR absorption data to the necessary outputs. In the realm of machine learning, algorithms include both training and testing phases. Machine learning algorithms use the acquired outcomes as outputs and the light absorption values as inputs during the training phase. In the test step, they predict the intended result based on the supplied light absorption values.

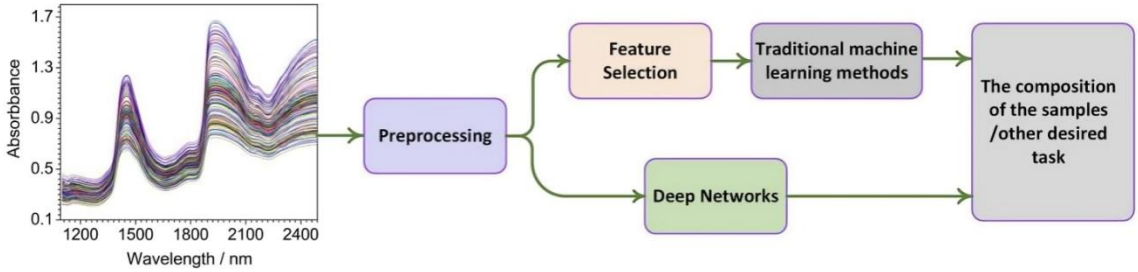

Fig. 2. Architecture of machine learning for NIR spectroscopy (Wenwen Zhang *et al*., 2022)

Spectral Preprocessing

In addition to the advancement of modeling algorithms, preprocessing algorithms have also made progress. This step is essential in analyzing spectral data as it deals with uninformative spectra caused by light scattering or system noise. In NIR spectroscopy, two commonly used preprocessing methods are spectral normalization and spectral derivatives. Spectral normalization corrects scattering impacts, while spectral derivatives handle peak overlap and baseline drifts (Rinnan, Van Den Berg, & Engelsen, 2009).

The elimination of multiplicative effects in spectral data is challenging, so there is significant interest in developing processing methods to address this issue. To a certain extent, Standard Normal Variate (SNV) along with Multiplicative Scatter Correction (MSC) and extended MSC (EMSC) are common employed techniques for eliminating multiplicative effects, thereby minimizing the impact of solid particle size (light scattering and variance in the effective path length) or scattering effect on spectral data (Wang *et al*., 2022). Furthermore, recently some improved algorithms have been applied. For example, to enhance the SNV preprocessing efficiency, Bi et al, partitioned the NIR spectra in to equally sized and separated sections, and processed with SNV preprocessing for each subinterval (Bi *et al*., 2016). The outcomes demonstrated that this particular local SNV preprocessing method exhibited remarkable efficacy, surpassing the effectiveness of global SNV. In order to account for the varying effects of physical factors on spectral variables, a normalization algorithm called Variable Sorting was created for Normalization (VSN). Before conducting the SNV algorithm, this algorithm assigns varying weights to different wavelength variables. (Rabatel, Marini, Walczak, & Roger, 2020). Denoising refers to the process of improving the signal-to-noise ratio (SNR) by eliminating or reducing random errors that are added to the raw spectral signals. The most used algorithms for denoising include Wavelet Transform (WT), Fourier Transform (FT), Savitzky-Golay (SG), and moving-average. Elimination of noise through these methods can be highly effective. Nevertheless, there is the risk of signal distortion, particularly when dealing with sharp spectra like raman, NMR, and X-ray diffraction.

The proposal of the fact that distorted peak denoising can be attributed to the insufficient sampling, which is a result of frequencies which are being scattered was explored by (Yao, Su, Yao, & Huang, 2021). In order to solve this problem, they suggested an operation method with yield adjustments based on a four-step approach. This method begins by determining the levels of signal and noise in the raw data. It subsequently adjusts the sampling density in areas characterized by high signal levels and improves them using linear interpretation. Next, it performs a smoothing operation to reshape the profile and finally, restores the original shape of the deformed profile. The proposed method demonstrated superior denoising performance when compared to S-G and WT denoising based on the experimental results.

The application of derivative preprocessing techniques, such as S-G derivation, enables efficient elimination of baseline and background interference while also facilitating the resolution of overlapping signals and enhancing spectral resolution and instrumental sensitivity. However, this method frequently introduces unwanted effects in to the frequencies which leads to a low signal-to-noise ratio (SNR). Furthermore, the noise becomes more prominent as the derivative order increases. As a result of this, the WT is commonly used for the computation of high derivatives such as the third or fourth order (Shao, Cui, Wang, & Cai, 2019). Additionally, the singular perturbation Spectra Estimator (SPSE) developed by Li et al is regarded as a reliable technique for calculating higher-order derivatives (Li, Wang, Lv, Ma, & Yang, 2015). In contrast to the derivative spectrum with integer orders, the fractional-order derivative spectrum has a greater ability to accurately depict changes in spectral details according to the derivative order while also addressing the conflict between spectral resolution and signal intensity (Hong *et al*., 2018; Hu *et al*., 2021). Zheng et al applied their novel fractional-Order Savitzky-Golay Derivative (FOSGD) algorithm to preprocess NIR spectral data as an example. They found that this algorithm resulted in improved model performance compared to using the integral order SG derivative (Zheng, Zhang, Tong, Yao, & Du, 2015).

Feature Selection

Due to the issue of including irrelevant or redundant information in spectral data which lead to noise and decreased model performance, application of variable selection is significant in spectral analysis to identify the most informative features. The goal of feature selection is to identify the most reliable, relevant, and unique set of features from a feature vector. Feature selection algorithms are capable of effectively reducing the size of spectral data and eliminating any duplicated information from the spectrum. Feature selection techniques in machine learning are divided in to three groups: filter methods, wrapper methods, and embedded methods (Wang *et al*., 2022). The primary difference of the mentioned techniques is the utilized learning algorithm. The variables in the filter method are assessed individually, disregarding any interdependence among them. Therefore, filter-based approaches ensure that the selected features do not overfit and are ranked based on their importance. The most applied techniques involve correlation coefficient method and analysis of variance (ANOVA) method. By considering the correlation between variables, the wrapper method determines the best combination based on how it affects the model performance. Therefore, wrapper-based characteristics have a tendency to overfit, and the majority of feature selection methods in NIR employ this approach. (Wenwen Zhang, Kasun, Wang, Zheng, & Lin, 2022). From variable selection algorithms of this method, interval PLS (iPLS), successive projections algorithm PLS (SPA-PLS), and genetic algorithm PLS (GA-PLS) can be mentioned. The inclusion of embedded approaches involves the utilization of a model learning factor that assesses the ability of chosen features to generalize. The strategy that is most commonly adopted in this regard is to add regular terms, such as the algorithm for least absolute shrinkage and selection operator, in order to decrease model's complexity (Wang, Bian, Tan, Wang, & Li, 2021). Random Forest (RF) variable selection is one of the most used popular algorithms in embedded method.

Modelling

The literature describes two main types of machine learning architectures for NIR: traditional methods and deep network architectures. Traditional methods involve selecting valuable features from the input data through feature learning and then applying traditional machine learning algorithms. These techniques application in spectroscopy which is called chemometrics is able to predict quantitative and qualitative features.

Multivariate Classification Models

One-class classification (OCC) techniques focus on modeling a single class independently of others, emphasizing the similarities within that class rather than the differences between classes. A widely used OCC technique in chemometrics is Soft Independent Modelling of Class Analogy (SIMCA) (Wold & Sjöström, 1977). SIMCA uses Principal Component Analysis (PCA) on the training data of the target class to create a defined acceptance region in multivariate space. A sample is assigned to a class if its residual distance falls within the statistical limit for that class. Interestingly, a sample can be assigned to more than one class if it meets the criteria for multiple classes (Kazemi *et al*., 2022). In simpler terms, PCA helps analyze the samples of each class and build classification models. If an unknown sample resembles the calibration samples, it will be classified as a member of that class (Basati, Jamshidi, Rasekh, & Abbaspour-Gilandeh, 2018). In contrast, two or multi-class classifiers, known as supervised discriminant methods, are used to establish boundaries between different classes. The most traditional method is Linear Discriminant Analysis (LDA), which identifies linear surfaces (hyperplanes) that effectively separate samples from different categories. This is done based on the relative positions of the groups' centroids and the within-class variance/covariance (Brereton *et al*., 2018). For implementing LDA, the number of training objects must be greater than the number of input variables. Therefore, it is often necessary to reduce the number of

variables using PCA before conducting statistical analysis.

Another supervised method is Partial Least Square-Discriminant Analysis (PLS-DA), which aims to maximize the separation between classes while minimizing variability within each class by creating linear decision boundaries (Xu, Xia, Min, & Xiong, 2022). PLS-DA generates new variables, known as Latent Variables (LVs), through linear combinations of the original variables. These LVs maximize the covariance between the predictor matrix (X) and the response matrix (Y). The Y matrix is binary, with as many rows as X and as many columns as there are groups in the dataset. Each column represents group membership using 0/1 variables, where a value of 1 indicates membership in a group, and 0 indicates otherwise (Næs, Isaksson, Fearn, & Davies, 2002). Support Vector Machine classification (SVMc) is another powerful technique based on statistical learning. It works by mapping the original data space into a higher-dimensional feature space using kernel functions, with the goal of finding the best separation between different classes in the training set through a hyperplane. The decision function of SVM is determined by a small number of support vectors located on the margins of the hyperplane. The success of an SVM model largely depends on the appropriate selection of kernel functions (De Girolamo *et al*., 2020).

Multivariate Calibration Models

Through the utilization of a multivariate calibration strategy, the combination of NIR data and reference values obtained from chemical analysis, enables the creation of calibration models with predictive capabilities and quantifiable properties for analogous sets of NIR data. The most commonly applied multivariate calibration models for NIR meat analysis are Principal Component Regression (PCR), Multiple Linear Regression (MLR), and Partial Least Square Regression (PLSR), (Dixit *et al*., 2017). In MLR technique, concentration is linked to absorbance through considering the concentrations of target analytes and other elements that contribute to the overall signal (Blanco & Villarroya, 2002). As an extension of PCA and an inverse calibration technique, PCR is similar to MLR in that it uses PCs from PCA as variables in an MLR model. The first step involves conducting PCA on the calibration data to produce PCA scores and loadings which is then followed by MLR (Gemperline, 2006). The mathematical model employed by PCR and PLSR is indistinguishable, except for how they handle data compression. While PCR focuses only on spectral information, PLS incorporates both spectral and concentration data. Latent Variables (LVs) are the compressed variables that are obtained in PLSR. By utilizing PLSR, the spectral data is mathematically correlated to a matrix of property of interest (chemical or physical properties), along with any other significant spectral components that interfere with the spectrum. (Hemmateenejad, Akhond, & Samari, 2007).

Deep Learning

As it was mentioned, there are two classifications for ML algorithms: traditional machine learning methods and deep network architectures. Unlike traditional machine learning methods, deep network architectures have multiple hidden layers like AlexNet and GoogleNet. Deep network architectures employ raw features unlike traditional machine learning methods that require an expert to engineer appropriate features.

NIR data has been effectively modeled by combining classical chemometric approaches, predominantly PCA and PLS-based techniques, with knowledge-driven spectroscopic preprocessing. For many years, ANNs have been utilized in the chemometric field. Nevertheless, there exists a distinction between the conventional ANNs and more recently developed deep NNs. In order to input data in to ANNs, which are like most Machine Learning (ML) algorithms, pre-extracted features extraction automatically, offering specialized proxies for spectroscopic

preprocessing (Fig. 3 b). DL can also include a larger number of layers than ANNs. Training can involve up to hundreds of layers with millions of parameters. This is possible due to the availability of enhanced computational power, graphic processing units (GPUs), refined regularization techniques and advanced model optimization approaches make this attainable (Mishra *et al.*, 2022).

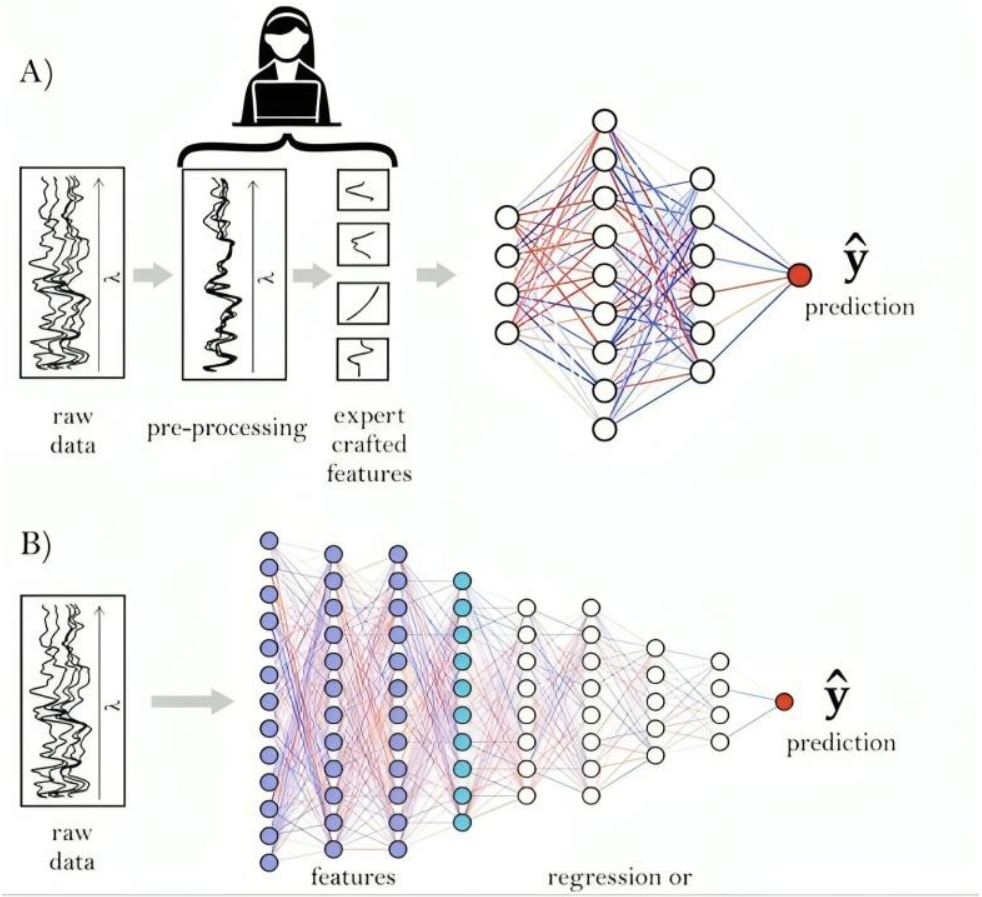

Fig. 3. (A) Classical ANN for data modelling, and (B) DL convolutional neural network (CNN) approach, which includes joint feature extraction and model building (Mishra *et al.*, 2022)

Challenges and Future Outlook

While spectral- and image acquisition techniques have advanced quickly, they still have some challenges when implemented in industrial environments. Firstly, the initial creation of certain models may require a significant investment of both time and money due to the lengthy calibration process. Moreover, the gathering of data is impacted by various acquisition parameters like scanning times and sample to detector distance, as well as environmental factors such as ambient temperature, humidity, illumination conditions, and sample temperature.

However, most testing techniques use a single detection method for a given detection index and provide acceptable predictive results, thus providing multiple pieces of information for a comprehensive evaluation of the sample is required in the future (Xiong, Sun, Pu, Gao, & Dai, 2017). Consequently, it becomes essential to integrate multiple detection methods and indicators, as well as utilize data fusion, for exploring the comprehensive evaluation technique for meat safety.

At this moment, the meat industry requires an online/real-time system for quickly verifying the authenticity of meat products. Despite some

initial success, further research is needed to implement online systems effectively. Implementing an online/real-time detection system for the rapid authentication of meat products would indeed have several benefits, but it also comes with its own set of drawbacks: Developing and implementing such a system can be expensive. There are costs associated with research and development, equipment procurement, installation, maintenance, and ongoing operational expenses. These costs may be prohibitive for some companies, particularly smaller businesses in the meat industry. In addition, creating a reliable online detection system for meat authentication requires advanced technology and expertise in areas such as sensor technology, data analysis, and machine learning. The complexity of integrating these components into a seamless and effective system can pose challenges. Furthermore, achieving high levels of accuracy in detecting and authenticating meat products in real-time can be difficult. Factors such as variations in meat composition, processing methods, and environmental conditions can affect the performance of the detection system. Ensuring consistently accurate results is essential for maintaining consumer trust and regulatory compliance. Another weak point is continuous maintenance and calibration of the detection system which are necessary to ensure its ongoing reliability and accuracy. This requires dedicated resources and expertise to address issues such as sensor degradation, software updates, and changes in production practices. Finally, introducing new technology into established meat industry practices may face resistance from stakeholders who are accustomed to traditional methods of authentication. Overcoming this resistance and fostering adoption of the new detection system can be a significant challenge.

Addressing these drawbacks requires careful planning, investment, and collaboration between industry stakeholders, technology developers, and regulatory authorities. Despite the challenges, the potential benefits of an online/real-time detection system for meat authentication make it a worthwhile endeavor for improving food safety and consumer confidence trends.

Despite these drawbacks, these nondestructive spectroscopy and imaging techniques may become more widely used in the future. These methods will continue to evolve as instrument technology improves, the meat industry urgently requires a real-time online system that can quickly authenticate meat products. The development of high-speed computers with sufficient storage capacity and appropriate chemical assays has made this possible. Implementing these fast and non-destructive systems could greatly impact the profitability of the meat industry and may become the leading trend in the future. Even though initial efforts yielded some success, additional investigation is needed to properly implement online systems.

Conclusion

This review provides a comprehensive review of how spectral methods and techniques have been used to swiftly assess the safety of ground meat illuminating the drawbacks of conventional methodologies and underscoring the necessity for enhanced, industry-specific alternatives. The present review paper concentrates on recently done research about the safety of minced meat using some spectral techniques and AI algorithms. Some new issues in application of AI, including feature selection and deep learning, were also discussed. The promising results acquired have highlighted the vast potential for implementation in the meat industry. In conclusion, these techniques could potentially be used in meat as a non-destructive security detection tool. Despite the current limitations, there are still various improvements and research possibilities for successful commercialization, especially for his HSI-based systems.

Declaration of Generative AI and AI-assisted Technologies in the Writing Process

During the preparation of this work the author used Tinywow in order to rewrite some

sentences. After using this tool, the author reviewed and edited the content as needed and take full responsibility for the content of the publication.

Author Contributions

Amir Kazemi: Conceptualization, Methodology, Software, Formal analysis, Investigation, Resources, Data curation, Writing–review & editing, Project administration, Writing-Original Draft, **Asghar Mahmoudi**: Conceptualization, Methodology, Data curation, Visualization, Investigation, Resources, **Mostafa Khojastehnazhand**: Software, Supervision, Validation, Writing-Reviewing, and Editing.

Founding Source

This research did not receive any specific grant from funding agencies in the public, commercial, or not-for-profit sectors.

References

1. Abidin, S.A.S.Z., Rosli, S.H., Bujang, A., Nordin, R., & Nizar, N.N.A. (2021). *Fourier Transform Infrared (FTIR) Spectroscopy for Determination of Offal in Beef Patties.* Paper presented at the 2021 IEEE 12th Control and System Graduate Research Colloquium (ICSGRC).
2. Achata, E.M., Mousa, M.A., Al-Qurashi, A.D., Ibrahim, O.H., Abo-Elyousr, K.A., Aal, A.M.A., & Kamruzzaman, M. (2023). Multivariate optimization of hyperspectral imaging for adulteration detection of ground beef: Towards the development of generic algorithms to predict adulterated ground beef and for digital sorting. *Food Control*, 109907. https://doi.org/10.1016/j.foodcont.2023.109907
3. Alaiz-Rodriguez, R., & Parnell, A.C. (2020). A machine learning approach for lamb meat quality assessment using FTIR spectra. *IEEE Access, 8*, 52385-52394. https://doi.org/10.1109/ACCESS.2020.2974623
4. Bai, Z., Gu, J., Zhu, R., Yao, X., Kang, L., & Ge, J. (2022). Discrimination of minced mutton adulteration based on sized-adaptive online NIRS information and 2D conventional neural network. *Foods, 11*(19), 2977. https://doi.org/10.3390/foods11192977
5. Banerjee, A. (2014). Fourier Transform Infrared Spectroscopy-A Review.
6. Barbin, D.F., Badaro, A.T., Honorato, D.C., Ida, E.Y., & Shimokomaki, M. (2020). Identification of turkey meat and processed products using near infrared spectroscopy. *Food Control, 107*, 106816. https://doi.org/10.1016/j.foodcont.2019.106816
7. Basati, Z., Jamshidi, B., Rasekh, M., & Abbaspour-Gilandeh, Y. (2018). Detection of sunn pest-damaged wheat samples using visible/near-infrared spectroscopy based on pattern recognition. *Spectrochimica Acta Part A: Molecular and Biomolecular Spectroscopy, 203*, 308-314. https://doi.org/10.1016/j.saa.2018.05.123
8. Bauer, A., Scheier, R., Eberle, T., & Schmidt, H. (2016). Assessment of tenderness of aged bovine gluteus medius muscles using Raman spectroscopy. *Meat Science, 115*, 27-33. https://doi.org/10.1016/j.meatsci.2015.12.020
9. Bi, Y., Yuan, K., Xiao, W., Wu, J., Shi, C., Xia, J., & Zhou, G. (2016). A local pre-processing method for near-infrared spectra, combined with spectral segmentation and standard normal variate transformation. *Analytica Chimica Acta, 909*, 30-40. https://doi.org/10.1016/j.aca.2016.01.010
10. Blanco, M., & Villarroya, I. (2002). NIR spectroscopy: a rapid-response analytical tool. *TrAC Trends in Analytical Chemistry, 21*(4), 240-250. https://doi.org/10.1016/S0165-9936(02)00404-1
11. Boyacı, I.H., Temiz, H.T., Uysal, R.S., Velioğlu, H.M., Yadegari, R.J., & Rishkan, M.M. (2014). A novel method for discrimination of beef and horsemeat using Raman spectroscopy. *Food Chemistry, 148*, 37-41. https://doi.org/10.1016/j.foodchem.2013.10.006
12. Brereton, R.G., Jansen, J., Lopes, J., Marini, F., Pomerantsev, A., Rodionova, O., Tauler, R. (2018). Chemometrics in analytical chemistry—part II: modeling, validation, and applications. *Analytical and Bioanalytical Chemistry*, *410*, 6691-6704. https://doi.org/10.1007/s00216-018-1283-4
13. Butler, H.J., Ashton, L., Bird, B., Cinque, G., Curtis, K., Dorney, J., Martin-Hirsch, P.L. (2016). Using Raman spectroscopy to characterize biological materials. *Nature Protocols, 11*(4), 664-687.

14. CANDOĞAN, K., DENİZ, E., ALTUNTAŞ, E.G., Naşit, İ., & Demiralp, D.Ö. (2020). Detection of pork, horse or donkey meat adulteration in beef-based formulations by Fourier transform infrared spectroscopy. *Gıda, 45*(2), 369-379. https://doi.org/10.15237/gida.GD19146
15. Cen, H., & He, Y. (2007). Theory and application of near infrared reflectance spectroscopy in determination of food quality. *Trends in Food Science & Technology, 18*(2), 72-83. https://doi.org/10.1016/j.tifs.2006.09.003
16. Chai, J., Zhang, K., Xue, Y., Liu, W., Chen, T., Lu, Y., & Zhao, G. (2020). Review of MEMS based Fourier transform spectrometers. *Micromachines, 11*(2), 214. https://doi.org/10.3390/mi11020214
17. Cheng, J.-H., Nicolai, B., & Sun, D.-W. (2017). Hyperspectral imaging with multivariate analysis for technological parameters prediction and classification of muscle foods: A review. *Meat Science, 123*, 182-191. https://doi.org/10.1016/j.meatsci.2016.09.017
18. Chophi, R., Sharma, S., Jossan, J.K., & Singh, R. (2021). Rapid and non-destructive analysis of eye-cosmetics using ATR-FTIR spectroscopy and chemometrics. *Forensic Science International, 329*, 111062. https://doi.org/10.1016/j.forsciint.2021.111062
19. Cruz-Tirado, J.P., Vieira, M.S.D.S., Correa, O.O.V., Delgado, D.R., Angulo-Tisoc, J.M., Barbin, D.F., & Siche, R. (2024). Detection of adulteration of Alpaca (*Vicugna pacos*) meat using a portable NIR spectrometer and NIR-hyperspectral imaging. *Journal of Food Composition and Analysis, 126*, 105901. https://doi.org/10.1016/j.jfca.2023.105901
20. Dashti, A., Müller-Maatsch, J., Roetgerink, E., Wijtten, M., Weesepoel, Y., Parastar, H., & Yazdanpanah, H. (2023). Comparison of a portable Vis-NIR hyperspectral imaging and a snapscan SWIR hyperspectral imaging for evaluation of meat authenticity. *Food Chemistry: X, 18*, 100667. https://doi.org/10.1016/j.fochx.2023.100667
21. Dashti, A., Müller-Maatsch, J., Weesepoel, Y., Parastar, H., Kobarfard, F., Daraei, B., Yazdanpanah, H. (2021). The feasibility of two handheld spectrometers for meat speciation combined with chemometric methods and its application for halal certification. *Foods, 11*(1), 71. https://doi.org/10.3390/foods11010071
22. Dashti, A., Weesepoel, Y., Müller-Maatsch, J., Parastar, H., Kobarfard, F., Daraei, B., & Yazdanpanah, H. (2022). Assessment of meat authenticity using portable Fourier transform infrared spectroscopy combined with multivariate classification techniques. *Microchemical Journal, 181*, 107735. https://doi.org/10.1016/j.microc.2022.107735
23. De Girolamo, A., Cervellieri, S., Mancini, E., Pascale, M., Logrieco, A.F., & Lippolis, V. (2020). Rapid authentication of 100% italian durum wheat pasta by FT-NIR spectroscopy combined with chemometric tools. *Foods, 9*(11), 1551. https://doi.org/10.3390/foods9111551
24. Deniz, E., Güneş Altuntaş, E., Ayhan, B., İğci, N., Özel Demiralp, D., & Candoğan, K. (2018). Differentiation of beef mixtures adulterated with chicken or turkey meat using FTIR spectroscopy. *Journal of Food Processing and Preservation, 42*(10), e13767. https://doi.org/10.1111/jfpp.13767
25. Dixit, Y., Casado-Gavalda, M.P., Cama-Moncunill, R., Cama-Moncunill, X., Markiewicz-Keszycka, M., Cullen, P., & Sullivan, C. (2017). Developments and challenges in online NIR spectroscopy for meat processing. *Comprehensive Reviews in Food Science and Food Safety, 16*(6), 1172-1187. https://doi.org/10.1111/1541-4337.12295
26. Edwards, K., Manley, M., Hoffman, L.C., & Williams, P.J. (2021). Non-destructive spectroscopic and imaging techniques for the detection of processed meat fraud. *Foods, 10*(2), 448. https://doi.org/10.3390/foods10020448
27. ElMasry, G., & Sun, D.-W. (2010). Principles of hyperspectral imaging technology *Hyperspectral imaging for food quality analysis and control* (pp. 3-43): Elsevier. https://doi.org/10.1016/B978-0-12-374753-2.10001-2
28. ElMasry, G., Sun, D.-W., & Allen, P. (2012). Near-infrared hyperspectral imaging for predicting colour, pH and tenderness of fresh beef. *Journal of Food Engineering, 110*(1), 127-140. https://doi.org/10.1016/j.jfoodeng.2011.11.028
29. Gemperline, P. (2006). *Practical guide to chemometrics*: CRC press. https://doi.org/10.1201/9781420018301

30. Green, R.O., Eastwood, M.L., Sarture, C.M., Chrien, T.G., Aronsson, M., Chippendale, B.J., & Solis, M. (1998). Imaging spectroscopy and the airborne visible/infrared imaging spectrometer (AVIRIS). *Remote Sensing of Environment, 65*(3), 227-248. https://doi.org/10.1016/S0034-4257(98)00064-9
31. Guo, B., Zhao, J., Weng, S., Yin, X., & Tang, P. (2020). *Rapid determination of minced beef adulteration using hyperspectral reflectance spectroscopy and multivariate methods.* Paper presented at the IOP Conference Series: Earth and Environmental Science. https://doi.org/10.1088/1755-1315/428/1/012049
32. Guo, Y., Ni, Y., & Kokot, S. (2016). Evaluation of chemical components and properties of the jujube fruit using near infrared spectroscopy and chemometrics. *Spectrochimica Acta Part A: Molecular and Biomolecular Spectroscopy, 153*, 79-86. https://doi.org/10.1016/j.saa.2015.08.006
33. Hemmateenejad, B., Akhond, M., & Samari, F. (2007). A comparative study between PCR and PLS in simultaneous spectrophotometric determination of diphenylamine, aniline, and phenol: Effect of wavelength selection. *Spectrochimica Acta Part A: Molecular and Biomolecular Spectroscopy*, *67*(3-4), 958-965. https://doi.org/10.1016/j.saa.2006.09.014
34. Hoffman, L., Ingle, P., Khole, A.H., Zhang, S., Yang, Z., Beya, M., & Cozzolino, D. (2023). Discrimination of lamb (*Ovis aries*), emu (*Dromaius novaehollandiae*), camel (*Camelus* dromedarius) and beef (*Bos taurus*) binary mixtures using a portable near infrared instrument combined with chemometrics. *Spectrochimica Acta Part A: Molecular and Biomolecular Spectroscopy, 294*, 122506. https://doi.org/10.1016/j.saa.2023.122506
35. Hong, T., Yin, J.-Y., Nie, S.-P., & Xie, M.-Y. (2021). Applications of infrared spectroscopy in polysaccharide structural analysis: Progress, challenge and perspective. *Food Chemistry: X, 12*, 100168. https://doi.org/10.1016/j.fochx.2021.100168
36. Hong, Y., Chen, Y., Yu, L., Liu, Y., Liu, Y., Zhang, Y., & Cheng, H. (2018). Combining fractional order derivative and spectral variable selection for organic matter estimation of homogeneous soil samples by VIS–NIR spectroscopy. *Remote Sensing, 10*(3), 479. https://doi.org/10.3390/rs10030479
37. Hu, W., Tang, R., Li, C., Zhou, T., Chen, J., & Chen, K. (2021). Fractional order modeling and recognition of nitrogen content level of rubber tree foliage. *Journal of Near Infrared Spectroscopy, 29*(1), 42-52. https://doi.org/10.1177/0967033520966693
38. Ignat, T., De Falco, N., Berger-Tal, R., Rachmilevitch, S., & Karnieli, A. (2021). A novel approach for long-term spectral monitoring of desert shrubs affected by an oil spill. *Environmental Pollution, 289*, 117788. https://doi.org/10.1016/j.envpol.2021.117788
39. Jiang, H., Cheng, F., & Shi, M. (2020). Rapid identification and visualization of jowl meat adulteration in pork using hyperspectral imaging. *Foods, 9*(2), 154. https://doi.org/10.3390/foods9020154
40. Jiang, H., Jiang, X., Ru, Y., Chen, Q., Wang, J., Xu, L., & Zhou, H. (2022). Detection and visualization of soybean protein powder in ground beef using visible and near-infrared hyperspectral imaging. *Infrared Physics & Technology, 127*, 104401. https://doi.org/10.1016/j.infrared.2022.104401
41. Jiang, H., Jiang, X., Ru, Y., Wang, J., Xu, L., & Zhou, H. (2020). Application of hyperspectral imaging for detecting and visualizing leaf lard adulteration in minced pork. *Infrared Physics & Technology, 110*, 103467. https://doi.org/10.1016/j.infrared.2020.103467
42. Jiang, H., Yang, Y., & Shi, M. (2021). Chemometrics in tandem with hyperspectral imaging for detecting authentication of raw and cooked mutton rolls. *Foods, 10*(9), 2127. https://doi.org/10.3390/foods10092127
43. Jing-yuan, Z., Jun-qin, Z., Mei, S., Xing-hai, C., & Ye-lin, L. (2022). Visualization of lamb adulteration based on hyperspectral imaging for non-destructive quantitative detection. *Food and Machinery, 38*(10), 61-68. https://doi.org/10.13652/j.spjx.1003.5788.2022.90174
44. Kamruzzaman, M., Makino, Y., & Oshita, S. (2016). Rapid and non-destructive detection of chicken adulteration in minced beef using visible near-infrared hyperspectral imaging and machine learning. *Journal of Food Engineering, 170*, 8-15. https://doi.org/10.1016/j.jfoodeng.2015.08.023
45. Kazemi, A., Mahmoudi, A., Veladi, H., & Javanmard, A. (2022). Detection of chicken and fat adulteration in minced lamb meat by VIS/NIR spectroscopy and chemometrics methods. *International Journal of Food Engineering, 18*(7), 525-535. https://doi.org/10.1515/ijfe-2021-0333
46. Kazemi, A., Mahmoudi, A., Veladi, H., Javanmard, A., & Khojastehnazhand, M. (2022). Rapid identification and quantification of intramuscular fat adulteration in lamb meat with VIS–NIR

spectroscopy and chemometrics methods. *Journal of Food Measurement and Characterization, 16*(3), 2400-2410. https://doi.org/10.1007/s11694-022-01352-y

47. Keshavarzi, Z., Barzegari Banadkoki, S., Faizi, M., Zolghadri, Y., & Shirazi, F. H. (2020). Comparison of transmission FTIR and ATR spectra for discrimination between beef and chicken meat and quantification of chicken in beef meat mixture using ATR-FTIR combined with chemometrics. *Journal of food science and technology, 57*, 1430-1438. https://doi.org/10.1007/s13197-019-04178-7
48. Khaled, A. Y., Parrish, C. A., & Adedeji, A. (2021). Emerging nondestructive approaches for meat quality and safety evaluation—A review. *Comprehensive Reviews in Food Science and Food Safety, 20*(4), 3438-3463. https://doi.org/10.1111/1541-4337.12781
49. Leng, T., Li, F., Xiong, L., Xiong, Q., Zhu, M., & Chen, Y. (2020). Quantitative detection of binary and ternary adulteration of minced beef meat with pork and duck meat by NIR combined with chemometrics. *Food Control, 113*, 107203. https://doi.org/10.1016/j.foodcont.2020.107203
50. Li, Z., Wang, Q., Lv, J., Ma, Z., & Yang, L. (2015). Improved quantitative analysis of spectra using a new method of obtaining derivative spectra based on a singular perturbation technique. *Applied Spectroscopy, 69*(6), 721-732. https://doi.org/10.1366/14-07642
51. López-Maestresalas, A., Insausti, K., Jarén, C., Pérez-Roncal, C., Urrutia, O., Beriain, M.J., & Arazuri, S. (2019). Detection of minced lamb and beef fraud using NIR spectroscopy. *Food Control, 98*, 465-473. https://doi.org/10.1016/j.foodcont.2018.12.003
52. Mabood, F., Boqué, R., Alkindi, A.Y., Al-Harrasi, A., Al Amri, I.S., Boukra, S., Naureen, Z. (2020). Fast detection and quantification of pork meat in other meats by reflectance FT-NIR spectroscopy and multivariate analysis. *Meat Science, 163*, 108084. https://doi.org/10.1016/j.meatsci.2020.108084
53. Meza Ramirez, C.A., Greenop, M., Ashton, L., & Rehman, I.U. (2021). Applications of machine learning in spectroscopy. *Applied Spectroscopy Reviews, 56*(8-10), 733-763. https://doi.org/10.1080/05704928.2020.1859525
54. Miller, M. F., Carr, M., Ramsey, C., Crockett, K., & Hoover, L. (2001). Consumer thresholds for establishing the value of beef tenderness. *Journal of Animal Science, 79*(12), 3062-3068. https://doi.org/10.2527/2001.79123062x
55. Mishra, P., Passos, D., Marini, F., Xu, J., Amigo, J.M., Gowen, A.A., Rutledge, D.N. (2022). Deep learning for near-infrared spectral data modelling: Hypes and benefits. *TrAC Trends in Analytical Chemistry*, 116804. https://doi.org/10.1016/j.trac.2022.116804
56. Næs, T., Isaksson, T., Fearn, T., & Davies, T. (2002). *A user-friendly guide to multivariate calibration and classification* (Vol. 6): NIR Chichester. https://doi.org/10.1002/cem.815
57. Oliveri, P., López, M.I., Casolino, M.C., Ruisánchez, I., Callao, M.P., Medini, L., & Lanteri, S. (2014). Partial least squares density modeling (PLS-DM)–A new class-modeling strategy applied to the authentication of olives in brine by near-infrared spectroscopy. *Analytica Chimica acta, 851*, 30-36. https://doi.org/10.1016/j.aca.2014.09.013
58. Pchelkina, V.A., Chernukha, IM., Fedulova, L.V., & Ilyin, N.A. (2022). Raman spectroscopic techniques for meat analysis: A review. *Теория и практика переработки мяса, 7*(2), 97-111. https://doi.org/10.21323/2414-438X-2022-7-2-97-111
59. Premanandh, J. (2013). Horse meat scandal–A wake-up call for regulatory authorities. *Food Control, 34*(2), 568-569. https://doi.org/10.1016/j.foodcont.2013.05.033
60. Rabatel, G., Marini, F., Walczak, B., & Roger, J.M. (2020). VSN: Variable sorting for normalization. *Journal of Chemometrics, 34*(2), e3164. https://doi.org/10.1002/cem.3164
61. Rady, A., & Adedeji, A.A. (2020). Application of hyperspectral imaging and machine learning methods to detect and quantify adulterants in minced meats. *Food Analytical Methods, 13*, 970-981. https://doi.org/10.1007/s12161-020-01719-1
62. Reinhard, E., Heidrich, W., Debevec, P., Pattanaik, S., Ward, G., & Myszkowski, K. (2010). *High dynamic range imaging: acquisition, display, and image-based lighting*: Morgan Kaufmann.
63. Rinnan, Å., Van Den Berg, F., & Engelsen, S.B. (2009). Review of the most common pre-processing techniques for near-infrared spectra. *TrAC Trends in Analytical Chemistry, 28*(10), 1201-1222. https://doi.org/10.1016/j.trac.2009.07.007

64. Robert, C., Fraser-Miller, S.J., Jessep, W.T., Bain, W.E., Hicks, T.M., Ward, J.F., Gordon, K.C. (2021). Rapid discrimination of intact beef, venison and lamb meat using Raman spectroscopy. *Food Chemistry*, *343*, 128441. https://doi.org/10.1016/j.foodchem.2020.128441
65. Saleem, M., Amin, A., & Irfan, M. (2021). Raman spectroscopy based characterization of cow, goat and buffalo fats. *Journal of food science and technology*, *58*, 234-243. https://doi.org/10.1007/s13197-020-04535-x
66. Shao, X., Cui, X., Wang, M., & Cai, W. (2019). High order derivative to investigate the complexity of the near infrared spectra of aqueous solutions. *Spectrochimica Acta Part A: Molecular and Biomolecular Spectroscopy*, *213*, 83-89. https://doi.org/10.1016/j.saa.2019.01.059
67. Shawky, E., El-Khair, R.M.., & Selim, D.A. (2020). NIR spectroscopy-multivariate analysis for rapid authentication, detection and quantification of common plant adulterants in saffron (*Crocus sativus* L.) stigmas. *Lwt*, *122*, 109032. https://doi.org/10.1016/j.lwt.2020.109032
68. Siddiqui, M.A., Khir, M.H.M., Witjaksono, G., Ghumman, A.S.M., Junaid, M., Magsi, S.A., & Saboor, A. (2021). Multivariate analysis coupled with M-SVM classification for lard adulteration detection in meat mixtures of beef, lamb, and chicken using FTIR spectroscopy. *Foods*, *10*(10), 2405. https://doi.org/10.3390/foods10102405
69. Silva, L.C., Folli, G.S., Santos, LP., Barros, I.H., Oliveira, B.G., Borghi, F.T., & Romao, W. (2020). Quantification of beef, pork, and chicken in ground meat using a portable NIR spectrometer. *Vibrational Spectroscopy*, *111*, 103158. https://doi.org/10.1016/j.vibspec.2020.103158
70. Stark, E., Luchter, K., & Margoshes, M. (1986). Near-infrared analysis (NIRA): A technology for quantitative and qualitative analysis. *Applied Spectroscopy Reviews*, *22*(4), 335-399.
71. Stuart, B.H. (2004). *Infrared spectroscopy: fundamentals and applications*: John Wiley & Sons.
72. Totaro, M.P., Squeo, G., De Angelis, D., Pasqualone, A., Caponio, F., & Summo, C. (2023). Application of NIR spectroscopy coupled with DD-SIMCA class modelling for the authentication of pork meat. *Journal of Food Composition and Analysis*, *118*, 105211. https://doi.org/10.1016/j.jfca.2023.105211
73. Wang, H.-P., Chen, P., Dai, J.-W., Liu, D., Li, J.-Y., Xu, Y.-P., & Chu, X.-L. (2022). Recent advances of chemometric calibration methods in modern spectroscopy: Algorithms, strategy, and related issues. *TrAC Trends in Analytical Chemistry*, *153*, 116648. https://doi.org/10.1016/j.trac.2022.116648
74. Wang, K., Bian, X., Tan, X., Wang, H., & Li, Y. (2021). A new ensemble modeling method for multivariate calibration of near infrared spectra. *Analytical Methods*, *13*(11), 1374-1380. https://doi.org/10.1039/D1AY00017A
75. Wang, L., Liang, J., Li, F., Guo, T., Shi, Y., Li, F., & Xu, H. (2024). Deep learning based on the Vis-NIR two-dimensional spectroscopy for adulteration identification of beef and mutton. *Journal of Food Composition and Analysis*, *126*, 105890. https://doi.org/10.1016/j.jfca.2023.105890
76. Weng, S., Guo, B., Tang, P., Yin, X., Pan, F., Zhao, J., & Zhang, D. (2020). Rapid detection of adulteration of minced beef using Vis/NIR reflectance spectroscopy with multivariate methods. *Spectrochimica Acta Part A: Molecular and Biomolecular Spectroscopy*, *230*, 118005. https://doi.org/10.1016/j.saa.2019.118005
77. Wold, S., & Sjöström, M. (1977). SIMCA: a method for analyzing chemical data in terms of similarity and analogy: ACS Publications. https://doi.org/10.1021/bk-1977-0052.ch012
78. Xiong, Z., Sun, D.-W., Pu, H., Gao, W., & Dai, Q. (2017). Applications of emerging imaging techniques for meat quality and safety detection and evaluation: A review. *Critical Reviews in Food Science and Nutrition*, *57*(4), 755-768. https://doi.org/10.1080/10408398.2014.954282
79. Xu, W., Xia, J., Min, S., & Xiong, Y. (2022). Fourier transform infrared spectroscopy and chemometrics for the discrimination of animal fur types. *Spectrochimica Acta Part A: Molecular and Biomolecular Spectroscopy*, *274*, 121034. https://doi.org/10.1016/j.saa.2022.121034
80. Yang, F., Sun, J., Cheng, J., Fu, L., Wang, S., & Xu, M. (2023). Detection of starch in minced chicken meat based on hyperspectral imaging technique and transfer learning. *Journal of Food Process Engineering*, *46*(4), e14304. https://doi.org/10.1111/jfpe.14304
81. Yao, Z., Su, H., Yao, J., & Huang, X. (2021). Yield-adjusted operation for convolution filter denoising. *Analytical Chemistry*, *93*(49), 16489-16503. https://doi.org/10.1021/acs.analchem.1c03606

82. Zahra, A., Qureshi, R., Sajjad, M., Sadak, F., Nawaz, M., Khan, H.A., & Uzair, M. (2023). Current advances in imaging spectroscopy and its state-of-the-art applications. *Expert Systems with Applications*, 122172. https://doi.org/10.1016/j.eswa.2023.122172
83. Zhang, W., Kasun, L.C., Wang, Q.J., Zheng, Y., & Lin, Z. (2022). A review of machine learning for near-infrared spectroscopy. *Sensors*, *22*(24), 9764. https://doi.org/10.3390/s22249764
84. Zhang, W., Ma, J., & Sun, D.-W. (2021). Raman spectroscopic techniques for detecting structure and quality of frozen foods: principles and applications. *Critical Reviews in Food Science and Nutrition*, *61*(16), 2623-2639. https://doi.org/10.1080/10408398.2020.1828814
85. Zhao, Z., Yu, H., Zhang, S., Du, Y., Sheng, Z., Chu, Y., & Deng, L. (2020). Visualization accuracy improvement of spectral quantitative analysis for meat adulteration using Gaussian distribution of regression coefficients in hyperspectral imaging. *Optik*, *212*, 164737. https://doi.org/10.1016/j.ijleo.2020.164737
86. Zheng, K.-Y., Zhang, X., Tong, P.-J., Yao, Y., & Du, Y.-P. (2015). Pretreating near infrared spectra with fractional order Savitzky–Golay differentiation (FOSGD). *Chinese Chemical Letters*, *26*(3), 293-296. https://doi.org/10.1016/j.cclet.2014.10.023

نشریه پژوهشهای علوم و صنایع غذایی ایران
https://ifstrj.um.ac.ir

مقاله مروری

جلد ۲۰، شماره ۶، بهمن-اسفند، ۱۴۰۳، ص. ۲۲۴-۲۰۱

تشخیص تقلب گوشت چرخ‌کرده با تکنیک‌های طیفی و هوش مصنوعی (۲۰۲۰-۲۰۲٤)

امیر کاظمی[۱*]- اصغر محمودی[۲]- مصطفی خجسته‌نژند[۳]

تاریخ دریافت: ۱۴۰۳/۰۳/۰۲
تاریخ پذیرش: ۱۴۰۳/۰۶/۱۹

چکیده

گوشت منبع مهمی از مواد مغذی مهم است و نقش حیاتی در رژیم غذایی انسان دارد. عدم نظارت بر کیفیت و ایمنی گوشت می‌تواند منجر به تهدید سلامتی شود. بررسی ایمنی گوشت با روش‌های شیمیایی پرهزینه و زمان‌بر است، بدون اینکه امکان نظارت به صورت زمان واقعی وجود داشته باشد. بنابراین، امروزه ارزیابی کیفیت گوشت با استفاده از تکنیک‌های طیفی مانند تصویربرداری طیفی و طیف‌سنجی، روش‌هایی امیدوارکننده محسوب می‌شوند و این تکنیک‌ها اخیراً دستخوش پیشرفت‌های سریعی شده و توجه عمومی را به خود جلب کرده است. بنابراین، هدف مقاله مروری حاضر ارائه مروری بر آخرین پیشرفت‌ها در روش‌های طیفی برای ارزیابی ایمنی گوشت چرخ شده است. اصول اولیه کار، فرآیند تحلیل و کاربردهای این تکنیک‌ها شرح داده شده است. محققان با بررسی امکان استفاده عملی از فناوری‌های تشخیص طیفی در ارزیابی ایمنی گوشت، چالش‌های موجود و چشم‌انداز تحقیقاتی آتی را مورد بحث قرار دادند. در ادامه، جدیدترین پیشرفت‌ها در کاربرد هوش مصنوعی همراه با تکنیک‌های ذکر شده نیز مورد بحث قرار گرفت.

واژه‌های کلیدی: تقلب، تصویربرداری طیفی، طیف‌سنجی NIR، گوشت چرخ‌کرده، یادگیری ماشین

۱ و ۲- دانشجوی دکتری و استاد، گروه مهندسی بیوسیستم، دانشگاه تبریز، تبریز، ایران
(*- نویسنده مسئول: Email: a.kazemi@tabrizu.ac.ir)
۳- دانشیار، گروه مهندسی مکانیک، دانشکده فنی و مهندسی، دانشگاه بناب، بناب، ایران

https://doi.org/10.22067/ifstrj.2024.88158.1335

بسم الله الرحمن الرحیم

مندرجات

نشریه پژوهشهای علوم و صنایع غذایی ایران

با شماره پروانه ۱۲۴/۸۴۷ و درجه علمی–پژوهشی شماره ۳/۱۱/۸۱۰ از وزارت علوم، تحقیقات و فناوری
۸۸/۵/۱۰
"براساس مصوبه وزارت عتف از سال ۱۳۹۸، کلیه نشریات دارای درجه "علمی–پژوهشی" به نشریه "علمی" تغییر نام یافتند. "

جلد ۲۰ **شماره ۶** **بهمن- اسفند ۱۴۰۳**

ناشر: دانشگاه فردوسی مشهد

این نشریه درپایگاه‌های زیر نمایه شده است:

AGRIS، Scopus، CABI، DOAJ، EBSCO، Google scholar، Internet Archive، پایگاه استنادی جهان اسلام (ISC)، سامانه نشریات علمی ایران، پایگاه اطلاعات علمی جهاد دانشگاهی (SID)، بانک اطلاعات نشریات کشور (MAGIRAN)، مرجع دانش CIVILICA

پست الکترونیکی: **ifstrj@um.ac.ir**

مقالات این شماره در سایت https://ifstrj.um.ac.ir به صورت مقاله کامل نمایه شده است.

این نشریه به تعداد ۶ شماره در سال و به صورت آنلاین منتشر می‌شود.

نشریه علمی
پژوهشهای علوم و صنایع غذایی ایران

جلد ۲۰ شماره ۶
سال ۱۴۰۳
شماره پیاپی ۹۰
شاپا: ۴۱۶۱-۱۷۳۵

عنوان مقالات